Irena Wojtowicz

„Zastosowanie dermatoskopii i dermatoskopii wzmocnionej ultrafioletem w ocenie raka podstawnokomórkowego.”

‘Application of dermatoscopy and ultraviolet-enhanced dermatoscopy in the assessment of basal cell carcinoma.’

Rozprawa na stopień doktora
w dziedzinie nauk medycznych i nauk o zdrowiu
w dyscyplinie nauki medyczne

Promotor: dr hab. n. med. Magdalena Żychowska, prof. UR
Zakład i Klinika Dermatologii, Wydział Medyczny, Collegium Medicum,
Uniwersytet Rzeszowski

Rzeszów 2025 r.

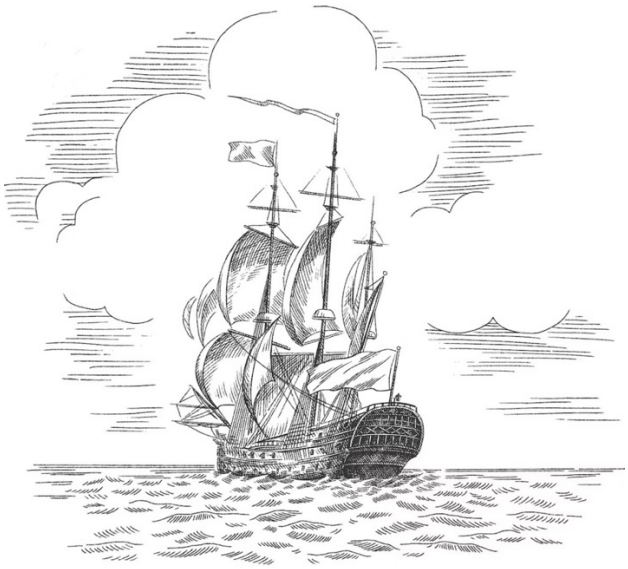

„Żaden wiatr nie sprzyja temu, kto nie wie, do jakiego portu zmierza.”

Seneka

Pragnę wyrazić serdecznie podziękowania:

Moim Najbliższym, a w szczególności Mężowi i Rodzicom,
za cierpliwość, niezachwianą wiarę, bezwarunkowe wsparcie i niezłomne trwanie przy mnie,

Pani Promotor, dr hab. n. med. Magdalenie Żychowskiej, prof. UR
za nieustającą inspirację, wiarę w moje możliwości i wsparcie, które było dla mnie niezastąpionym drogowskazem – zarówno naukowo, jak i życiowo.

Laurze, mojej córeczce,

aby zawsze pamiętała, że choć droga do marzeń bywa trudna,
to właśnie wytrwałość prowadzi do celu,
a każda wielka podróż zaczyna się od pierwszego kroku.

Spis treści

Rozdział 1.

Curriculum Vitae

Doświadczenie zawodowe i wykształcenie

2023-obecnie	**Uniwersytecki Szpital Kliniczny im. Fryderyka Chopina w Rzeszowie,** **Klinika Dermatologii i Dermatologii Onkologicznej** Stanowisko: lekarz rezydent w trakcie specjalizacji z dermatologii i wenerologii
2020-2023	**Wojewódzki Szpital Podkarpacki im. Jana Pawła II w Krośnie** Stanowisko: lekarz rezydent w trakcie specjalizacji z dermatologii i wenerologii
2018-2019	**Kliniczny Szpital Wojewódzki Nr 1 w Rzeszowie** Stanowisko: lekarz stażysta
2012-2018	**Uniwersytet Jagielloński w Krakowie, Collegium Medicum** Kierunek: lekarski Ukończenie studiów z wyróżnieniem. Uzyskanie tytułu zawodowego lekarza z wynikiem bardzo dobrym.
2009-2012	**IV Liceum Ogólnokształcące im. Mikołaja Kopernika w Rzeszowie** Profil: biologiczno-chemiczny Uzyskanie świadectwa maturalnego z wyróżnieniem.

Publikacje:

(z wyłączeniem prac będących częścią rozprawy doktorskiej)

1. **Wojtowicz I**., Krawczyk-Wołoszyn K., Ostańska E., Reich A., Żychowska M. Choose your biopsy site wisely — the utility of dermoscopy in the diagnosis of Bowen's disease of the face. *Forum Dermatologicum*, 2024, 10(2), 50–53.

2. **Wojtowicz I**., Reich A. Hidradenitis suppurativa – co dotychczas wiadomo? *Wiadomości Dermatologiczne,* 2024; 22. Dostępne na: https://www.wiadomoscidermatologiczne.pl/artykul/hidradenitis-suppurativa-co-dotychczas-wiadomo [dostęp: 31.05.2025].

3. **Wojtowicz I**., Żychowska M. Dermoskopia w świetle ultrafioletowym w dermatoonkologii. *W:* Diagnostyka obrazowa złośliwych nowotworów skóry. Pod redakcją: Kamińska-Winciorek G. Warszawa: Polskie Towarzystwo Chirurgii Onkologicznej, Biblioteka Chirurga Onkologa – *w trakcie procesu publikacji*

Doniesienia zjazdowe:

1. **Wojtowicz I**., Reich A., Żychowska M. Ultraviolet-induced fluorescence dermoscopy features of basal cell carcinomas in the H- and non-H-zones of the head and neck area. *Spring Symposium of the European Academy of Dermatology and Venereology*, Praga, 22–24 maja 2025.

2. **Wojtowicz I.** Zastosowanie dermatoskopii i dermatoskopii wzmocnionej ultrafioletem w ocenie raka podstawnokomórkowego. *Zjazd Sekcji Forum Młodych Polskiego Towarzystwa Dermatologicznego*, Łódź, 24–25 października 2024.

3. **Wojtowicz I.** Xanthogranuloma necrobioticum. *Konferencja naukowa „Cyklówki dermatologiczne" pod egidą Oddziału Podkarpackiego Polskiego Towarzystwa Dermatologicznego*, Rzeszów, 6 grudnia 2024.

Działalność dydaktyczna i organizacyjna:

1. Współprowadzenie warsztatów pt. „Dermatoskopia chorób wieku dziecięcego” – prezentacja tematu „Melanonychia u dzieci” podczas konferencji „Podkarpackie Dni Dermatologii”, która odbyła się w dniach 27–29 marca 2025 r. w Rzeszowie.

Nagrody i wyróżnienia

1. **Wyróżnienie Specjalne** w kategorii "Praca Kliniczna" za pracę pt. *"Zastosowanie dermatoskopii i dermatoskopii wzmocnionej ultrafioletem w ocenie raka podstawnokomórkowego"*, podczas Zjazdu Sekcji Forum Młodych Polskiego Towarzystwa Dermatologicznego, Łódź, 24–25 października 2024 r.

2. **Stypendium Mentorship Award** przyznane przez International Society of Dermatology (ISD) na realizację 2-miesięcznego stażu klinicznego w Australii, obejmującego szkolenie w wiodących ośrodkach dermatologicznych: w Melbourne pod kierunkiem prof. Rosemary Nixon oraz w Sydney pod kierunkiem prof. Dedee Murrell.

Rozdział 2.

Wykaz skrótów

AI – sztuczna inteligencja (ang *artificial intelligence*)

BCC – rak podstawnokomórkowy (ang. *basal cell carcinoma*)

BSC – rak podstawnokomórkowy o cechach płaskonabłonkowych (ang. *basosquamous carcinoma*)

EVD – dermoskopia ex vivo (ang. *ex vivo dermoscopy*)

MAY globules – liczne, zgrupowane, żółto-białe globule (ang. *multiple aggregated yellow-white globules*)

NPD – dermoskopia niespolaryzowana (ang. *non-polarized dermoscopy*)

OCT – optyczna koherentna tomografia (ang. *optical coherence tomography*)

OSHMD – optyczna dermoskopia dużych powiększeń (ang. *optical super-high magnification dermoscopy*)

PD – dermoskopia spolaryzowana (ang. *polarized dermoscopy*)

PDT – terapia fotodynamiczna (ang. *photodynamic therapy*)

PPV – dodatnia wartość predykcyjna (ang. *positive predictive value*)

RCM – refleksyjna mikroskopia konfokalna (ang. *reflectance confocal microscopy)*

SCC – rak kolczystokomórkowy (ang. *squamous cell carcinoma*)

SD – odchylenie standardowe (ang. *standard deviation*)

UV – światło ultrafioletowe (ang. *ultraviolet light*)

UVFD – dermoskopia wzmocniona ultrafioletem (ang. *ultraviolet-enhanced fluorescence dermoscopy*)

WADD – dermoskopia z zastosowaniem szerokiego pola widzenia (ang. *wide-area digital dermoscopy*)

Rozdział 3

Wykaz publikacji stanowiących rozprawę doktorską

1. Praca przeglądowa

Tytuł: **Dermoscopy of Basal Cell Carcinoma Part 1: Dermoscopic Findings and Diagnostic Accuracy – A Systematic Literature Review**

Autorzy: **Irena Wojtowicz**, Magdalena Żychowska

Cancers, 2025; 17(3):493. doi: 10.3390/cancers17030493

IF = 4.5 | MNiSW = 140 points | Q1

2. Praca przeglądowa

Tytuł: **Dermoscopy of Basal Cell Carcinoma Part 2: Dermoscopic Findings by Lesion Subtype, Location, Age of Onset, Size and Patient Phototype**

Autorzy: **Irena Wojtowicz**, Magdalena Żychowska

Cancers, 2025; 17(2):176. doi: 10.3390/cancers17020176

IF = 4.5 | MNiSW = 140 points | Q1

3. Praca przeglądowa

Tytuł: **Dermoscopy of Basal Cell Carcinoma Part 3: Differential Diagnosis, Treatment Monitoring and Novel Technologies**

Autorzy: **Irena Wojtowicz**, Magdalena Żychowska

Cancers, 2025; 17(6):1025. doi: 10.3390/cancers17061025

IF = 4.5 | MNiSW = 140 points | Q1

4. Praca oryginalna

Tytuł: **Application of Ultraviolet-Enhanced Fluorescence Dermoscopy in Basal Cell Carcinoma**

Autorzy: **Irena Wojtowicz**, Magdalena Żychowska

Cancers, 2024; 16(15):2685. doi: 10.3390/cancers16152685

IF = 4.5 | MNiSW = 140 points | Q1

5. Praca oryginalna

Tytuł: **Polarized Dermoscopy and Ultraviolet-Induced Fluorescence Dermoscopy of Basal Cell Carcinomas in the H- and Non-H-Zones of the Head and Neck**

Autorzy: **Irena M. Wojtowicz**, Adam A. Reich, Magdalena Żychowska

Dermatology and Therapy (Heidelb), 2025. https://doi.org/10.1007/s13555-025-01432-z

IF = 3.5 | MNiSW = 100 points | Q2

Podsumowanie bibliometryczne

Łączny Impact Factor (IF): 21,5

Łączna punktacja MNiSW: 660 punktów

Rozdział 4.

Wstęp

Rak podstawnokomórkowy (ang. *basal cell carcinoma*, BCC) jest najczęściej występującym złośliwym nowotworem skóry i nowotworem ogółem [1]. Choć rzadko prowadzi do zgonu, jego miejscowo agresywny wzrost może powodować istotne uszkodzenia tkanek, prowadząc do deformacji anatomicznych i poważnych konsekwencji funkcjonalnych oraz estetycznych. Aktualne dane wskazują, że ryzyko zachorowania na BCC w ciągu życia wynosi około 20%, co oznacza, że problem ten dotyczy co piątej osoby [2]. Co więcej, częstość występowania BCC jest szacowana jako 18–20 razy wyższa niż czerniaka, co dodatkowo podkreśla skalę tego zagadnienia w populacji ogólnej [3].

We wczesnym rozpoznaniu BCC w codziennej praktyce klinicznej szczególnie przydatna jest dermoskopia – nieinwazyjna technika umożliwiająca wizualizację struktur skórnych od naskórka aż po warstwę brodawkowatą skóry właściwej, niewidocznych golym okiem [4]. Dermoskopia znacznie zwiększa czułość wykrywania zmian nowotworowych w porównaniu do badania klinicznego, osiągając czułość na poziomie od 67,6% do 98,6% oraz dodatnią wartość predykcyjna (ang. *positive predictive value*, PPV) rzędu 85,9%–97% [5,6,7]. Pomimo wysokiej skuteczności, nadal istnieje ryzyko błędnej interpretacji, zwłaszcza w przypadku zmian o nietypowym obrazie dermoskopowym.

W codziennej praktyce trudności mogą sprawiać zmiany takie jak podrażnione lub zmienione zapalnie brodawki łojotokowe, włókniaki twarde z obrazem imitującym BCC czy BCC zlokalizowane na kończynach dolnych [8,9,10,11]. Ponadto, rzadko występujące zmiany, takie jak m.in. nerwiakowłókniak śluzowy, skórny mięśniak gładkokomórkowy czy nowotwory przydatkowe skóry pozostają często nierozróżnialne za pomocą klasycznej dermoskopii [12,13,14]. W takich przypadkach niezbędna pozostaje weryfikacja histopatologiczna – złoty standard w diagnostyce i podstawowe narzędzie decydujące o dalszym postępowaniu terapeutycznym [14]. Co istotne, zdarzają się sytuacje, w których zmiany rozpoznawane wstępnie jako BCC, w rzeczywistości okazują się innymi jednostkami chorobowymi np. chłoniakami skóry z komórek B, przerzutami raka nerki czy skórną postacią histoplazmozy [15,16,17].

Powyższe trudności diagnostyczne oraz ograniczenia obecnych technik obrazowania skłaniają do poszukiwania nowych metod wspomagających nieinwazyjne wczesne rozpoznawanie BCC. Jednym z kierunków rozwoju dermoskopii jest integracja dodatkowych technologii, takich jak wykorzystanie światła ultrafioletowego (ang. *ultraviolet light,* UV).

Dermoskopia fluorescencyjna wzmocniona ultrafioletem (ang. *ultraviolet-enhanced fluorescence dermoscopy,* UVFD) to metoda, która wykorzystuje promieniowanie UV o długości fali 365 nm, znane dotychczas z zastosowania w lampie Wooda, w celu wzbudzenia fluorescencji endogennych chromoforów skóry, takich jak melanina i hemoglobina. W wyniku zjawiska przesunięcia Stokesa pochłonięta energia świetlna powoduje wzbudzenie elektronów, które powracając do stanu podstawowego emitują światło o dłuższej fali, mieszczące się w zakresie widzialnym. Uzyskana fluorescencja pozwala na uwidocznienie różnic w strukturze i składzie chemicznym tkanek, co może zwiększać kontrast obrazu i poprawiać dokładność diagnostyczną w ocenie zmian skórnych [18].

Rozdział 5.

Cele

Celem pracy była analiza wykorzystania UVFD w ocenie BCC, z uwzględnieniem obecnych struktur dermoskopowych i ich występowania w zależności od lokalizacji, wielkości i podtypu klinicznego nowotworu.

Szczegółowe cele pracy:

1. Analiza stanu wiedzy na temat wykorzystania klasycznej dermoskopii w ocenie BCC (Publikacje 1, 2, 3)

2. Identyfikacja i zdefiniowanie struktur dermoskopowych widocznych w BCC w UVFD (Publikacja 4)

3. Analiza częstości występowania poszczególnych cech UVFD w BCC i ich korelacji ze strukturami obecnymi w PD (Publikacja 4)

4. Porównanie obrazu BCC w UVFD w zależności od lokalizacji, wielkości nowotworu oraz podtypu klinicznego (Publikacja 4)

5. Analiza obrazu BCC w UVFD i PD w poszczególnych rejonach głowy i szyi ze szczególnym uwzględnieniem strefy H (Publikacja 5)

Rozdział 6.

Materiały i metody

Niniejsza rozprawa doktorska składa się z pięciu prac. W trzech pracach przeglądowych (publikacja nr 1, 2, 3) podsumowano dotychczasowy stan wiedzy na temat tzw. klasycznej dermoskopii, obejmującej PD oraz dermoskopię niespolaryzowaną (ang. *non-polarized dermoscopy*, NPD) w ocenie BCC. Dwa badania oryginalne koncentrowały się na ocenie cech dermoskopowych BCC widocznych w PD oraz w UVFD. Analiza uwzględniała lokalizację zmian zarówno na twarzy, jak i poza nią, ich rozmiar oraz kliniczny podtyp BCC (publikacja nr 4), a także szczegółowe rejony anatomiczne w obrębie głowy i szyi (publikacja nr 5).

Publikacja 1: **Dermoscopy of Basal Cell Carcinoma Part 1: Dermoscopic Findings and Diagnostic Accuracy – A Systematic Literature Review**

Publikacja 2: **Dermoscopy of Basal Cell Carcinoma Part 2: Dermoscopic Findings by Lesion Subtype, Location, Age of Onset, Size and Patient Phototype**

Publikacja 3: **Dermoscopy of Basal Cell Carcinoma Part 3: Differential Diagnosis, Treatment Monitoring and Novel Technologies**

Powyższe przeglądy systematyczne zostały przeprowadzone zgodnie z wytycznymi PRISMA [19]. Przeszukano bazę danych PubMed od jej powstania do września 2024 roku, stosując kombinacje słów kluczowych odnoszących się do BCC oraz dermoskopii.

Włączono wyłącznie artykuły oryginalne w języku angielskim zawierające dane na temat cech dermoskopowych oraz dokładności diagnostycznej dermoskopii (publikacja nr 1), obrazu dermoskopowego w zależności od podtypu BCC, jego lokalizacji, wielkości, wieku zachorowania i fototypu skóry pacjenta (publikacja nr 2), roli dermoskopii w diagnostyce różnicowej, monitorowaniu terapii oraz opisujące nowoczesne metody diagnostyczne będące modyfikacją tzw. klasycznej dermoskopii (publikacja nr 3). Dodatkowo przeszukano listy bibliograficzne wybranych publikacji w celu identyfikacji potencjalnie istotnych badań nieujętych w początkowym wyszukiwaniu. Wykluczono

prace poglądowe, komentarze redakcyjne, opinie eksperckie, publikacje bez dostępu do pełnego tekstu oraz napisane w języku innym niż angielski.

Publikacja 4

Praca oryginalna: **Application of Ultraviolet-Enhanced Fluorescence Dermoscopy in Basal Cell Carcinoma**

Badanie przeprowadzono w Klinice Dermatologii w Rzeszowie. Do analizy włączono pacjentów zgłaszających się do Kliniki z podejrzeniem BCC, wysuniętym w oparciu o ocenę kliniczną i dermoskopową. Ostateczne rozpoznanie każdorazowo potwierdzano histopatologicznie. W badaniu użyto dermatoskop Dermlite DL5, umożliwiający obrazowanie w trybie PD oraz UVFD (UV o długości fali 365 nm). Zdjęcia wykonywano za pomocą telefonu iPhone 7 Plus, a następnie zapisywano i analizowano.

Obserwacje dermoskopowe w trybie PD oceniano zgodnie ze standardowymi kryteriami stosowanymi w dermatoonkologii, uwzględniając obecność struktur naczyniowych (np. naczynia rozgałęziające się drzewkowato, drobne, krótkie teleangiektazje), struktur barwnikowych (np. obszary przypominające liście klonu, duże szaro-niebieskie gniazda owalne, obszary w kształcie kół ze szprychami) oraz innych cech, takich jak owrzodzenia, homogenne obszary czerwono-białe czy wyraźne granice guza.

Obraz BCC w UVFD nie był dotychczas analizowany i opisywany w literaturze. Na podstawie własnych obserwacji wyróżniono nastepujące struktury:

- Ciemną sylwetkę guza (ang. *dark silhouettes*)
- Zaburzony wzorzec ujść mieszków włosowych (ang. *interrupted follicle pattern*)
- Brak niebiesko-zielonej fluorescencji w obrębie guza (ang. *lack of blue-green fluorescence*)
- Brak różowo-pomarańczowej fluorescencji w obrębie guza (ang. *lack of pink-range fluorescence*)
- Obecność różowo-pomarańczowej fluorescencji (ang. *pink-range fluorescence*)
- Obecność błękitnych włókien fluorescencyjnych (ang. *blue fluorescent fibers*)
- Nadżerki i owrzodzenia (ang. *erosions and ulcerations*)
- Biało-niebieską łuskę (ang. *white-blue scales*)

- Naczynia rozgałęziające się drzewkowato (ang. *arborizing vessels*)
- Czarne globule (ang. *black globules*)
- Ogniska białej depigmentacji (ang. *white depigmentation*)
- Białe grudki/globule (ang. *white clods*)
- Dobrze widoczne granice guza (ang. *well-demarcated borders*)

Większość z wymienionych struktur zaprezentowano na Rycinie 1.

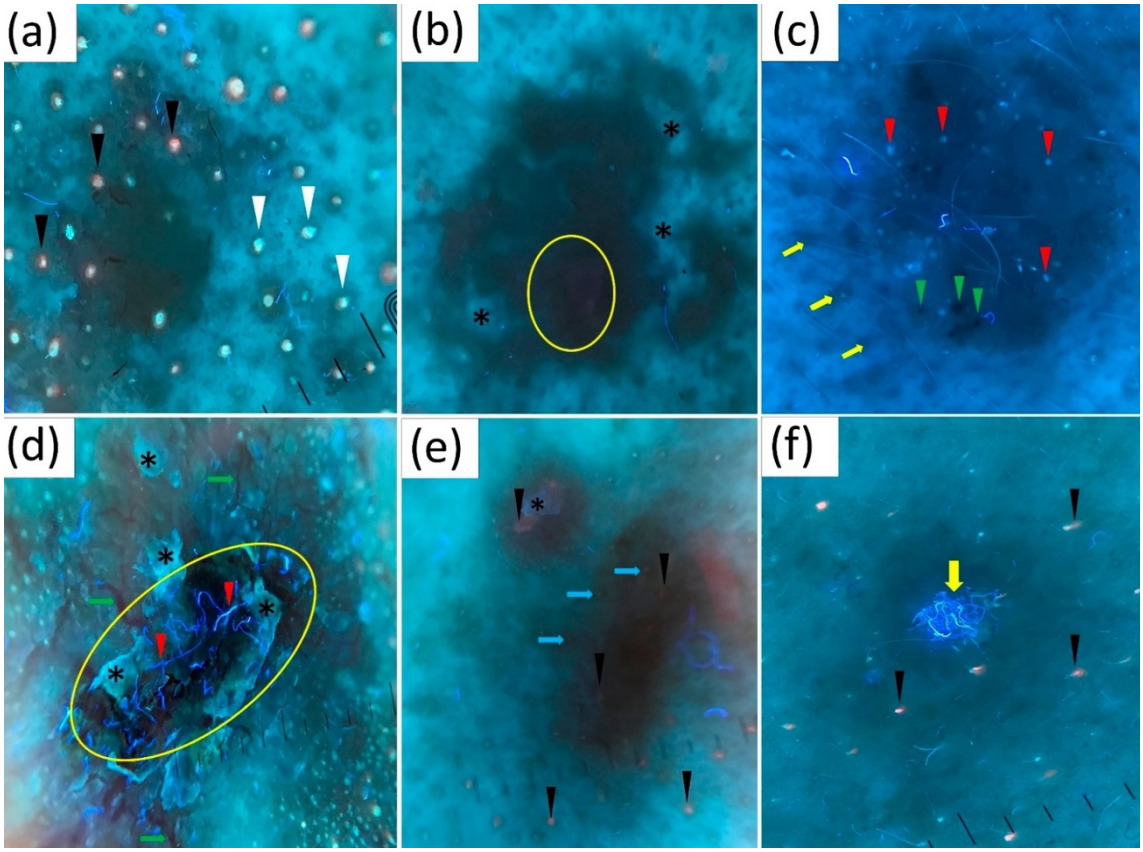

Ryc. 1. Struktury obserwowane w raku podstawnokomórkowym (ang. *basal cell carcinoma,* BCC) w dermoskopii wzmocnionej ultrafioletem (ang. *ultraviolet-enhanced fluorescence dermoscopy,* UVFD). (a) Ciemna sylwetka guza, różowo-pomarańczowa (czarne groty strzałek) i niebiesko-zielona (białe groty strzałek) fluorescencja w skórze otaczającej i ich brak w obrębie guza. (b) Ciemna sylwetka guza z ogniskami białej depigmentacji (czarne gwiazdki) i różowo-pomarańczową fluorescencją (żółty okrąg). (c) Białe grudki (czerwone groty strzałek), czarne globule (zielone groty strzałek), zachowany wzorzec ujść mieszkowych w otoczeniu (żółte strzałki) i jego zaburzenie w obrębie zmiany. (d) Biało-niebieska łuska (czarne gwiazdki), błękitne włókna fluorescencyjne (czerwone groty strzałek), naczynia rozgałęziające się drzewkowato (zielone strzałki). (e) Ciemna sylwetka guza, różowo-pomarańczowa fluorescencja (czarne groty strzałek) w skórze otaczającej i jej brak w obrębie guza, biało-niebieska łuska (czarna gwiazdka), zachowany wzorzec ujść mieszkowych w otoczeniu i jego zaburzenie w obrębie guza (niebieskie strzałki). (f) Błękitne włókna fluorescencyjne (żółta strzałka), różowo-pomarańczowa fluorescencja (czarne groty strzałek) w skórze otaczającej i jej brak w obrębie guza. Ta rycina jest częścią publikacji nr 4.

„Ciemna sylwetka” odnosiła się do obszaru zmiany nowotworowej, który wykazywał wyraźnie ciemniejsze zabarwienie w porównaniu do otaczającej skóry. „Zaburzony wzorzec ujść mieszków włosowych” identyfikowano na podstawie obecności regularnie rozmieszczonych, ciemnych, okrągłych lub owalnych struktur odpowiadających ujściom mieszków włosowych w skórze zdrowej, których brak stwierdzano w obrębie guza. „Brak fluorescencji mieszkowej niebiesko-zielonej czy różowo-pomarańczowej” definiowano jako obecność tych wzorców fluorescencji w skórze otaczającej zmianę z jednoczesnym ich całkowitym brakiem w obrębie nowotworu. Z kolei „biała depigmentacja” była rozumiana jako intensywnie jasna, jednorodna strefa o białym zabarwieniu, wyraźnie odróżniająca się zarówno od reszty guza, jak i od skóry sąsiadującej.

W badaniu analizowano obraz PD oraz UVFD z uwzględnieniem lokalizacji BCC (porównując zmiany umiejscowione na twarzy i poza jej obszarem), rozmiaru (małe <5 mm średnicy, średnie 5-10 mm, duże >10 mm) oraz podtypu klinicznego (guzkowy i powierzchowny). Dodatkowo oceniano korelację struktur widocznych w PD oraz UVFD.

Analizę statystyczną wykonano przy użyciu programu SPSS. Zmienne kategoryczne przedstawiono jako liczby bezwzględne i procenty, natomiast zmienne ciągłe jako średnie ± odchylenie standardowe (ang. *standard deviation*, SD). Do porównań międzygrupowych zastosowano test Fishera. Za istotny statystycznie przyjęto poziom $p < 0,05$.

Publikacja 5

Praca oryginalna: **Polarized Dermoscopy and Ultraviolet-Induced Fluorescence Dermoscopy of Basal Cell Carcinomas in the H- and Non-H-Zones of the Head and Neck**

Badanie przeprowadzono w Klinice Dermatologii w Rzeszowie w okresie od stycznia 2024 roku do stycznia 2025 roku. Podobnie jak w publikacji nr 4, analizie poddano pacjentów zgłaszających się z podejrzeniem BCC, wysuniętym na podstawie oceny klinicznej i dermoskopowej, a następnie potwierdzonym histopatologicznie.

W badaniu oceniano BCC zlokalizowane w najczęstszym obszarze ich występowania – w rejonie głowy i szyi. Obraz dermoskopowy analizowano zarówno w odniesieniu do konkretnych, szczegółowych lokalizacji anatomicznych, jak i z uwzględnieniem tzw. strefy H. Stefę H wyróżniono ze uwagi na szczególne znaczenie kliniczne związane z wyższym ryzykiem agresywnego wzrostu nowotworu oraz większym prawdopodobieństwem nawrotu. Obejmuje ona okolicę nosa, uszu, oczu, ust, skroni oraz brody.

Do obrazowania użyto tego samego sprzętu co w poprzedniej pracy oryginalnej: dermatoskopu Dermlite DL5 umożliwiającego pracę w trybie PD oraz w trybie UVFD. Zdjęcia wykonywano telefonem iPhone 7 Plus, a następnie archiwizowano i analizowano. Obecność poszczególnych struktur w trybie PD oceniano według uznanych kryteriów dermatoonkologicznych. W trybie UVFD oceniano obecność struktur zdefiniowanych w Publikacji nr 4. Analizę statystyczną przeprowadzono analogicznie jak w Publikacji nr 4, z wykorzystaniem oprogramowania SPSS. Zastosowano test dokładny Fishera ($p < 0,05$), a dane przedstawiono jako liczby i procenty (zmienne kategorialne) oraz średnie ± SD (zmienne ciągłe).

Badania zostały objęte zgodą Komisji Bioetycznej Okręgowej Izby Lekarskiej w Rzeszowie (Uchwała nr 50/2024/B).

Rozdział 7.

Wyniki

W ramach przeglądu systematycznego zidentyfikowano 848 publikacji w bazie PubMed. Po wstępnej selekcji do analizy włączono 292 artykuły. Spośród nich:

- 56 prac uwzględniono w części pierwszej, obejmującej ocenę dokładności diagnostycznej dermoskopii oraz opis cech dermoskopowych BCC,
- 107 publikacji uwzględniono w części drugiej, koncentrującej się na obrazie dermoskopowym BCC w zależności od podtypu zmiany, jej lokalizacji, wielkości, wieku wystąpienia i fototypu pacjenta,
- 129 artykułów włączono do części trzeciej, obejmującej zagadnienia związane z diagnostyką różnicową, monitorowaniem leczenia oraz wykorzystaniem nowoczesnych technologii obrazowania w ocenie BCC.

Publikacja 1: **Dermoscopy of Basal Cell Carcinoma Part 1: Dermoscopic Findings and Diagnostic Accuracy – A Systematic Literature Review**

Dokładność diagnostyczna

Analiza dostępnych publikacji wykazała, że dermoskopia cechuje się wysoką dokładnością diagnostyczną w rozpoznawaniu BCC, szczególnie w przypadku podtypów barwnikowych. W większości badań uzyskano wysokie wartości czułości i PPV, sięgające odpowiednio 95,4% i 97% [5,7]. Niższą swoistość notowano w analizach obejmujących wyłącznie zmiany amelanotyczne lub słabopigmentowane (np. 51,7%–69,5%), co tłumaczono większym ryzykiem błędnego rozpoznania [20].

Zaobserwowano, że czułość diagnostyczna wzrasta wraz z nabywaniem doświadczenia, osiągając stabilny poziom po około siedmiu miesiącach praktyki, co niestety może korelować ze spadkiem swoistości. Najczęściej BCC mylono z brodawką łojotokową lub znamieniem barwnikowym.

Niektóre prace sugerowały możliwość prognozowania wariantu histopatologicznego BCC z dokładnością do 93,3%, szczególnie w przypadkach podtypu guzkowego i powierzchownego [21]. Jednak wyniki te nie zostały jednoznacznie potwierdzone dla postaci agresywnych.

Dane wskazują również na wpływ lokalizacji zmiany – niższa czułość notowana była dla zmian zlokalizowanych na tułowiu i kończynach, co tłumaczono mniejszą częstością występowania barwnika i przewagą postaci powierzchownych.

Struktury dermoskopowe

W pracy przeglądowej podsumowano ponad 20 struktur dermoskopowych obserwowanych w BCC z uwzględnieniem ich definicji, mechanizmu powstania, korelacji z obrazem histopatologicznym oraz znaczenia w rozpoznawaniu BCC. Odnotowano, że istotną cechą złośliwych zmian skórnych – w tym BCC – są połyskujące białe linie widoczne w PD. Dodatkowo, niektóre struktury, jak liczne, zgrupowane, żółto-białe globule (ang. *multiple aggregated yellow-white globules,* MAY globules*)*, wykazują związek z bardziej agresywnymi podtypami BCC, wspierając ocenę ryzyka nawrotu i progresji.

Publikacja 2: **Dermoscopy of Basal Cell Carcinoma Part 2: Dermoscopic Findings by Lesion Subtype, Location, Age of Onset, Size and Patient Phototype**

Podtyp

W dostępnej literaturze znaleziono dane na temat opisów dermoskopowych 17 podtypów BCC, jednak żaden pojedynczy wzorzec dermoskopowy nie pozwala na jednoznaczną identyfikację konkretnego wariantu histologicznego. Pewne kombinacje struktur mogą jednak sugerować przynależność do określonego podtypu. Na przykład obecność naczyń rozgałęziających się drzewkowato, przejrzystości i owalnych niebiesko-szarych gniazd przemawia za podtypem guzkowym, natomiast krótkie teleangiektazje, liczne nadżerki, struktury przypominające liście klonu, koła ze szprychami oraz lśniące czerwono-białe obszary częściej obserwowane są w podtypie powierzchownym.

Z praktycznego punktu widzenia ważniejsze od identyfikacji konkretnego podtypu jest rozróżnienie BCC niskiego i wysokiego ryzyka. Do podtypów wysokiego ryzyka – cechujących się większą złośliwością miejscową i skłonnością do nawrotów – zaliczamy BCC twardzinopodobny, mikroguzkowy, naciekający oraz BCC o cechach płaskonabłonkowych (ang. *basosquamous carcinoma*, BSC). Wysokie ryzyko należy podejrzewać w przypadku zmian niepigmentowanych, klinicznie białych, wykazujących naczynia rozgałęziające się drzewkowato lub kłębuszkowe, rozległe owrzodzenia (obejmujące >90% powierzchni zmiany), liczne niebiesko-szare globule, struktury koncentryczne oraz brak obszarów różowych lub owalnych niebiesko-szarych gniazd.

Lokalizacja

BCC najczęściej rozwija się w okolicy twarzy i szyi. W tych lokalizacjach typowy jest guzkowy podtyp choroby z obecnością naczyń rozgałęziających się drzewkowato w obrazie dermoskopowym. Na twarzy dominują zmiany niepigmentowane, które częściej wiążą się z naciekającym wzrostem i potencjalnie bardziej agresywnym podtypem histologicznym.

Na szczególną uwagę kliniczną zasługuje tzw. strefa H. W tej lokalizacji BCC ma większą skłonność do głębokiego naciekania i owrzodzeń. W strefie H częściej również występują bardziej agresywne warianty nowotworu, co przekłada się na podwyższone ryzyko nawrotów. W innych rejonach głowy i szyi, nienależących do strefy H, częściej występują w dermoskopii naczynia przecinkowate i kłębuszkowe niż klasyczne naczynia rozgałęziające się drzewkowato.

Około jedna piąta zmian BCC zlokalizowanych w obrębie głowy i szyi rozwija się na powiekach. Utrata rzęs (madaroza) w tej okolicy może być istotnym sygnałem sugerującym złośliwy proces nowotworowy.

Na tułowiu najczęściej spotykane są powierzchowne postacie BCC, które dermoskopowo wykazują struktury przypominające koła ze szprychami, drobne teleangiektazje oraz niewielkie nadżerki.

Rozpoznanie BCC na kończynach dolnych może być utrudnione – zmiany często cechują się polimorficznym wzorcem naczyniowym, obecnością lśniących białych struktur oraz

owrzodzeń, natomiast naczynia rozgałęziajace się drzewkowato są w tych rejonach obserwowane rzadko.

BCC może także występować w lokalizacjach nieeksponowanych na słońce, np. w okolicy sromu, gdzie obraz dermoskopowy jest zbliżony do klasycznego.

Wiek

U osób poniżej 50. roku życia BCC częściej były niepigmentowane, a typowym znaleziskiem były niebiesko-szare globule przy braku widocznych naczyń. U pacjentów starszych dominowały natomiast klasyczne cechy BCC, takie jak naczynia rozgałęziające się drzewkowato, owalne niebiesko-szare gniazda oraz owrzodzenia.

Wielkość

W przeglądzie systematycznym literatury wykazano, że wraz ze wzrostem średnicy nowotworu rośnie liczba widocznych struktur dermoskopowych typowych dla BCC, jednak nie pojawiają się nowe cechy, charakterystyczne wyłącznie dla większych zmian. Małe guzy częściej wykazywały obecność licznych niebiesko-szarych kropek i owalnych niebiesko-szarych gniazd. Z kolei większe zmiany częściej prezentowały naczynia rozgałęziające się drzewkowato, owrzodzenia oraz lśniące białe struktury, przy czym naczynia rozgałęziające się drzewkowato zwykle pojawiały się w guzach powyżej 6 mm. Różnice w definicjach małych i dużych BCC pomiędzy badaniami utrudniały bezpośrednie porównania, jednak niektóre cechy, takie jak obecność niebiesko-szarych struktur, mogą wspierać wczesne rozpoznanie nowotworu.

Fototyp skóry

W populacjach o ciemniejszych fototypach skóry (III–VI) BCC występuje rzadziej, co związane jest z ochronnymi właściwościami melaniny. Wraz ze wzrostem fototypu rośnie jednak częstość występowania barwnikowego wariantu BCC, sięgając 100% wśród osób czarnoskórych. U tych pacjentów najczęściej obserwowano dermoskopowo: niebiesko-szare kropki, owalne niebiesko-szare gniazda, struktury przypominające liście klonu,

niebiesko-biały welon, owrzodzenia, naczynia rozgałęziające się drzewkowato i krótkie teleangiektazje. Podtyp guzkowy dominował i był silnie związany z obecnością owrzodzeń, niebiesko-białego welonu i naczyń rozgałęziających się drzewkowato. W BCC powierzchownym częściej obserwowano struktury przypominające liście klonu, obszary czerwono-białe, małe nadżerki, a zwłaszcza koła ze szprychami. U osób czarnoskórych występowały również takie cechy dermoskopowe jak uwydatniona siatka barwnikowa oraz centralna hipopigmentacja, co może imitować włókniaka twardego. U osób z albinizmem BCC występował ponad dwukrotnie częściej niż rak kolczystokomórkowy (ang. *squamous cell carcinoma*, SCC), z typowymi cechami dermoskopowymi jak naczynia rozgałęziające się drzewkowato, owalne niebiesko-szare gniazda i struktury przypominające koła ze szprychami.

Publikacja 3: **Dermoscopy of Basal Cell Carcinoma Part 3: Differential Diagnosis, Treatment Monitoring and Novel Technologies**

Diagnostyka różnicowa

Przeprowadzona analiza wykazała, że dermoskopia jest cennym narzędziem w różnicowaniu BCC, zwłaszcza w przypadku wczesnych zmian i guzów w lokalizacjach o dużym znaczeniu estetycznym, jak twarz. Choć wiele schorzeń skóry ma charakterystyczny obraz dermoskopowy, niektóre — jak podrażniona brodawka łojotkowa czy atypowy włókniak twardy — mogą imitować BCC i sprawiać trudności diagnostyczne.

W przypadku rzadkich guzów (np. neurothekeoma, retikulohistiocytoma, nerwiaki, nowotwory przydatkowe) rozpoznanie opiera się na badaniu histopatologicznym, poprzedzonym podejrzeniem dermoskopowym. Bywa, że zmiana przypomina BCC w badaniu dermoskopowym, a po weryfikacji histopatologicznej rozpoznawana jest inna jednostka, np. chłoniak skóry czy przerzut raka piersi.

Dla zwiększenia trafności diagnostycznej zaleca się łączenie dermoskopii z innymi nieinwazyjnymi technikami obrazowania, takimi jak refleksyjna mikroskopia konfokalna

(ang. *reflectance confocal microscopy*, RCM) czy optyczna koherentna tomografia (ang. *optical coherence tomography*, OCT), co pozwala ograniczyć niepotrzebne biopsje.

Wyznaczanie granic BCC

Dermoskopia odgrywa istotną rolę w wyznaczaniu granic BCC przed leczeniem chirurgicznym, w tym przed zabiegiem Mohsa oraz klasyczną chirurgią. Pomaga ograniczyć ryzyko dodatnich marginesów bocznych i zmniejsza liczbę etapów chirurgii Mohsa, co prowadzi do mniejszych ubytków. Ułatwia także wybór miejsca biopsji oraz planowanie radioterapii. W przypadku zmian zlokalizowanych na twarzy nie zaleca się opierać oceny marginesu jedynie na obecności naczyń rozgałęziających się drzewkowato, które mogą występować w tej lokalizacji fizjologicznie. Pomocna może się okazać tzw. *dermoskopia z naciąganiem skóry* (*stretching dermoscopy*). Technika ta poprawia widoczność opalizującego zabarwienia związanego ze zmianami stromalnymi charakterystycznymi dla BCC. Napięcie skóry powoduje zmniejszenie przepływu krwi w drobnych naczyniach otaczających guz, nie wpływając na większe naczynia rozgałęziające się drzewkowato będące częścią guza, dzięki czemu struktury te stają się łatwiejsze do rozróżnienia i umożliwiają dokładniejszą ocenę granic zmiany.

Monitorowanie leczenia

Dermoskopia jest cennym narzędziem w monitorowaniu leczenia BCC – pozwala ocenić skuteczność terapii, wykrywać resztkowe zmiany i wczesne nawroty. Jej zastosowanie udokumentowano w przypadku terapii imikwimodem, mebutynianem ingenolu, vismodegibem, w leczeniu skojarzonym fluorouracylem i kwasem salicylowym a także w terapii fotodynamicznej (ang. *photodynamic therapy*), radioterapii i brachyterapii. Niektóre cechy dermoskopowe mają wartość prognostyczną – np. nadżerki i owrzodzenia rokują dobrą odpowiedź na imikwimod, a struktury koncentryczne, przypominające liście klonu i koła ze szprychami wiążą się z gorszą odpowiedzią na PDT. Obserwacja zmian w obrazie dermoskopowym w trakcie leczenia pomaga ocenić skuteczność terapii i zidentyfikować zmiany wymagające dalszej kontroli.

Nowe technologie

W ostatnich latach obserwuje się dynamiczny rozwój nowych technologii uzupełniających klasyczną dermoskopię w ocenie BCC. Optyczna dermoskopia dużych powiększeń (ang. *optical super-high magnification dermoscopy*, OSHMD) pozwala dostrzec nowe, wcześniej nieopisywane cechy charakterystyczne dla powierzchownych BCC, szczególnie w przypadkach o skąpej pigmentacji lub całkowitym braku barwnika.

W histopatologii coraz większą rolę odgrywa dermoskopia ex vivo (ang. *ex vivo dermoscopy*, EVD), umożliwiająca precyzyjne oznaczenie obszarów podejrzanych i skrócenie czasu analizy mikroskopowej. Z kolei technika dermoskopii z zastosowaniem szerokiego pola widzenia (ang. *wide-area digital dermoscopy*, WADD) ułatwia ocenę większych guzów, choć jej zastosowanie wymaga dodatkowego sprzętu i więcej czasu.

Nowe technologie obrazowania, takie jak dermatofluoroskopia, multispektralna dermoskopia czy autofluorescencyjna dermoskopia multispektralna, wykazują potencjał w wykrywaniu i mapowaniu BCC, jednak ich kliniczna użyteczność wymaga dalszych badań.

Coraz większe znaczenie zyskuje sztuczna inteligencja (ang *artificial intelligence*, AI), która może wspierać ocenę obrazów dermoskopowych. Pełne wdrożenie tej technologii wymaga jednak rozwiązania problemów z jakością danych, standaryzacją oraz ochroną prywatności pacjentów.

W kręgu nowych, nieinwazyjnych metod diagnostycznych znajduje się również UVFD, jednak jak dotąd ta modyfikacja dermoskopii nie była wykorzystywana w ocenie BCC.

Publikacja 4

Praca oryginalna: **Application of Ultraviolet-Enhanced Fluorescence Dermoscopy in Basal Cell Carcinoma**

W badaniu przeanalizowano 163 przypadki BCC, potwierdzone histopatologicznie, u 52 pacjentów, z czego 55,8% stanowiły kobiety. Większość badanych charakteryzowała się jasnym fototypem skóry (I–II według Fitzpatricka). Najczęstszą lokalizacją zmian była twarz (50,9%), a następnie plecy (27,6%). Nie odnotowano przypadków BCC zlokalizowanych na kończynach dolnych. W badanej populacji dominował podtyp powierzchowny (55,8%) oraz bezbarwnikowy (55,2%). Średnia średnica guza w momencie rozpoznania wynosiła 8,1 ± 5 mm, a 38,6% zmian miało mniej niż 5 mm.

W ocenie dermoskopowej w trybie PD najczęściej obserwowano homogenne czerwono-białe obszary (51,5%), krótkie drobne teleangiektazje (48,5%), naczynia rozgałęziające się drzewkowato (30,7%), owrzodzenia (34,4%), białe bezstrukturalne obszary (31,3%), łuskę (28,8%) oraz niebiesko-szare globule (21,5%).

Natomiast w UVFD dominującymi cechami były: ciemna sylwetka guza (82,2%), zaburzenie wzorca ujść mieszków włosowych (31,9%), brak niebiesko-zielonej fluorescencji w obrębie guza (33,1%), obecność czarnych globul (29,4%), biało-niebieska łuska (28,8%), brak różowo-pomarańczowej fluorescencji w obrębie guza (26,4%) oraz wyraźnie granice zmiany (23,9%).

Analizując zależności pomiędzy cechami obserwowanymi w PD i UVFD wykazano m.in., że ciemna sylwetka guza w UVFD częściej współwystępowała z czerwono-białymi obszarami homogennymi oraz krótkimi teleangiektazjami widocznymi w PD. Obecność błękitnych włókien fluorescencyjnych w UVFD zawsze towarzyszyła owrzodzeniom zidentyfikowanym w PD, co może sugerować ich użyteczność jako wskaźnika obecności ubytku naskórka. Czarne globule obserwowane w UVFD silnie korelowały z pigmentowymi strukturami w PD. Ponadto, utrata fluorescencji mieszkowej oraz zaburzenie wzorca ujść mieszków włosowych w UVFD częściej występowały w guzach, które w PD wykazywały naczynia rozgałęziające się drzewkowato oraz dobrze odgraniczone brzegi.

Obraz UVFD analizowano również w zależności od lokalizacji, wielkości i podtypu klinicznego BCC wykazując istotne statystycznie różnice.
W przypadku małych guzów (<5 mm) częściej obserwowano zaburzony wzorzec ujść mieszków włosowych, brak różowo-pomarańczowej fluorescencji w obrębie guza oraz wyraźnie zaznaczone granice zmiany. Większe guzy częściej wykazywały obecność biało-niebieskiej łuski oraz nadżerek i owrzodzeń.
Odmiana guzkowa BCC częściej cechowała się brakiem fluorescencji mieszkowej, zarówno niebiesko-zielonej, jak i różowo-pomarańczowej. Większość zmian, które prezentowały nadżerki lub owrzodzenia, naczynia rozgałęziające się drzewkowato i zaburzony wzorzec ujść mieszków włosowych mieszków, była podtypem guzkowym BCC. Powierzchowne BCC istotnie częściej prezentowały ogniska białej depigmentacji. Barwnikowy wariant BCC charakteryzował się obecnością czarnych globul w UVFD, natomiast bezbarwnikowe guzy częściej wykazywały utratę fluorescencji mieszkowej, zaburzony wzorzec ujść mieszków włosowych i obecność naczyń rozgałęziających się drzewkowato.
Guzy zlokalizowane na twarzy częściej wykazywały wyraźne granice, zaburzony wzorzec ujść mieszków włosowych, utratę różowo-pomarańczowej fluorescencji oraz obecność nadżerek i owrzodzeń.

Szczegółowe wyniki pracy zaprezentowane są na stronach 103 - 112 niniejszej rozprawy doktorskiej.

Publikacja 5

Praca oryginalna: **Polarized Dermoscopy and Ultraviolet-Induced Fluorescence Dermoscopy of Basal Cell Carcinomas in the H- and Non-H-Zones of the Head and Neck**

Analizie poddano 151 przypadków BCC, potwierdzonych histopatologicznie, zlokalizowanych wyłącznie w obrębie głowy i szyi. Najczęstszym umiejscowieniem zmian była tzw. strefa H (61,6%), a zwłaszcza okolica nosa. Średni wiek pacjentów wynosił 69 ± 12 lat, a 65% badanych stanowili mężczyźni. Dominowały osoby z jasnymi fototypami skóry (I–II wg Fitzpatricka). Najczęściej rozpoznawanym podtypem

klinicznym był guzkowy BCC (59,6%), a aż 78,8% zmian miało charakter bezbarwnikowy. Średnica guza wynosiła średnio 8,1 ± 5 mm.

Wśród najczęściej obserwowanych w PD cech były: naczynia rozgałęziające się drzewkowato (55,6%), krótkie teleangiektazje (52,3%), czerwono-białe obszary homogenne (50,3%) oraz owrzodzenia (33,8%).

W trybie UVFD dominowały: ciemna sylwetka guza (78,8%), zaburzony wzorzec ujść mieszków włosowych (53%), brak niebiesko-zielonej (45%) i różowo-pomarańczowej fluorescencji w obrębie guza (39,1%), obecność biało-niebieskiej łuski (30,5%) oraz nadżerki i owrzodzenia (23,2%). Wyraźne granice guza były lepiej widoczne w UVFD w porównaniu do PD.
Zauważono różnice w częstości występowania ciemnej sylwetki guza, zaburzeń wzorca ujść mieszków włosowych oraz braku fluorescencji mieszkowej w zależności od lokalizacji. Przykładowo, zaburzenie wzorca ujść mieszków było najczęstsze w okolicy ust (75%) oraz nosa i okolicy nosowej (71,4%), co może wynikać z większej aktywności gruczołów łojowych i szerokich ujść mieszków w tych rejonach. Brak fluorescencji niebiesko-zielonej i różowo-pomarańczowej w obrębie guza również dominowały w wymienionych powyżej lokalizacjach oraz na szyi. Obecność nadżerek i owrzodzeń w UVFD była najczęściej widoczna na szyi, uszach i nosie.

W przypadku BCC zlokalizowanych w strefie H, w UVFD zaobserwowano istotnie statystycznie częstsze występowanie owrzodzeń, błękitnych włókien fluorescencyjnych oraz brak niebiesko-zielonej fluorescencji w obrębie guza.

Szczegółowe rezultaty badania zostały przedstawione na stronach 118 - 123 niniejszej rozprawy doktorskiej.

Rozdział 8.

Dyskusja

Wyniki uzyskane w ramach niniejszej rozprawy potwierdzają rosnącą rolę dermoskopii w diagnostyce BCC. Przeprowadzony przegląd systematyczny literatury stanowił podstawę do przeprowadzenia badań nad nowoczesną modyfikacją klasycznej dermoskopii, czyli UVFD, oraz pozwolił umieścić wyniki prac własnych w szerszym kontekście naukowym i praktycznym.

Obie oryginalne publikacje, stanowiące trzon rozprawy, dostarczają nowych danych dotyczących obserowanych struktur w UVFD w przypadku BCC.

W analizach własnych obserwowano częstsze występowanie podtypu guzkowego i bezbarwnikowego BCC na twarzy, zwłaszcza w strefie H. Jest to zgodne z wcześniejszymi doniesieniami literaturowymi, również sugerującymi bardziej agresywny charakter zmian w tej lokalizacji oraz wyższe ryzyko wznowy. W celu ograniczenia liczby niepotrzebnych biopsji w tym estetycznie wrażliwym rejonie, a także ułatwienia postawienia wstępnej diagnozy na możliwie wczesnym etapie, kiedy istnieje szansa na radykalne wycięcie zmiany z zachowaniem odpowiedniego marginesu tkanek zdrowych, niezbędne jest dalsze udoskonalanie nieinwazyjnych metod diagnostycznych. Wydaje się, że coraz więcej nowych, jeszcze nie w pełni zbadanych, możliwości może dawać szczególna modyfikacja klasycznej dermoskopii – UVFD.

W przeprowadzonych badaniach wykazano, że większość zmian BCC w UVFD prezentowała tzw. ciemną sylwetkę oraz zaburzenie wzorca ujść mieszków włosowych. Zaburzenie prawidłowej architektury ujść mieszków było szczególnie widoczne w przypadku zmian zlokalizowanych w obrębie głowy i szyi, co najprawdopodobniej wynika z większej aktywności gruczołów łojowych, a tym samym lepszej wizualizacji ujść mieszków w dermoskopii. W tych rejonach częściej obserwowano także brak fluorescencji mieszkowej, zarówno niebiesko-zielonej, jak i różowo-pomarańczowej, w obrębie obszaru guza. Jednocześnie, UVFD prawdopodobnie pozwala na uwidocznienie granic obszaru zajętego przez guz lepiej niż PD, zwłaszcza w obrębie głowy i szyi. Obserwacja ta wymaga jednak dalszej weryfikacji w kolejnych badaniach. Ponadto, wyniki prac własnych wykazały, że niektóre struktury widoczne w UVFD – jak błękitne

włókna fluorescencyjne czy czarne globule – korelują z dobrze znanymi cechami obserowanymi w PD, co może mieć praktyczne znaczenie diagnostyczne. Wykazano również, że obecność błękitnych włókien w UVFD, niewidocznych „gołym okiem" oraz w klasycznej dermoskopii, koreluje z występowaniem owrzodzeń / nadżerek w PD, co potwierdza ich wartość pomocniczą w lokalizacji ubytków naskórka.

Z praktycznego punktu widzenia, łączenie PD z nową techniką jaką jest UVFD potencjalnie może zwiększyć trafność diagnostyczną, ograniczyć konieczność biopsji oraz usprawnić planowanie leczenia chirurgicznego oraz radioterapii. Komplementarne stosowanie obu metod może stanowić nowy standard w ocenie BCC, szczególnie w lokalizacjach trudnych chirurgicznie lub estetycznie wrażliwych.

Mimo istotnych zalet, należy również mieć na uwadze ograniczenia UVFD. W prowdzonych badaniach zanotowowano, że struktury naczyniowe (naczynia linijne rozgałęzione, cienkie teleangiektazje), które stanowią ważną cechę dermoskopową BCC, były istotnie rzadziej widoczne w UVFD niż w PD. Również wykrywalność nadżerek i owrzodzeń była niższa w UVFD w porównaniu z PD. To wskazuje na konieczność traktowania UVFD jako techniki wspomagającej, uzupełniającej standardowe badanie dermoskopowe, a nie zastępującej je.

Pewnym ograniczeniem rozprawy jest fakt, że badania były prowadzone w pojedynczym ośrodku z dominującą populacją pacjentów o fototypie I i II. Uniemożliwia to uogólnienie wyników na inne populacje, zwłaszcza o wyższym fototypie skóry.

Zastosowanie nowatorskiej nieinwazyjnej techniki obrazowania BCC w projekcie – szczególnie w kontekście próby klasyfikacji obserwowanych zjawisk – stanowi istotny wkład do dalszego rozwoju tej techniki w praktyce klinicznej.

Rozdział 9.

Publikacje stanowiące rozprawę doktorską

cancers

MDPI

Review

Dermoscopy of Basal Cell Carcinoma Part 1: Dermoscopic Findings and Diagnostic Accuracy—A Systematic Literature Review

Irena Wojtowicz and Magdalena Żychowska *

Department of Dermatology, Faculty of Medicine, Medical College of Rzeszow University, 35-310 Rzeszow, Poland
* Correspondence: magda.zychowska@gmail.com

Simple Summary: Basal cell carcinoma (BCC) is the most common malignant skin tumor, which can cause significant tissue damage. BCC may present with a wide range of dermoscopic findings, including white, yellow, blue and pigmented structures, vascular structures (predominantly arborizing vessels or short fine teleangiectasias), multiple small erosions/ulcerations and/or features of regression. Dermoscopy improves the diagnostic accuracy of early BCC detection when compared with clinical examination alone. Diagnostic accuracy also increases with training and experience, which constitutes the premise for the need to expand dermoscopic knowledge.

Abstract: Introduction: Basal cell carcinoma (BCC) is the most common malignant skin tumor. While rarely fatal, it can cause local tissue damage. Part I of the review summarizes the dermoscopic features of BCC and the diagnostic accuracy of dermoscopy in the diagnosis of BCC. Methods: A search of the PubMed database was performed for studies reporting on the diagnostic accuracy of dermoscopy or dermoscopic findings in BCC, either pigmented or non-pigmented, located anywhere on the body, of any histopathologic subtype, size and at any age of onset. Results: BCC was found to present with a wide range of dermoscopic features, including white structures (shiny white lines, shiny white areas, rosettes), yellow structures (milia-like cysts, yellow lobular-like structures), multiple aggregated yellow-white globules (MAY globules), blue structures (blue ovoid nests), vascular structures (arborizing vessels, short fine telangiectasias), multiple small erosions/ulcerations, features of regression (pepper-like structures, white scar-like areas) and pigmented structures (spoke-wheel areas, maple leaf-like areas (MLLAs), blue/gray dots). Dermoscopy showed a sensitivity of 67.6–98.6% and a positive predictive value (PPV) of 85.9–97% in identifying BCC. The physician's experience and training improve the accuracy, however, BCCs on the trunk and extremities, particularly of superficial subtypes, may still constitute a challenge. Conclusions: Dermoscopy, especially when performed by a trained physician, increases the accuracy of early BCC detection.

Keywords: dermoscopy; dermatoscopy; basal cell carcinoma; polarized; non-polarized

Academic Editor: Alfonso Baldi

Received: 5 December 2024
Revised: 26 January 2025
Accepted: 27 January 2025
Published: 1 February 2025

Citation: Wojtowicz, I.; Żychowska, M. Dermoscopy of Basal Cell Carcinoma Part 1: Dermoscopic Findings and Diagnostic Accuracy—A Systematic Literature Review. *Cancers* **2025**, *17*, 493. https://doi.org/10.3390/cancers17030493

1. Introduction

Basal cell carcinoma (BCC) is the most common malignant skin tumor, accounting for 75–90% of skin cancers and occurring 18–20 times more often than melanoma. It is also the most prevalent malignant disease overall [1–3]. About one in five people will develop BCC at some point in life, with a higher incidence in men [4,5].

BCC grows slowly, usually less than 1 mm^2 per month, and while rarely fatal or metastatic, it can cause significant local tissue damage [6–8]. Dermoscopy is a noninvasive method that visualizes skin features from the surface to the papillary dermis and facilitates appropriate lesion management [1,9].

Part I of the systematic review summarizes the dermoscopic features of BCC and the diagnostic accuracy of dermoscopy in the diagnosis of BCC.

2. Methods

A search of the PubMed database was performed using the terms "(BCC OR basal cell carcinoma OR basalioma) AND (dermoscopy OR dermatoscopy)". All records from the establishment of the PubMed database through September 2024 were analyzed. Only English-language publications were included. Additionally, the reference lists of all the reports were checked for relevant articles. Two reviewers (I.W. and M.Ż.) initially checked the titles and abstracts of all of the records. If a title or abstract suggested the study might be relevant, the full article was reviewed. The criteria for including studies were: (1) Patients with histopathologically confirmed BCC who underwent a dermoscopic examination; (2) The studies reported on the diagnostic accuracy of dermoscopy, dermoscopic findings of BCC, both pigmented or non-pigmented, located anywhere on the body, of any histopathologic subtype, size and at any age of onset. Figure 1 shows the process of selecting articles based on the PRISMA (Preferred Reporting Items for Systematic Reviews and Meta-Analyses) guidelines.

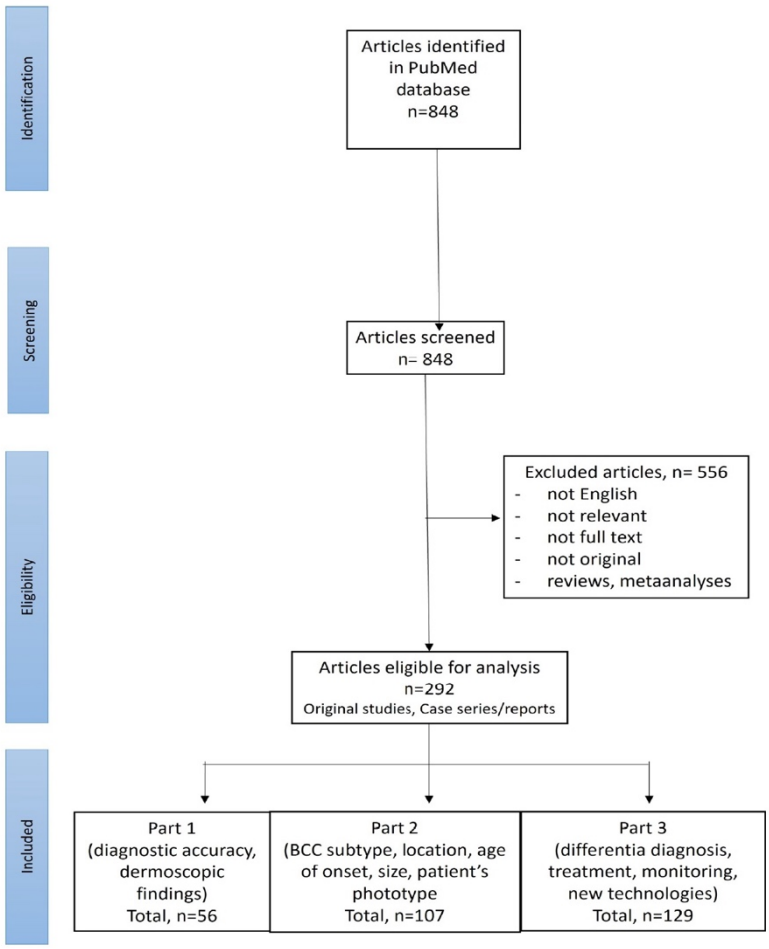

Figure 1. PRISMA flow chart showing the screening process (available also: Wojtowicz I et al. [10]).

3. Results

The literature search initially identified 848 studies. After screening abstracts, 292 articles were selected for further review. Of these, 56 articles reported on the diagnostic accuracy of dermoscopy or characterized dermoscopic features of BCC and were included in Part 1 of the review.

3.1. Diagnostic Accuracy of Dermoscopy

Several studies assessed the diagnostic accuracy of dermoscopy in BCC, with most being retrospective and conducted in Western countries. A large Swedish study analyzing 1180 histologically confirmed BCCs found that diagnosis with dermoscopic evaluation had a sensitivity of 95.4% and a positive predictive value (PPV) of 85.9% [11]. Similar results were reported by Altamura et al., with an even higher PPV of up to 96% [12]. Nelson et al. reported a sensitivity of 67.6% and a PPV of 97.0%, although the lower sensitivity was explained by the study's design, which assessed the decision to refer patients directly for definitive treatment without an incisional biopsy [13]. Dermoscopy was shown to have a specificity of 100%, sensitivity of 80%, PPV of 100% and a negative predictive value (NPV) of 94.12% for identifying malignant lesions [14].

Dermoscopic accuracy for BCC diagnosis was reported to be higher in case of pigmented lesions [1,6]. An analysis of 934 BCCs in a Japanese population, of which 96.4% were pigmented, showed that the diagnostic sensitivity and specificity were 92.2% and 96.0%, respectively [6]. Rosendahl et al. demonstrated a sensitivity of 98.6% for pigmented BCCs. The authors also found that adding dermoscopy to clinical examination improved diagnostic accuracy for pigmented lesions, but this improvement was statistically significant only for nonmelanocytic lesions [15].

In a multicenter prospective study on 740 BCCs, the sensitivity and specificity of dermoscopy were 93.2% and 51.7%, with a PPV of 84.4% and an NPV of 73.3%. The lower specificity was explained by the high number (87%) of hypopigmented/amelanotic lesions in the study group [1]. Low specificity (51.8% and 69.5% for two observers) was also shown by Guitera et al., who recruited to their study only amelanotic and light-colored lesions [16]. The study of 'pink' cutaneous lesions resulted in an overall BCC sensitivity of 85.1% and specificity of 92.4%, with a PPV of 89.8% [17].

Yuki et al. found that sensitivity was significantly lower for BCCs located on the trunk and extremities, attributing this to alower frequency of pigmentation and a higher proportion of superficial BCCs in those areas [6].

Another factor influencing diagnostic accuracy by dermoscopy was the doctor's experience. Nelson et al. showed that gaining expertise resulted in higher sensitivity at the cost of specificity in direct referral to surgery [12]. Yuki et al. also observed that sensitivity increased with experience, reaching a plateau after seven months [6]. The most common misdiagnosis for BCC was seborrheic keratosis, followed by melanocytic nevus [6].

Some studies suggested that dermoscopy can predict histopathologic subtypes with up to 93.3% accuracy, with the highest value for superficial and nodular variants [18–21]. However, others did not confirm these results, especially in cases of aggressive variants of BCC [13,22,23]. Popadić and Brasanac concluded that dermoscopy does not accurately reflect histopathologic findings in aggressive BCCs [19].

3.2. Dermoscopy Findings

A wide range of dermoscopic findings in BCC have been reported in the literature and, taking into account common features, they were divided into the following groups: white structures (shiny white lines, shiny white areas, rosettes), yellow structures (milia-like cysts, yellow lobular-like structures), MAY globules, blue structures (blue ovoid nests), vascular

structures (predominantly arborizing vessels or short fine teleangiectasias), multiple small erosions/ulcerations, features of regression ("blue areas", "blue hue", "pepper-like structures", "white scar-like areas", "white areas", "milky way areas") and pigmented structures (spoke-wheel areas, maple leaf-like areas–MLLAs, large blue-gray ovoid nests and less frequently multiple blue/gray globules, multiple in-focus blue/gray dots, blue-whitish veils, brown dots or globules, concentric structures, pigment networks). Several novel findings, such as negative maple leaf-like areas (NMLLAs), brown homogenous blotches, large blue-gray structureless areas, interrupted radial streaking, rainbow patterns and semitranslucent areas, are also discussed below.

3.2.1. White Structures

White structures observed in the dermoscopy of BCC include shiny white lines, shiny white areas (blotches) and rosettes. A key feature is that these structures are visible only under polarized light (contact or non-contact) and are not seen with non-polarized dermoscopy [24–28].

Shiny white lines, described as bright whitish lines, were initially referred to as 'chrysalis structures', though this term was considered a misnomer. The preferred term now is 'crystalline structures' or 'crystalline lines'. They include both short lines and longer strands [28]. Apart from BCCs, they can be observed in various malignant and benign lesions, including melanoma, squamous cell carcinoma (SCC), lichen planus-like keratosis (LPLK), Spitz nevi, scars, dermatofibromas, porokeratosis and even on extensively sun-damaged skin of the bald scalp [25–29].

In a prospective observational study analyzing 11,225 lesions, Balagula et al. found that only 1.8% of lesions presented shiny white lines. These lines were primarily seen in dermatofibromas (75.2%) and scars (90.5%), but also in BCC (47.6%) and invasive melanomas (84.6%), and rarely in nevi. The study demonstrated that these structures were 2.5 times more likely to be observed in malignant tumors compared to benign lesions [29]. In another study Shitara et al. concluded that the presence of shiny white lines is associated with a ten times higher risk of malignancy [25].

Navarrete-Dechent et al. found that shiny white strands and/or blotches (white clods or larger structureless areas) had a diagnostic specificity of 91% and should be considered a reliable criterion for detecting BCC, although the study's limitation was that it included only non-pigmented neoplasms [26]. Liebman et al. confirmed that the presence of these structures is suggestive of a BCC [28]. To date, no statistically significant difference in the prevalence of these structures across different histopathological subtypes of BCC has been reported [24–26]. However, shiny white strands are considered to be more frequently present in BCCs with ulceration [25].

According to Liebman et al., in BCC, larger whitish strands were observed more often than short lines (41% vs. 12%), and they were typically arranged in parallel or disorganized rather than orthogonally oriented (35.8% vs. 44.4% vs. 19.8%, respectively). In contrast, in melanomas, short shiny white lines were more frequently present and were typically arranged orthogonally, without accompanying shiny white areas [28].

Examples of BCCs displaying shiny white lines are shown in Figure 2, while those with shiny white blotches are illustrated in Figure 3.

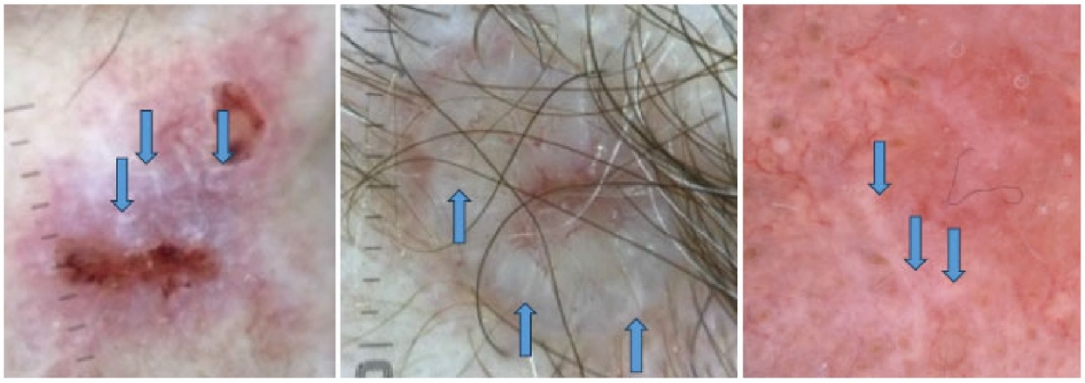

Figure 2. Dermoscopy images of basal cell carcinomas (BCCs) with shiny white lines (blue arrows).

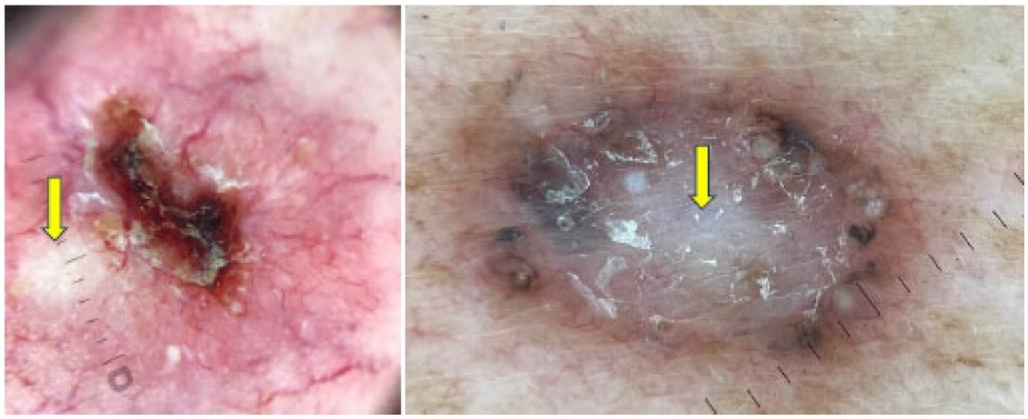

Figure 3. Dermoscopy images of BCCs with shiny white blotches (yellow arrows).

Rosettes, defined as four bright white points clustered together, are significantly more likely to be seen in actinic tumors than in other lesions [28]. Liebman et al. reported that 46.3% of actinic keratoses and 27% of SCCs showed rosettes [28]. Navarrete-Dechent et al. concluded that rosettes were not associated with a diagnosis of BCC [26].

A study from 1998 identified an additional whitish dermoscopic feature: a milky-red peripheral ring with intersecting blood vessels, referred to as "corona". This feature was found in nodular and infiltrative BCC, but rarely in the superficial subtype [9]. However, this finding has not been reported in more recent studies.

3.2.2. Yellow Structures

Yellowish structures observed in the dermoscopy of BCC include milia-like cysts (MLCs) and yellow lobular-like structures.

According to Bellucci et al., MLCs show starry and cloudy formations, which may also appear white in color. The starry formations are bright at the center with variably sharp borders, while the cloudy ones are larger, have fluffy borders and are approximately oval in shape. In an analysis of 400 BCCs, MLCs were present in 7.75% of cases [30]. MLCs are typically found in seborrheic keratoses (more often as cloudy MLCs) and congenital melanocytic nevi and were identified as useful features for differentiating benign lesions from melanoma [30]. They are more clearly visible under non-polarized dermoscopy [24]. Figure 4 shows examples of BCCs with MLCs.

Figure 4. Dermoscopy images of BCCs with milia-like cysts (MLCs) (green arrows).

Yellow lobular-like structures are round or oval in shape, vary in size and may be either isolated or clustered together. In the aforementioned study, they were noted in 4.2% of BCCs. Moreover, they have been thought to be characteristic for sebaceous hyperplasia, sebaceous adenoma and nevus sebaceous of Jadassohn [30]. Figure 5 illustrates BCCs with yellow lobular-like structures.

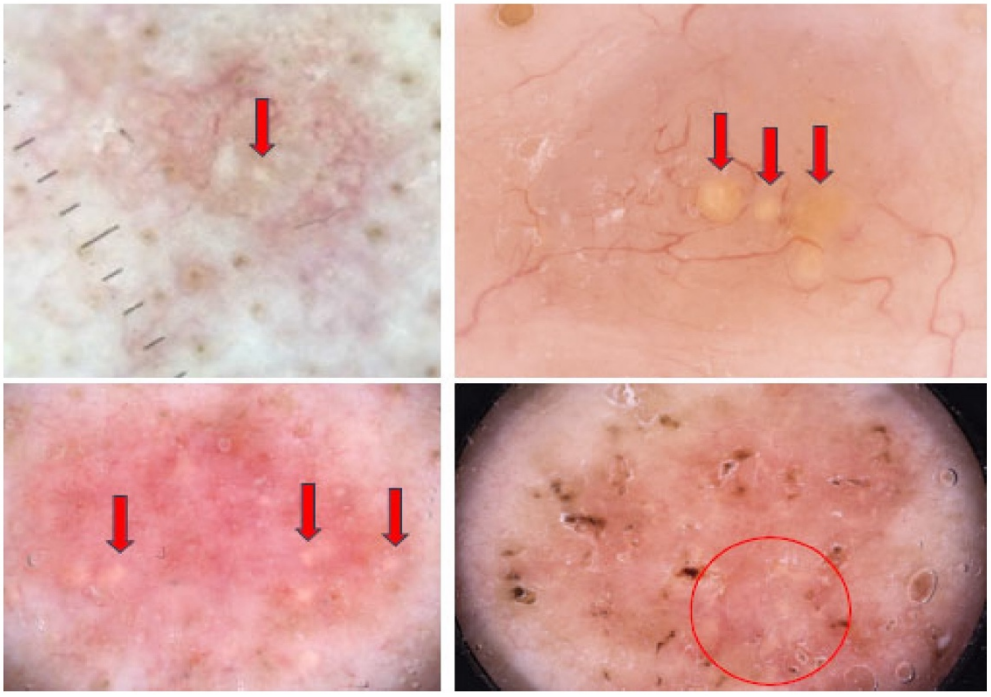

Figure 5. Dermoscopy images of BCCs with yellow lobular-like structures (red arrows and red circle).

Notably, the study found that both types of yellow structures were more frequently seen in BCCs located on the face and in nodular subtypes. The authors concluded that their presence should not rule out a BCC diagnosis when other specific dermoscopic criteria are present [30].

In 2021, Roda and Oliveira reported a case of a "half-yellow BCC". On histopathology, the yellow color corresponded to cholesterol clefts, which might have resulted from microtrauma or long-lasting disease [31].

3.2.3. MAY Globules

MAY globules, defined as clustered white-yellow structures (multiple aggregated yellow-white globules), are primarily associated with BCC. Some examples are present in Figure 6. These globules are visible under both polarized and non-polarized light [32,33].

In a case-control study on 656 non-pigmented lesions, MAY globules were found in 21.0% of BCCs, but were rare in other diagnoses (only 0.8% of cases), including SCC and desmoplastic trichoepithelioma. Among BCCs located on the head and neck, 38.7% exhibited MAY globules, compared to just 4.2% of lesions other than BCC. Their presence can be helpful in distinguishing BCC from intradermal nevi, effectively excluding the latter [34].

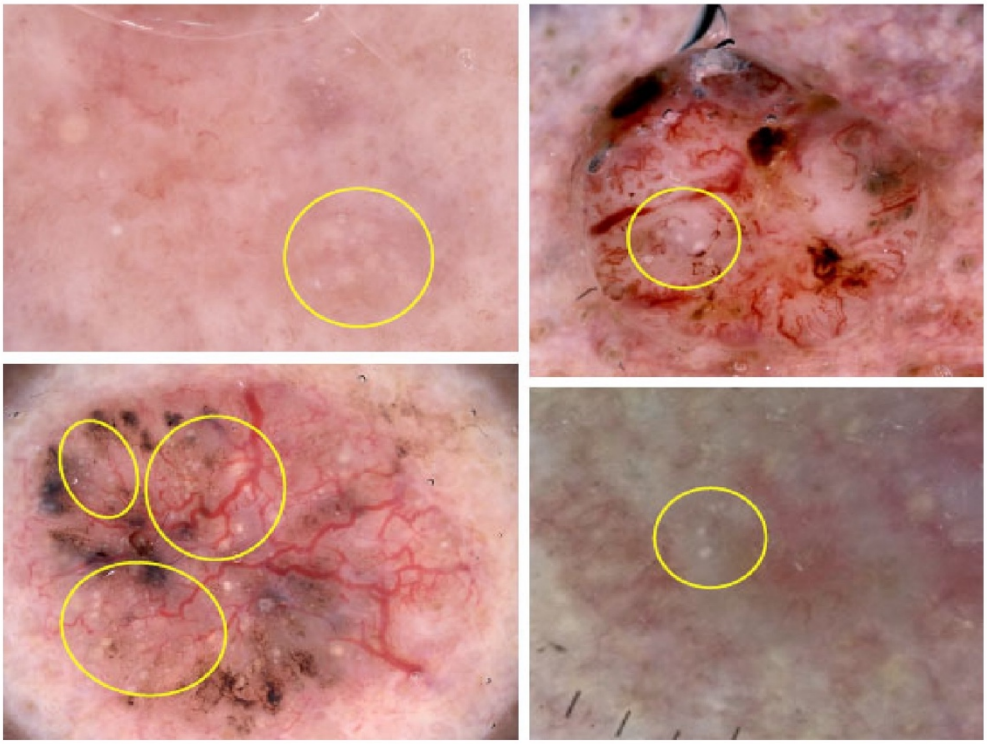

Figure 6. Dermoscopy images of BCCs with multiple aggregated yellow-white globules (MAY globules) (yellow circles).

In the aforementioned study, MAY globules were significantly associated with high-risk histologic subtypes of BCC, such as infiltrative and morpheaform types, where they were 6.5 times more likely to occur. Notably, they were not observed in any case of superficial BCC [32].

In several cases, MAY globules were linked with calcifications observed in histopathology, supporting earlier findings that calcifications are more common in high-risk subtypes [32]. Pagnoni et al. reported a case of calcifying micronodular BCC with MAY globules and concluded that calcifications, as well as micronodular histopathologic changes, were associated with aggressive subtypes of BCC [33].

3.2.4. Blue Structures

Under dermoscopy, a blue color has been a known indicator of malignancy. In 2017, Papadić et al. reported that nearly two-thirds of lesions with blue structures were likely to be malignant. In their analysis, BCCs constituted 21% of 144 pigmented lesions displaying a blue color under dermoscopy. The authors found the distribution of color to be crucial. Structureless peripheral or patchy blue color were most frequently observed in melanoma, while blue clods were more indicative of BCC. Among 28 lesions with blue clods, 17 (60.7%) were confirmed to be BCCs. These blue clods, metaphorically referred to as blue ovoid nests, were also observed in nevi (14.3%), seborrheic keratoses (7.14%) and angiomas (3.57%) [35].

3.2.5. Vascular Structures

Vascular structures are crucial in the diagnosis of BCC, particularly in non-pigmented lesions, where the lack of characteristic pigmented features makes diagnosis more challenging. According to Micantonio et al., nearly all BCCs (91.5%, 461 out of 504) presented with at least one vascular pattern [36]. Sakakibara et al. reported a slightly lower but still significant incidence of 87% in the BCCs diagnosed in Japanese population [34]. Vessels are more clearly visible in non-contact dermoscopy due to the absence of pressure applied to the surface, which occurs in contact dermoscopy [24].

The two most common vascular patterns in BCC are arborizing vessels and short fine telangiectasias [24,37–40]. Arborizing vessels, defined as large stem vessels ($\geq$0.2 mm) that branch irregularly in a tree-like pattern, were the most frequently observed in nodular and pigmented subtypes [36,40]. Gürsel et al. noted arborizing vessels as the most common BCC feature [38], with a sensitivity of 72% and specificity of 100% in the Japanese population [37]. Figure 7 presents dermoscopy images of these structures.

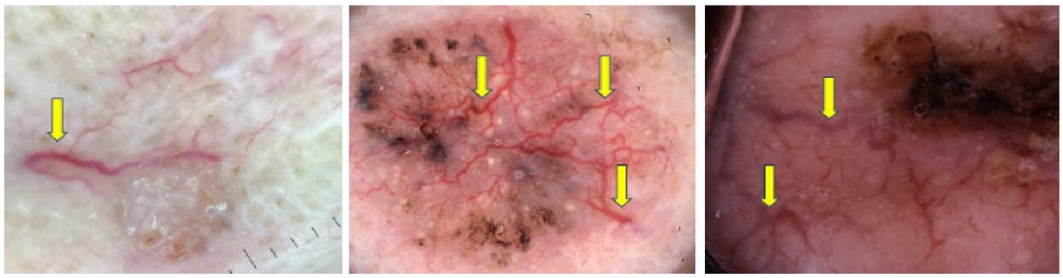

Figure 7. Dermoscopy images of BCCs with arborizing vessels (yellow arrows).

Short fine telangiectasias are defined as fine, kinked vessels of small caliber and length with few branches [36]. They are observed in 10% of BCCs and are considered an early form of arborizing vessels [12]. These vessels are typical of superficial BCC, particularly observed in the non-pigmented subtype [34,36]. Figure 8 shows some BCCs with short fine telangiectasias.

Figure 8. Dermoscopy images of BCCs with short fine telangiectasias (green arrows and circles).

Arpaia et al. analyzed the type and prevalence of vascular patterns in ulcerated and non-ulcerated portions of BCC. They found that dotted, linear-irregular, hairpin, comma and polymorphous patterns were highly represented in the ulcerated areas, while the arborizing vessels were prevalent in the non-ulcerated portion. Moreover, the correct diagnosis of BCC was statistically more likely when the ulcerated portion showed an arborizing pattern or when glomerular or hairpin patterns were absent. Additionally, the absence of dotted vessels in the non-ulcerated areas also increased the likelihood of an accurate diagnosis [34].

Additional vascular structures appear in less than 10% of BCCs and are almost always associated with arborizing vessels or short fine telangiectasias. These additional structures can include hairpin, glomerular, dotted, comma or polymorphous vessels, with decreasing incidence respectively. When a lesion contains two or more vascular patterns, it is referred to as polymorphous and needs further investigation to exclude amelanotic/hypomelanotic melanoma and SCC [36].

3.2.6. Multiple Small Erosions/Ulcerations

By definition, erosions are characterized by superficial tissue loss, whereas ulcerations involve deeper, full-thickness loss of the entire epidermis and superficial dermis [41,42]. The occurrence of multiple small erosions was reported to be the key dermoscopic feature that distinguished superficial BCC from other histopathological subtypes [43]. Figure 9 illustrates several BCCs with multiple small erosions/ulcerations.

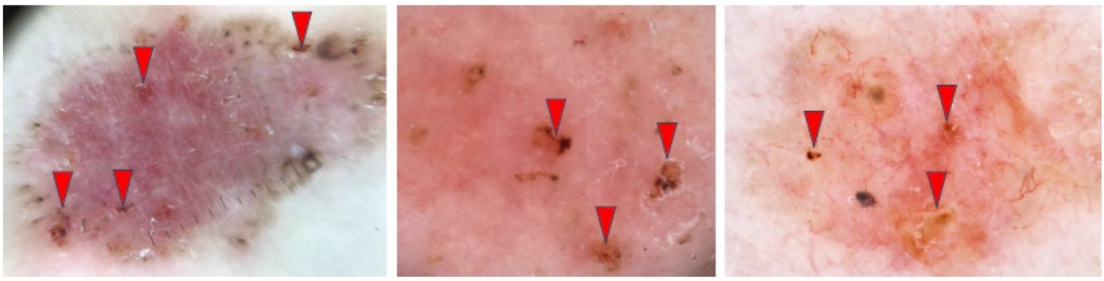

Figure 9. Dermoscopy images of BCCs with multiple small erosions/ulcerations (red arrowheads).

3.2.7. Features of Regression

In dermoscopy, features of regression may appear as bluish areas (due to the accumulation of melanin) or as white/reddish areas (indicating fibroplasia with the formation of blood vessels). The former, shown in Figure 10, are often referred to as "blue areas", "blue hue" or "pepper-like structures", while the latter, presented in Figure 11, are commonly called "white scar-like areas", "white areas" or "milky way areas". These features disrupt the overall dermoscopic presentation of the lesion, making the diagnosis more challenging. Features of regression are primarily considered to be a sign of melanoma. However, they may also be seen in many other lesions, including BCC, SCC, Bowen's disease, pigmented actinic keratoses and seborrheic keratoses. Therefore, regression should not be considered an independent indicator of melanoma but rather assessed in combination with other dermoscopic features [44].

Figure 10. Dermoscopy images of BCCs with bluish features of regression called "blue areas" or "blue hue" (yellow circles) and "pepper-like structures" (green circles).

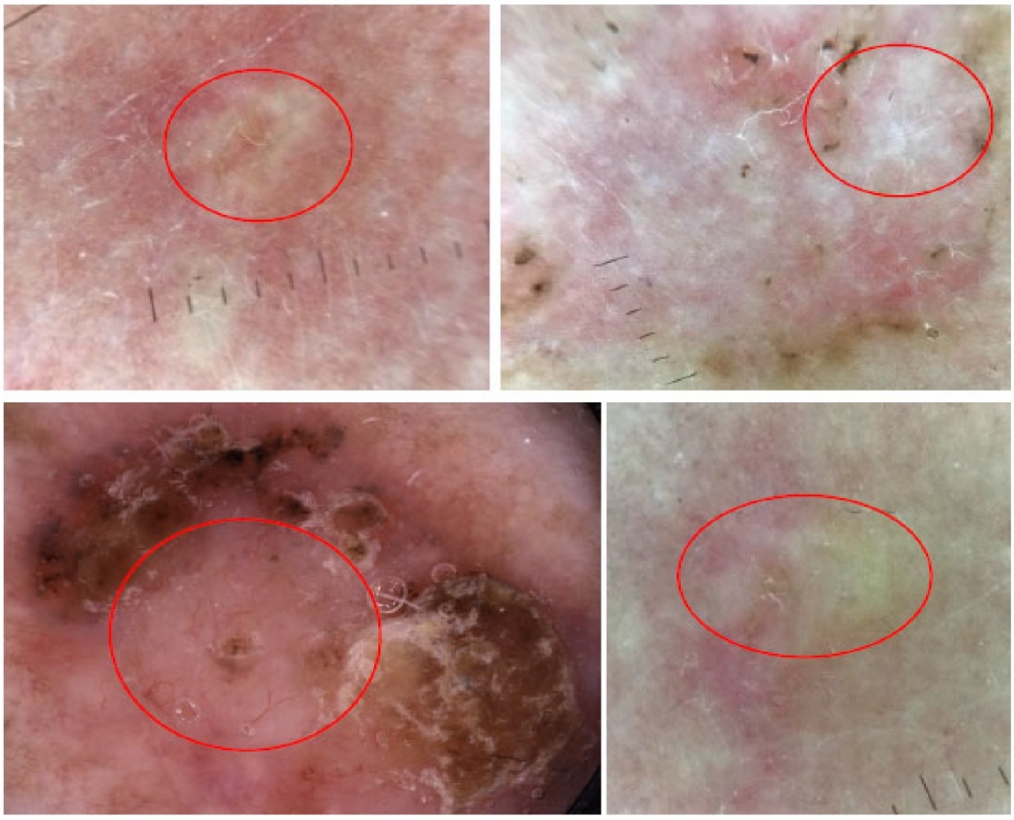

Figure 11. Dermoscopy images of BCCs with white/reddish features of regression called "white scar-like areas", "white areas" or "milky way areas" (red circles).

3.2.8. Pigmented Structures

Diagnostic criteria for pigmented BCC were presented by Menzies et al. in 2000. They included an absence of pigment network and the presence of one or more of the following six features: spoke-wheel areas, MLLAs, large gray-blue ovoid nests, multiple gray-blue globules, ulceration and arborizing vessels [3,7,12,45]. The method was demonstrated to have a sensitivity of 97% for diagnosing pigmented BCCs, and a specificity of 93% for invasive melanoma and 92% for benign pigmented skin lesions [45].

Peris et al. assessed the interobserver agreement, with five observers with varying levels of dermoscopy experience, of each dermoscopic feature proposed by Menzies. Full agreement was reached for the absence of a pigment network. Spoke-wheel areas and arborizing vessels showed very good agreement, while ulceration and multiple blue-gray globules had good agreement. However, there was no agreement on the definitions of MLLAs and large blue-gray ovoid nests, as these structures were often confused with each other; ovoid nests may be misinterpreted as globules or MLLAs and the latter as ovoid nests or localized pigmentation [46].

The pigment network is the most characteristic feature of melanocytic lesions and generally should not be found in BCC. However, in a study analyzing 412 BCCs, pigment network or network-like structures were observed in 3.4% of BCCs. In 64.3% of these cases, the presence of the pigment network was due to the collision of BCC with another skin neoplasm, such as solar lentigo, nevus or actinic keratosis. Such findings may result from the lesion's location on photodamaged skin and, most importantly, should always be carefully distinguished from atypical or malignant melanocytic lesions [7,47,48].

Spoke-wheel areas are well-circumscribed radial projections, typically brown but occasionally blue or gray, converging at a central axis that is often darker in color (e.g.,

dark brown, black or blue), as illustrated in Figure 12 [45]. They are considered to be highly specific indicator of pigmented BCC, with specificity reaching 100% in some studies [42,46,49,50]. Longo et al. demonstrated that the presence of spoke-wheel or concentric structures was the most significant factor in predicting a BCC diagnosis [1]. In a study analyzing BCC thickness, spoke-wheel areas were more limited in thicker tumors, while they covered wider areas in thinner tumors [4].

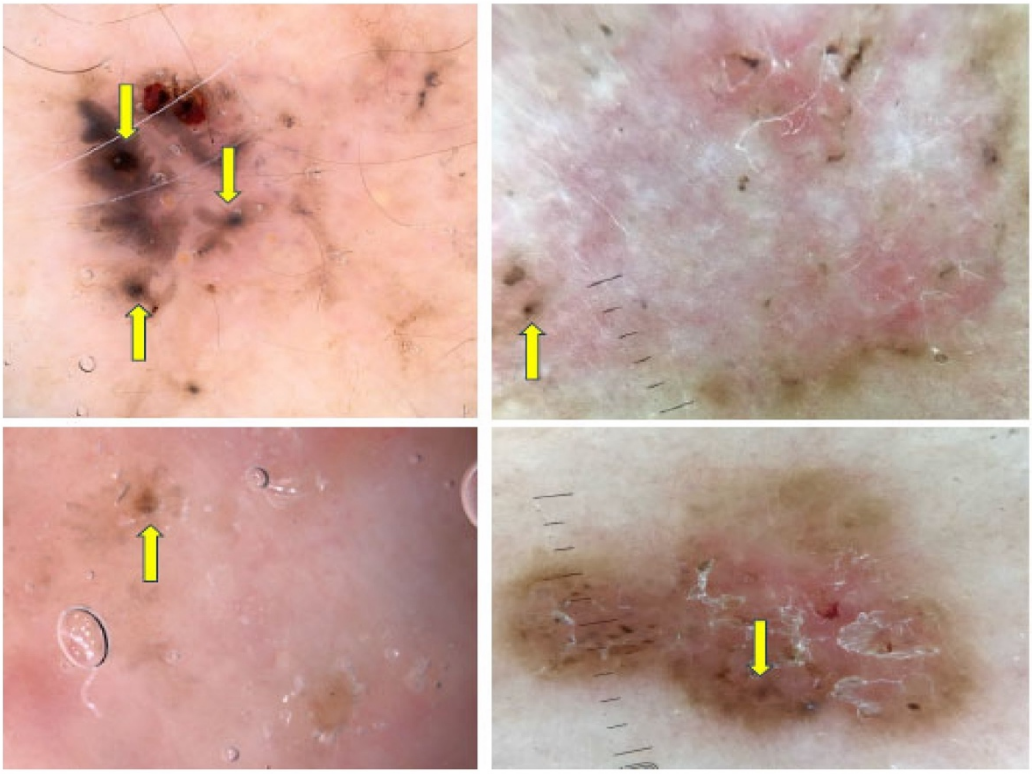

Figure 12. Dermoscopy images of BCCs with spoke-wheel areas (yellow arrows).

MLLAs are brown to gray-blue bulbous extensions that create a leaf-like pattern. Some examples are shown in Figure 13. Unlike pseudopods, these areas are distinct pigmented nests (islands) that do not arise from a pigment network and generally do not arise from an adjacent confluent pigmented area [45]. MLLAs were more frequently observed in younger individuals compared to other BCC features and were more commonly found in lesions with smaller diameters, suggesting that they may be an early sign of pigmented BCC [51].

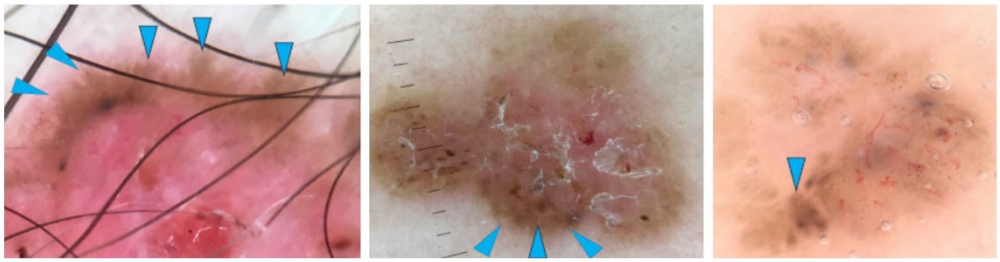

Figure 13. Dermoscopy images of BCCs with maple leaf-like areas—MLLAs (blue arrowheads).

Large blue-gray ovoid nests are well-defined pigmented areas (either ovoid or elongated) larger than globules that are confluent or nearly confluent and not directly connected to the main pigmented tumor body [45]. Figure 14 illustrates some of them. The pres-

ence of blue ovoid nests has been reported to be associated with increased BCC thickness, confirmed both by ultrasound and histopathology [4].

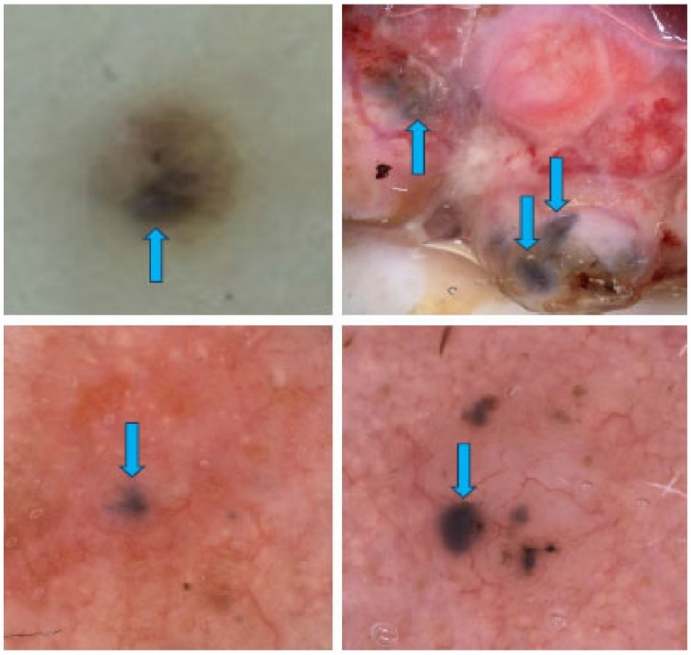

Figure 14. Dermoscopy images of BCCs with blue-gray ovoid nests (blue arrows).

In a study conducted by Tabanlıoğlu et al., 57.5% of pigmented BCCs presented with a blue-whitish veil, suggesting that this feature might play a more significant role in identifying pigmented BCC than previously thought, as this finding has traditionally been associated with melanoma [51,52]. A blue-whitish veil is better seen in non-polarized dermoscopy [11].

Brown dots or globules may occasionally be observed in BCC; however, they are typically seen in melanocytic lesions [53].

Concentric structures and multiple in-focus blue/gray dots were first reported by Altamura et al. and observed in 7.6% and 5.1% of the BCCs, respectively. The authors concluded that concentric structures represent the early stage of a spoke-wheel area, while multiple in-focus blue/gray dots indicate the early phase of multiple blue/gray globules [12]. Examples of BCCs with concentric structures, multiple blue-gray globules, and multiple in-focus blue-gray dots are presented in Figures 15, 16 and 17, respectively.

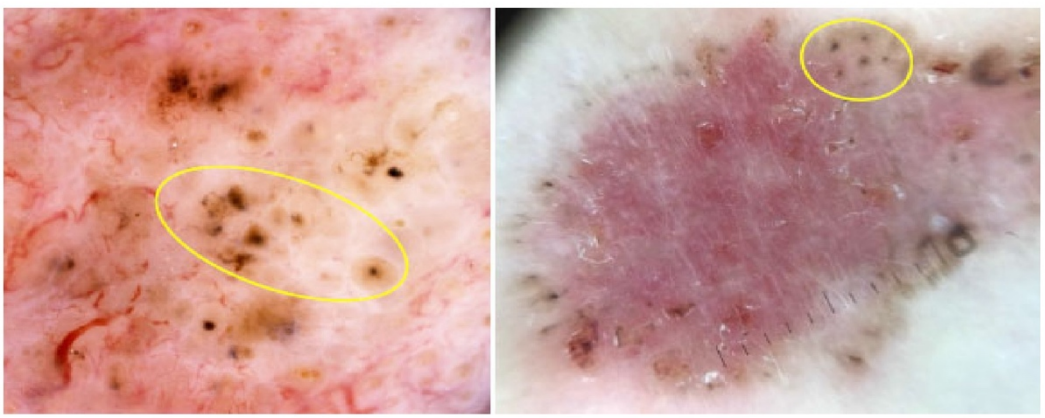

Figure 15. Dermoscopy images of BCCs with concentric structures (yellow circles).

Figure 16. Dermoscopy images of BCCs with multiple blue/gray globules (red circles).

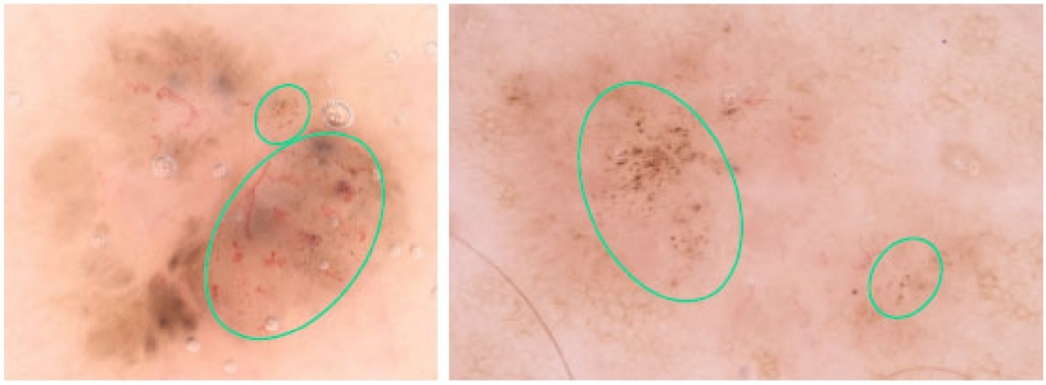

Figure 17. Dermoscopy images of BCCs with multiple in-focus blue/gray dots (green circles).

It is worth mentioning that the classic dermoscopic features of pigmented BCC (large blue/gray ovoid nests, multiple blue/gray globules and ulceration) can be disrupted by previous treatments with ablative lasers, which makes the diagnosis more challenging. Interestingly, arborizing vessels and certain nonclassical dermoscopic patterns (short fine superficial telangiectasia, multiple small erosions, concentric structures, multiple in-focus blue/gray dots) were found to be predominantly preserved after such procedures [54].

3.2.9. Novel Findings

Negative Maple Leaf-like Areas

NMLLAs, described in 2024 by Palmisano et al., are a non-pigmented version of the MLLAs initially characterized by Menzies et al. in 2000 [2,45]. They are characterized by round, non-pigmented bulbous structures with a homogeneous whitish background and well-defined borders. This newly described feature is associated with superficial BCC and reflects non-pigmented tumor nests at the dermal-epidermal junction [2].

Brown Homogeneous Blotches (BHB)

In 2023 Manca et al. reported presence of patches of uniform brown pigmentation without any other dermoscopic structures, except for occasionally present arborizing vessels or globules/dots, in 61 of 90 cases of pigmented BCC. Based on this, the authors introduced "brown homogeneous blotches" as a new dermoscopic finding in pigmented BCC. They demonstrated a sensitivity of 67.8% and a specificity of 93.3%. These values were comparable with those of well-known dermoscopic criteria of pigmented BCC. BHB showed an even higher sensitivity than some already established features, such as concentric structures (21.1%), spoke-wheel areas (6.7%) and MLLAs (32.2%) [3]. Figure 18 presents BCC with BHB.

Figure 18. Dermoscopy image of BCC with brown homogeneous blotches (BHB) (yellow circles).

Large Blue-Gray Structureless Areas

In a study from 2021 evaluating the relationship between BCC size and dermoscopic features, a high incidence (56%) of diffuse blue-gray patches was noted in large BCCs. The authors suggested that this finding results from the integration of large blue-gray ovoid nests and may serve as an important clue for identification of large BCCs [55]. An example of BCC with large blue-gray structureless areas is presented in Figure 19.

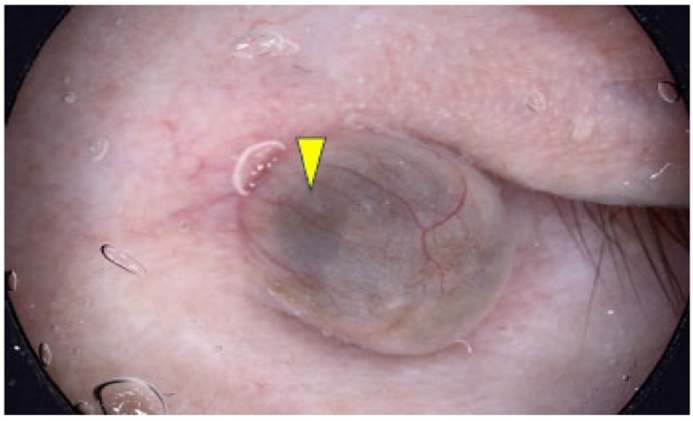

Figure 19. Dermoscopy image of BCC with large blue-gray structureless areas (yellow arrowhead).

Rainbow Pattern

In polarized dermoscopy, as mentioned by Garcia-Garcia and Perez-Oliva in 2010, BCC may present with various colors of the rainbow spectrum (ranging from red to violet). However, this multicolored pattern has been predominantly observed in Kaposi sarcoma, melanoma, stasis dermatitis and lichen planus [56].

Semitranslucent Areas

In 2009 Stoecker et al. observed multiple colors in BCC, ranging from reddish pink in thicker regions, dull orange at the periphery, to occasionally gray areas, which the authors termed semitranslucent areas. This phenomenon is best seen under non-contact polarized dermoscopy. While contact polarized imaging may reduce the typical color, it preserves the contrast in smoothness with the surrounding areas, which is key to this "jelly-like" phenomenon. This feature was found to correlate in histopathology with basaloid tumor nodules located near the surface, as well as with reduced epidermal thickness and a thinner collagen layer [57]. The BCC presenting this feature is shown in Figure 20.

Figure 20. Dermoscopy image of BCC with semitranslucent areas (red circle).

Interrupted Radial Streaking

In a single case reported by Bakos et al. in 2007, a patient with phototype IV presented with superficial pigmented BCC that exhibited numerous long and short pigmented streaks, ranging from brown to black. These streaks were arranged in an interrupted radial and centrifugal pattern, occasionally fusing together, creating an interrupted pigment network, which could easily be misdiagnosed as melanoma [47].

The summary of dermoscopic findings seen in BCC is presented in Table 1.

Table 1. A summary of dermoscopic findings in basal cell carcinoma (BCC).

Dermoscopy Finding	Definition	Mechanism of Formation and Corresponding Pathological Findings	Remarks
Shiny white lines (‘crystalline structures’ or ‘crystalline lines’)	Bright whitish lines visible only under polarized light; include short lines and longer strands; longer strands are typically arranged in parallel or disorganized; more frequently present in BCCs with ulceration	Interaction of polarized light with collagen orientation in the stromal tissue of tumor characterized by elevated amount of dermal collagen [25]	Higher risk of malignancy; reliable criterion for detecting BCC; other lesions include melanoma, SCC, dermatofibromas, scars, sun-damaged skin
Shiny white areas (blotches)	Large structureless white areas seen only under polarized light;	Interaction of polarized light with collagen orientation in the stromal tissue of tumor characterized by elevated amount of dermal collagen [25]	Reliable criterion for detecting BCC
Rosettes	Four bright white points seen only under polarized light	Optical phenomenon caused by the interaction of polarized light with keratin-filled adnexal openings [26]	Not typically associated with BCC, more common in AK and SCC
Milia-like cysts (MLCs)	Starry (bright center, variably sharp borders) or cloudy (larger, fluffy borders, oval in shape) yellow or white formations; more clearly visible under non-polarized dermoscopy	No correlation with pathology was found in the literature analyzed in the study	Not specific to BCC (typically in seborrheic keratosis and congenital melanocytic nevi); their presence should not rule out a BCC diagnosis when other specific dermoscopic criteria are present;

Table 1. *Cont.*

Dermoscopy Finding	Definition	Mechanism of Formation and Corresponding Pathological Findings	Remarks
Yellow lobular-like structures	Round or oval yellow structures	No correlation with pathology was found in the literature analyzed in the study	More common in BCCs on the face and nodular BCC; characteristic of sebaceous hyperplasia, sebaceous adenoma, nevus sebaceous of Jadassohn
MAY globules	Clustered white-yellow structures; visible under polarized and non-polarized light	Localized, circular regions of abnormal calcification within or surrounding tumor masses, accompanied by calcified keratocysts [32]	High-risk histologic subtypes of BCC (infiltrative, morpheaform, micronodular); helpful in distinguishing BCC from intradermal nevi, excluding the latter; present also in SCC or desmoplastic trichoepithelioma
Arborizing vessels	Large vessels branching in a tree-like pattern; more clearly visible in non-contact dermoscopy	Main vessels measuring ≥0.2 mm in diameter with irregular, tree-like branching [30]; Arborizing microvessels indicate telangiectasia smaller than 0.2 mm in diameter [42]	The most common BCC feature; associated with nodular, pigmented and non-ulcerated BCC; In non-BCC, the number of ramifications was lower than in BCC, and the diameter of vessels decreased more acutely from the stem vessel to the first branch
Short fine telangiectasias	Small kinked vessels of small caliber; an early form of arborizing vessels; more clearly visible in non-contact dermoscopy	Thin, twisted vessels of small diameter and short length, with minimal branching [36]	Associated with superficial and non-pigmented BCC
Multiple small erosions/ulcerations	Erosion—superficial tissue loss; ulceration—loss of the entire epidermis and superficial dermis	Erosion—superficial tissue loss; ulceration—loss of the entire epidermis and superficial dermis [41]	Multiple small erosions are characteristic for superficial BCC
Regression features ("blue areas", "blue hue", "pepper-like structures, "white scar-like areas", "white areas", "milky way areas")	Bluish or white/reddish areas indicating melanin accumulation (bluish) or fibroplasia with the formation of blood vessels (white/reddish)	"Blue areas", "blue hue" and "pepper-like structures" correspond to increased melanin deposition in the dermis. "White areas", "white scar-like areas" and the "milky way areas" indicate fibroplasia associated with blood vessel formation, leading to a whitish appearance with varying reddish shades [42]	Regression features disrupt the overall dermoscopic presentation of the lesion, making the diagnosis more challenging; should not be considered an independent indicator of melanoma
Pigment network	Intersecting brown lines creating a reticular pattern with hypopigmented holes	Melanin present within keratinocytes and/or melanocytes along the junction of the epidermis and dermis [42]	Proves against the diagnosis of BCC; mostly associated with the collision of BCC with another skin neoplasm (e.g., solar lentigo, nevus or actinic keratosis) or lesion's location on photodamaged skin

Table 1. *Cont.*

Dermoscopy Finding	Definition	Mechanism of Formation and Corresponding Pathological Findings	Remarks
Spoke-wheel areas	Radial brown, blue or gray projections converging at a central axis darker in color	Clusters of pigmented basaloid cells extending from the follicular epithelium [42]	The most significant factor in predicting pigmented BCC; most common in thinner tumors
Maple leaf-like areas (MLLAs)	Brown to gray-blue bulbous extensions; do not arise from a pigment network and an adjacent confluent pigmented area	Extensive, complex masses of pigmented basaloid cells located in the upper dermis [42]	May indicate early stage pigmented BCC
Large gray-blue ovoid nests	Large ovoid pigmented areas not directly connected to the main tumor body	Prominent clusters of pigmented basaloid cells within the dermis [42]	Associated with increased thickness of pigmented BCC; higher risk of malignancy; rarely observed also in nevi, seborrheic keratoses or angiomas
Multiple blue/gray globules	Multiple globules blue or gray in color	Compact clusters of pigmented basaloid cells found in the dermis [42]	Classic dermoscopic features of pigmented BCC
Multiple in-focus blue/gray dots	Foci of multiple blue/gray dots that appear "in focus" at dermoscopic examination	Smaller than in globules clusters of melanocytes or melanin granules in the papillary dermis [42]	Indicate the early phase of multiple blue/gray globules in pigmented BCC
Blue-whitish veil	Blue structureless zone; better seen in non-polarized dermoscopy	Brown pigment deposition in the dermis consisting of melanin-laden melanocytes and/or melanophages, with orthokeratosis, hypergranulosis and occasional parakeratosis above the pigment [51]	Traditionally associated with melanoma, however also frequently seen in pigmented BCC
Brown dots/globules	Dots or globules brown in color	Smaller clusters (dots) or larger clusters (globules) of melanocytes or melanin granules at the dermoepidermal junction [42]	Proves against the diagnosis of BCC (typical for melanocytic lesions)
Concentric structures	Irregularly shaped globular-like structures with different colors (blue, gray, brown, black) and darker central area	No correlation with pathology was found in the literature analyzed in the study	Represent the early stage of a spoke-wheel area in pigmented BCC
Negative maple leaf-like areas (NMLLAs)	Non-pigmented version of the MLLAs	Non-pigmented tumor clusters at the dermal-epidermal junction [2]	Superficial BCC
Brown homogeneous blotches	Patches of uniform brown pigmentation	The study reporting on BHB did not provide any correlation with pathology [3]	Pigmented BCC
Large blue-gray structureless areas	Diffuse blue-gray patches	The authors who first reported on this feature suggested that it results from the integration of large blue-gray ovoid nests; however, no correlation with pathology was assessed [55]	Important clue for identification of large BCC
Interrupted radial streaking	Brown or black streaks arranged in an interrupted radial and centrifugal pattern	Pigmented multicentric superficial BCC with melanophages present in the fibrotic upper dermis [47]	Can be confused with melanoma

Table 1. *Cont.*

Dermoscopy Finding	Definition	Mechanism of Formation and Corresponding Pathological Findings	Remarks
Rainbow pattern	Multicolored pattern seen under polarized dermoscopy	The study reporting on rainbow pattern did not provide any correlation with pathology [56]	Rare in BCC, more common in other entitites (e.g., Kaposi's sarcoma, melanoma, stasis dermatitis, lichen planus)
Semitranslucent areas	Jelly-like phenomenon with reddish pink or gray color, seen under non-contact polarized dermoscopy	Basaloid tumor nodules located near the surface, reduced epidermal thickness and a thinner collagen layer [57]	In BCC correlates with basaloid tumor nodules located near the surface, reduced epidermal thickness and a thinner collagen layer

4. Discussion

The current review highlights the high diagnostic accuracy of dermoscopy in identifying BCC when compared with clinical examination alone. Dermoscopy has proven especially valuable in distinguishing pigmented and non-pigmented variants of BCC. The studies show high sensitivity (ranging from 67.6% to 98.6%) and PPV (ranging from 85.9% to 97%) in the detection of BCC. The high specificity (up to 100% for malignant skin lesions in general) underscores dermoscopy's reliability as a diagnostic tool for skin malignancies.

However, some challenges remain. Diagnostic sensitivity appears to be lower for lesions located on the trunk and extremities, particularly those of a superficial subtype, which are often hypopigmented or amelanotic. This highlights the importance of considering lesion-specific characteristics in dermoscopic analysis. Studies also show that the experience and training of the physician significantly improve diagnostic accuracy.

In terms of dermoscopic features, BCC presents a wide range of patterns. Pigmented BCCs often show features like large gray-blue ovoid nests, multiple gray-blue globules and arborizing vessels, while non-pigmented BCCs typically display vascular patterns like arborizing vessels and fine telangiectasias. The presence of shiny white lines, seen with polarized light, is an important sign of malignant lesions, including BCC and melanoma. Additionally, structures like MAY globules have been linked to more aggressive BCC subtypes, helping with risk assessment.

The limitation of the current review is that the search was restricted to the PubMed database. Additionally, a limitation in the literature is the need for histopathological confirmation to accurately predict aggressive BCC subtypes. While some studies suggest dermoscopy can predict these subtypes with over 93% accuracy, particularly for superficial and nodular variants, aggressive BCC subtypes are harder to diagnose dermoscopically, perhaps because they invade deeper. Further research is needed to identify specific dermoscopic features that can reliably indicate these more challenging cases.

Some recently identified dermoscopic features, like NMLLAs, brown homogeneous blotches and large blue-gray structureless areas, show promise but need more validation. Although these features may improve diagnostic accuracy, their role in routine practice has yet to be clearly defined.

5. Conclusions

In summary, dermoscopy is a noninvasive, highly accurate method for diagnosing BCC, with distinct dermoscopic features that are associated with both pigmented and non-pigmented subtypes. While the accuracy of dermoscopy is particularly high for pigmented BCC, there are ongoing challenges with non-pigmented lesions. Future research

should focus on standardizing dermoscopic criteria for aggressive BCC variants and further exploring newer dermoscopic features. These efforts will enhance the effectiveness of dermoscopy in diagnosing BCC.

Author Contributions: I.W. and M.Ż.; methodology: I.W. and M.Ż.; manuscript—draft preparation: I.W.; manuscript—final version editing: I.W. and M.Ż. All named authors meet the International Committee of Medical Journal Editors (ICMJE) criteria for authorship for this article, take responsibility for the integrity of the work as a whole. All authors have read and agreed to the published version of the manuscript.

Funding: This research received no external funding.

Institutional Review Board Statement: This review is based on the analysis of data from literature. All sample dermoscopic images presented in the article were taken during routine patient care and come from the Department of Dermatology, University of Rzeszow. All patients gave consent for the examination and publication of the dermoscopic images.

Informed Consent Statement: Written informed consent was obtained from all patients involved in the study to publish this paper.

Data Availability Statement: No original datasets were generated for this article.

Conflicts of Interest: The authors declare no conflicts of interest.

References

1. Longo, C.; Guida, S.; Mirra, M.; Pampena, R.; Ciardo, S.; Bassoli, S.; Casari, A.; Rongioletti, F.; Spadafora, M.; Chester, J.; et al. Dermatoscopy and reflectance confocal microscopy for basal cell carcinoma diagnosis and diagnosis prediction score: A prospective and multicenter study on 1005 lesions. *J. Am. Acad. Dermatol.* **2024**, *90*, 994–1001. [CrossRef] [PubMed]
2. Palmisano, G.; Cano, C.O.; Fontaine, M.; Lenoir, C.; Cinotti, E.; Tognetti, L.; Rubegni, P.; Perez-Anker, J.; Puig, S.; Malvehy, J.; et al. Dermoscopic criteria explained by LC-OCT: Negative maple leaf-like areas. *J. Eur. Acad. Dermatol. Venereol.* **2024**, *38*, e271–e273. [CrossRef] [PubMed]
3. Manca, R.; Dattolo, A.; Valenzano, F.; Castriota, M.; Martella, A.; Galdo, G.; Argenziano, G.; Abeni, D.; Fania, L. Proposal of a new dermoscopic criterion for pigmented basal cell carcinoma: A multicentre retrospective study. *Dermatol. Rep.* **2023**, *16*, 9691. [CrossRef] [PubMed]
4. Coppola, R.; Barone, M.; Zanframundo, S.; Devirgiliis, V.; Roberti, V.; Perrella, E.; Donati, M.; Palese, E.; Tenna, S.; Persichetti, P.; et al. Basal cell carcinoma thickness evaluated by high-frequency ultrasounds and correlation with dermoscopic features. *Ital. J. Dermatol. Venerol.* **2021**, *156*, 610–615. [CrossRef] [PubMed]
5. Wang, W.; Chen, Y.; Wang, C.; Wang, J.; Chang, C. Dermoscopic features of pigmented basal cell carcinoma according to size. *Int. J. Dermatol.* **2024**, *63*, 916–921. [CrossRef]
6. Yuki, A.; Takatsuka, S.; Abe, R.; Takenouchi, T. Diagnostic accuracy of dermoscopy for 934 basal cell carcinomas: A single-center retrospective study. *J. Dermatol.* **2023**, *50*, 64–71. [CrossRef]
7. Rossiello, L.; Zalaudek, I.; Cabo, H.; Ferrara, G.; Gabriel, C.; Argenziano, G. Dermoscopic-pathologic correlation in an unusual case of pigmented basal cell carcinoma. *Dermatol. Surg.* **2006**, *32*, 1509–1512. [CrossRef]
8. Sykes, A.J.; Wlodek, C.; Trickey, A.; Clayton, G.L.; Oakley, A. Growth rate of clinically diagnosed superficial basal cell carcinoma and changes in dermoscopic features over time. *Australas. J. Dermatol.* **2020**, *61*, 330–336. [CrossRef]
9. Carroll, D.M.; Billingsley, E.M.; Helm, K.F. Diagnosing basal cell carcinoma by dermatoscopy. *J. Cutan. Med. Surg.* **1998**, *3*, 62–67. [CrossRef]
10. Wojtowicz, I.; Żychowska, M. Dermoscopy of Basal Cell Carcinoma Part 2: Dermoscopic Findings by Lesion Subtype, Location, Age of Onset, Size, and Patient Phototype. *Cancers* **2025**, *17*, 176. [CrossRef]
11. Ahnlide, I.; Bjellerup, M. Accuracy of clinical skin tumour diagnosis in a dermatological setting. *Acta Derm. Venereol.* **2013**, *93*, 305–308. [CrossRef]
12. Altamura, D.; Menzies, S.W.; Argenziano, G.; Zalaudek, I.; Soyer, H.P.; Sera, F.; Avramidis, M.; De Ambrosis, K.; Fargnoli, M.C.; Peris, K. Dermatoscopy of basal cell carcinoma: Morphologic variability of global and local features and accuracy of diagnosis. *J. Am. Acad. Dermatol.* **2010**, *62*, 67–75. [CrossRef] [PubMed]
13. Nelson, S.A.; Scope, A.; Rishpon, A.; Rabinovitz, H.S.; Oliviero, M.C.; Laman, S.D.; Cole, C.M.; Chang, Y.H.; Swanson, D.L. Accuracy and confidence in the clinical diagnosis of basal cell cancer using dermoscopy and reflex confocal microscopy. *Int. J. Dermatol.* **2016**, *55*, 1351–1356. [CrossRef]

14. Stoica, L.E.; Voiculescu, M.; Cirstea, C. Dermatoscopic and histopathological aspects of preneoplasia and skin cancers—Study on 74 patients. *Curr. Health Sci. J.* **2015**, *41*, 186–195. [CrossRef] [PubMed]
15. Rosendahl, C.; Tschandl, P.; Cameron, A.; Kittler, H. Diagnostic accuracy of dermatoscopy for melanocytic and nonmelanocytic pigmented lesions. *J. Am. Acad. Dermatol.* **2011**, *64*, 1068–1073. [CrossRef] [PubMed]
16. Guitera, P.; Menzies, S.; Argenziano, G.; Longo, C.; Losi, A.; Drummond, M.; Scolyer, R.; Pellacani, G. Dermoscopy and in vivo confocal microscopy are complementary techniques for the diagnosis of difficult amelanotic and light-colored skin lesions. *Br. J. Dermatol.* **2016**, *175*, 1311–1319. [CrossRef] [PubMed]
17. Witkowski, A.M.; Łudzik, J.; De Carvalho, N.; Ciardo, S.; Longo, C.; Di Nardo, A.; Pellacani, G. Non-invasive diagnosis of pink basal cell carcinoma: How much can we rely on dermoscopy and reflectance confocal microscopy? *Skin Res. Technol.* **2016**, *22*, 230–237. [CrossRef]
18. Longo, C.; Lallas, A.; Kyrgidis, A.; Rabinovitz, H.; Moscarella, E.; Ciardo, S.; Zalaudek, I.; Oliviero, M.; Losi, A.; Gonzalez, S.; et al. Classifying distinct basal cell carcinoma subtype by means of dermatoscopy and reflectance confocal microscopy. *J. Am. Acad. Dermatol.* **2014**, *71*, 716–724.e1. [CrossRef]
19. Popadić, M.; Brasanac, D. The use of dermoscopy in distinguishing the histopathological subtypes of basal cell carcinoma: A retrospective, morphological study. *Indian J. Dermatol. Venereol. Leprol.* **2022**, *88*, 598–607. [CrossRef]
20. Emiroglu, N.; Cengiz, F.P.; Kemeriz, F. The relation between dermoscopy and histopathology of basal cell carcinoma. *An. Bras. Dermatol.* **2015**, *90*, 351–356. [CrossRef]
21. Ahnlide, I.; Zalaudek, I.; Nilsson, F.; Bjellerup, M.; Nielsen, K. Preoperative prediction of histopathological outcome in basal cell carcinoma: Flat surface and multiple small erosions predict superficial basal cell carcinoma in lighter skin types. *Br. J. Dermatol.* **2016**, *175*, 751–761. [CrossRef] [PubMed]
22. Popadić, M. Dermoscopic features in different morphologic types of basal cell carcinoma. *Dermatol. Surg.* **2014**, *40*, 725–732. [PubMed]
23. Popadić, M. Dermoscopy of aggressive basal cell carcinomas. *Indian J. Dermatol. Venereol. Leprol.* **2015**, *81*, 608–610. [CrossRef] [PubMed]
24. Liebman, T.N.; Jaimes-Lopez, N.; Balagula, Y.; Rabinovitz, H.S.; Wang, S.Q.; Dusza, S.W.; Marghoob, A.A. Dermoscopic features of basal cell carcinomas: Differences in appearance under non-polarized and polarized light. *Dermatol. Surg.* **2012**, *38*, 392–399. [CrossRef]
25. Shitara, D.; Ishioka, P.; Alonso-Pinedo, Y.; Palacios-Bejarano, L.; Carrera, C.; Malvehy, J.; Puig, S. Shiny white streaks: A sign of malignancy at dermoscopy of pigmented skin lesions. *Acta Derm. Venereol.* **2014**, *94*, 132–137. [CrossRef]
26. Navarrete-Dechent, C.; Bajaj, S.; Marchetti, M.A.; Rabinovitz, H.; Dusza, S.W.; Marghoob, A.A. Association of shiny white blotches and strands with nonpigmented basal cell carcinoma: Evaluation of an additional dermoscopic diagnostic criterion. *JAMA Dermatol.* **2016**, *152*, 546–552. [CrossRef]
27. Salerni, G.; Alonso, C.; Bussy, R.F. Crystalline structures as the only dermoscopic clue for the diagnosis of basal cell carcinoma. *Arch. Dermatol.* **2012**, *148*, 776. [CrossRef]
28. Liebman, T.N.; Rabinovitz, H.S.; Dusza, S.W.; Marghoob, A.A. White shiny structures: Dermoscopic features revealed under polarized light. *J. Eur. Acad. Dermatol. Venereol.* **2012**, *26*, 1493–1497. [CrossRef]
29. Balagula, Y.; Braun, R.P.; Rabinovitz, H.S.; Dusza, S.W.; Scope, A.; Liebman, T.N.; Mordente, I.; Siamas, K.; Marghoob, A.A. The significance of crystalline/chrysalis structures in the diagnosis of melanocytic and nonmelanocytic lesions. *J. Am. Acad. Dermatol.* **2012**, *67*, 194.e1–194.e8. [CrossRef]
30. Bellucci, C.; Arginelli, F.; Bassoli, S.; Magnoni, C.; Seidenari, S. Dermoscopic yellow structures in basal cell carcinoma. *J. Eur. Acad. Dermatol. Venereol.* **2014**, *28*, 651–654. [CrossRef]
31. Roda, Â.; Oliveira, A. An unexpected shade of yellow. *Dermatol. Pract. Concept.* **2021**, *11*, e2021052. [CrossRef] [PubMed]
32. Navarrete-Dechent, C.; Liopyris, K.; Rishpon, A.; Marghoob, N.G.; Cordova, M.; Dusza, S.W.; Sahu, A.; Kose, K.; Oliviero, M.; Rabinovitz, H.; et al. Association of multiple aggregated yellow-white globules with nonpigmented basal cell carcinoma. *JAMA Dermatol.* **2020**, *156*, 882–890. [CrossRef] [PubMed]
33. Pagnoni, A.; Giroud, S.; Koulouri, A.; Hohl, D.; Gaide, O. White globules in basal cell carcinoma: A dermoscopic sign with preoperative implications. *Dermatol. Pract. Concept.* **2020**, *11*, e2021103. [CrossRef] [PubMed]
34. Arpaia, N.; Filoni, A.; Bonamonte, D.; Giudice, G.; Fanelli, M.; Vestita, M. Vascular patterns in cutaneous ulcerated basal cell carcinoma: A retrospective blinded study including dermoscopy. *Acta Derm. Venereol.* **2017**, *97*, 612–616. [CrossRef]
35. Popadić, M.; Sinz, C.; Kittler, H. The significance of blue color in dermatoscopy. *J. Dtsch. Dermatol. Ges.* **2017**, *15*, 302–307. [CrossRef]
36. Micantonio, T.; Gulia, A.; Altobelli, E.; Di Cesare, A.; Fidanza, R.; Riitano, A.; Fargnoli, M.C.; Peris, K. Vascular patterns in basal cell carcinoma. *J. Eur. Acad. Dermatol. Venereol.* **2011**, *25*, 358–361. [CrossRef]
37. Sakakibara, A.; Kamijima, M.; Shibata, S.; Yasue, S.; Kono, M.; Tomita, Y. Dermoscopic evaluation of vascular structures of various skin tumors in Japanese patients. *J. Dermatol.* **2010**, *37*, 316–322. [CrossRef]

38. Ürün, G.Y.; Fiçicioğlu, S.; Ürün, M.; Can, N. Clinical, dermoscopic and histopathological evaluation of basal cell carcinoma. *Dermatol. Pract. Concept.* **2023**, *13*, e2023004. [CrossRef]
39. Camela, E.; Ilut Anca, P.; Lallas, K.; Papageorgiou, C.; Manoli, S.M.; Gkentsidi, T.; Eftychidou, P.; Liopyris, K.; Sgouros, D.; Apalla, Z.; et al. Dermoscopic clues of histopathologically aggressive basal cell carcinoma subtypes. *Medicina* **2023**, *59*, 349. [CrossRef]
40. Trigoni, A.; Lazaridou, E.; Apalla, Z.; Vakirlis, E.; Chrysomallis, F.; Varytimiadis, D.; Ioannides, D. Dermoscopic features in the diagnosis of different types of basal cell carcinoma: A prospective analysis. *Hippokratia* **2012**, *16*, 29–34.
41. Scalvenzi, M.; Lembo, S.; Francia, M.G.; Balato, A. Dermoscopic patterns of superficial basal cell carcinoma. *Int. J. Dermatol.* **2008**, *47*, 1015–1018. [CrossRef] [PubMed]
42. Popadić, M. Statistical evaluation of dermoscopic features in basal cell carcinomas. *Dermatol. Surg.* **2014**, *40*, 718–724. [PubMed]
43. Namiki, T.; Nojima, K.; Hanafusa, T.; Miura, K.; Yokozeki, H. Superficial basal cell carcinoma: Dermoscopic and histopathological features of multiple small erosions. *Australas. J. Dermatol.* **2018**, *59*, 69–71. [CrossRef] [PubMed]
44. De Giorgi, V.; Massi, D.; Salvini, C.; Sestini, S.; Carli, P. Features of regression in dermoscopic diagnosis: A confounding factor? Two clinical, dermoscopic-pathologic case studies. *Dermatol. Surg.* **2006**, *32*, 282–286. [CrossRef] [PubMed]
45. Menzies, S.W.; Westerhoff, K.; Rabinovitz, H.; Kopf, A.W.; McCarthy, W.H.; Katz, B. Surface microscopy of pigmented basal cell carcinoma. *Arch. Dermatol.* **2000**, *136*, 1012–1016. [CrossRef]
46. Peris, K.; Altobelli, E.; Ferrari, A.; Fargnoli, M.C.; Piccolo, D.; Esposito, M.; Chimenti, S. Interobserver agreement on dermoscopic features of pigmented basal cell carcinoma. *Dermatol. Surg.* **2002**, *28*, 643–645. [CrossRef]
47. Bakos, R.M.; Bakos, L.; Cartell, A.; Manzoni, A.P.; Prati, C. Radial streaking: Unusual dermoscopic pattern in pigmented superficial basal cell carcinoma. *J. Eur. Acad. Dermatol. Venereol.* **2007**, *21*, 1263–1265. [CrossRef]
48. Gulia, A.; Altamura, D.; De Trane, S.; Micantonio, T.; Fargnoli, M.C.; Peris, K. Pigmented reticular structures in basal cell carcinoma and collision tumours. *Br. J. Dermatol.* **2010**, *162*, 442–444. [CrossRef]
49. Demirtaşoğlu, M.; Ilknur, T.; Lebe, B.; Kuşku, E.; Akarsu, S.; Ozkan, S. Evaluation of dermoscopic and histopathologic features and their correlations in pigmented basal cell carcinomas. *J. Eur. Acad. Dermatol. Venereol.* **2006**, *20*, 916–920. [CrossRef]
50. Wang, S.Q.; Katz, B.; Rabinovitz, H.; Kopf, A.W.; Oliviero, M. Lessons on dermoscopy #4. Poorly defined pigmented lesion. Diagnosis: Pigmented BCC. *Dermatol. Surg.* **2000**, *26*, 605–606. [CrossRef]
51. Tabanlıoğlu Onan, D.; Sahin, S.; Gököz, O.; Erkin, G.; Cakır, B.; Elçin, G.; Kayıkçıoğlu, A. Correlation between the dermatoscopic and histopathological features of pigmented basal cell carcinoma. *J. Eur. Acad. Dermatol. Venereol.* **2010**, *24*, 1317–1325. [CrossRef] [PubMed]
52. Felder, S.; Rabinovitz, H.; Oliviero, M.; Kopf, A. Dermoscopic pattern of pigmented basal cell carcinoma, blue-white variant. *Dermatol. Surg.* **2006**, *32*, 569–570. [CrossRef] [PubMed]
53. Ferrari, A.; De Angelis, L.; Peris, K. Unusual clinical and dermoscopic features in two cases of pigmented basal cell carcinoma. *J. Am. Acad. Dermatol.* **2005**, *53*, 1087–1089. [CrossRef] [PubMed]
54. Kim, W.J.; Song, M.; Kim, H.S.; Ko, H.C.; Kim, M.B.; Kim, B.S. History of laser ablation in pigmented basal cell carcinoma conceals classic dermoscopic patterns. *Dermatol. Surg.* **2014**, *40*, 733–738.
55. Xu, L.J.; Zheng, L.L.; Zhu, W. Effect of tumor size on dermoscopic features of pigmented basal cell carcinoma. *Chin. Med. J.* **2021**, *134*, 1866–1868. [CrossRef]
56. Garcia-Garcia, B.; Perez-Oliva, N. Dermoscopic rainbow pattern in basal cell carcinoma. *J. Eur. Acad. Dermatol. Venereol.* **2010**, *24*, 499–500. [CrossRef]
57. Stoecker, W.V.; Kolm, I.; Rabinovitz, H.S.; Oliviero, M.C.; Xu, J.; Malters, J.M. Semitranslucency in dermoscopic images of basal cell carcinoma. *Arch. Dermatol.* **2009**, *145*, 224. [CrossRef]

cancers

MDPI

Review

Dermoscopy of Basal Cell Carcinoma Part 2: Dermoscopic Findings by Lesion Subtype, Location, Age of Onset, Size and Patient Phototype

Irena Wojtowicz and Magdalena Żychowska *

Department of Dermatology, Institute of Medical Sciences, Medical College, Rzeszow University, 35-310 Rzeszow, Poland
* Correspondence: magda.zychowska@gmail.com

Simple Summary: Basal cell carcinoma (BCC) is the most common form of skin cancer with different levels of aggressiveness depending on the subtype. High-risk BCCs can be suspected when the correlation of certain vascular and structural features occurs, especially in areas like the nose, eyes and ears. On the other hand, pigmented features have been found to be more common in less aggressive subtypes. Dermoscopy, a non-invasive diagnostic tool, improves early detection of BCC and helps in determining the subtype. Nevertheless, dermoscopic challenges remain, particularly in the case of lesions located on the lower limbs.

Abstract: Introduction: Basal cell carcinoma (BCC) is the most prevalent type of skin cancer worldwide. Despite its low metastatic potential, certain subtypes present an aggressive clinical course. Part II focuses on the different dermoscopic patterns observed in BCC, depending on the lesion subtype, its location on the body, the patient's age, the size of the tumor, and skin phototype. **Methods**: A search of the PubMed database was conducted for studies reporting dermoscopic findings in BCC across all body locations, histopathologic subtypes, tumor sizes, ages of onset and skin phototypes. **Results:** There are no dermoscopic features indicative of a particular BCC subtype. However, arborizing, truncated or glomerular vessels, shiny white lines, ulceration, white areas, absence of pink zones and large blue-gray ovoid nests suggest high-risk BCCs (morpheaform, micronodular, infiltrative, basosquamous). Pigmented features can occur in all BCC types, though increased pigmentation indicates less aggressive subtypes (nodular, superficial, fibroepithelioma of Pinkus, adenoid). BCCs most commonly develop on the head, typically presenting as nodular and non-pigmented tumors. Those on the nose, eyes and ears may be more aggressive and prone to recurrence. On the trunk, BCCs are usually superficial and pigmented. Lower limb lesions often show polymorphous vessels rather than arborizing ones, which makes the dermoscopic diagnosis challenging. Dermoscopy aids early detection, with larger tumors exhibiting more established features but no size-specific patterns. Aggressive subtypes display similar dermoscopic findings regardless of size. **Conclusions:** Dermoscopy is a valuable tool for the early detection of BCC, though no specific dermoscopic features can definitively identify subtypes. High-risk BCCs can be suspected when distinct vascular and structural patterns are present, particularly in lesions located on the face, especially around the nose, eyes and ears, while pigmented features may indicate less aggressive subtypes.

Keywords: dermoscopy; dermatoscopy; basal cell carcinoma; BCC subtypes; nodular BCC; superficial BCC; high-risk BCC

Academic Editor: Alfonso Baldi

Received: 5 December 2024
Revised: 4 January 2025
Accepted: 7 January 2025
Published: 8 January 2025

Citation: Wojtowicz, I.; Żychowska, M. Dermoscopy of Basal Cell Carcinoma Part 2: Dermoscopic Findings by Lesion Subtype, Location, Age of Onset, Size and Patient Phototype. *Cancers* **2025**, *17*, 176. https://doi.org/10.3390/cancers17020176

1. Introduction

Basal cell carcinoma (BCC) is the most common skin cancer, with incidence rising globally [1–3]. Although typically slow-growing and rarely metastatic, certain subtypes are more aggressive, increasing the risk of recurrence and morbidity [4]. Early and precise diagnosis is crucial for effective management. Dermoscopy, a non-invasive tool, helps clinicians identify specific patterns and has been proven to play crucial role in the initial detection of BCC [1,4–6]. Part 2 of the review summarizes the prevalence of the dermoscopic findings in BCC with particular emphasis on variations depending on lesion subtype, location, age of onset, size and patient phototype.

2. Methods

A search of PubMed was performed for English-language publications using the following search term: "(BCC OR basal cell carcinoma OR basalioma) AND (dermoscopy OR dermatoscopy)". Records available from the inception of the PubMed database until September 2024 were screened. The references of the initially identified papers were also checked. Two reviewers (I.W. and M.Ż.) performed the screening of the abstracts and, if considered relevant, the full texts were subsequently reviewed. Only original studies or cases reporting dermoscopic features in histopathologically confirmed BCCs (located anywhere on the body, of any histopathologic subtype, size and at any age of onset) were included. Figure 1 illustrates the selection process of the articles according to the PRISMA (Preferred Reporting Items for Systematic Reviews and Meta-Analyses) standard.

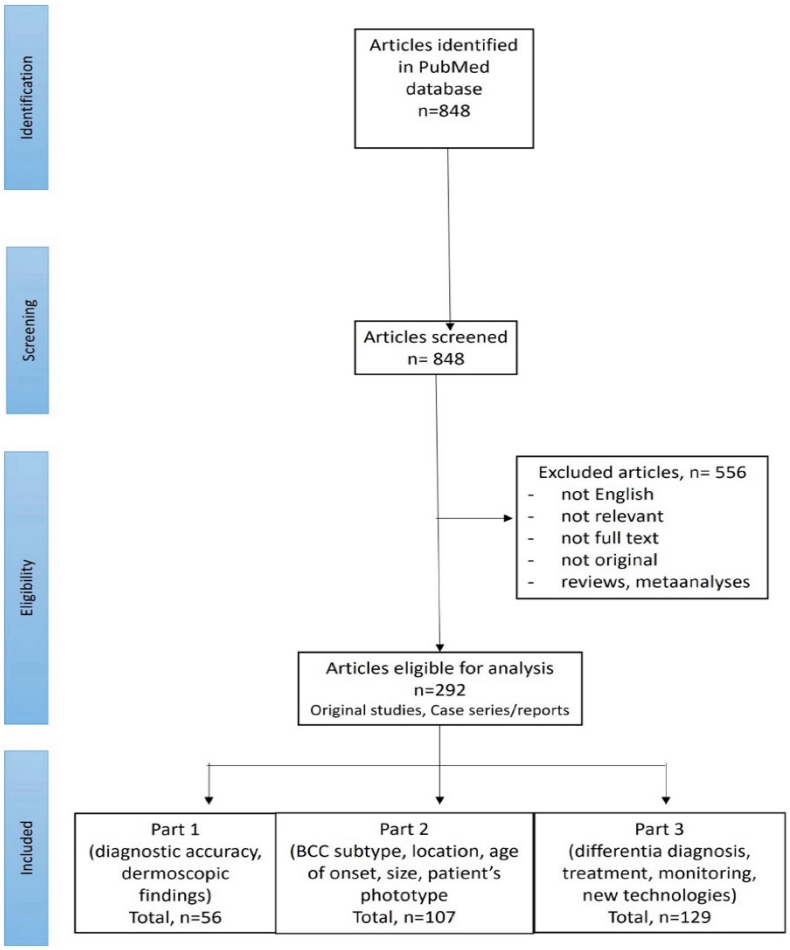

Figure 1. PRISMA flow chart illustrating the screening procedure.

3. Results

Out of 848 studies initially identified in the literature search, 292 were selected for further review. Of these, 107 articles discussed dermoscopic findings in BCCs depending on the lesion subtype, location, age of onset, size or patient phototype and are included in Part 2 of the review.

3.1. Dermoscopic Findings by BCC Subtype

The literature search revealed 52 studies that focused on the dermoscopic features of various BCC subtypes.

More than 26 different variants of BCC have been distinguished in the literature [7]. Some subtypes exhibit more aggressive behavior, with increased morbidity and recurrence risk. These "high-risk" or "aggressive" subtypes, comprising nearly 5% of all BCCs, include sclerodermiform (also known as morpheaform, morphoeic or sclerosing), micronodular, infiltrative, and basosquamous BCCs. In contrast, "low-risk" or "non-aggressive" subtypes include nodular, superficial, fibroepithelioma of Pinkus and adenoid BCCs [8–19].

No specific dermoscopic structures have been found to be indicative of a particular BCC subtype [9,11]. Furthermore, studies show that dermoscopic findings are rather correlated with tumor thickness than with subtype [9,13,20]. Negrutiu et al. reported that the depth of invasion index was directly related to the presence of arborizing vessels and ulceration, but negatively correlated with short, fine telangiectasias, maple-leaf-like areas and spoke-wheel areas [20].

Verduzco-Martínez et al. identified arborizing and truncated (short, linear path, diameter of 0.01–0.02 mm, abrupt interruption) vessels as highly specific for diagnosing high-risk BCCs. The authors also noted that ulceration should raise suspicion of an aggressive subtype [17]. Other studies confirmed that arborizing vessels should be considered the most significant feature indicative of aggressive BCCs [13,21]. Pyne et al. found that aggressive BCCs often lack pink areas or they constitute less than half of the tumor area [16]. Kim et al. created a "dermatoscopic index of BCC aggressiveness", assigning "+1" for multiple blue-gray globules, arborizing telangiectasia and concentric structures and "−1" for large blue-gray ovoid nests. A score over "+2" indicated aggressive BCCs [14].

3.1.1. Sclerodermiform BCC

Dermoscopic features of sclerodermiform BCC include arborizing vessels or microvessels on a milky red, pink-white or porcelain-white background, along with multiple erosions or ulcerations [9,10,15,18,22]. Arborizing vessels and ulcerations were found to be more common in the head and neck than on the body [22]. Diagnosis is often delayed due to the deep invasive nature of this variant. Typically, the tumor needs to reach a larger size before the arborizing microvessels can be seen under dermoscopy [23]. Ulcerations can form a ring, as noted by Inamura [24]. Sclerodermiform BCC typically has poorly defined margins and is non-pigmented [10,22].

3.1.2. Micronodular BCC

Under dermoscopy, the micronodular subtype of BCC was frequently pigmented with brown globules and blue globules/nests. Common dermoscopic findings also included short fine telangiectasias, arborizing vessels, milky red structureless areas, ulceration and white clods or milia-like cysts [10,11]. The micronodular subtype of BCC is presented in Figure 2.

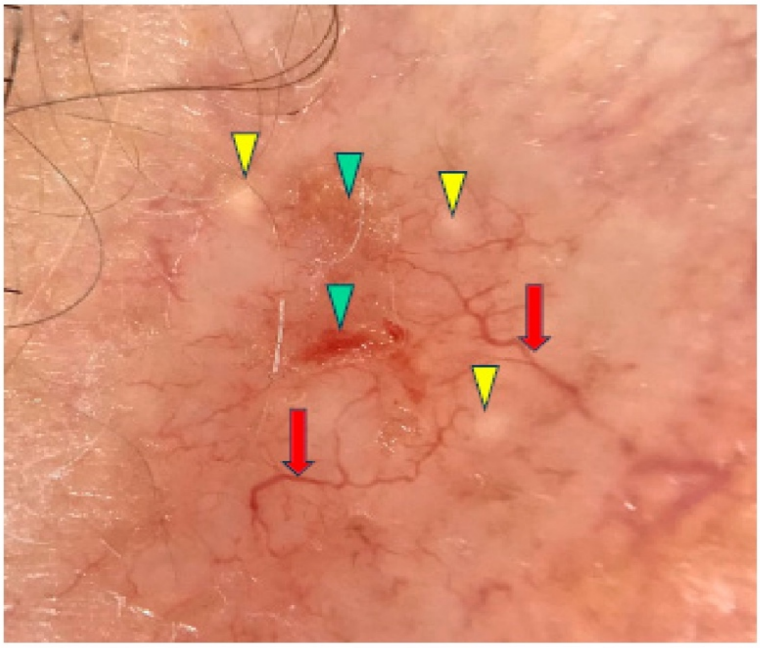

Figure 2. Dermoscopy image of micronodular BCC showing arborizing vessels (red arrows), erosions (green arrowheads), milia-like cyst (yellow arrowheads).

3.1.3. Infiltrative BCC

Infiltrative BCC (iBCC) is typically non-pigmented and presents under dermoscopy with arborizing telangiectasia, superficial fine telangiectasia, ulceration/multiple erosions, shiny white-red structureless background and white structureless areas [9–11,17,25,26]. Popadić et al. observed that dermoscopic features of iBCC correlated with tumor thickness; thicker areas showed multiple erosions and pigmentation, while thinner areas displayed white structureless zones [15]. Pyne et al. described a dermoscopic "stellate pattern" in iBCC, characterized by geometrical extensions from the tumor margin formed by vessels, surface folds or white linear structures. This feature showed a sensitivity of 31.7% and specificity of 94.1% [27]. "Halo phenomenon" was also reported in a single case of iBCC [28].

3.1.4. Basosquamous BCC

Basosquamous BCC (BSC) shows overlapping dermoscopic features of BCC and invasive SCC. Giacomel et al. suggested that BSC should be considered in the differential diagnosis when at least one dermoscopic finding of both BCC and SCC was present [29]. BCC-related features typically include polymorphous or monomorphous vasculature, while SCC-related findings are linked to keratinization [30]. Polymorphous vascular patterns in BSC consisted of combinations of branched, serpentine, straight, coiled or looped vessels, while monomorphous patterns showed unfocused arborizing vessels [29,30]. Keratinization signs included keratin masses, blood spots on keratin, superficial scales and white clods. Other common features were white structureless areas, shiny white-red background, ulceration and blue-grey blotches [29,30]. Akay et al. introduced two new dermoscopic criteria: "four dots in a square" (rosettes) to differentiate BSC from BCC, and "adherent fibers" (a sign of ulceration) to differentiate BSC from actinic keratosis [30].

3.1.5. Nodular BCC

Arborizing vessels are reported to be characteristic of nodular BCCs (nBCCs), though other vascular patterns like short fine telangiectasias, dots, coils and loops have also been observed [9,11,16,21,31–36]. However, one study contradicted these findings and reported

no differences in vascular patterns between sBCCs and nBCCs [32]. Translucency is the second most common feature of nBCCs [9,34,36]. Blue-gray ovoid nests are frequently present and, in the study by Popadić et al., were found to have the highest diagnostic accuracy for nBCCs [9,11,13,17,26,36,37]. Other pigmented structures such as blue-gray dots, blue-gray globules and structureless hyperpigmentation are also common [9,21,26,32,36]. Maple-leaf-like structures and spoke-wheel-like areas were identified by Enache et al. as some of the most common dermoscopic findings in pigmented nBCCs [36]. In addition, nBCCs often present with a shiny white-red structureless background or milky red background, though Popadić et al. stated that this finding lacked statistical significance for the nodular variant [9,11]. Among whitish structures, shiny white areas were frequently noted [11,32,36]. Whitish globules may indicate amyloid deposition, as suggested by Park et al. [38]. Interestingly, blue-white veil-like structures and the rainbow pattern were reported more frequently in nBCC than in sBCC [32]. Figure 3 shows examples of nBCCs.

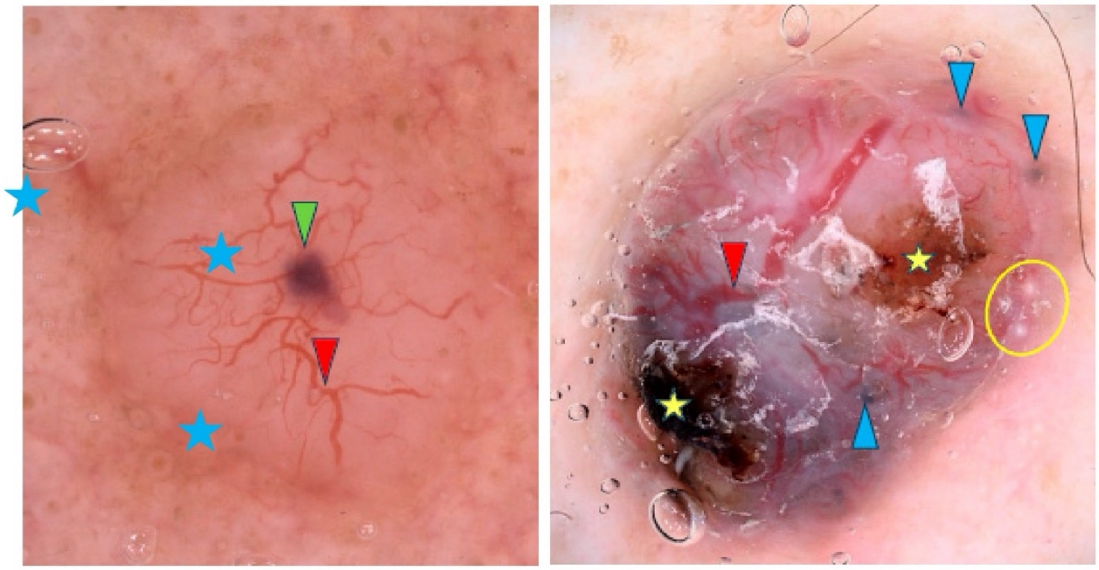

Figure 3. Dermoscopy images of nodular BCCs (nBCCs). The nBCC on the left shows arborizing vessels (red arrowhead), blue clod/ovoid nest (green arrowhead), milky way areas (blue asterisks). The nBCC on the right presents arborizing vessels (red arrowhead), multiple gray-blue globules (blue arrowheads), erosions (yellow asterisks), milia-like cyst (yellow circle).

3.1.6. Superficial BCC

Studies are in agreement that short fine teleangiectasias and multiple erosions are significantly associated with superficial BCC (sBCC) [9,11,13,20,25,26,32,33,39–45].

Some authors have also identified truncated vessels [17] and arborizing microvessels (diameter < 0.2 mm) as typical for this subtype, underlining that arborizing vessels have not been observed [16,21,34,45]. Shiny white to red areas [9,11,16,33–35,40,43–45], maple-leaf-like areas [9,20,21,25,26,32,37,40,45] and spoke-wheel areas [17,20,32,37,40,46] have also been found as highly specific for sBCC. Other dermoscopic findings frequently observed in sBCC included concentric structures [32], multiple blue-gray globules or dots and ovoid nests [21,26].

Lallas et al. found that the presence of maple-leaf-like areas and short fine superficial telangiectasias, in association with the absence of arborizing vessels, blue-gray ovoid nests and ulceration, was predictive of sBCC with a sensitivity of 81.9% and a specificity of 81.8% [45]. Some examples of sBCCs are shown in Figure 4.

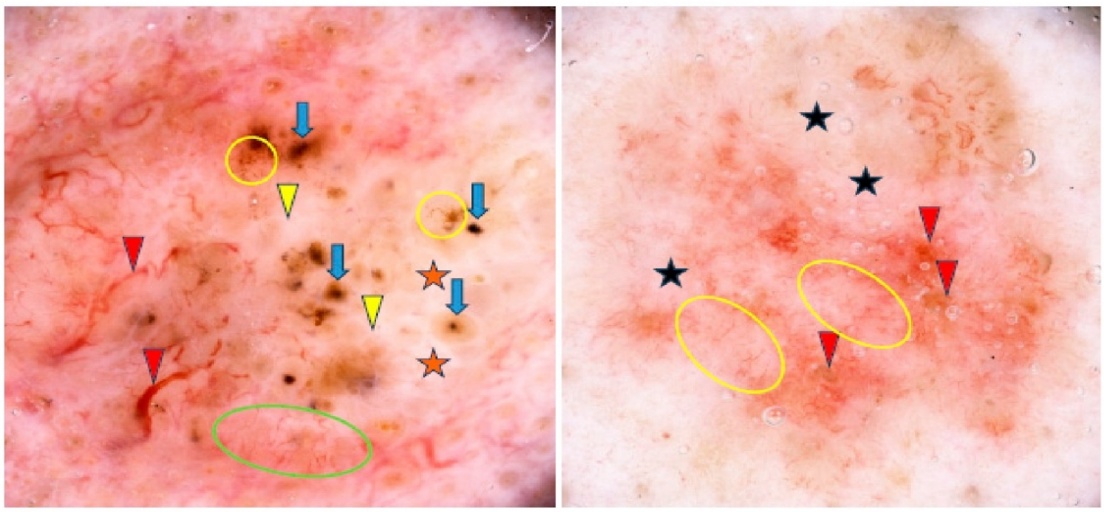

Figure 4. Dermoscopy images of superficial basal cell carcinomas (sBCCs). The sBCC on the left shows arborizing vessels (red arrowheads), shiny white areas/blotches (orange asterisks), concentric structures (blue arrows), short fine teleangiectasias (green circle), shiny white lines (yellow arrowheads), multiple in-focus blue/gray dots (yellow circles). The sBCC on the right presents short fine teleangiectasias (yellow circles), erosions (red arrowheads), milky way areas (black asterisks).

3.1.7. Fibroepithelioma of Pinkus

Seven articles reported the dermoscopic features of fibroepithelioma of Pinkus (FEP) and were included in the analysis [19,47–50]. In 2006, Zalaudek et al. analyzed 10 FEPs. All were clinically misdiagnosed as benign lesions but were correctly identified on dermoscopy in 90% of the cases. Key features included fine arborizing vessels, dotted vessels, white streaks and, additionally, gray-brown areas with gray-blue dots in pigmented FEPs (40% of cases). In 2020, Nanda et al. analyzed 48 FEPs, and, apart from serpentine, dotted, or polymorphous vessels and shiny white lines, identified a novel FEP feature—hypopigmented to pink lines intersecting at acute angles (HPLA). This structure has also been reported in hypopigmented melanoma and Spitz nevi [51]. In single case reports, negative network, comedo-like openings and novel findings, including negative maple-leaf-like areas and negative spoke-wheel areas, were reported [47,48,50].

3.1.8. Infundibulocystic BCC

Few cases of infundibulocystic BCC have been reported in the literature, most involving multiple lesions associated with genetic syndromes, with only one case documenting dermoscopic findings. The BCC presented with short fine telangiectasias, maple-leaf-like areas, multiple scattered blue-gray dots and globules, as well as white shiny streaks [52].

3.1.9. Cystic BCC

Cystic BCC is another rare variant of BCC, with only a few reports in the literature, out of which only two included descriptions of dermoscopic findings. Both cases showed arborizing telangiectasia, with one also displaying a homogeneous blue-black area. The blue-black area was suggested to correspond to the cystic regions of the tumor resulting from massive cell necrosis [53].

3.1.10. Blue-White BCC

In one study, the clinically blue-white variant of BCC (n = 32) was analyzed. The authors concluded that the blue color in dermoscopy may result from blue-gray globules, multiple blue-gray dots and/or blue-gray ovoid nests, along with a new dermoscopic

finding—homogeneous blue pigmentation, observed in 59% of cases. The homogenous blue pigmentation was suggested to correspond to a large ovoid nest. On the other hand, clinically present white color was linked to dermoscopic structureless white areas, shiny white structures and another novel feature—whitish septa, observed in 44% of BCCs. The blue-white BCCs also frequently presented with ulcerations and fine arborizing vessels [54].

3.1.11. Polypoid BCC

There have been few cases of polypoid BCC reported in the literature, with only three documenting dermoscopic findings. All cases showed arborizing vessels and two also revealed multiple blue-gray globules and ovoid nests [55–57].

3.1.12. Large Pore BCC

Lösch et al. described a case of BCC with a central dilated pore, surrounded by a poorly defined whitish-pink area and noticeable branched vessels on dermoscopy. Gray pigmentation and yellowish-white scales were also present around the pore [58].

3.1.13. Linear BCC

The three cases of linear BCCs reported by Alcántara-Reifs et al. were pigmented and showed maple-leaf-like areas and spoke-wheel structures on dermoscopy [59].

3.1.14. Keloidal BCC

A keloid-like portion of BCC displayed arborizing vessels on a pinkish-white background without pigmented components, as reported in one study [60].

3.1.15. BCC with Myoepithelial Differentiation

In BCC with myoepithelial differentiation, dermoscopy revealed irregular linear vessels and arborizing vessels on a whitish background with several dark brown areas [61].

3.1.16. Radiation-Induced BCC

BCCs developing in areas previously treated with radiotherapy showed a predominance of ovoid nests and arborizing vessels on a pink background [62].

3.1.17. Pigmented BCC

Pigmented BCC (pBCC) accounts for less than 10% of BCCs in fair-skinned populations, whereas it represents more than 50%, and even up to 90%, in individuals with skin of color [8,37,63–66]. However, not all cases of pBCC are clinically evident. Dermoscopy can reveal features of pigmentation in about 30% of clinically non-pigmented BCCs [37,67]. Pigmentation in BCCs results not only from increased melanin but also from a higher number of melanocytes [63,66]. Lallas et al. found that pigmentation is significantly more common in nodular lesions and those located on the trunk [37]. On the other hand, Wolner et al. reported significantly higher incidence of pBCCs on the upper extremities compared with the head and neck region [68].

Park et al. found that increased pigmentation under dermoscopy was associated with a lower likelihood of infiltration and may predict a non-aggressive BCC subtype [63]. This could be linked to the anticarcinogenic properties of melanin, which reduces ultraviolet radiation (UVR) penetration through the epidermis and prevents malignant transformation and tumor cell infiltration. pBCCs were demonstrated to require smaller surgical margins for complete excision, and as a result, they are more often excised with adequate margins. When dermoscopy shows pigmentation within BCC on a level of 11% to 15%, clinicians should anticipate the need for more aggressive surgical treatment [63].

Nevertheless, pBCC is not classified as a separate subtype, as pigmented features can occur in all BCC types [37]. Xavier-Júnior et al. distinguished pBCC subtypes with higher-risk morphologies, such as sclerosing or micronodular, and demonstrated that the prognosis is rather related to morphological findings than to the presence of pigmented structures [69]. Examples of pBCCs are shown in Figure 5, whereas non-pigmented variants are illustrated in Figure 6.

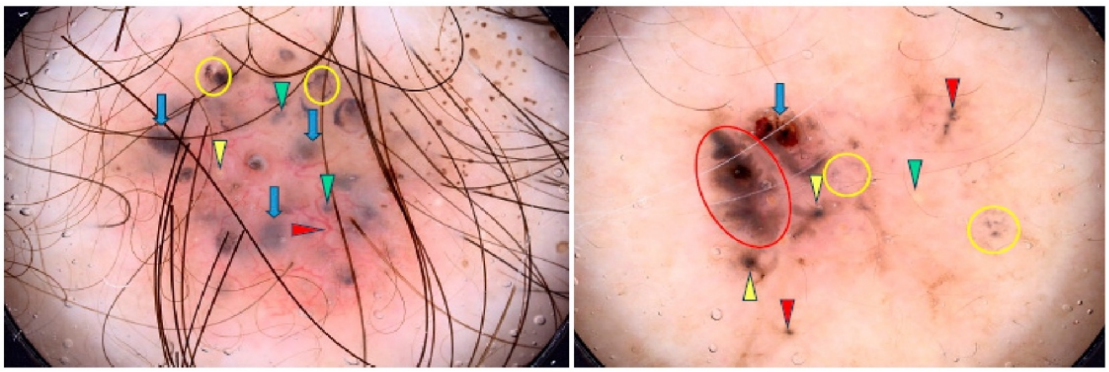

Figure 5. Dermoscopy images of pigmented BCCs (pBCCs). The pBCC on the left shows multiple gray-blue globules (green arrowheads), arborizing vessel (red arrowhead), blue clods/ovoid nests (blue arrows), multiple in-focus blue/gray dots (yellow circles), milia-like cyst (yellow arrowhead). The pBCC on the right presents erosion (blue arrow), maple-leaf-like areas (red circle), multiple gray-blue globules (red arrowheads), multiple in-focus blue/gray dots (yellow circles), milia-like cyst (green arrowhead), spoke-wheel areas (yellow arrowheads).

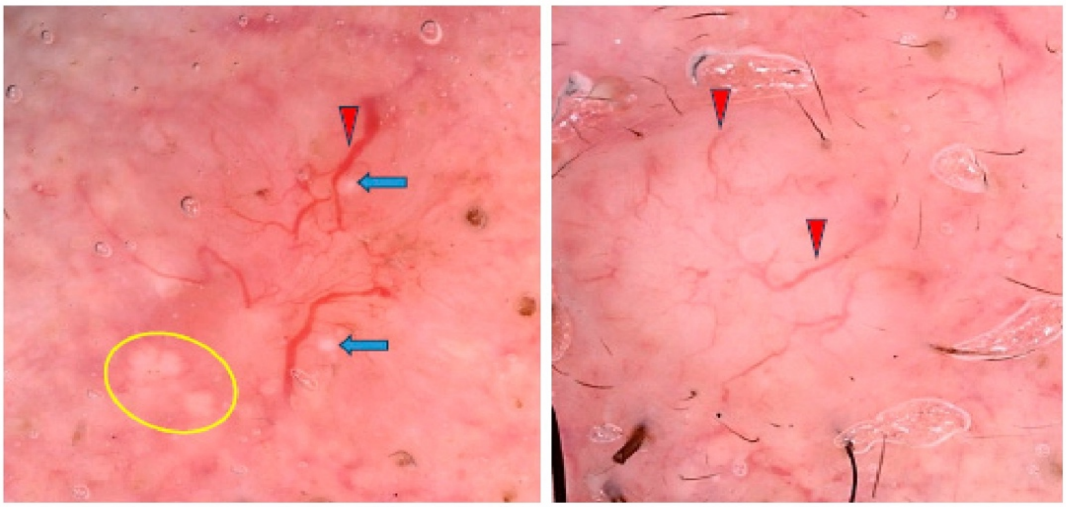

Figure 6. Dermoscopy images of non-pigmented BCCs. The BCC on the left shows MAY globules (yellow circle), milia-like cysts (blue arrows), arborizing vessel (red arrowhead). The BCC on the right presents arborizing vessels (red arrowheads).

3.1.18. Recurrent BCC

BCCs extremely rarely metastasize, and therefore, classical cancer staging systems do not apply to them. Instead, they have been divided based on the risk of local recurrence into two categories—low and high risk.

In the study by Sgouros et al., prognostic features associated with high-risk BCC included clinically apparent white color, the presence of shiny white lines on dermoscopy, nodular morphology and prominent clinico-dermatoscopic ulceration (covering more than 90% of the lesion's surface). High-risk BCCs more frequently exhibited glomerular vessels

and were non-pigmented. Dermatoscopic evidence of pigmentation, on the other hand, was indicative of a low-risk BCC [70].

In another study, a statistically significant correlation was found between arborizing telangiectasia and blue-gray globules with BCC recurrence [55]. Cuellar et al. noted that the first sign of early relapse was the appearance of brown-gray pigmented foci, even when the original tumors were not pigmented [71].

3.1.19. Summary of Dermoscopic Findings by BCC Subtype

In summary, no single dermoscopic finding definitively indicates a specific BCC subtype; however, certain combinations of features may suggest particular subtypes. For instance, the presence of arborizing vessels, translucency and blue-gray ovoid nests may point to nBCC, while short fine telangiectasias, multiple erosions, maple-leaf-like areas, spoke-wheel areas and shiny white-to-red areas are more commonly observed in sBCC. BSC often exhibits a "stellate pattern" and halo phenomenon and sclerodermiform BCC is characterized by arborizing or microvessels on a milky-red, pink-white or porcelain-white background. Table 1 summarizes the dermoscopic characteristics of different BCC subtypes.

Table 1. Key dermoscopic features of different basal cell carcinoma (BCC) subtypes.

Subtype	Key Dermoscopic Features
Superficial BCC (sBCC)	Spoke-wheel areas, maple-leaf-like areas, multiple erosions, shiny white to red areas, short fine telangiectasias + absence of arborizing vessels, blue-gray ovoid nests and ulceration
Nodular BCC (nBCC)	Arborizing vessels, blue-gray ovoid nests, translucent background, shiny white areas
Basosquamous BCC (BSC)	"Four dots in a square", adherent fibers, keratin masses
Sclerodermiform BCC	Arborizing vessels on a porcelain-white background, along with multiple erosions or ulcerations (often forming a ring), poorly defined margins
Infiltrative BCC (iBCC)	Stellate pattern, halo phenomenon
Micronodular BCC	Brown and blue globules, white clods, milia-like cysts, arborizing vessels or short fine telenagiectasias, milky red structureless areas, ulceration
Infundibulocystic BCC	Short fine telangiectasias, maple-leaf-like areas, blue-gray dots and globules, shiny white streaks
Cystic BCC	Homogeneous blue-black areas, arborizing telangiectasia
Blue-white BCC	Homogeneous blue pigmentation, whitish septa, blue-gray dots/globules/nests
Polypoid BCC	Arborizing vessels, blue-gray globules, ovoid nests
Large Pore BCC	Central dilated pore surrounded by a poorly defined whitish-pink area, branched vessels, gray pigmentation, yellowish-white scales
Linear BCC	Maple-leaf-like areas, spoke-wheel structures
Keloidal BCC	Arborizing vessels on a pinkish-white background
Fibroepithelioma of Pinkus	Hypopigmented to pink lines intersecting at acute angles (HPLA), fine arborizing, dotted or serpentine vessels, shiny white lines, gray-brown areas, gray-blue dots
BCC with Myoepithelial Differentiation	Irregular linear vessels, arborizing vessels, whitish background, dark brown areas
Radiation-induced BCC	Ovoid nests, arborizing vessels, pink background
Recurrent BCC	Arborizing telangiectasia, blue-gray globules, brown-gray pigmented foci

Nevertheless, from a clinical perspective, differentiating between "high-risk" and "low-risk" subtypes is more critical than recognizing specific subtypes. High-risk subtypes, including sclerodermiform, micronodular, infiltrative and basosquamous carcinoma, display more aggressive behavior, with greater morbidity and recurrence risk. High-risk BCCs should be suspected in non-pigmented, clinically white lesions that exhibit arborizing, truncated or glomerular vessels; extensive ulceration, especially when covering more than 90% of the lesion's surface; multiple blue-gray globules; concentric structures and a lack of pink areas or large blue-gray ovoid nests.

3.2. Dermoscopic Findings by BCC Location

3.2.1. Face and Scalp

BCC most commonly (up to 80%) develops on the head, particularly on the face and neck, where it typically presents as a nodule with arborizing vessels on dermoscopy [32,33,68,72,73]. In in-depth analysis, Fagotti et al. found that the frontonasal area is the most prevalent location for the nodular subtype, while sclerodermiform BCC is more commonly found in the periauricular area [33]. Facial BCCs, especially in the H-zone (nose, eyes, ears), are more likely to ulcerate and have a higher risk of deeper invasion, indicating more aggressive histological subtypes and a higher risk of recurrence [33,72]. Pogorzelska-Dyrbuś et al. reported a lower prevalence of brown globules in the H-zone and a higher prevalence of glomerular and comma vessels in non-H-zone areas [72,74]. BCCs on the face, particularly in fair and extensively sun-damaged skin, may also appear more subtle, presenting as a white macule or papule. Interestingly, Liopyris et al. observed that 28.9% of these lesions lacked any classic BCC criteria and 13.3% presented with milia-like cysts, making diagnosis particularly challenging. The authors suggested that the white color of the lesion may be attributed to the presence of abundant dermal collagen. Pigmented BCCs are less common on the face [31]. In contrast, scalp BCCs more often display pigmented structures and, surprisingly, also melanocytic patterns, while showing vascular patterns less frequently than BCCs in other locations [32].

3.2.2. Eyelid

In the United States and Western countries, BCC constitutes the most common eyelid malignancy, accounting for up to 90.8% of non-melanoma skin cancers [73,75]. About 20% of BCCs in the head and neck region occur on the eyelids, predominantly on the lower eyelid, especially on the margin, likely due to higher UV exposure [73,75–78]. Vaccari et al. found that the lateral half of the eyelid margin is most often affected, usually without local symptoms [75]. Pigmented eyelid margin BCCs (EMBCCs) account for 10% of cases, similar to the prevalence in the head region [76]. Madarosis (eyelash loss) is a key sign of EMBCCs and other malignant eyelid tumors [75–77].

In dermoscopy, EMBCCs show arborizing, thin linear and polymorphous vessels, as well as linear vessels running perpendicular to the eyelid margin, a feature unique for this location [75–78]. However, arborizing vessels, while typical for BCC, are not specific to the eyelid [77]. Jaworska et al. highlighted that linear perpendicular vessels are not pathognomonic for EMBCC, as they also occur in normal eyelid margins and other lesions. The authors observed structureless pink areas and starry milia-like cysts in EMBCCs [78]. Williams et al. also reported pink or skin-colored background [77], while Cinotti et al. noted intense pink, yellow and white colors, with yellow possibly due to crusts on erosions [76].

3.2.3. Trunk

In 2022, Jaworska et al. reported that truncal BCCs develop more frequently in younger men. These lesions tend to grow larger and are frequently multiple, likely due to genetic susceptibility and UV-induced oxidative damage to the skin [78]. BCCs on the trunk

are mostly superficial and, on dermoscopy, are associated with short fine telangiectasias, spoke-wheel areas and small erosions [32,68].

3.2.4. Areola

BCCs developing on the areola are very uncommon and have been referred to as "BCC of the nipple-areola complex (BCC-NAC)". Suggested causal factors include UV radiation and radiation therapy, with the latter increasing the risk of multiple BCC-NAC cases, especially when exposure occurs early in life [79]. Kitamura et al. reported a unique dermoscopic finding in BCC-NAC, which they called "large black web". This feature was characterized by a black network with a mesh thicker than the typical pigment network. Noteworthy is that the pigment network is naturally observed on the areola since it is one of the few naturally pigmented areas of the body [80].

3.2.5. Umbilicus

In 2011, Ramirez et al. reported a case of umbilical BCC in a 21-year-old patient. The small papule was first detected during a full-body mole mapping. Dermoscopy revealed an unpigmented lesion with superficial ulcerations and polymorphic vessels, including arborizing vessels, all suggestive of BCC. The authors underscored that the umbilicus, due to its proximity to various anatomical structures, may facilitate tumor spread. Although only a few cases of umbilical BCC have been documented to date, the case mentioned above is the only one that reported the dermoscopic findings [81].

3.2.6. Limbs

Four studies on BCCs developing on the limbs were included in our analysis. Wolner et al. evaluated 392 BCCs, of which 54 (13.8%) were located on the lower extremities (LE) and 40 (10.2%) on the upper extremities (UE). BCCs on the LE were more common in women, were diagnosed at a younger age and often showed a superficial subtype. Arborizing vessels were significantly less common on the LE, while ulceration/erosions, polymorphous vessels and shiny white structures were more frequently observed [68]. The BCC located on the LE (shank) is presented in Figure 7.

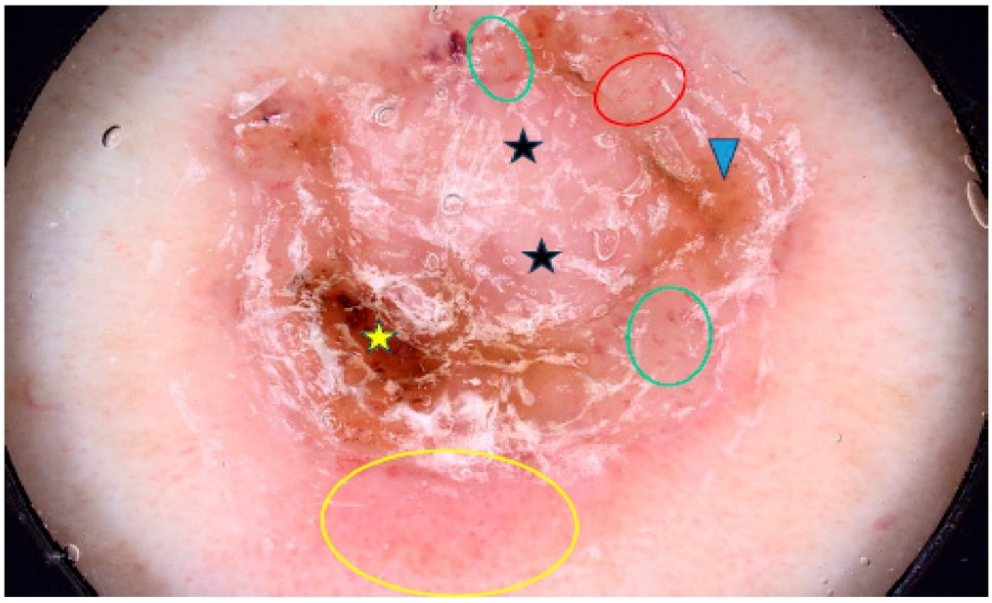

Figure 7. Dermoscopy image of BCC located on the shank showing erosion (yellow asterisk), dotted vessels (yellow circle), looped vessels (red circle), glomerular vessels (green circles), milky way areas (black asterisks), brown homogenous blotch (blue arrowhead).

Two of these studies focused on acral BCCs, which are extremely rare on glabrous skin since BCCs usually develop in hair-bearing areas due to follicular germinative cell differentiation [82]. Factors such as repeated trauma, burns, chronic ulceration, ionizing radiation and arsenic exposure may contribute to their development. Acral BCCs are more common in patients with genetic syndromes such as nevoid basal cell carcinoma syndrome, Bazex syndrome and xeroderma pigmentosum [82,83]. Another explanation is the spread via eccrine ducts [83]. Acral BCCs primarily affect women, though the role of sex hormones is unconfirmed [82]. In dermoscopy, BCCs on glabrous skin present with ulcers, dotted vessels, blue-gray ovoid nests and the absence of arborizing vessels, although one case of periungual BCC did show typical arborizing vessels [82–84].

3.2.7. Genitals

UV radiation is considered to be the primary contributing factor of BCC, but it may also develop in non-sun-exposed areas. Advanced age, local trauma, chronic inflammation and radiotherapy may be causative factors in such cases [85]. Studies indicate that vulvar BCC accounts for less than 1–2% of all BCCs and only 2–5% of all vulvar cancers [85–87]. Dobrosavljevic Vukojevic et al. reported an even higher prevalence of vulvar BCC, ranging from 2% to 4.9% of all vulvar cancers in Europe, and up to 8% in China [88].

Genital BCCs typically develop on the labium majus and minus of postmenopausal women, with an average age of 70 [85,87–89]. Pigmentation in vulvar BCCs is rare in Caucasians (3%) but common in China (81%) [47,86,88]. These cancers are often diagnosed late, usually when the tumor is larger than 1 cm and symptoms like itching, a palpable mass and pain are often misdiagnosed as inflammatory conditions [86,87]. Dermoscopy reveals similar features to cutaneous BCCs, including blue ovoid nests, blue globules, fine telangiectasias, arborizing telangiectasia and white shiny structures, with ulcerations occurring in 28% of cases; however, brown dots have also been described [86,88,89]. In the reviewed literature, no reports of dermoscopic findings for BCC on male genitalia were identified.

3.2.8. Summary of Dermoscopic Findings by BCC Location

In conclusion, BCC most commonly occurs on the head, particularly on the face and neck, where it typically presents as a nodule with arborizing vessels. Non-pigmented BCCs predominate on the face, suggesting a higher likelihood of infiltration and potentially indicating a more aggressive subtype. In the H-zone (nose, eyes, and ears), BCCs are more prone to ulceration, deeper invasion and association with aggressive histological subtypes, leading to an increased risk of recurrence. BCCs in non-H-zone areas more frequently display glomerular and comma vessels rather than arborizing vessels. Approximately 20% of head and neck BCCs occur on the eyelids, with madarosis (eyelash loss) serving as a key sign of EMBCC or other malignant eyelid tumors. On the trunk, BCCs are typically superficial, exhibiting features such as SFT, spoke-wheel areas and small erosions. BCC-NAC should be suspected when a unique dermoscopic feature, described as a “large black web”, is observed. On the lower extremities, diagnosis of BCC is particularly challenging. Lesions in this region more often present with ulceration, polymorphous vessels and SWS, while arborizing vessels are rarely observed. BCC can also occur in non-sun-exposed areas, such as the genital region (vulva) in postmenopausal women, where its dermoscopic features are similar to those seen in cutaneous BCC.

3.3. Dermoscopic Features by Age on BCC Onset

A study of 448 BCCs found that early-onset cases (in patients under 50 years of age) were less pigmented and often showed blue-gray globules with no visible vessels. In

contrast, arborizing telangiectasia, large blue-gray ovoid nests and ulceration were more common in older patients [90].

3.4. Dermoscopic Features by BCC Size

Twelve studies reporting the dermoscopic findings in BCC by tumor size were included in the analysis [21,91–101]. The values used to differentiate between small and large BCCs varied across studies; one study set the cutoff at 15 mm, three at 10 mm, two at 6 mm, two at 5 mm, one at 4 mm, and one at 3 mm [21,91,92,95–101]. Very small BCCs (vsBCCs) were defined as those measuring 2–3 mm, while micro-BCCs referred to tumors of 2 mm or smaller [21,93].

The included studies demonstrated that the number of established dermoscopic features of BCC increased with tumor size, but no additional size-specific features were observed. However, some dermoscopic findings may be observed with different frequencies, facilitating diagnosis at various stages [91,95,98,100]. Particularly, Ishizaki underscored that dermoscopy contributes to recognizing BCCs in their early stages [96].

Predictors of small BCCs included SFT, small erosions, multiple blue-gray dots and large blue-gray ovoid nests [91,97,98]. On the other hand, some studies led to opposite conclusions. Two of them reported SFT and small erosions to be more frequent in large BCCs [97,99]. Moreover, Wang et al. reported that pigmented structures started to appear at 2 mm, with no difference in frequencies across pBCC sizes [91].

vsBCCs were statistically more likely to present with pigmented structures, particularly blue-gray dots and ovoid nests, but less frequently showed SFT, shiny white structures, ulceration, micro-erosions and scales [21]. The three cases reported thus far of pigmented micro-BCCs demonstrated high dermoscopic variability [93].

In larger BCCs, arborizing vessels, ulceration and SWS are significantly more common [91,94,101]. Arborizing vessels typically appeared when tumors exceeded 6 mm [91]. Kinzel-Maluje et al. concluded that arborizing vessels are the only statistically significant predictor against small BCCs [92].

Arias-Rodriguez et al. demonstrated that aggressive BCC subtypes had similar frequencies of dermoscopic findings regardless of tumor size [21]. Examples of small (3.5 mm diameter) and large (18 mm diameter) BCCs are shown in Figure 8.

Direct comparisons were challenging due to the varying definitions of small and large BCCs used across the publications. Table 2 summarizes findings from the studies included.

3.5. Dermoscopic Features by Patient Phototype

We included five studies on dermoscopy in BCC among patients with darker phototypes (III–VI) [66,102–105] and one study on individuals with albinism [106]. Due to the protective properties of melanin, the incidence of BCC is lower in darker skin tones. The incidence rate of pBCC increases with darker phototypes, from 91.8% in phototypes II-IV to 100% in Black individuals [102,104].

Frequent dermoscopic features included blue-grey dots, ovoid nests, maple-leaf-like areas, blue-white veil, ulceration, arborizing vessels and SFT. Nodular BCC was the most common subtype significantly associated with ulceration, blue-white veil and arborizing vessels [102,103,105]. Maple-leaf-like areas, red-white structureless areas, multiple small erosions and spoke wheel areas were commonly found in sBCC, with the strongest correlation seen for the latter [102,105]. Micronodular BCC showed predominantly arborizing and dotted vessels and blue-white veil [103]. A dermoscopic rainbow pattern was seen in a third of Indian patients [103]. In Black individuals, 55.6% of BCCs had an accentuated reticular network, and 33.3% showed central hypopigmentation, which could be mistaken for a dermatofibroma [104].

In Africans with albinism, BCC was 2.3 times more frequent than SCC, similar to Caucasians, and the most frequent dermoscopic findings included arborizing telangiectasia, ovoid nests and spoke-wheel-like structures [106].

Table 2. Summary of dermoscopic features associated with basal cell carcinoma (BCC) sizes across different studies.

Primary Author, Year, Country	Definitions of BCC Sizes	Dermoscopic Features Predominantly Observed in Specific Sizes
Wang et al., 2024, Taiwan [91]	Small: <6 mm; Large: >6 mm	Small: Short fine telangiectasias, small erosions. Large: Arborizing vessels (appeared in tumors larger than 6 mm), ulcerations, shiny white structures. Pigment patterns appeared at 2 mm and were consistent regardless of size.
Kinzel-Maluje et al., 2024, Brazil [92]	Small: ≤4 mm; Large: >4 mm	Small: Short fine telangiectasia in nodular BCC, concentric structures in micronodular BCC. Large: Arborizing vessels.
Foltz et al., 2023, United States [93]	Micro-BCC: ≤2 mm	Micro-BCC: Dermoscopic variability. The findings include blue-gray dots, blue-gray ovoid nests, spoke-wheel structures, maple-leaf-like structures.
Arias-Rodriguez et al., 2023, Colombia [21]	Very Small: ≤3 mm; Small: 3–10 mm	Very Small: More pigmented structures, including blue-gray dots, globules and ovoid nests, fewer vessels (primarily short fine telangiectasias (SFT)), reduced presence of shiny white structures (SWSs), scales, ulcerations and micro-erosions. Small: Increased number of vessels, more SWS, scales, ulcerations and micro-erosions.
Sykes et al., 2020, New Zealand [94]	Small: ≤41.9 cm^2 Large: >41.9 cm^2	Large sBCC: Gain SWS, small blue clods and brown clods over time.
Persechino et al., 2020, Italy [95]	Small: <3 mm	Small pBCCs show typical dermoscopic features of BCC.
Xu et al., 2021, China [101]	Small: <1 cm; Large: ≥1 cm	Large: Blue-gray dots, arborizing vessels, SWS, ulcerations and large blue-gray structureless areas. Large BCCs in heavily pigmented lesions (>70% pigmentation) more frequently exhibited large blue-gray structureless areas, SWS and ulceration.
Ishizaki et al., 2016, Japan [96]	Small: <15 mm; Large: ≥15 mm	Increased detection of smaller BCCs due to dermoscopy; however, no specific dermoscopic findings were evaluated.
Longo et al., 2017, Italy [97]	Small: <5 mm; Large: >5 mm	Small: Multiple blue-gray dots, large blue-gray ovoid nests. Large: Ulceration, multiple small erosions.
Takahashi et al., 2016, Japan [98]	Very Small: ≤3 mm; Small: 4–6 mm	Very Small: Fewer positive dermoscopic features. Both groups: Large blue-gray ovoid nests and multiple blue-gray globules.
Popadić et al., 2015, Serbia [99]	Small: ≤10 mm; Large: >10 mm	Large: Arborizing vessels, short fine telangiectasias, multiple small erosions.
Sanchez-Martin et al., 2012, Spain [100]	Small: ≤5 mm	Small BCCs show typical dermoscopic features of BCC.

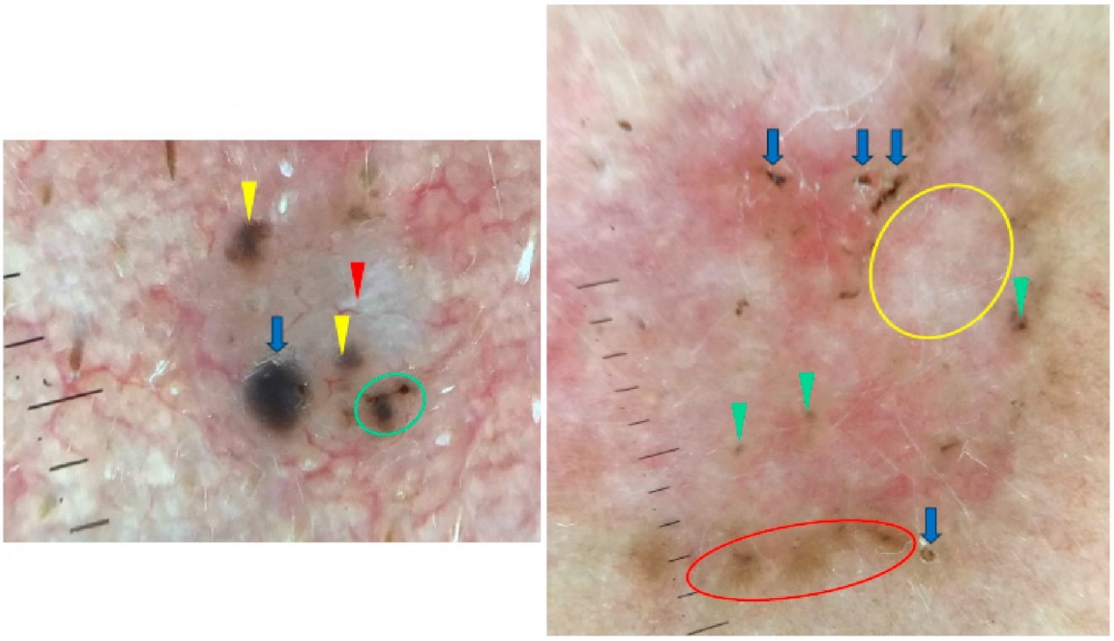

Figure 8. Dermoscopy images of BCCs in different sizes. The small BCC on the left shows blue clod/ovoid nest (blue arrow), multiple gray-blue globules (yellow arrowheads), concentric structures (green circle), shiny white line (red arrowheads). The large BCC on the right presents multiple gray-blue globules (green arrowheads), maple-leaf-like areas (red circle), white areas (yellow circle), multiple erosions (blue arrows).

4. Discussion

In the current review, we analyzed the variations of dermoscopic features in BCC based on tumor subtype, location, age of onset, size and skin phototype. Data from the literature indicate that there is no single feature that is pathognomonic for a certain BCC subtype or specific to a particular location. This underscores the fact that a combination of dermoscopic features is more relevant for an accurate diagnosis of BCC.

In patients with darker skin phototypes, the incidence of BCC is lower than in lighter skin tones; however, the percentage of pBCCs increases in this group, with blue-grey dots, ovoid nests, maple-leaf-like areas and blue-white veil being frequent findings.

There is also a variety of studies in the English literature on the dermoscopic findings in BCC depending on the tumor size. However, comparing the results between these studies is difficult due to the different ranges of diameter adopted by individual authors. The main attention has been drawn to pigmented structures, which were detected even in 2 mm tumors. Pigmented structures were suggested to be more common in smaller BCCs; however, we presume that their presence rather allows for faster detection of suspicious lesion.

Several factors, beyond the inconsistent definitions of tumor size, may further complicate the interpretation and comparison of results. For example, variability in sample representativeness—such as differences in ethnicity, gender and age distributions—can influence findings. Additionally, the accuracy and reproducibility of dermoscopic assessments, as well as differences in equipment and techniques used in various studies, present further challenges. Addressing these variables is crucial for improving the reliability and generalizability of research on BCC dermoscopy. On the other hand, a limitation of the current review is that only the PubMed database was searched. Another limitation is the lack of consistency in the literature in the division of BCC into clinical and histological subtypes, which causes confusion and makes it difficult to standardize dermoscopic findings.

To address these limitations, future studies should focus on standardizing the definitions of tumor size, improving the diversity and representativeness of samples and establishing protocols for consistent dermoscopic evaluations across populations. Efforts should also aim to develop guidelines for the harmonization of equipment and techniques. Comparative analyses with similar studies could help identify the unique contributions of each work, while also explaining differences or consistencies in findings. This would not only strengthen the understanding of BCC dermoscopy but also enhance its clinical application.

5. Conclusions

There is a wide variety of data in the literature on the dermoscopic presentation of BCC depending on the tumor subtype, location, age of onset, size and skin phototype. Despite the evidence confirming the differences in the dermoscopic presentations of BCC, it was not possible to find any pathognomonic feature for any subtype or location.

Author Contributions: Concept and design: I.W. and M.Ż.; methodology: I.W. and M.Ż.; manuscript—draft preparation: I.W.; manuscript—final version editing: I.W. and M.Ż. All named authors meet the International Committee of Medical Journal Editors (ICMJE) criteria for authorship for this article, take responsibility for the integrity of the work as a whole. All authors have read and agreed to the published version of the manuscript.

Funding: The publication fee was covered with the internal funds of University of Rzeszow. This research received no external funding.

Institutional Review Board Statement: This review is based on the analysis of data from literature. All sample dermoscopic images presented in the article were taken during routine patient care and come from the Department of Dermatology, University of Rzeszow. The study was conducted in accordance with the Declaration of Helsinki and approved by the Ethics Committee at the Regional Medical Chamber in Rzeszow (protocol code 50/2024/B, date of approval 21 October 2024).

Informed Consent Statement: Written informed consent has been obtained from the patients to publish this paper.

Data Availability Statement: No original datasets were generated for this article.

Conflicts of Interest: The authors declare no conflicts of interest.

References

1. Longo, C.; Guida, S.; Mirra, M.; Pampena, R.; Ciardo, S.; Bassoli, S.; Casari, A.; Rongioletti, F.; Spadafora, M.; Chester, J.; et al. Dermatoscopy and reflectance confocal microscopy for basal cell carcinoma diagnosis and diagnosis prediction score: A prospective and multicenter study on 1005 lesions. *J. Am. Acad. Dermatol.* **2024**, *90*, 994–1001. [CrossRef] [PubMed]
2. Palmisano, G.; Orte Cano, C.; Fontaine, M.; Lenoir, C.; Cinotti, E.; Tognetti, L.; Rubegni, P.; Perez-Anker, J.; Puig, S.; Malvehy, J.; et al. Dermoscopic criteria explained by LC-OCT: Negative maple leaf-like areas. *J. Eur. Acad. Dermatol. Venereol.* **2024**, *38*, e271–e273. [CrossRef]
3. Coppola, R.; Barone, M.; Zanframundo, S.; Devirgiliis, V.; Roberti, V.; Perrella, E.; Donati, M.; Palese, E.; Tenna, S.; Persichetti, P.; et al. Basal cell carcinoma thickness evaluated by high-frequency ultrasounds and correlation with dermoscopic features. *Ital. J. Dermatol. Venerol.* **2021**, *156*, 610–615. [CrossRef]
4. Yuki, A.; Takatsuka, S.; Abe, R.; Takenouchi, T. Diagnostic accuracy of dermoscopy for 934 basal cell carcinomas: A single-center retrospective study. *J. Dermatol.* **2023**, *50*, 64–71. [CrossRef] [PubMed]
5. Ahnlide, I.; Bjellerup, M. Accuracy of clinical skin tumour diagnosis in a dermatological setting. *Acta Derm. Venereol.* **2013**, *93*, 305–308. [CrossRef] [PubMed]
6. Carroll, D.M.; Billingsley, E.M.; Helm, K.F. Diagnosing basal cell carcinoma by dermatoscopy. *J. Cutan. Med. Surg.* **1998**, *3*, 62–67. [CrossRef]
7. McDaniel, B.; Badri, T.; Steele, R.B. Basal Cell Carcinoma. In *StatPearls*; StatPearls Publishing: Treasure Island, FL, USA, 2024. Available online: https://www.ncbi.nlm.nih.gov/books/NBK482439 (accessed on 15 November 2024).
8. Popadić, M. Statistical evaluation of dermoscopic features in basal cell carcinomas. *Dermatol. Surg.* **2014**, *40*, 718–724. [PubMed]
9. Popadić, M. Dermoscopic features in different morphologic types of basal cell carcinoma. *Dermatol. Surg.* **2014**, *40*, 725–732.

10. Camela, E.; Ilut Anca, P.; Lallas, K.; Papageorgiou, C.; Manoli, S.M.; Gkentsidi, T.; Eftychidou, P.; Liopyris, K.; Sgouros, D.; Apalla, Z.; et al. Dermoscopic clues of histopathologically aggressive basal cell carcinoma subtypes. *Medicina* **2023**, *59*, 349. [CrossRef] [PubMed]
11. Gürsel Ürün, Y.; Fiçicioğlu, S.; Ürün, M.; Can, N. Clinical, dermoscopic, and histopathological evaluation of basal cell carcinoma. *Dermatol. Pract. Concept.* **2023**, *13*, e2023004. [CrossRef] [PubMed]
12. Popadić, M.; Sinz, C.; Kittler, H. The significance of blue color in dermatoscopy. *J. Dtsch. Dermatol. Ges.* **2017**, *15*, 302–307. [CrossRef] [PubMed]
13. Popadić, M.; Brasanac, D. The use of dermoscopy in distinguishing the histopathological subtypes of basal cell carcinoma: A retrospective, morphological study. *Indian J. Dermatol. Venereol. Leprol.* **2022**, *88*, 598–607. [CrossRef]
14. Kim, H.S.; Park, J.M.; Mun, J.H.; Song, M.; Ko, H.C.; Kim, B.S.; Kim, M.B. Usefulness of Dermatoscopy for the Preoperative Assessment of the Histopathologic Aggressiveness of Basal Cell Carcinoma. *Ann. Dermatol.* **2015**, *27*, 682–687. [CrossRef]
15. Popadić, M. Dermoscopy of aggressive basal cell carcinomas. *Indian J. Dermatol. Venereol. Leprol.* **2015**, *81*, 608–610. [CrossRef] [PubMed]
16. Pyne, J.; Sapkota, D.; Wong, J.C. Aggressive basal cell carcinoma: Dermatoscopy vascular features as clues to the diagnosis. *Dermatol. Pract. Concept.* **2012**, *2*, 203a02. [CrossRef] [PubMed]
17. Verduzco-Martínez, A.P.; Quiñones-Venegas, R.; Guevara-Gutiérrez, E.; Tlacuilo-Parra, A. Correlation of dermoscopic findings with histopathologic variants of basal cell carcinoma. *Int. J. Dermatol.* **2013**, *52*, 718–721. [CrossRef]
18. Zhang, L.W.; Shen, X.; Fu, L.X.; Meng, H.M.; Lu, Y.H.; Chen, T.; Xu, R.H. Dermoscopy, reflectance confocal microscopy, and high-frequency ultrasound for the noninvasive diagnosis of morphea-form basal cell carcinoma. *Skin Res. Technol.* **2022**, *28*, 766–768. [CrossRef]
19. Lupu, M.; Clatici, V.G.; Barinova, E.; Voiculescu, V.M. Fibroepithelioma of Pinkus: Dermoscopic and reflectance confocal microscopic patterns. *Dermatol. Ther.* **2021**, *34*, e14831. [CrossRef] [PubMed]
20. Negrutiu, M.; Danescu, S.; Popa, T.; Focșan, M.; Vesa, Ș.C.; Baican, A. Advancements in Basal Cell Carcinoma Diagnosis: Non-Invasive Imaging and Multimodal Approach. *J. Clin. Med.* **2023**, *13*, 39. [CrossRef] [PubMed]
21. Arias-Rodriguez, C.; Muñoz-Monsalve, A.M.; Cuesta, D.; Mejia-Mesa, S.; Aluma-Tenorio, M.S. Dermoscopy of very small basal cell carcinoma ($\leq$3 mm). *An. Bras. Dermatol.* **2023**, *98*, 755–763. [CrossRef] [PubMed]
22. Conforti, C.; Pizzichetta, M.A.; Vichi, S.; Toffolutti, F.; Serraino, D.; Di Meo, N.; Giuffrida, R.; Deinlein, T.; Giacomel, J.; Rosendahl, C.; et al. Sclerodermiform basal cell carcinomas vs. other histotypes: Analysis of specific demographic, clinical, and dermatoscopic features. *J. Eur. Acad. Dermatol. Venereol.* **2021**, *35*, 79–87. [CrossRef]
23. Husein-ElAhmed, H. Sclerodermiform basal cell carcinoma: How much can we rely on dermatoscopy to differentiate from non-aggressive basal cell carcinomas? Analysis of 1256 cases. *An. Bras. Dermatol.* **2018**, *93*, 229–232. [CrossRef] [PubMed]
24. Inamura, Y.; Imafuku, K.; Kitamura, S.; Hata, H.; Shimizu, H. Morphoeic basal cell carcinoma with ring-form ulceration. *Int. J. Dermatol.* **2016**, *55*, e415–e416. [CrossRef]
25. Longo, C.; Lallas, A.; Kyrgidis, A.; Rabinovitz, H.; Moscarella, E.; Ciardo, S.; Zalaudek, I.; Oliviero, M.; Losi, A.; Gonzalez, S.; et al. Classifying distinct basal cell carcinoma subtypes by means of dermatoscopy and reflectance confocal microscopy. *J. Am. Acad. Dermatol.* **2014**, *71*, 716–724.e1. [CrossRef] [PubMed]
26. Pampena, R.; Parisi, G.; Benati, M.; Borsari, S.; Lai, M.; Paolino, G.; Cesinaro, A.M.; Ciardo, S.; Farnetani, F.; Bassoli, S.; et al. Clinical and Dermoscopic Factors for the Identification of Aggressive Histologic Subtypes of Basal Cell Carcinoma. *Front. Oncol.* **2021**, *10*, 630458. [CrossRef]
27. Pyne, J.H.; Fishburn, P.; Dicker, A.; David, M. Infiltrating basal cell carcinoma: A stellate peri-tumor dermatoscopy pattern as a clue to diagnosis. *Dermatol. Pract. Concept.* **2015**, *5*, 21–26. [CrossRef] [PubMed]
28. Basak, P.Y.; Meric, G.; Ciris, M. Basal cell carcinoma with halo phenomenon in a young female: Significance of dermatoscopy in early diagnosis. *Indian J. Dermatol.* **2015**, *60*, 214.
29. Giacomel, J.; Lallas, A.; Argenziano, G.; Reggiani, C.; Piana, S.; Apalla, Z.; Ferrara, G.; Moscarella, E.; Longo, C.; Zalaudek, I. Dermoscopy of basosquamous carcinoma. *Br. J. Dermatol.* **2013**, *169*, 358–364. [CrossRef]
30. Akay, B.N.; Saral, S.; Heper, A.O.; Erdem, C.; Rosendahl, C. Basosquamous carcinoma: Dermoscopic clues to diagnosis. *J. Dermatol.* **2017**, *44*, 127–134. [CrossRef]
31. Liopyris, K.; Navarrete-Dechent, C.; Yélamos, O.; Marchetti, M.A.; Rabinovitz, H.; Marghoob, A.A. Clinical, dermoscopic, and reflectance confocal microscopy characterization of facial basal cell carcinomas presenting as small white lesions on sun-damaged skin. *Br. J. Dermatol.* **2019**, *180*, 229–230. [CrossRef]
32. Suppa, M.; Micantonio, T.; Di Stefani, A.; Soyer, H.P.; Chimenti, S.; Fargnoli, M.C.; Peris, K. Dermoscopic variability of basal cell carcinoma according to clinical type and anatomic location. *J. Eur. Acad. Dermatol. Venereol.* **2015**, *29*, 1732–1741. [CrossRef] [PubMed]

33. Fagotti, S.; Pizzichetta, M.A.; Corneli, P.; Toffolutti, F.; Serraino, D.; Di Meo, N.; Zalaudek, I. Dermoscopic features of face and scalp basal and squamous cell carcinomas according to clinical histopathologic characteristics and anatomical location. *J. Eur. Acad. Dermatol. Venereol.* **2021**, *35*, e237–e239. [CrossRef]
34. Emiroglu, N.; Cengiz, F.P.; Kemeriz, F. The relation between dermoscopy and histopathology of basal cell carcinoma. *An. Bras. Dermatol.* **2015**, *90*, 351–356. [CrossRef]
35. Trigoni, A.; Lazaridou, E.; Apalla, Z.; Vakirlis, E.; Chrysomallis, F.; Varytimiadis, D.; Ioannides, D. Dermoscopic features in the diagnosis of different types of basal cell carcinoma: A prospective analysis. *Hippokratia* **2012**, *16*, 29–34. [PubMed]
36. Enache, A.O.; Pătrașcu, V.; Simionescu, C.E.; Ciurea, R.N.; Văduva, A.; Stoica, L.E. Dermoscopy Patterns and Histopathological Findings in Nodular Basal Cell Carcinoma-Study on 68 Cases. *Curr. Health Sci. J.* **2019**, *45*, 116–122. [CrossRef]
37. Lallas, A.; Argenziano, G.; Kyrgidis, A.; Apalla, Z.; Moscarella, E.; Longo, C.; Ferrara, G.; Piana, S.; Benati, E.; Zendri, E.; et al. Dermoscopy uncovers clinically undetectable pigmentation in basal cell carcinoma. *Br. J. Dermatol.* **2014**, *170*, 192–195. [CrossRef] [PubMed]
38. Park, J.Y.; Jung, J.Y.; Park, B.W.; Cho, E.B.; Park, E.J.; Kim, K.H.; Kim, K.J. A rare dermoscopic pattern of nodular basal cell carcinoma with amyloid deposition. *J. Am. Acad. Dermatol.* **2017**, *76*, S55–S56. [CrossRef]
39. Altamura, D.; Menzies, S.W.; Argenziano, G.; Zalaudek, I.; Soyer, H.P.; Sera, F.; Avramidis, M.; DeAmbrosis, K.; Fargnoli, M.C.; Peris, K. Dermatoscopy of basal cell carcinoma: Morphologic variability of global and local features and accuracy of diagnosis. *J. Am. Acad. Dermatol.* **2010**, *62*, 67–75. [CrossRef]
40. Liebman, T.N.; Jaimes-Lopez, N.; Balagula, Y.; Rabinovitz, H.S.; Wang, S.Q.; Dusza, S.W.; Marghoob, A.A. Dermoscopic features of basal cell carcinomas: Differences in appearance under non-polarized and polarized light. *Dermatol. Surg.* **2012**, *38*, 392–399. [CrossRef] [PubMed]
41. Namiki, T.; Nojima, K.; Hanafusa, T.; Miura, K.; Yokozeki, H. Superficial basal cell carcinoma: Dermoscopic and histopathological features of multiple small erosions. *Australas. J. Dermatol.* **2018**, *59*, 69–71. [CrossRef]
42. Ahnlide, I.; Zalaudek, I.; Nilsson, F.; Bjellerup, M.; Nielsen, K. Preoperative prediction of histopathological outcome in basal cell carcinoma: Flat surface and multiple small erosions predict superficial basal cell carcinoma in lighter skin types. *Br. J. Dermatol.* **2016**, *175*, 751–761. [CrossRef] [PubMed]
43. Scalvenzi, M.; Lembo, S.; Francia, M.G.; Balato, A. Dermoscopic patterns of superficial basal cell carcinoma. *Int. J. Dermatol.* **2008**, *47*, 1015–1018. [CrossRef] [PubMed]
44. Giacomel, J.; Zalaudek, I. Dermoscopy of superficial basal cell carcinoma. *Dermatol. Surg.* **2005**, *31*, 1710–1713. [CrossRef]
45. Lallas, A.; Tzellos, T.; Kyrgidis, A.; Apalla, Z.; Zalaudek, I.; Karatolias, A.; Ferrara, G.; Piana, S.; Longo, C.; Moscarella, E.; et al. Accuracy of dermoscopic criteria for discriminating superficial from other subtypes of basal cell carcinoma. *J. Am. Acad. Dermatol.* **2014**, *70*, 303–311. [CrossRef]
46. Stephens, A.; Fraga-Braghiroli, N.; Oliviero, M.; Rabinovitz, H.; Scope, A. Spoke wheel-like structures in superficial basal cell carcinoma: A correlation between dermoscopy, histopathology, and reflective confocal microscopy. *J. Am. Acad. Dermatol.* **2013**, *69*, e219–e221. [CrossRef]
47. Yonan, Y.; Maly, C.; DiCaudo, D.; Mangold, A.; Pittelkow, M.; Swanson, D. Dermoscopic description of fibroepithelioma of Pinkus with negative network. *Dermatol. Pract. Concept.* **2019**, *9*, 246–247. [CrossRef] [PubMed]
48. Cuenca-Barrales, C.; Ruiz-Carrascosa, J.C.; Ruiz-Villaverde, R. Fibroepithelioma of Pinkus: A Basal Cell Carcinoma with Distinctive Dermoscopic Features. *Actas Dermosifiliogr.* **2018**, *109*, 908–909. [CrossRef] [PubMed]
49. Inskip, M.; Longo, C.; Haddad, A. Two adjacent individual fibroepithelioma of Pinkus of the umbilicus-One pink, one pigmented-a case report and review of the literature. *Dermatol. Pract. Concept.* **2016**, *6*, 17–20. [CrossRef] [PubMed]
50. Zalaudek, I.; Leinweber, B.; Ferrara, G.; Soyer, H.P.; Ruocco, E.; Argenziano, G. Dermoscopy of fibroepithelioma of Pinkus. *J. Am. Acad. Dermatol.* **2005**, *52*, 168–169. [CrossRef]
51. Nanda, J.K.; Marghoob, N.; Forero Cuevas, D.M.; Lee, K.R.; Levy, M.; Reiter, O.; Busam, K.J.; Marghoob, A.A. Clinical and dermoscopic features of fibroepithelioma of Pinkus: Case series with an emphasis on hypopigmented to pink lines intersecting at acute angles. *Arch. Dermatol. Res.* **2021**, *313*, 633–640. [CrossRef]
52. Roldán-Marín, R.; Leal-Osuna, S.; Lammoglia-Ordiales, L.; Toussaint-Caire, S. Infundibulocystic basal cell carcinoma: Dermoscopic findings and histologic correlation. *Dermatol. Pract. Concept.* **2014**, *4*, 51–54. [CrossRef]
53. Yoneta, A.; Horimoto, K.; Nakahashi, K.; Mori, S.; Maeda, K.; Yamashita, T. A case of cystic basal cell carcinoma which shows a homogenous blue/black area under dermatoscopy. *J. Skin Cancer* **2011**, *2011*, 450472. [CrossRef] [PubMed]
54. Quiñones-Venegas, R.; Paniagua-Santos, J.E.; Guevara-Gutierrez, E.; Esteban-Salerni, G.; Gonzalez-Ramirez, R.A.; Tlacuilo-Parra, A. Basal cell carcinoma, blue-white variant: Dermatoscopic findings in 32 cases. *Indian J. Dermatol. Venereol. Leprol.* **2021**, *87*, 29–33. [CrossRef] [PubMed]
55. Hirakawa, M.; Ishikura, Y.; Futatsuya, T.; Yamaguchi, R.; Shimizu, A. Polypoid basal cell carcinoma on the nose tip. *Case Rep. Dermatol. Med.* **2022**, *2022*, 4087202. [CrossRef]

56. Yildiz, S.; Karaarslan, I.; Yaman, B.; Ozdemir, F. Dermoscopy and reflectance confocal microscopy in pedunculated basal cell carcinoma. *Dermatol. Pract. Concept.* **2017**, *7*, 51–52. [CrossRef]
57. Feito-Rodríguez, M.; Sendagorta-Cudós, E.; Moratinos-Martínez, M.; González-Beato, M.J.; de Lucas-Laguna, R.; Pizarro, A. Dermatoscopic characteristics of acrochordon-like basal cell carcinomas in Gorlin-Goltz syndrome. *J. Am. Acad. Dermatol.* **2009**, *60*, 857–861. [CrossRef]
58. Lösch, A.I.; González, V.M.; Vigovich, F.A.; Larralde, M. Large Pore Basal Cell Carcinoma: A Case Report. *Dermatol. Pract. Concept.* **2021**, *11*, e2021021. [CrossRef]
59. Alcántara-Reifs, C.M.; Salido-Vallejo, R.; González-Menchen, A.; García-Nieto, A.V. Linear basal cell carcinoma: Report of three cases with dermoscopic findings. *Indian J. Dermatol. Venereol. Leprol.* **2016**, *82*, 708–711. [CrossRef]
60. Nagashima, K.; Demitsu, T.; Nakamura, T.; Nakamura, S.; Yamada, T.; Kakurai, M.; Umemoto, N.; Dohmoto, T.; Imagawa, I.; Yoneda, K. Keloidal basal cell carcinoma possibly developed from classical nodulo-ulcerative type of basal cell carcinoma: Report of a case. *J. Dermatol.* **2015**, *42*, 427–429. [CrossRef] [PubMed]
61. Namiki, T.; Miura, K.; Ueno, M.; Tanaka, K.; Yokozeki, H. Case of basal cell carcinoma with myoepithelial differentiation: Its characteristic clinical and histopathological features. *J. Dermatol.* **2016**, *43*, 1109–1110. [CrossRef]
62. Siqueira, M.L.; Trope, B.M.; Cavalcante, R.B.; Campos-do-Carmo, G.; Ramos-E-Silva, M. Dermoscopy of multiple radiation-induced basal cell carcinomas in a patient treated previously for pinealoma. *J. Dermatol. Case Rep.* **2014**, *8*, 115–117. [CrossRef] [PubMed]
63. Park, J.H.; Jo, J.Y.; Park, H.; Kim, I.H. Dermoscopic and histopathologic analysis of the correlation between the pigmentation of basal cell carcinoma and tumor aggressiveness. *Ann. Dermatol.* **2023**, *35*, 451–460. [CrossRef] [PubMed]
64. Kinnera, B.; Devi, V.N.; Satyanarayana, V.V.V. The dermoscopy of pigmented basal cell carcinoma. *J. Cutan. Aesthet. Surg.* **2020**, *13*, 365–367. [CrossRef] [PubMed]
65. Tabanlıoğlu Onan, D.; Sahin, S.; Gököz, O.; Erkin, G.; Cakır, B.; Elçin, G.; Kayıkçıoğlu, A. Correlation between the dermoscopic and histopathological features of pigmented basal cell carcinoma. *J. Eur. Acad. Dermatol. Venereol.* **2010**, *24*, 1317–1325. [CrossRef]
66. Demirtaşoğlu, M.; Ilknur, T.; Lebe, B.; Kuşku, E.; Akarsu, S.; Ozkan, S. Evaluation of dermoscopic and histopathologic features and their correlations in pigmented basal cell carcinomas. *J. Eur. Acad. Dermatol. Venereol.* **2006**, *20*, 916–920. [CrossRef] [PubMed]
67. Manca, R.; Dattolo, A.; Valenzano, F.; Castriota, M.; Martella, A.; Galdo, G.; Argenziano, G.; Abeni, D.; Fania, L. Proposal of a new dermoscopic criterion for pigmented basal cell carcinoma: A multicentre retrospective study. *Dermatol. Rep.* **2023**, *16*, 9691. [CrossRef] [PubMed]
68. Wolner, Z.J.; Bajaj, S.; Flores, E.; Carrera, C.; Navarrete-Dechent, C.; Dusza, S.W.; Rabinovitz, H.S.; Marchetti, M.A.; Marghoob, A.A. Variation in dermoscopic features of basal cell carcinoma as a function of anatomical location and pigmentation status. *Br. J. Dermatol.* **2018**, *178*, e136–e137. [CrossRef] [PubMed]
69. Xavier-Júnior, J.C.C.; Ocanha-Xavier, J.P.; Camilo-Júnior, D.J.; Pires D'ávilla, S.C.G.; Mattar, N.J. Is pigmented BCC a unique histological variant or is it only a clinical presentation? *Australas. J. Dermatol.* **2020**, *61*, 80–81. [CrossRef] [PubMed]
70. Sgouros, D.; Rigopoulos, D.; Panayiotides, I.; Apalla, Z.; Arvanitis, D.K.; Theofili, M.; Theotokoglou, S.; Syrmali, A.; Theodoropoulos, K.; Pappa, G.; et al. Novel insights for patients with multiple basal cell carcinomas and tumors at high risk for recurrence: Risk factors, clinical morphology, and dermatoscopy. *Cancers* **2021**, *13*, 3208. [CrossRef] [PubMed]
71. Cuellar, F.; Vilalta, A.; Puig, S.; Palou, J.; Zaballos, P.; Malvehy, J. Dermoscopy of early recurrent basal cell carcinoma. *Arch. Dermatol.* **2008**, *144*, 1254. [CrossRef] [PubMed]
72. Pogorzelska-Dyrbuś, J.; Salwowska, N.; Bergler-Czop, B. Dermoscopic pattern of basal cell carcinoma in H- and non-H-zones. *Dermatol. Pract. Concept.* **2023**, *13*, e2023125. [CrossRef] [PubMed]
73. Rana, H.; Stokkermans, T.J.; Purt, B.; Chou, E. Malignant Eyelid Lesions. In *StatPearls*; StatPearls Publishing: Treasure Island, FL, USA, 2024. Available online: https://www.ncbi.nlm.nih.gov/books/NBK551710 (accessed on 15 November 2024).
74. Pogorzelska-Dyrbuś, J.; Salwowska, N.; Bergler-Czop, B. Vascular pattern in dermoscopy of basal cell carcinoma in the H- and non-H-zone. *Postep. Dermatol. Alergol.* **2023**, *40*, 273–276. [CrossRef] [PubMed]
75. Vaccari, S.; Barisani, A.; Schiavi, C.; Baraldi, C.; Pepe, F.; Roda, M.; Patrizi, A.; Tosti, G. Basal cell carcinoma of the eyelid margin: Dermoscopic clues in a case series. *Dermatol. Ther.* **2021**, *34*, e15006. [CrossRef] [PubMed]
76. Cinotti, E.; La Rocca, A.; Labeille, B.; Grivet, D.; Lambert, V.; Kaspi, M.; Nami, N.; Cambazard, F.; Fimiani, M.; Thuret, G.; et al. Dermoscopy for the diagnosis of eyelid margin tumours. *Br. J. Dermatol.* **2019**, *181*, 397–398. [CrossRef] [PubMed]
77. Williams, N.M.; Navarrete-Dechent, C.; Marghoob, A.A.; Abarzua-Araya, Á.; Salerni, G.; Jaimes, N. Differentiating basal cell carcinoma from intradermal nevi along the eyelid margin with dermoscopy: A case series. *J. Am. Acad. Dermatol.* **2021**, *84*, 173–175. [CrossRef] [PubMed]
78. Jaworska, K.; Sławińska, M.; Wyszomirski, A.; Lakomy, J.; Sobjanek, M. Dermoscopic features of eyelid margin tumors: A single-center retrospective study. *J. Dermatol.* **2022**, *49*, 851–861. [CrossRef]
79. Fujii, M.; Harimoto, A.; Namiki, T. Basal cell carcinoma of the nipple-areola complex with multiple lesions: Possible causative role of radiation. *J. Dtsch. Dermatol. Ges.* **2018**, *16*, 193–195. [CrossRef] [PubMed]

80. Kitamura, S.; Hata, H.; Yamaguchi, Y.; Imafuku, K.; Yanagi, T.; Shimizu, H. The unique dermoscopic structure 'Large black web' in basal cell carcinoma on the areola. *J. Eur. Acad. Dermatol. Venereol.* **2016**, *30*, e221–e223. [CrossRef]
81. Ramirez, P.; Sendagorta, E.; Feito, M.; Gonzalez-Beato, M.; Mayor, M.; Pizarro, A. Umbilical basal cell carcinoma in a 21-year-old man: Report of an exceptional case and dermatoscopic evaluation. *Dermatol. Online J.* **2011**, *17*, 16. Available online: https://pubmed.ncbi.nlm.nih.gov/21272507 (accessed on 15 November 2024). [CrossRef]
82. Machida, M.; Ansai, S.; Hida, Y.; Kubo, Y.; Arase, S.; Kuramoto, K. Basal cell carcinoma arising on the palm. *J. Dermatol.* **2011**, *38*, 94–96. [CrossRef]
83. Dávila, J.J.; Aguilar, K.; Cabrera, F.; Boadas, A. Dermoscopic features of acral basal cell carcinoma. *Int. J. Dermatol.* **2019**, *58*, e54–e55. [CrossRef] [PubMed]
84. Tavares, L.L.; Costa, J.C.M.D.; Delcourt, N.C.; Rodrigues, N.C.D.S. Periungual basal cell carcinoma. *An. Bras. Dermatol.* **2018**, *93*, 114–115. [CrossRef] [PubMed]
85. Bertaina, C.; Salerni, G.; Celoria, M.; Lombardo, S.; Gorosito, M.; Molteni, A.; Fernández-Bussy, R. Dermoscopy of pigmented vulvar basal cell carcinoma. *Dermatol. Pract. Concept.* **2019**, *9*, 239–240. [CrossRef]
86. Cinotti, E.; Tonini, G.; Perrot, J.L.; Habougit, C.; Luisi, S.; Rubegni, P. Dermoscopic and reflectance confocal microscopy features of two cases of vulvar basal cell carcinoma. *Dermatol. Pract. Concept.* **2018**, *8*, 68–71. [CrossRef]
87. de Giorgi, V.; Massi, D.; Mannone, F.; Checcucci, V.; De Magnis, A.; Sestini, S.; Papi, F.; Lotti, T. Dermoscopy in vulvar basal cell carcinoma. *Arch. Dermatol.* **2007**, *143*, 426–427. [CrossRef] [PubMed]
88. Dobrosavljevic Vukojevic, D.; Djurisic, I.; Lukic, S.; Kastratovic-Kotlica, B.; Vukicevic, J. Dermatoscopy in vulvar basal cell carcinoma. *J. Eur. Acad. Dermatol. Venereol.* **2017**, *31*, e180–e181. [CrossRef]
89. Scotti, B.; Vaccari, S.; Maltoni, L.; Robuffo, S.; Veronesi, G.; Dika, E. Clinic and dermoscopy of genital basal cell carcinomas: A retrospective analysis among 169 patients referred with genital skin neoplasms. *Arch. Dermatol. Res.* **2024**, *316*, 307. [CrossRef] [PubMed]
90. Song, Z.; Wang, Y.; Meng, R.; Chen, Z.; Gao, Y.; An, X.; Yang, J.; Yin, Y.; Chen, L.; Xin, L.; et al. Clinical and dermoscopic variation of basal cell carcinoma according to age of onset and anatomic location: A multicenter, retrospective study. *Arch. Dermatol. Res.* **2023**, *315*, 1655–1664. [CrossRef] [PubMed]
91. Wang, W.E.; Chen, Y.T.; Wang, C.H.; Wang, J.H.; Chang, C.H. Dermoscopic features of pigmented basal cell carcinoma according to size. *Int. J. Dermatol.* **2024**, *63*, 916–921. [CrossRef] [PubMed]
92. Kinzel-Maluje, F.; González-Godoy, D.; Vargas-Mora, P.; Muñoz, P. Dermoscopy of small diameter basal cell carcinoma: A case-control study. *An. Bras. Dermatol.* **2024**, *99*, 111–114. [CrossRef] [PubMed]
93. Foltz, E.; Ludzik, J.; Witkowski, A. Dermoscopy and reflectance confocal microscopy-augmented characterization of pigmented micro-basal cell carcinoma (less than 2 mm diameter). *Skin Res. Technol.* **2023**, *29*, e13250. [CrossRef]
94. Sykes, A.J.; Wlodek, C.; Trickey, A.; Clayton, G.L.; Oakley, A. Growth rate of clinically diagnosed superficial basal cell carcinoma and changes in dermoscopic features over time. *Australas. J. Dermatol.* **2020**, *61*, 330–336. [CrossRef] [PubMed]
95. Persechino, F.; Franceschini, C.; Iorio, A.; Carbone, A.; Ferrari, A.; Buccini, P.; Piemonte, P.; Eibenschutz, L.; Sperduti, I.; Cota, C.; et al. Clinical management of very small pigmented lesions: Improved clinical outcome through dermoscopy and reflectance confocal microscopy combination. *Skin Res. Technol.* **2020**, *26*, 718–726. [CrossRef] [PubMed]
96. Ishizaki, S.; Tanaka, M.; Dekio, I.; Sawada, M.; Fujibayashi, M.; Shimizu, S. The contribution of dermoscopy to early excision of basal cell carcinoma: A study on the tumor sizes acquired between 1998 and 2013 at a university hospital in Japan. *J. Dermatol. Sci.* **2016**, *84*, 360. [CrossRef]
97. Longo, C.; Specchio, F.; Ribero, S.; Coco, V.; Kyrgidis, A.; Moscarella, E.; Ragazzi, M.; Peris, K.; Argenziano, G. Dermoscopy of small-size basal cell carcinoma: A case-control study. *J. Eur. Acad. Dermatol. Venereol.* **2017**, *31*, e273–e274. [CrossRef]
98. Takahashi, A.; Hara, H.; Aikawa, M.; Ochiai, T. Dermoscopic features of small size pigmented basal cell carcinomas. *J. Dermatol.* **2016**, *43*, 543–546. [CrossRef] [PubMed]
99. Popadić, M.; Vukićević, J. What is the impact of tumour size on dermoscopic diagnosis of BCC? *J. Eur. Acad. Dermatol. Venereol.* **2015**, *29*, 2474–2478. [CrossRef]
100. Sanchez-Martin, J.; Vazquez-Lopez, F.; Perez-Oliva, N.; Argenziano, G. Dermoscopy of small basal cell carcinoma: Study of 100 lesions 5 mm or less in diameter. *Dermatol. Surg.* **2012**, *38*, 947–950. [CrossRef]
101. Xu, L.J.; Zheng, L.L.; Zhu, W. Effect of tumor size on dermoscopic features of pigmented basal cell carcinoma. *Chin. Med. J.* **2021**, *134*, 1866–1868. [CrossRef] [PubMed]
102. Khalili, M.; Mirahmadi, S.; Shamsimeymandi, S.; Dabiri, S.; Amiri, R.; Rezaei Zadeh Rukerd, M.; Aflatoonian, M. Diagnostic value of dermoscopic structures in predicting superficial basal cell carcinoma in the skin of color. *Adv. Biomed. Res.* **2024**, *13*, 23. [CrossRef]
103. Vinay, K.; Ankad, B.S.; Narayan, R.V.; Chatterjee, D.; Bhat, Y.J.; Neema, S.; Shah, S.; Chauhan, P.; Khare, S.; Rajput, C.; et al. A multicentric study on dermoscopic patterns and clinical-dermoscopic-histological correlates of basal cell carcinoma in Indian skin. *Clin. Exp. Dermatol.* **2022**, *47*, 1982–1990. [CrossRef]

104. Manci, R.N.; Dauscher, M.; Marchetti, M.A.; Usatine, R.; Rotemberg, V.; Dusza, S.W.; Marghoob, A.A. Features of skin cancer in Black individuals: A single-institution retrospective cohort study. *Dermatol. Pract. Concept.* **2022**, *12*, e2022075. [CrossRef]
105. Behera, B.; Kumari, R.; Thappa, D.M.; Gochhait, D.; Srinivas, B.H.; Ayyanar, P. Dermoscopic features of basal cell carcinoma in skin of color: A retrospective cross-sectional study from Puducherry, South India. *Indian J. Dermatol. Venereol. Leprol.* **2023**, *89*, 254–260. [CrossRef] [PubMed]
106. Enechukwu, N.A.; Ogun, G.O.; Ezejiofor, O.I.; Chukwuanukwu, T.O.; Yaria, J.; George, A.O.; Ogunbiyi, A.O. Histopathologic patterns of cutaneous malignancies in individuals with oculocutaneous albinism in Anambra state, Nigeria: A paradigm swing? *Ecancermedicalscience* **2020**, *14*, 1013. [CrossRef]

cancers

MDPI

Review

Dermoscopy of Basal Cell Carcinoma Part 3: Differential Diagnosis, Treatment Monitoring and Novel Technologies

Irena Wojtowicz and Magdalena Żychowska *

Department of Dermatology, Faculty of Medicine, Collegium Medicum, University of Rzeszów, 35-310 Rzeszów, Poland; wojtowicz.irena.maria@gmail.com
* Correspondence: magda.zychowska@gmail.com

Simple Summary: Basal cell carcinoma (BCC) is the most common skin cancer, but its diagnosis can be challenging due to overlapping features with other skin conditions. Dermoscopy is a key tool for preliminary diagnosis. It helps to differentiate BCC from other lesions, plan treatment, monitor the efficacy of therapies and identify recurrences. New technologies, such as ultraviolet-induced fluorescence dermoscopy (UVFD) and optical super-high magnification dermoscopy (OSHMD), show promise in improving diagnostic accuracy. However, some BCCs remain indistinguishable with dermoscopy, emphasizing that histopathology remains the gold standard for confirming the diagnosis.

Abstract: Introduction: Basal cell carcinoma (BCC) is the most frequently diagnosed skin cancer globally. Despite the well-established dermoscopic features of BCC, overlapping characteristics with other benign and malignant skin conditions cause challenges in differential diagnosis. Part III of this review highlights the role of dermoscopy in differential diagnosis, treatment planning, therapy monitoring and the integration of novel technologies including ultraviolet-induced fluorescence dermoscopy (UVFD) and optical super-high magnification dermoscopy (OSHMD). **Methods:** A search of the PubMed database was conducted for studies reporting on advances in the dermoscopic assessment of BCC, including differential diagnosis, treatment, monitoring and novel diagnostic technologies. **Results:** Even entities with well-defined dermoscopic features distinguishing them from BCC can sometimes mimic BCC. Additionally, rare lesions such as neurothekeoma, reticulohistiocytoma, solitary circumscribed neuroma, dermal leiomyosarcoma and various adnexal tumors often remain dermoscopically indistinguishable from BCC, which underscores the importance of histopathology as the diagnostic gold standard. Dermoscopy aids in delineating the tumor margins, optimizing Mohs micrographic surgery (MMS) and traditional excision. It may also help to monitor therapeutic effects by detecting the disappearance of BCC patterns, the presence of residual tumor or recurrences. Dermoscopy may aid in the prediction of therapeutic responses to imiquimod, photodynamic therapy or vismodegib. UVFD and OSHMD appear to be valuable complementary diagnostic techniques for detecting BCC. UVFD seems to be particularly valuable for the detection of small tumors (<5 mm), facial lesions and nodular or non-pigmented BCC subtypes, while OSHMD is useful for the assessment of superficial and non-pigmented BCCs. Three-dimensional total-body photography enhances diagnostic precision but, so far, only when used in combination with traditional dermoscopy. **Conclusions:** Dermoscopy is valuable for margin delineation, therapy monitoring and differential diagnosis but can be inconclusive, which highlights the role of histopathology as the gold standard. Modifications in dermoscopy technique may further enhance its accuracy.

Academic Editor: Alfonso Baldi

Received: 19 February 2025
Revised: 14 March 2025
Accepted: 16 March 2025
Published: 19 March 2025

Citation: Wojtowicz, I.; Żychowska, M. Dermoscopy of Basal Cell Carcinoma Part 3: Differential Diagnosis, Treatment Monitoring and Novel Technologies. *Cancers* **2025**, *17*, 1025. https://doi.org/10.3390/cancers17061025

Keywords: dermoscopy; dermatoscopy; basal cell carcinoma; BCC; ultraviolet-induced fluorescence dermoscopy; UVFD; UV-dermoscopy; UV-dermatoscopy; optical super-high magnification dermoscopy; OSHMD

1. Introduction

Basal cell carcinoma (BCC) remains the most common skin cancer worldwide, accounting for 80–90% of all such tumors [1]. Currently, approximately 20% of individuals will develop BCC in their lifetime, with the risk increasing with age [2]. Additionally, men are more prone to developing BCC than women [1]. Its diagnosis and management continue to evolve due to advances in dermoscopy and imaging technologies [1,3]. While the dermoscopic features of BCC are well-established, challenges in differential diagnosis arise due to overlapping characteristics with other benign and malignant skin conditions [4,5]. Furthermore, the accurate delineation of tumor margins and monitoring of therapeutic outcomes are critical for optimizing patient care. Recent developments, including ultraviolet-induced fluorescence dermoscopy (UVFD) and optical super-high magnification dermoscopy (OSHMD), have introduced new opportunities for enhancing diagnostic and treatment precision. Part III of this review focuses on the dermoscopic findings relevant to the differential diagnosis of BCC, the role of dermoscopy in treatment planning and therapy monitoring, and the potential of novel diagnostic techniques as modifications of traditional dermoscopy.

2. Methods

In September 2024, PubMed database was searched for English publications available since the database onset using the search terms: (BCC OR basal cell carcinoma OR basalioma) AND (dermoscopy OR dermatoscopy). The exclusion criteria included: not relevant papers, reviews and meta-analyses, no full text available, no English-language version available. The authors (I.W. and M.Ż.) performed the screening of the abstracts first, and, if the article was considered relevant, the full texts and the references of the articles were reviewed. The literature search and selection of included papers was performed according to the PRISMA (preferred reporting items for systematic reviews and meta-analyses) guidelines. Details are presented in Figure 1.

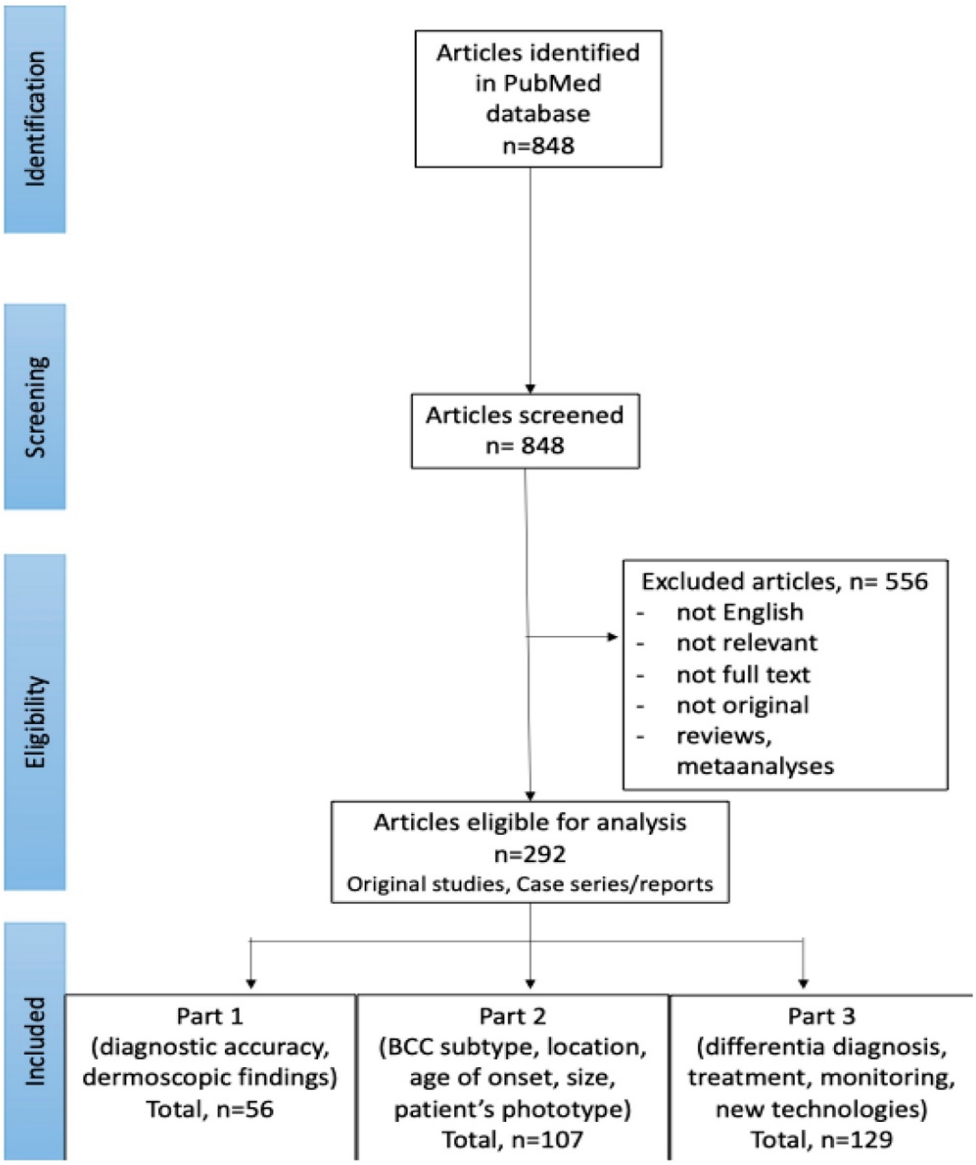

Figure 1. PRISMA flow chart of the literature search and article selection (available also: Wojtowicz I.; Żychowska M. [4,6]).

3. Results

Of the 848 studies initially identified through the literature search, 292 were selected for further review. Among these, 129 articles focused on advances in the dermoscopic assessment of BCC, including differential diagnosis, treatment, monitoring of therapeutic efficacy and novel diagnostic technologies, and were included in Part 3 of the Review.

3.1. Differential Diagnosis

We included 129 studies on entities that may be challenging to differentiate from BCC. While the dermoscopic features of BCC are well-established and extensively studied, the dermoscopic diagnosis of BCC is not always straightforward [4]. Even arborizing vessels, one of the most characteristic findings, can appear in other lesions. Jin et al. demonstrated that arborizing vessels may also be present in various tumors, mainly epidermal cysts, hypertrophic scars/keloids, intradermal nevi and actinic keratoses, as well as in conditions like necrobiosis lipoidica, morphea and porokeratosis. The authors found that arborizing

vessels in BCC are focused (bright red and passing over the central parts of the lesion), while in non-BCC lesions they are unfocused (blurred in color and distributed at the periphery of the lesion), have fewer branches, and show a sharper decrease in vessel diameter from the stem to the first branch [5].

Dermoscopy, while not always conclusive, significantly narrows the differential diagnosis. Often, the clinical–dermoscopic correlation can lead to the diagnosis of a specific condition [7,8]. When uncertainty persists, histopathology remains the gold standard for establishing a definitive diagnosis.

3.1.1. Intradermal Nevi

A study analyzing 77 intradermal nevi (IDN) and 118 BCCs found that IDN most frequently exhibited hair (83.3%), brown pigment (79.5%), comma-shaped vessels (66.7%) and brown globules (66.7%). Hairpin vessels were observed in 25.6% of IDN. In contrast, BCCs commonly displayed large arborizing vessels (94.1%), microvessels (89%) and structureless hypopigmented areas. Focused vessels were identified as a key feature for diagnosing BCC [9]. On the eyelid margin, nearly half of BCCs caused eyelash disruption, while IDN did not. Additionally, 25% of IDN showed arborizing vessels. Lesions with a pink background or eyelash disruption suggested BCC, whereas a brown background or globules indicated IDN [10].

3.1.2. Melanocytic Nevi

In a study in Chinese patients on 3503 lesions, which were clinically diagnosed as melanocytic nevi (MN), 2.5% of them were histopathologically found to be malignant, with the predominant diagnosis of BCC (84.9% of malignant diagnoses) [11]. Key differences between BCCs and MN include vascular features, pigmentation and ulceration. BCC typically shows prominent arborizing vessels, while MN exhibit more regular vascular structures or may lack visible vasculature. In terms of pigmentation, BCC displays rather aggregated structures like blue-gray ovoid nests or maple leaf-like areas, whereas MN are characterized by organized reticular pigmentation or homogeneous coloration. Ulceration is common in BCC, particularly in aggressive subtypes, but is rare in MN [12].

3.1.3. Actinic Keratosis

Exposure to ultraviolet (UV) rays is a key etiopathogenetic factor for both actinic keratosis (AK) and BCC, with over 30% of patients having both types of lesions simultaneously [13]. Di Carlo et al. identified the strawberry pattern, red pseudonetwork and keratotic hair follicles as the main dermoscopic criteria for AK. However, dermoscopy failed to differentiate between AK and BCC in 22% of cases [13]. Tschandl et al. noted that the most valuable dermoscopic clues for differentiating pigmented AK from other lesions were the presence of scales, white circles and a sharply demarcated border [14].

3.1.4. Bowen's Disease

Dermoscopy aids in the differentiation of the two nonpigmented skin cancers, SCC in situ (Bowen's disease, BD) and superficial BCC (sBCC), which can clinically look very similar. BD typically presents with dotted or glomerular vessels, while sBCC is characterized by leaf-like areas, spoke-wheel areas, concentric structures and arborizing vessels. However, when sBCC occurs on the lower extremities, it may also display dotted vessels, making differentiation more challenging. In such cases, clinicians should consider short fine telangiectasias (SFT) and white shiny blotches or strands as additional indicators of sBCC [15,16].

3.1.5. Squamous Cell Carcinoma

Squamous cell carcinoma (SCC) is more frequently misdiagnosed as BCC than the other way round. Factors such as pigmentation and an elevated border contribute to SCC being mistaken for BCC, while the presence of scaling may lead to BCC being misidentified as SCC [17]. SCC can exhibit dermoscopic features resembling BCC, including multiple linear-branching vessels over a pinkish-reddish background, blue-gray ovoid nests and short white streaks, creating a clinical, dermoscopic and even confocal appearance similar to BCC [18]. A cystic-variant keratoacanthoma (KA)-type SCC was reported to present with a central pinpoint white crust, mimicking nodular BCC or an acneiform lesion. In such cases, optical coherence tomography (OCT) enabled the preliminary diagnosis of SCC [19]. Additionally, erosions are more commonly associated with BCC, whereas scales and keratin masses are indicative of SCC [20].

3.1.6. Seborrheic Keratosis

Seborrheic keratosis (SK) typically shows dermoscopic features such as thick lines (fissures and ridges), black-to-brown clods (comedo-like openings), white clods (milia-like cysts) and hairpin vessels with white halos [21]. Takenouchi reported that approximately 85% of SK lesions in a study involving Japanese patients showed at least one of the first three features mentioned above [22]. However, certain SK variants, including irritated/inflamed SK [21,23], pigmented clonal SK [24] and adenoid SK [25], may mimic pigmented BCC (pBCC). Irritated or inflamed SK can present with chaotic multi-colored plaques, erosions/ulcerations, pinkish-white areas, brown-gray dots, blue-gray globules or arborizing telangiectasia [21,23]. In one case, pigmented clonal SK clinically resembled pBCC but was easily diagnosed dermoscopically by the presence of multiple milia-like cysts, potentially preventing unnecessary surgery [24]. Adenoid SK, in contrast, closely mimicked pBCC even in dermoscopy, displaying blue-gray globules, leaf-like areas and hairpin vessels without white halos, with histopathology required for confirmation [25]. In the large study conducted by Zhang et al. in 2024, 1089 samples clinically diagnosed as SK were analyzed, and notably, 5.7% were identified as malignant tumors, with half of them being BCCs [11]. A rare keratotic BCC variant, described in one case by Yanagihara et al., mimicked SK dermoscopically, showing dark violaceous to black botryoid structures with a partial gray-white veil and hyperkeratotic areas [26].

3.1.7. Lichenoid Keratosis

A study of 51 histopathologically confirmed lichenoid keratosis (LK) cases revealed that 52.9% were misdiagnosed preoperatively as BCC, with only 1.9% correctly identified. LK was categorized into six dermoscopic subtypes. The flat pigmented type displayed dotted and linear vessels with coarse bluish-grey granules, while the flat erythematous type showed dotted and linear vessels, milky red-white areas, and structures with a cerebriform appearance. Plaque-like LK featured short, pigmented lines, comedo-like openings, spoke-wheel areas, and coarse brown granules. Morpheaform LK presented with telangiectasias and short pigmented lines, while papulo-keratotic LK showed brownish globules, cerebriform patterns, eccentric or central hyperpigmentation and short pigmented lines. Nodular LK exhibited white scar-like areas, comedo-like openings and blue ovoid nests. Telangiectasias in LK were fewer, non-arborizing, and less focused than in BCC. Blue ovoid nests appeared only in nodular LK, while grey-blue granules in LK were coarser and more regularly distributed. The authors concluded that differentiating BCC from LK might be challenging when dermoscopic features specific for BCC, such as maple leaf–like areas, ovoid nests and spoke-wheel structures, are lacking [27].

3.1.8. Melanoma

sBCC misdiagnosed as malignant melanoma (MM) often displays atypical network (55.9%) and regression structures (35.5%), while non-sBCCs typically show atypical vascular pattern (58.8%) and irregular blotches (58.8%) [28]. Pigmented fibroepithelioma of Pinkus can mimic MM due to dermoscopic features such as circumferential radial lines, eccentric black areas, gray-black dots and clods, white lines, bluish-gray structureless areas and pigmented fenestrated structures resembling an atypical, pigmented network [29,30].

BCCs on the lower extremities may present overlapping features with MM, including shiny white streaks, linear vessels, or blue-black granular pigmentation. Shiny white streaks are seen in both conditions, while linear vessels could be interpreted as the dilated vessels of BCC or the irregular vessels of MM. Blue-black granular pigmentation, commonly associated with regression in melanocytic lesions, can also be misleading [31]. Similarly, MM can mimic BCC. For example, nodular MM on the upper eyelid was reported to display blue-gray ovoid nests, ulceration, arborizing vessels, comedo-like openings, and "moth-eaten" borders. Asahara et al. emphasized that typical dermoscopic features of pBCCs can also appear in melanomas [32].

A prospective study on 240 flat pigmented facial lesions found that circles were predictive of lentigo maligna, while clods were linked to BCC and gray coloration strongly indicated malignancy on the face. In the aforementioned study, dermoscopic clues that were almost exclusive to BCC included branched or serpentine vessels, and ulceration [14].

Vascular patterns require careful analysis. Non-/hypopigmented nodular melanoma typically exhibits densely packed vessels of small diameter, while non-/hypopigmented nodular BCC is characterized by arborizing vessels of larger caliber with lower density [33]. Di Matteo et al. developed a scoring system for distinguishing MM from BCC, based on 12 dermoscopic features. Features suggestive of MM received positive scores: regression structures (+3), irregular dots or globules (+3), irregular blotches (+2), irregular streaks (+2), white-red structureless areas (+1), and white streaks (+1). Features indicative of BCC received negative scores: spoke-wheel areas (−1), in-focus dots (−1), multiple blue-gray globules (−1), arborizing vessels (−2), concentric structures (−3), and maple leaf-like areas (−3). A total score greater than 2 was suggestive of MM, while a score of 2 or less indicated BCC. The model achieved a sensitivity of 94.08% and specificity of 79.45% [34].

3.1.9. Adnexal Tumors

Trichoblastoma

No single dermoscopic feature is pathognomonic for trichoblastoma (TB); however, the presence of fine, short, poorly branching telangiectasia can help differentiate it from nodular BCC, which typically exhibits more prominent arborizing vessels [35]. In a study comparing 502 BCC cases with 61 trichoblastic tumors (TT), including TB, trichoepithelioma (TE) and desmoplastic trichoepithelioma (DTE), ulceration was found to be less frequently present in TT under dermoscopy. Pigmented structures, particularly brown dots and globules, were significantly more common in TT. Additionally, TT more frequently displayed cloudy or starry milia-like cysts and yellow globules. Nevertheless, histopathological examination remains the gold standard for differentiating between BCC and TT [36]. Histologically, TB should also be distinguished from trichoblastic BCC (tBCC) [37]. Ghigliotti et al. found that blue-gray ovoid nests and blue-gray globules were much more frequently observed in tBCC than in TB [38].

Trichoepithelioma

TE, a histopathological variant of TB, is classified into three subtypes: solitary, multiple and DTE [35,39,40]. TE can mimic BCC both clinically and dermoscopically [39–41] and,

reversely, BCC can mimic TE [42]. Both tumors may display arborizing vessels; however, in DTE, these vessels are typically sparsely branched, contrary to the more prominent arborizing vessels often seen in BCC [42]. TE is characterized by a pearl-white background within the lesion, particularly in the desmoplastic variant. Additional features may include multiple milia-like cysts or keratin cysts, and an absence of BCC-specific structures such as leaf-like areas and ovoid nests [39,40]. Dermoscopic findings should always be evaluated alongside clinical information, including the patient's age and the lesion's growth pattern. TE commonly appears in young adults and exhibits a very slow growth rate, while BCC generally arises in individuals over 50 and shows a more significant and gradual increase in size [39,41].

Trichoadenoma

Trichoadenoma was reported to dermoscopically resemble BCC. The dermoscopic findings in trichoadenoma included shiny white lines, a blue-gray ovoid area, diffuse, in-focus linear vessels and small whitish circles with a diffuse distribution. The latter has been previously described in adnexal tumors but is considered to be absent in BCCs [43].

Trichilemmoma

Trichilemmomas typically develop over long-standing nevus sebaceous and are typically non-pigmented. However, pigmented desmoplastic trichilemmoma may mimic dermoscopically pBCC. In a single case report of pigmented desmoplastic tricholemmoma, multiple pigmented dots, a gray-blue globule, a pink structureless area, shiny white lines and rosettes were observed [44].

Basaloid Follicular Hamartoma

Linear and unilateral basaloid follicular hamartoma (BFH) is a rare condition presenting as papules and plaques along Blaschko's lines. Although benign, it carries a long-term risk of BCC arising within the lesion [45,46]. Dermoscopy of BFH may reveal rounded structures containing brown-gray linear and arciform elements, globules, dots, spoke wheel–like structures without a central dark point, keratotic plugs, irregular crown vessels, short fine telangiectasias and structureless areas with telangiectasias. These features alone cannot reliably differentiate BFH from BCC. However, the presence of arborizing vessels, blue-gray ovoid nests, ulcerations, erosions, spoke wheel areas with central dark points, concentric structures and white streaks can aid in distinguishing BCC from BFH [45].

Inverted Follicular Keratosis

Cases featuring a yellowish-white amorphous central area surrounded by a radial arrangement of polymorphic vascular patterns, including arborizing vessels, linear irregular vessels and corkscrew vessels, could be misdiagnosed as BCC [47].

Poroma

Poromas typically appear as non-pigmented nodules, although 17% may exhibit pigmentation, mimicking pBCC by presenting arborizing vessels and large blue-gray ovoid nests [48–52]. While histopathology remains the gold standard for diagnosis, dermoscopy can provide valuable clues. Unlike pBCC, poromas lack maple leaf-like structures and spoke-wheel areas and their arborizing vessels are less prominent with fewer branches. Additionally, pigmented poromas often exhibit regular shapes, sharply demarcated nodules and smooth-edged blue-gray ovoid nests, whereas pBCCs are more likely to display irregularities, such as unclear boundaries and rough-edged blue-gray ovoid nests [48,51,52].

Spiradenoma

Spiradenoma, a painful skin tumor, shows arborizing vessels and blue clods on a pink-to-red background under dermoscopy. Distinguishing features between spiradenomas and pBCCs include telangiectasias with minimal branching in spiradenomas and pure blue clods, compared to the blue-gray in pBCC [53,54].

Tubular Apocrine Adenoma

Ito et al. described a case of tubular apocrine adenoma (TAA) presenting on dermoscopy with short fine telangiectasias (SFTs) and large blue-gray ovoid nests arranged in a floriform pattern. The authors emphasized that the combination of such findings is rarely seen in BCC. They proposed that the coexistence of SFTs and mature large blue-gray ovoid nests in a floriform arrangement may be a distinguishing dermoscopic feature of TAA [55].

Pilomatricoma

Pilomatricomas can occasionally mimic BCC on dermoscopy, especially in elderly patients. The most common dermoscopic pattern in pilomatricomas includes irregular white structures, white streaks, polymorphous or atypical vessels, ulceration, structureless gray-blue areas and absence of specific dermoscopic criteria for other skin tumors [56].

Sebaceoma

Sebaceoma is characterized dermoscopically by yellow structures, such as a yellow-pinkish or yellow-white background and yellow homogeneous areas, accompanied by less bright red crown vessels. In contrast, BCC typically presents with bright red, sharply focused arborizing vessels, blue-gray dots, globules or nests and lacks the yellowish background seen in sebaceoma [57].

Sebaceous Carcinoma

Dermoscopy of sebaceous carcinoma reveals a polymorphic vessel pattern along with whitish-pink areas, yellowish structures and yellowish structureless areas. The presence of yellowish structures is a key dermoscopic feature that helps differentiate sebaceous carcinoma from BCC [58].

Apocrine Hidrocystoma

According to Hidalgo et al., dermoscopy can help differentiate BCC from apocrine hidrocystoma (AH) on the eyelid. BCC typically shows eyelash destruction and in-focus arborizing telangiectasias. In contrast, although AH is clinically similar, dermoscopy reveals translucent homogeneous areas, linear whitish structures and no eyelash involvement [59].

Microcystic Adnexal Carcinoma

This malignant adnexal carcinoma presents on dermoscopy with a central pinkish-white structureless area, overlying scale-crusts and hemorrhage, sharply in-focus arborizing vessels, yellow-white clods and gray-brown dots, features that mimic BCC. Notably, the presence of "whitish clods", which are absent in BCC, may aid in preliminary identification of microcystic adnexal carcinoma [60].

3.1.10. Dermatofibroma

A study analyzing dermatofibromas (DF) found that 3.8% exhibited a "BCC-like" pattern, characterized by arborizing vessels, blue-gray ovoid nest-like structures or peripheral brown-black leaf-like structures [61].

3.1.11. Linear Lesions—Scars, Scratches/Erosions and Tattoos

Linear BCC (LBCC) is a rare morphologic variant of BCC, defined by a length-to-width ratio of at least 3:1, as noted by Navarrete-Dechent et al. Clinically, LBCC can mimic scars, scratches, erosions, or even tattoos, leading to potential misdiagnosis. While no unique dermoscopic features have been identified for this subtype, dermoscopy frequently reveals pigmentation (83.3%) with blue-grey globules being the most common finding, helping in accurate diagnosis [8].

3.1.12. Acne Vulgaris

BCC can occasionally mimic acneiform lesions, especially in fair-skinned older adults. Dermoscopically, acne papules typically display a neutral yellow background, central punctum and arborizing-like vessels. However, in excoriated lesions, the neutral yellow background may resemble the yellow ulceration of BCC, and the presence of arborizing-like vessels may further lead to misdiagnosis [19].

3.1.13. Psoriasis

Patients with psoriasis often undergo phototherapy or immunosuppressive treatments, which can increase the risk of developing skin malignancies. Additionally, BCC can be easily overlooked among inflammatory psoriatic lesions. Dermoscopy proved to be highly valuable in these cases. Psoriatic lesions typically display a homogeneous vascular pattern consisting of red dots on a light-red background. The diagnostic accuracy can reach 99% when these features are present. In contrast, BCC exhibits characteristic dermoscopic features, including arborizing vessels, short fine telangiectasias, erosions, blue-gray dots and/or milky-pink background [62–65].

3.1.14. Acrochordons

Acrochordons, also known as skin tags, are benign, pedunculated neoplasms commonly found on the neck, axillae, or groin and are generally simple to diagnose clinically. However, atypical presentations can pose a diagnostic challenge. A solitary erythematous lesion with firm consistency located in the lumbar region may resemble fibroepithelioma of Pinkus, a rare variant of BCC that often occurs in the lumbosacral area. Dermoscopy of such ischemic acrochordons was reported to show regularly arranged dotted vessels on a violaceous background with bullae filled with serous fluid. In contrast, fibroepithelioma of Pinkus is more likely to exhibit fine arborizing vessels, sometimes accompanied by dotted vessels and white streaks [66].

3.1.15. Scarring Alopecia

Tomasini et al. reported on a case of progressive hair loss over five years, initially misdiagnosed as female androgenetic alopecia and treated with minoxidil. However, dermoscopy revealed a large (15 × 15 cm) BCC, characterized by multiple arborizing vessels, structureless hypopigmentation, and complete loss of follicular openings, leading to the correct diagnosis [67].

3.1.16. Granuloma Faciale

Flat-type granuloma faciale (GF) can present dermoscopically as diffuse orange structureless areas with elongated linear vessels resembling branching vessels, mimicking BCC. Unlike flat GF, raised GF may display follicular features [68]. Lallas et al. observed that GF vessels tend to be larger, more numerous, and arranged in parallel, with less extensive branching compared to BCC [69]. Savoia et al. reported cases of GF plaques, showing both wide and thin linear vessels with evident branching, further complicating differentiation.

Due to these similarities in arborizing vessels, histology remains essential for accurate diagnosis [68].

3.1.17. Vulvar Hidradenoma Papilliferum

Vulvar hidradenoma papilliferum was reported to exhibit dermoscopic features closely resembling non-pigmented BCC. In a single case, the lesion displayed a prominent vascular pattern, including well-focused arborizing vessels over a pinkish background and whitish areas. This similarity highlights the importance of histopathological confirmation to make an accurate diagnosis [70].

3.1.18. Trigeminal Trophic Syndrome

Ulceration on the face, characterized by a flat, well-demarcated, polygonal, erythematous outline with scattered short linear vessels and a base appearing irregularly raised, homogeneously reddish, with peripheral homogenous whitish areas and scarce chrysalis structures and vessels on dermoscopy, may initially suggest BCC. However, loss of pain and temperature sensation around the lesion and absence of typical BCC dermoscopic features should suggest trigeminal trophic syndrome, caused by damage to the sensory branches of the trigeminal nerve [71].

3.1.19. Cutaneous Metastasis

Kuraitis and Pei reported a case of cutaneous metastasis of renal cancer, showing a translucent papule with tortuous arborizing vessels and centrally located lacunae under dermoscopy. This vascular pattern closely mimicked BCC, making the diagnosis based on dermoscopy alone very difficult [72].

3.1.20. Mammary Carcinoma

Horikawa et al. described a case of pigmented invasive ductal carcinoma of the areola, mimicking BCC on dermoscopy. The lesion displayed blue-gray areas with white scales containing brown areas and brown to bluish-white globules surrounded by a hyperpigmented border on the periphery. The definite diagnosis was made using histopathology [73].

3.1.21. Cutaneous Histoplasmosis

Immunosuppressed patients can develop rare conditions with unusual presentations. One such case involved a patient treated with anti-TNF drugs for psoriasis for approximately three years. After discontinuing the treatment, a tumor appeared on the eyebrow. Dermoscopy suggested BCC due to the presence of arborizing telangiectasias at the lesion's periphery and superficial scaling. However, biopsy revealed structures characteristic of *Histoplasma capsulatum* [74].

3.1.22. Dermal Leiomyosarcoma

Lozano Salazar et al. reported a case of a tumor presenting as a raised, indurated, erythematous lesion with the destruction of eyebrow follicles and a surrounding firm, edematous border. Dermoscopy showed a homogeneous brown pattern. Although BCC was initially suspected, histopathology was consistent with the diagnosis of dermal leiomyosarcoma (derived from the hair erector muscle). The dermoscopic features of this entity have not been established to date [75].

3.1.23. Neuroma

Solitary circumscribed neuroma, also known as palisaded encapsulated neuroma (PEN), is a benign cutaneous tumor often misdiagnosed as BCC. Fernández-Crehuet et al. reported two cases—one of a BCC and one of a PEN—both exhibiting arborizing vessels

on a pink background under dermoscopy, with the definitive diagnosis confirmed by histopathology. The authors concluded that the presence of arborizing telangiectasia on a pink-white background should prompt the consideration of diagnoses other than BCC [76].

3.1.24. Reticulohistiocytoma

Reticulohistiocytoma, also referred to as solitary cutaneous reticulohistiocytosis, is a type of non-Langerhans cell histiocytosis that can mimic BCC in dermoscopy. Reticulohistiocytoma was reported to display arborizing vessels on a yellowish-pink background. This underscores the importance of histopathologic examination in confirming the diagnosis of BCC [77].

3.1.25. Targetoid Hemosiderotic Hemangioma

Targetoid hemosiderotic hemangiomas (THH) exhibit a characteristic dermoscopic pattern in 52% of cases, typically showing central lagoons surrounded by a yellowish circular intermediate area and a purple or ecchymotic peripheral ring, or central lagoons with a homogeneous peripheral area. However, Enei et al. reported a THH case initially misdiagnosed as BCC due to the presence of arborizing vessels and a bluish-gray ovoid structure [78].

3.1.26. Angiokeratoma

Angiokeratomas and pBCCs may be confused clinically and dermoscopically. Angiokeratomas typically display dark lacunae—multiple, well-defined, round or oval structures that are dark blue, violaceous or black—with no vascular structures inside. The features demonstrate high diagnostic accuracy (sensitivity: 93.8%; specificity: 99.1%). In contrast, pBCC may present with multiple, round or oval, poorly defined grayish-blue structures, distinct from typical large, blue-gray ovoid nests and mimicking lacunae. However, Zaballos Diego highlighted that the presence of arborizing vessels within the grayish-blue structures should prompt the diagnosis of pBCC [79].

3.1.27. Adult Xanthogranuloma

Juvenile xanthogranuloma in adulthood is a rare non-Langerhans cell histiocytosis that can clinically and dermoscopically resemble BCC, particularly due to the presence of arborizing vessels. However, the distinctive yellowish-orange hue, indicative of a xanthomatized tumor, serves as a crucial clue for dermoscopic diagnosis [80].

3.1.28. Neurothekeoma

Aydingoz et al. reported a case of neurothekeoma, a slow-growing benign tumor of nerve sheath origin, in an immunosuppressed patient undergoing treatment for non-Hodgkin lymphoma. Dermoscopically, the lesion mimicked BCC, displaying only thick, arborizing vessels on the surface of the nodule. The definitive diagnosis was made upon histopathology [81].

3.1.29. Primary Cutaneous B-Cell Lymphoma

A study analyzing the dermoscopic features of primary cutaneous B-cell lymphomas (PCBCL) revealed that 17.4% of cases were misdiagnosed as BCC by two blinded dermoscopy experts, with primary cutaneous follicle center lymphoma being particularly prone to misdiagnosis (30.2%). In 58 PCBCL cases, the authors identified salmon-colored background and prominent blood vessels, most commonly serpentine vessels, as the predominant dermoscopic features. These findings may also be seen in superficial BCC [82].

Table 1 summarizes the differential diagnosis of BCC, highlighting key dermoscopic features.

Table 1. Summary of the differential diagnoses of basal cell carcinoma (BCC).

Disease	Key Dermoscopic Features
Intradermal Nevi (IDN) [9,10]	Hair, comma-shaped vessels, brown pigment, brown globules, hairpin vessels [9]
Melanocytic Nevi (MN) [11,12]	Organized reticular pigmentation, regular vascular structures or lack of visible vasculature [12]
Actinic Keratosis (AK) [13,14]	Strawberry pattern, red pseudonetwork, keratotic hair follicles, scales, white circles [13,14]
Bowen's Disease (BD) [15,16]	Dotted/glomerular vessels, regularly distributed on a pink background [15,16]
Squamous Cell Carcinoma (SCC) [17–20]	Scales without both pigmentation and rolled border, keratin masses [17,20]
Seborrheic Keratosis (SK) [11,21,23–26]	Thick lines (fissures and ridges), black-to-brown clods (comedo-like openings), white clods (milia-like cysts), hairpin vessels with white halos [21]
Lichenoid Keratosis (LK) [27]	Dotted and linear vessels, coarse bluish-gray granules, comedo-like openings, cerebriform patterns, short, pigmented lines [27]
Melanoma (MM) [14,28–34]	Atypical network, regression structures, atypical vascular pattern, shiny white streaks, irregular blotches/streaks, blue-black granular pigmentation [28,31]
Trichoblastoma (TB) [35–38]	Fine, short, poorly branching telangiectasias, pigmented structures (brown dots, globules), milia-like cysts, yellow globules [35,36]
Trichoepithelioma (TE) [35,39–42]	Pearl-white background, multiple milia-like cysts, sparsely branched arborizing vessels [39,40,42]
Trichoadenoma [43]	Shiny white lines, blue-gray ovoid nests, in-focus linear vessels, small whitish circles [43]
Trichilemmoma [44]	Typically—non-pigmented; in pigmented cases: multiple pigmented dots, gray-blue globules, pink structureless areas, shiny white lines, rosettes [44]
Basaloid Follicular Hamartoma (BFH) [45,46]	Brown-gray linear (along Blaschko's lines)/arciform elements, globules, dots, spoke-wheel–like structures without a central dark point, keratotic plugs, irregular crown vessels, short fine telangiectasias, structureless areas [45,46]
Inverted Follicular Keratosis (IFK) [47]	Yellowish-white amorphous central area, radial polymorphic vascular patterns (arborizing, linear, corkscrew vessels) [47]
Poroma [48–52]	Typically non-pigmented, sharply demarcated nodules. In pigmented cases: arborizing vessels, large blue-gray ovoid nests [48–52]
Spiradenoma [53,54]	Arborizing vessels, blue clods on pink-to-red background [53,54]
Tubular Apocrine Adenoma (TAA) [55]	Short fine telangiectasias (SFTs), large blue-gray ovoid nests in a floriform pattern [55]
Pilomatricoma [56]	Irregular white structures, white streaks, polymorphous or atypical vessels [56]
Sebaceoma [57]	Yellowish-pink or yellow-white background, yellow homogeneous areas, crown vessels [57]
Sebaceous Carcinoma [58]	Polymorphic vessels, whitish-pink areas, yellowish structures, yellowish structureless areas [58]
Apocrine Hidrocystoma (AH) [59]	AH on the eyelid: translucent homogeneous areas, linear whitish structures, no eyelash involvement [59]

Table 1. *Cont.*

Disease	Key Dermoscopic Features
Microcystic Adnexal Carcinoma (MAC) [60]	Central pinkish-white structureless area, scale-crusts, hemorrhage, sharply in-focus arborizing vessels, yellow-white clods, gray-brown dots [60]
Dermatofibroma (DF) [61]	Typical pattern: peripheral pigment network + central white patch "BCC-like" pattern: blue-gray ovoid nests, peripheral brown-black leaf-like structures [61]
Linear Lesions (Scars, Scratches/Erosions, Tattoos) [8]	Depending on type of lesion, linear arrangement [8]
Acne Vulgaris [19]	Yellow background, central punctum, radial crowning vessels (arborizing-like vessels) [19]
Psoriasis [62–65]	Homogeneous vascular pattern, red dots distributed regularly on a light-red background [62–65]
Acrochordons (Skin Tags) [66]	In ischemic acrochordons: regularly arranged dotted vessels, violaceous background, bullae with serous fluid [66]
Scarring Alopecia [67]	Complete loss of follicular openings, structureless hypopigmentation [67]
Granuloma Faciale (GF) [68,69]	Diffuse orange structureless areas, elongated linear vessels [68]
Vulvar Hidradenoma Papilliferum [70]	Prominent vascular pattern—arborizing vessels, pink background, whitish areas [70]
Trigeminal Trophic Syndrome [71]	Ulceration on the face with polygonal, well-demarcated, erythematous borders, linear vessels, irregularly raised base [71]
Cutaneous Metastasis [72]	Various presentations, including translucent papule, tortuous arborizing vessels, lacunae [72]
Mammary Carcinoma [73]	Blue-gray areas, white scale, brown areas, brown to bluish-white globules, hyperpigmented border [73]
Cutaneous Histoplasmosis [74]	Scaling, arborizing telangiectasias at lesion periphery [74]
Dermal Leiomyosarcoma [75]	Erythematous nodule, homogeneous brown pattern, destruction of follicles, surrounding halo [75]
Neuroma [76]	Arborizing vessels, pink background [76]
Reticulohistiocytoma [77]	Arborizing vessels on a yellowish-pink background [77]
Targetoid Hemosiderotic Hemangioma (THH) [78]	Central lagoons, yellowish circular intermediate area, purple or ecchymotic peripheral ring or homogeneous peripheral area [78]
Angiokeratoma [79]	Dark lacunae [79]
Adult Xanthogranuloma [80]	Yellowish-orange hue, arborizing vessels [80]
Neurothekeoma [81]	thick, arborizing vessels on the surface of the nodule [81]
Primary cutaneous B-cell lymphomas (PCBCL) [82]	salmon-colored background, serpentine vessels [82]

3.2. Treatment and Monitoring

3.2.1. Detecting Tumor Margins

After reviewing the literature, we identified 11 studies [83–93] highlighting the benefits of dermoscopy for delineating tumor margins and five studies [94–98] suggesting limited utility.

The studies favoring dermoscopy reported reduced positive lateral margins (19% vs. 53%), fewer stages and smaller defects in Mohs micrographic surgery (MMS), especially for pigmented tumors [83–85,91]. Dermoscopic mapping during MMS, referred to as "Der-Mohscopy", enabled immediate correlation between dermoscopic and histopathologic findings [93]. Adding videodermoscopy (40× magnification) reduced the number of required stages to one in most patients compared to curettage [84]. Jawed et al. highlighted dermoscopy's role in accurately identifying biopsy sites, describing scars as homogeneous pink patches with clusters of small-caliber vessels under dermoscopy [87]. When using dermoscopy before MMS, the mean margin increase was 1.26 ± 0.4 mm (range 1–2 mm) [83]. A study analyzing 295 MMS procedures with prior dermoscopic margin delineation suggested a 1 mm initial margin for well-defined, non-aggressive BCCs smaller than 6 mm in cosmetically sensitive areas. For larger or more aggressive BCCs, wider margins are necessary: 3 mm—for nodular tumors under 6 mm, 4 mm—for well-defined tumors between 6 and 19 mm, 5 mm—for ill-defined, non-aggressive tumors, and 7 mm—for ill-defined aggressive ones [99].

Presurgical dermoscopic analysis of BCC margins has proven valuable even before traditional surgical excision for nodular, infiltrative and morpheaform subtypes [88,89]. It reduces suboptimal margins from 22% (with clinical evaluation alone) to 7% [88]. Mun et al. cautioned against relying on arborizing vessels to define margins, especially on the face, as they may represent normal vessels and lead to unnecessary excision [100]. In such cases, "stretching dermoscopy" can enhance margin assessment by improving the visualization of the opalescent color associated with stromal changes in BCC. Stretching the skin reduces the blood flow in smaller vessels surrounding the tumor without affecting larger arborizing vessels, thereby improving their distinction. Contact dermoscopy can compress both normal and tumoral vessels [101]. A study of 200 BCCs showed that 2 mm dermoscopically detected margins achieved complete histological excision in 98.5% of cases, with tumor extensions rarely exceeding 1 mm [90]. In a Japanese study, dermoscopic margins closely matched histopathological findings, with no tumors spreading beyond 1 mm. A 2–3 mm margin achieved a 99% complete removal rate for well-defined, primary pBCCs [102]. Another study reported a mean margin extension of 0.59 mm after dermoscopy, concluding that dermoscopy aids in determining both lateral and deep tumor margins, especially when using high magnification (120×) to achieve a three-dimensional view [92].

Dermoscopic identification of BCC peripheral borders is a quick and effective method for planning radiotherapy and evaluating tumor persistence or recurrence at the treatment margins [86].

Imbernón-Moya et al. highlighted that negative maple leaf-like areas may predict residual disease or recurrence after surgical or non-surgical treatment. This new dermoscopic criterion could aid in identifying tumor borders and defining adequate surgical margins, particularly in non-pigmented superficial BCCs [103].

Several studies have questioned the effectiveness of dermoscopy in improving surgical outcomes for BCC. A study involving 317 cases found no reduction in MMS stages or improvement in margin identification, regardless of clinician experience or the clinical and histopathological tumor subtype [94]. Similarly, smaller studies reported no advantage in using dermoscopy for margin delineation or stage reduction during MMS [95–98]. Cerci et al. observed that dermoscopy had limited accuracy in assessing lateral margins

in superficial, micronodular, infiltrative, morpheaform and mixed BCCs. However, the lack of a control group in this study meant it could not establish whether dermoscopy outperformed clinical evaluation. The study identified predictors of histologically positive margins, including superficial fine telangiectasias, shiny white-red structureless areas and white streaks [104].

3.2.2. Monitoring Effectiveness of Therapies

Imiquimod Cream 5%

Dermoscopy has proven to be an effective non-invasive tool for assessing and monitoring the outcomes of 5% imiquimod treatment, including the detection of residual tumor or recurrence. It enables the evaluation of lesion clearance without the need for biopsies; however, persistent dermoscopic features indicate the need for a biopsy [105–110].

Dermoscopic features such as leaf-like areas and spoke-wheel areas showed early regression by week 4 of therapy. Similarly, arborizing vessels in sBCCs disappeared early, likely due to their smaller size. In contrast, larger structures like blue-gray ovoid nests required a longer treatment period to resolve [109]. Another study found that ulceration and neovascularization were the first dermoscopic features to fully clear, typically by week 4. Among pigmented features, blue-gray globules showed the fastest clearance (50% by week 4), followed by leaf-like areas and large blue-gray ovoid nests [110].

In a study of 134 BCCs, multiple small erosions (common in sBCCs) increased the likelihood of complete response to imiquimod by 38 times, while large ulcerations and solitary small erosions were associated with eight- and seven-fold higher odds, respectively [106]. Dermoscopy also identified eruptive epidermoid cysts, a local immune reaction to imiquimod treatment, showing particularly in mid-facial areas (nose, chin, and lips). These cysts appeared as yellow-whitish plaques resembling "popcorn", with minimal vascularization, typically observed at the endpoint of therapy [108].

Photodynamic Therapy

Spoke-wheel patterns, concentric structures and leaf-like areas were linked to poor response to PDT, likely due to limited light penetration through these features. Deeper pigmented structures, such as globules, commonly seen in nBCCs, were associated with higher recurrence rates [111].

Apalla et al. analyzed 98 sBCCs treated with imiquimod or PDT and introduced "residual disease-associated dermoscopic criteria" (RDADC), including pigmented structures, ulcerations or arborizing vessels as indicators of residual disease. RDADC accurately predicted sBCC presence in histopathology, while their disappearance correlated with complete clearance. The reappearance of RDADC during follow-up suggests recurrence. Post-treatment white/red structureless areas or superficial fine telangiectasias may reflect treatment-related changes (upper dermal fibrosis and atrophy of the overlying epidermis) rather than neoplasia but require close monitoring for early recurrence [112].

Ingenol Mebutate

A study on four sBCCs demonstrated a rapid disappearance of dermoscopic features one month after treatment with ingenol mebutate gel 0.015% (for the face/scalp) and 0.05% (for the trunk/extremities). The authors suggested that in the future, lesion follow-up after this treatment could be performed without the need for punch biopsies [113].

Treatment with 0.5% 5-Fluorouracil and 10% Salicylic Acid

Diluvio et al. treated pBCCs with a combination of 0.5% 5-fluorouracil and 10% salicylic acid applied once daily for six weeks. Dermoscopy proved valuable in detecting the rapid disappearance of characteristic patterns (maple leaf-like areas, in-focus blue–gray

dots, concentric structures and spoke-wheel areas) one month after starting treatment. Additionally, six-month follow-up dermoscopic evaluations revealed no sBCC-specific features, confirming the absence of residual tumor or recurrence [114].

Vismodegib

In a study on long-term intermittent vismodegib treatment for multiple BCCs, lesions exhibiting in-focus dots at baseline, arborizing vessels after 12 weeks of treatment and concentric structures after 24 consecutive weeks were indicative of the histological persistence of BCC at the end of therapy (week 72). Moreover, pigmented structures observed at week 56 were significantly associated with a positive final histological examination, further suggesting treatment resistance [115].

High-Intensity Focused Ultrasound (HIFU)

Calik et al. introduced a novel non-invasive method for treating BCC using high-intensity focused ultrasound (HIFU). Dermoscopy played a crucial role in accurately delineating the treatment area and offered valuable insights into the healing process following HIFU treatment [116].

Radiotherapy and Brachytherapy

Two studies highlighted the utility of dermoscopy as an effective monitoring tool for patients with BCCs undergoing high-dose-rate (HDR) brachytherapy [114,115]. The authors observed a significantly faster reduction in dermoscopic features compared to topical therapies, followed by the development of ulceration, which may be attributed to the deeper tissue penetration of HDR. This effect was particularly pronounced in older patients. Additionally, dermoscopy proved to be highly sensitive in detecting recurrence or residual BCC [117,118].

Navarrete-Dechent et al. evaluated BCCs treated with high-dose ionizing radiation therapy and observed that only arborizing vessels became less prominent during follow-up. They also noted that short fine telangiectasias and shiny white blotches and strands lose diagnostic specificity in biopsied lesions, as these features may also appear in scars. Additionally, they reported a gradual increase in "white color", likely due to fibrosis, and "orange color", attributed to inflammatory cell accumulation. However, the study was limited by its small sample size and lack of a control group [119,120].

3.3. New Technologies

3.3.1. Ultraviolet-Induced Fluorescence Dermoscopy (UVFD)

The integration of ultraviolet light (365 nm) into dermatoscopes was demonstrated to improve the evaluation of BCC biopsy sites prior to dermatologic surgery. Navarrete-Dechent et al. observed that biopsy sites appear darker than surrounding skin under UVFD, likely due to inflammation and hypervascularity in scar tissue caused by the procedure [121]. However, Gil-Pallares et al. noted that even non-biopsied BCCs exhibit a darker appearance. This was attributed to the "umbrella effect", where skin tumors block UV light penetration, reducing fluorescence from underlying collagen and elastin. Recent scars appeared slightly less dark than tumors, while older hypopigmented scars were seen as brighter areas [122].

In a study of 163 BCCs, the UVFD features were reported for the first time. Common findings included dark silhouettes (82.2%), interrupted follicle patterns (31.9%), absence of blue-green fluorescence (33.1%), black globules (29.4%), white-blue scales (28.8%), lack of pink-orange fluorescence (26.4%) and well-demarcated borders (23.9%). UVFD was suggested as a valuable complementary tool to polarized dermoscopy (PD), particularly for small tumors, facial lesions and nodular or non-pigmented subtypes. BCCs of a diameter

less than 5 mm more often showed interrupted follicle patterns, the absence of pink-orange fluorescence and well-demarcated borders. Facial lesions frequently displayed clearly defined borders and interrupted follicle patterns, while nodular BCCs were associated with interrupted follicle patterns and absence of pink-orange fluorescence. Non-pigmented BCCs commonly exhibited the absence of blue-green fluorescence and interrupted follicle patterns. The study also found that erosions, ulcerations and vascular structures were less visible under UVFD compared to PD [123]. Figure 2 illustrates various characteristics of BCC observed under UVFD.

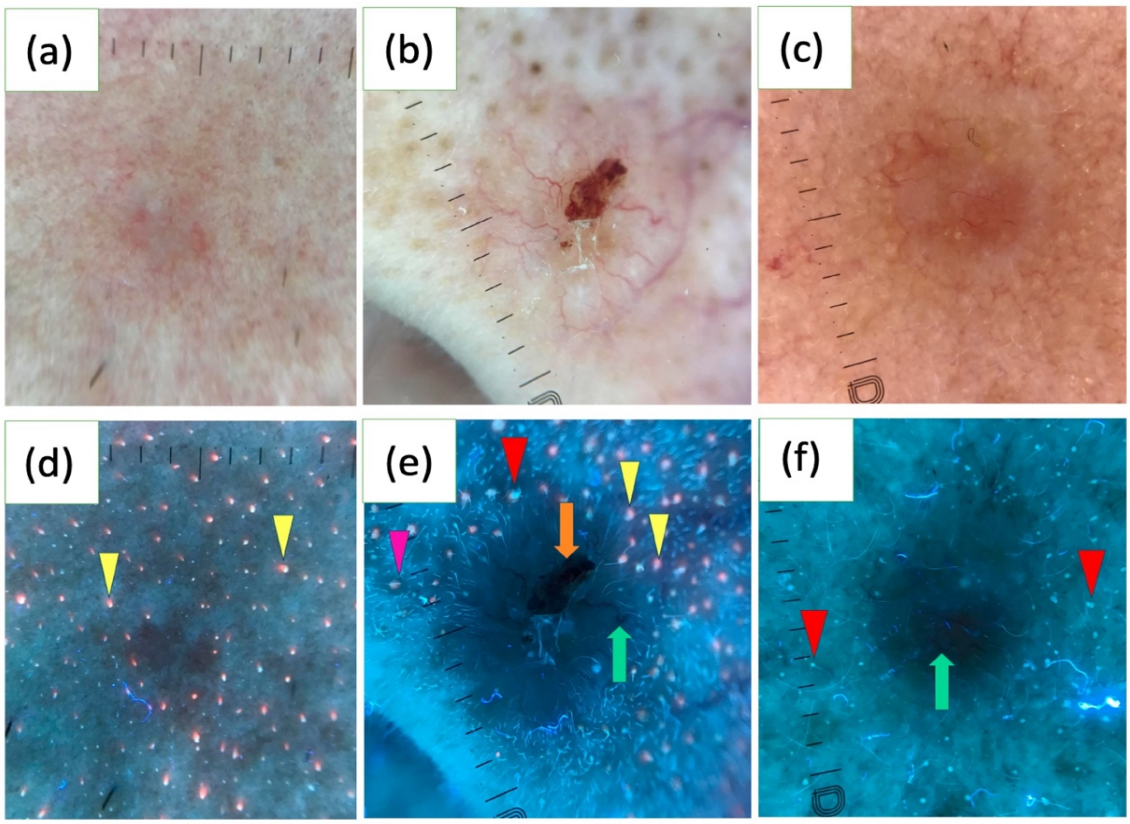

Figure 2. Polarized light dermoscopy (PD) presentation of basal cell carcinoma (BCC) on the face (**a**–**c**). Corresponding images in ultraviolet-induced fluorescence dermoscopy (UVFD) (**d**–**f**). (**d**) Dark silhouette, pink-orange follicular fluorescence at the periphery of the tumor (yellow arrowheads), absence of pink-orange fluorescence within the BCC. (**e**) Dark silhouette, erosion (orange arrow), arborizing vessel (green arrow), blue-green follicular fluorescence at the periphery of the BCC (red arrowhead), pink-orange follicular fluorescence at the periphery of the tumor (yellow arrowheads), absence of both types of fluorescence within the BCC, follicle pattern in the surrounding skin (pink arrowhead), interrupted follicle pattern within the lesion. (**f**) Dark silhouette, blue-green follicular fluorescence at the periphery of the BCC (red arrowheads), absence of blue-green fluorescence within the BCC, arborizing vessel (green arrow).

3.3.2. Optical Super-High Magnification Dermoscopy (OSHMD)

OSHMD, offering up to 400× magnification, improves the visualization of BCC. In a study involving 400 BCCs, a novel feature termed light brown nests was identified, which may aid in the early recognition of superficial BCCs, particularly in non-pigmented or slightly pigmented lesions that lack classic dermoscopic patterns. Light brown nests were observed in 30.3% of superficial BCCs and 14.3% of non-pigmented BCCs, being more distinctly visible at 50–70× magnification. These nests can appear either homogeneous or structured, often containing gray-blue structures or aggregated dots and commas [124].

Additionally, OSHMD revealed looped vessels as the most common vascular pattern in BCCs (63.4%). This feature can rarely be seen with conventional dermoscopy. A new vascular pattern, consisting of thin linear vessels circumferential to pigmented structures, was also identified in 53.7% of the BCCs analyzed [125].

In two BCC cases, an unusual vascular pattern, named "oak-leaf-like" vessels due to their resemblance to an oak leaf, was identified. Notably, the presence of "oak-leaf-like" vessels seems to be independent of lesion thickness as they were observed both in nodular and superficial BCCs [126].

OSHMD may also enhance the differentiation between IDN and BCC by revealing features invisible with standard dermoscopy. These include circular cells, likely corresponding to typical melanocytes in IDN, and fine pigmented structures resembling dots or globules, suggestive of BCC [127]. Figure 3 presents some characteristics of BCC observed under OSHMD.

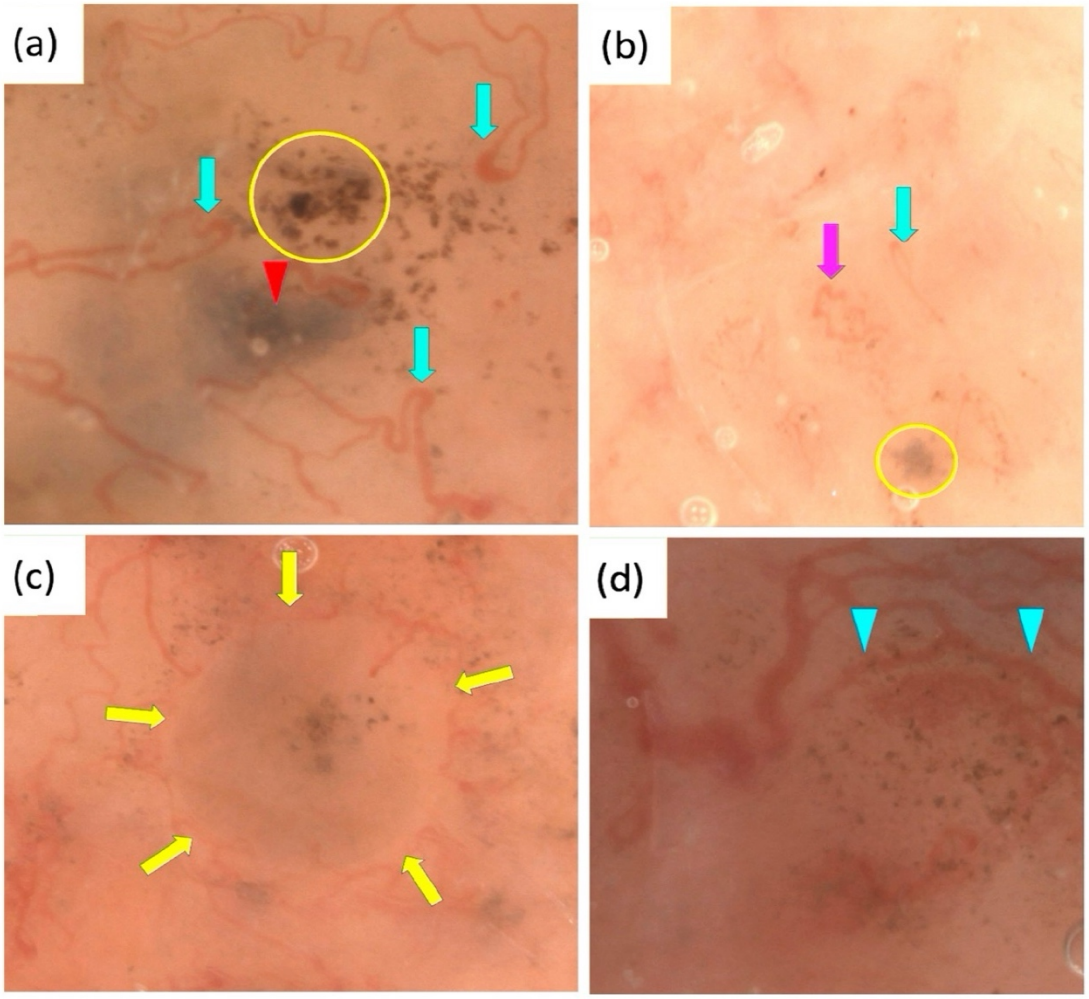

Figure 3. Optical super-high magnification dermoscopy (OSHMD) presentation of basal cell carcinoma (BCC) (**a**–**d**). (**a**) Light brown nest containing aggregated dots (yellow circle), blue-gray ovoid nest (red arrowhead), looped vessels (green arrows). (**b**) Light brown nest containing gray-blue structures (yellow circle), looped vessel (green arrow), "oak-leaf-like" vessel (pink arrow). (**c**) Light brown nest containing gray-blue structures and aggregated dots inside surrounded by linear vessels circumferential to pigmented structures (yellow arrows). (**d**) Linear vessels circumferential to pigmented structures—multiple in-focus blue/gray dots (blue arrowheads).

3.3.3. Ex Vivo Dermoscopy

Ex vivo dermoscopy (EVD) allows dermatopathologists to quickly identify areas of interest, reducing the risk of missing malignant lesions and improving diagnostic specificity by 3.0% in malignant nonmelanocytic lesions [128]. Most structures are well preserved in EVD images, though they appear darker, with new blue areas observed in 41.1% of BCC cases, white areas in 33.1% and a loss of red in 87.9%. Additionally, new crystalline structures were noted in 16.1% of BCC cases. Blood vessels were lost in 66.1% of observations. Scales and crusts also often disappeared, likely due to detachment during specimen fixation and handling [129].

Combining EVD with dermoscopy-guided cutting (DD) enhances the detection of positive margins in BCC, increasing from 8.3% to 11.1%, with a notable improvement in superficial BCC [130]. This approach also reduces the turnaround time (time from tissue cutting to pathological protocol) for BCC diagnosis from 2 days to 1 day, improving the efficiency of histopathologic evaluations [130].

3.3.4. Total Body Photography

Three-dimensional total body photography (3D-TBP) creates a 3D body model using images from multiple angles, enabling precise lesion mapping. Hobelsberger et al. found that 3D-TBP has slightly lower sensitivity (73% vs. 79%) and specificity (77% vs. 82%) compared to dermoscopy for BCC, though these differences were not statistically significant. Diagnostic accuracy for 3D-TBP was lower than dermoscopy (75% vs. 80%) but improved significantly to 85% when only high-confidence lesions, previously assessed with dermoscopy, were included. Additionally, 12 out of 182 lesions were not visible on 3D-TBP due to their location under hair or on the nasal septum [131].

3.3.5. Wide Area Digital Dermoscopy and Acrylic Globe Magnifier Dermoscopy

The wide area digital dermoscopy (WADD) method captures overlapping dermoscopic images of large lesions using a standard dermoscope and combines them with image editing software into a single, wide-field view. This technique seems to be useful for assessing large lesions, such as BCC, as described by Dellatorre and Gadens, that cannot be fully visualized under a dermoscope due to the limited diameter of its lenses. Additionally, WADD may be beneficial for evaluating extensive congenital melanocytic nevi and diseases affecting hairy areas. However, the method has limitations, requires 30% photo overlap (essential for the software to accurately align and merge the images) and professional software for image composition [132].

An older method for the dermoscopic assessment of large lesions, described in 2008, is acrylic globe magnifier dermoscopy. This technique involves using a camera with an acrylic globe magnifier and macro lens to photograph lesions, with immersion oil applied to reduce artifacts. Reflections are minimized by angling the light source and images are evaluated by dermatologists in a randomized order. The method demonstrated a 94% agreement with classical dermoscopy, with a sensitivity of 85% and specificity of 100% for BCC, providing diagnostic accuracy comparable to epiluminescence microscopy [133].

3.3.6. Dermatofluoroscopy

Dermatofluoroscopy is a diagnostic method that uses two-photon excitation to measure melanin fluorescence in skin lesions. It has proven effective in diagnosing melanomas, characterized by a fluorescence shift to the red spectrum. However, the technique also demonstrates high sensitivity for detecting pBCCs, with 88.9% of pBCCs identified as melanin-bearing malignant tumors. The spectral profiles of BCCs and melanomas appear

very similar, and the results of the fluorescence analysis should lead to recommendations for surgical excision [134].

3.3.7. Multispectral Skin Dermoscopy

Multispectral skin dermoscopy uses polarized light at various wavelengths to capture the optical absorption spectra of skin chromophores, such as melanin and hemoglobin, generating a "pigment contrast map" and a "blood contrast map". These maps enhance the visualization of vascular and pigment structures, aiding in the diagnosis of pBCC. In flat erythematous lesions, the blood contrast map helps differentiate between sBCC, which shows fine linear vessels, and BD, characterized by glomerular vessels [135].

3.3.8. Multispectral Autofluorescence Dermoscopy

Multispectral autofluorescence dermoscopy uses fluorescence lifetime imaging microscopy (FLIM) to analyze the natural autofluorescence of skin tissues, focusing on molecules like NADH, FAD and collagen. A laser excites the tissue and the emitted light is measured to capture both the intensity and timing of the fluorescence. This helps to detect changes in tissue structure and metabolism, enabling the distinction between cancerous and healthy skin. The method has been reported to be effective in identifying and mapping nBCC margins, potentially improving precision during surgical removal [136].

4. Discussion

In Part 3 of the review, we analyzed the dermoscopic features of BCC and its mimickers. While some conditions such as acne vulgaris, acrochordons or psoriasis typically can be easily distinguished, challenging cases can arise, particularly in early-stage or isolated lesions. Dermoscopy proves valuable in these situations, especially for early lesions or those located on the face, where the aesthetic outcome of a biopsy is always an issue. Other well-known conditions like SK, IDN, MN, melanoma, AK, SCC, BD and DF have well-defined dermoscopic features that distinguish them from BCC. However, lesions such as an irritated/inflamed SK, DF with a "BCC-like" pattern or BCC on the legs can pose diagnostic challenges. Moreover, rare lesions, including neurothekeoma, reticulohistiocytoma, solitary circumscribed neuroma, dermal leiomyosarcoma and various adnexal tumors, remain largely indistinguishable with dermoscopy. In such cases, a definitive diagnosis depends on histopathological analysis, typically initiated by dermoscopic suspicion of BCC. Interestingly, histopathological findings can occasionally reveal surprising diagnoses in lesions initially resembling BCC on dermoscopy, such as primary cutaneous B-cell lymphomas, mammary carcinomas or cutaneous histoplasmosis. This underscores the critical role of histopathology as the gold standard in confirming diagnoses and guiding appropriate management. To improve diagnostic accuracy, integrating dermoscopy with other non-invasive imaging techniques such as reflectance confocal microscopy (RCM) and optical coherence tomography (OCT) can be highly beneficial. RCM allows real-time, high-resolution imaging of the skin, providing additional insights into cellular structures that can distinguish BCC from benign lesions or other skin cancers. Similarly, OCT offers cross-sectional imaging that can aid in assessing tumor depth and structure. Combining these modalities with dermoscopy enhances diagnostic precision, minimizes unnecessary biopsies, and helps identify cases where histopathological confirmation is essential [137].

Although some studies reported conflicting findings, the majority demonstrated that dermoscopy effectively aids in delineating tumor margins before MMS and traditional surgical excision. It helps to reduce positive lateral margins and decrease the number of MMS stages required, which in turn results in smaller defects, particularly for pBCCs. For facial lesions, however, relying on arborizing vessels for margin delineation is not

advised, as these may represent normal vessels in this location. In such cases, dermoscopy performed on stretched skin can improve the visualization of BCC margins. For MMS, a 1 mm initial margin is suggested for well-defined, non-aggressive BCCs smaller than 6 mm in cosmetically sensitive areas, while a 2–3 mm margin appears sufficient for traditional surgery. Additionally, dermoscopy is valuable in identifying biopsy sites in healed lesions when total excision is necessary. Dermoscopy has also proven useful in planning BCC radiotherapy by aiding in defining the treatment area and evaluating tumor persistence or recurrence.

Dermoscopy has also been demonstrated to be a valuable tool for treatment monitoring, including the detection of the disappearance of characteristic patterns, as well as identifying residual tumors or recurrences. This has been shown for various treatment methods, including 5% imiquimod cream, PDT, ingenol mebutate gel, a combination of 0.5% 5-fluorouracil and 10% salicylic acid, radiotherapy, brachytherapy and vismodegib. Before treatment, certain dermoscopic features can help predict therapeutic outcomes. For example, multiple small erosions, large ulcerations and solitary small erosions are associated with a better response to 5% imiquimod cream, while the presence of spoke-wheel patterns, concentric structures and leaf-like areas predicts a poor response to PDT. Additionally, some dermoscopic findings may indicate a higher risk of recurrence after specific therapies. These include deeper pigmented structures, such as globules, often observed in nodular BCCs, which have been linked to increased recurrence rates following PDT. During treatment, changes in dermoscopic features can help assess treatment efficacy. For instance, the presence of in-focus dots at baseline, arborizing vessels after 12 weeks, concentric structures after 24 weeks, and pigmented structures at week 56 in vismodegib-treated lesions have been associated with histological persistence of BCC. Post-treatment, dermoscopy assists in detecting residual disease or early recurrence.

Recent years have also brought the development of various modifications in classical dermoscopy. UVFD appears to be a valuable complementary diagnostic tool to PD, particularly for small tumors (<5 mm), facial lesions and nodular or non-pigmented BCC subtypes. OSHMD may assist in recognizing BCC by identifying newly described features not typically observed in traditional dermoscopy. This method seems particularly useful for diagnosing superficial BCCs, especially in non-pigmented or slightly pigmented lesions that lack classic dermoscopic patterns. Additionally, OSHMD can aid in distinguishing between IDN and BCC. In EVD, most structures are well-preserved, enabling pathologists to precisely select areas for further histopathological assessment. Combining EVD with dermoscopy-guided cutting has proven particularly effective, enhancing the detection of positive margins and reducing the time from tissue cutting to pathological evaluation. Although 3D-TBP alone does not significantly improve diagnostic accuracy and cannot yet replace traditional dermoscopy, its combination with dermoscopy has been shown to enhance diagnostic precision. Modifications to traditional dermoscopy, such as WADD and acrylic globe magnifier dermoscopy, allow the visualization of larger BCCs that exceed the dermoscope lens size, creating a wide-field view. However, creating such a view requires additional devices, is time-consuming, and is better suited for evaluating individual lesions rather than for quick clinical assessments. A single study highlighted dermatofluoroscopy as valuable in detecting pBCCs, multispectral skin dermoscopy as effective for identifying pBCC and differentiating between sBCC and BD, and multispectral autofluorescence dermoscopy as useful for identifying and mapping nBCC margins. Further studies are necessary to fully evaluate the potential of these emerging diagnostic technologies for BCC assessment.

Moreover, artificial intelligence (AI) is rapidly advancing dermatological diagnostics, including BCC assessment. Maron et al. compared a state-of-the-art convolutional neural

network (CNN) model with 112 dermatologists in diagnosing skin lesions, including BCC. While sensitivity was similar (73.8%), the AI model outperformed dermatologists in specificity (99.5% vs. 97.8%), highlighting its potential in non-invasive imaging [138]. However, challenges such as inconsistent data, lack of standardization, and privacy concerns limit its clinical application. Despite these challenges, AI is expected to enhance dermoscopy, improving diagnostic accuracy and efficiency [139].

5. Conclusions

Dermoscopy is a valuable tool for the differential diagnosis of BCC, assisting in tumor margin delineation before MMS and traditional excision, treatment planning for radiotherapy and monitoring therapy effectiveness. However, in some rare or ambiguous cases, it remains inconclusive. Recent advancements, including RCM, OCT, UVFD, OSHMD and AI-assisted analysis have shown promise in improving diagnostic accuracy, but challenges such as standardization and data variability persist, underscoring the role of histopathology as the diagnostic gold standard. Future research should focus on optimizing multimodal imaging approaches to enhance diagnostic precision and treatment outcomes.

Author Contributions: Concept and design: I.W. and M.Ż.; methodology: I.W. and M.Ż.; manuscript—draft preparation: I.W.; manuscript—final version editing: I.W. and M.Ż. All named authors meet the International Committee of Medical Journal Editors (ICMJE) criteria for authorship for this article, take responsibility for the integrity of the work as a whole. All authors have read and agreed to the published version of the manuscript.

Funding: This article was not supported by any funding or sponsorship. The publication fee was covered with the internal funds of University of Rzeszow.

Institutional Review Board Statement: This review is based on the analysis of data from the literature. All sample dermoscopic images presented in the article were taken during routine patient care and come from the Department of Dermatology, University of Rzeszow. All patients gave consent for the examination and publication of the dermoscopic images. The study was conducted in accordance with the Declaration of Helsinki and approved by the Ethics Committee at the Regional Medical Chamber in Rzeszow (protocol code 50/2024/B, date of approval 21 October 2024).

Informed Consent Statement: Written informed consent has been obtained from the patients to publish this paper.

Data Availability Statement: No original datasets were generated for this article.

Conflicts of Interest: Irena Wojtowicz and Magdalena Zychowska declare that they have no conflicts of interest.

References

1. Coppola, R.; Barone, M.; Zanframundo, S.; Devirgiliis, V.; Roberti, V.; Perrella, E.; Donati, M.; Palese, E.; Tenna, S.; Persichetti, P.; et al. Basal Cell Carcinoma Thickness Evaluated by High-Frequency Ultrasounds and Correlation with Dermoscopic Features. *Ital. J. Dermatol. Venerol.* **2021**, *156*, 610–615. [CrossRef] [PubMed]
2. Wang, W.E.; Chen, Y.T.; Wang, C.H.; Wang, J.H.; Chang, C.H. Dermoscopic Features of Pigmented Basal Cell Carcinoma According to Size. *Int. J. Dermatol.* **2024**, *63*, 916–921. [CrossRef] [PubMed]
3. Palmisano, G.; Orte Cano, C.; Fontaine, M.; Lenoir, C.; Cinotti, E.; Tognetti, L.; Rubegni, P.; Perez-Anker, J.; Puig, S.; Malvehy, J.; et al. Dermoscopic Criteria Explained by LC-OCT: Negative Maple Leaf-Like Areas. *J. Eur. Acad. Dermatol. Venereol.* **2024**, *38*, e271–e273. [CrossRef] [PubMed]
4. Wojtowicz, I.; Żychowska, M. Dermoscopy of Basal Cell Carcinoma Part 1: Dermoscopic Findings and Diagnostic Accuracy—A Systematic Literature Review. *Cancers* **2025**, *17*, 493. [CrossRef]
5. Jin, H.; Yang, M.Y.; Kim, J.M.; Kim, G.W.; Kim, H.S.; Ko, H.C.; Kim, B.S.; Kim, M.B. Arborizing Vessels on Dermoscopy in Various Skin Diseases Other Than Basal Cell Carcinoma. *Ann. Dermatol.* **2017**, *29*, 288–294. [CrossRef]
6. Wojtowicz, I.; Żychowska, M. Dermoscopy of Basal Cell Carcinoma Part 2: Dermoscopic Findings by Lesion Subtype, Location, Age of Onset, Size and Patient Phototype. *Cancers* **2025**, *17*, 176. [CrossRef]

7. Eldaboush, A.M.; Marghoob, A.A. Challenging Diagnosis of Basal Cell Carcinoma: A Case Report Emphasizing the Clinical Utility of Dermoscopy. *Cureus* **2024**, *16*, e59274. [CrossRef]
8. Navarrete-Dechent, C.; Marchetti, M.A.; Uribe, P.; Schwartz, R.J.; Liopyris, K.; Marghoob, N.G.; Galimany, L.; Castro, J.C.; Jaimes, N.; Rabinovitz, H.S.; et al. Dermoscopy of Linear Basal Cell Carcinomas, a Potential Mimicker of Linear Lesions: A Descriptive Case-Series. *Dermatol. Pract. Concept.* **2022**, *12*, e2022195. [CrossRef]
9. Conforti, C.; Giuffrida, R.; Agozzino, M.; Cannavó, P.S.; Dianzani, C.; di Meo, N.; Nardello, C.; Neagu, N.; Guarneri, F.; Zalaudek, I. Basal Cell Carcinoma and Dermal Nevi of the Face: Comparison of Localization and Dermatoscopic Features. *Int. J. Dermatol.* **2021**, *60*, 996–1002. [CrossRef]
10. Williams, N.M.; Navarrete-Dechent, C.; Marghoob, A.A.; Abarzua-Araya, Á.; Salerni, G.; Jaimes, N. Differentiating Basal Cell Carcinoma from Intradermal Nevi Along the Eyelid Margin with Dermoscopy: A Case Series. *J. Am. Acad. Dermatol.* **2021**, *84*, 173–175. [CrossRef]
11. Zhang, J.; Wang, Y.; Zhang, W.; Cai, L.; Feng, J.; Zhu, Y.; Lu, H. Clinical Misdiagnosis of Cutaneous Malignant Tumors as Melanocytic Nevi or Seborrheic Keratosis: A Retrospective Analysis of a Chinese Population. *Clin. Cosmet. Investig. Dermatol.* **2024**, *17*, 465–476. [CrossRef] [PubMed]
12. Amirnia, M.; Ranjkesh, M.R.; Azimpouran, M.; Karkon-Shayan, F.; Alikhah, H.; Jafari-Asl, M.; Piri, R.; Naghavi-Behzad, M. Comparative Study of Dermatoscopic and Histopathologic Results in Facial Basal Cell Carcinoma and Melanocytic Nevi. *Asian Pac. J. Cancer Prev.* **2016**, *17*, 425–429. [CrossRef] [PubMed]
13. Di Carlo, A.; Elia, F.; Desiderio, F.; Catricalà, C.; Solivetti, F.M.; Laino, L. Can Video Thermography Improve Differential Diagnosis and Therapy Between Basal Cell Carcinoma and Actinic Keratosis? *Dermatol. Ther.* **2014**, *27*, 290–297. [CrossRef] [PubMed]
14. Tschandl, P.; Rosendahl, C.; Kittler, H. Dermatoscopy of Flat Pigmented Facial Lesions. *J. Eur. Acad. Dermatol. Venereol.* **2015**, *29*, 120–127. [CrossRef]
15. Felder, S.; Rabinovitz, H.; Oliviero, M.; Kopf, A. Dermoscopic Differentiation of a Superficial Basal Cell Carcinoma and Squamous Cell Carcinoma in Situ. *Dermatol. Surg.* **2006**, *32*, 423–425. [CrossRef]
16. Papageorgiou, C.; Apalla, Z.; Variaah, G.; Matiaki, F.C.; Sotiriou, E.; Vakirlis, E.; Lazaridou, E.; Ioannides, D.; Lallas, A. Accuracy of Dermoscopic Criteria for the Differentiation Between Superficial Basal Cell Carcinoma and Bowen's Disease. *J. Eur. Acad. Dermatol. Venereol.* **2018**, *32*, 1914–1919. [CrossRef]
17. Ryu, T.H.; Kye, H.; Choi, J.E.; Ahn, H.H.; Kye, Y.C.; Seo, S.H. Features Causing Confusion Between Basal Cell Carcinoma and Squamous Cell Carcinoma in Clinical Diagnosis. *Ann. Dermatol.* **2018**, *30*, 64–70. [CrossRef]
18. Cornacchia, L.; Longo, C.; Piana, S.; Lai, M.; Pellacani, G.; Peris, K.; Pampena, R. 'Eternal Sunshine of the Spotless Islands': How Dermoscopy May Influence Confocal Microscopy When Dealing with Squamous Cells Carcinoma Simulating Basal Cell Carcinoma. *J. Eur. Acad. Dermatol. Venereol.* **2019**, *33*, e277–e280. [CrossRef]
19. Markowitz, O.; Utz, S. Differentiating Early Stage Cystic Keratoacanthoma, Nodular Basal Cell Carcinoma, and Excoriated Acne Vulgaris by Clinical Exam, Dermoscopy, and Optical Coherence Tomography: A Report of 3 Cases. *J. Clin. Aesthet. Dermatol.* **2015**, *8*, 48–50.
20. Neagu, N.; Lallas, K.; Maskalane, J.; Salijuma, E.; Papageorgiou, C.; Gkentsidi, T.; Spyridis, I.; Morariu, S.H.; Apalla, Z.; Lallas, A. Minimizing the Dermatoscopic Morphologic Overlap Between Basal and Squamous Cell Carcinoma: A Retrospective Analysis of Initially Misclassified Tumours. *J. Eur. Acad. Dermatol. Venereol.* **2020**, *34*, 1999–2003. [CrossRef]
21. Mansur, A.T.; Yildiz, S. A Diagnostic Challenge: Inflamed and Pigmented Seborrheic Keratosis. Clinical, Dermoscopic, and Histopathological Correlation. *Dermatol. Online J.* **2019**, *25*, 14. [CrossRef]
22. Takenouchi, T. Key Points in Dermoscopic Diagnosis of Basal Cell Carcinoma and Seborrheic Keratosis in Japanese. *J. Dermatol.* **2011**, *38*, 59–65. [CrossRef] [PubMed]
23. Álvarez-Salafranca, M.; Gómez-Martín, I.; Bañuls, J.; Serrano, P.; Medina, C.; Llambrich, A.; Pizarro, Á.; Ara, M.; Zaballos, P. Dermoscopy of Inflamed Seborrheic Keratosis: A Great Mimic of Malignancy. *Australas. J. Dermatol.* **2022**, *63*, 53–61. [CrossRef]
24. Al Jalbout, S.; Moscarella, E.; Longo, C.; Argenziano, G.; Piana, S.; Zalaudek, I. Dermoscopy Should Always Be Performed. . .Even in Clear-Cut Cases! *J. Am. Acad.Dermatol.* **2013**, *69*, e159–e160. [CrossRef]
25. Gao, Y.Y.; An, X.J.; Yang, J.; Huang, C.Z.; Tao, J. Seborrheic Keratosis Mimicking Basal Cell Carcinoma Under Dermoscopy: A Case Report. *Chin. Med. J.* **2020**, *133*, 2139–2140. [CrossRef]
26. Yanagihara, S.; Yoshida, Y.; Tsuruta, D.; Yamamoto, O. Basal Cell Carcinoma Showing Surface Hyperkeratosis Clinically Mimicking Seborrheic Keratosis. *J. Dermatol.* **2015**, *42*, 1195–1196. [CrossRef]
27. Gori, A.; Oranges, T.; Janowska, A.; Savarese, I.; Chiarugi, A.; Nardini, P.; Salvati, L.; Palleschi, G.M.; Scarfì, F.; Massi, D.; et al. Clinical and dermoscopic features of lichenoid keratosis: A retrospective case study. *J. Cutan. Med. Surg.* **2018**, *22*, 561–566. [CrossRef]
28. Peccerillo, F.; Mandel, V.D.; Di Tullio, F.; Ciardo, S.; Chester, J.; Kaleci, S.; de Carvalho, N.; Del Duca, E.; Giannetti, L.; Mazzoni, L.; et al. Lesions Mimicking Melanoma at Dermoscopy Confirmed Basal Cell Carcinoma: Evaluation with Reflectance Confocal Microscopy. *Dermatology* **2019**, *235*, 35–44. [CrossRef]

29. Akay, B.N.; Kirmizi, A.; Demirdag, H.G.; Erdem, C.; Okcu Heper, A. Heavily Pigmented Fibroepithelioma of Pinkus Mimicking Melanoma. *Int. J. Dermatol.* **2018**, *57*, 753–754. [CrossRef]
30. Gómez-Martín, I.; Moreno, S.; Pujol, R.M.; Segura, S. Pigmented Fibroepithelioma of Pinkus: A Potential Dermoscopic Simulator of Malignant Melanoma. *J. Dermatol.* **2017**, *44*, 542–543. [CrossRef]
31. Alarcon, I.; Carrera, C.; Turegano, P.; Malvehy, J.; Puig, S. Basal Cell Carcinoma with Spontaneous Regression: Added Value of Reflectance Confocal Microscopy When the Dermoscopic Diagnosis is Uncertain. *J. Am. Acad. Dermatol.* **2014**, *71*, e7–e9. [CrossRef] [PubMed]
32. Asahara, M.; Hoashi, T.; Shirakawa, N.; Matano, Y.; Funasaka, Y.; Saeki, H. Case of Nodular Melanoma on the Upper Eyelid Dermoscopically Mimicking Pigmented Basal Cell Carcinoma. *J. Dermatol.* **2017**, *44*, 543–545. [CrossRef] [PubMed]
33. Giuffrida, R.; Conforti, C.; Blum, A.; Buljan, M.; Guarneri, F.; Hofmann-Wellenhof, R.; Longo, C.; Paoli, J.; Rosendahl, C.; Soyer, H.P.; et al. Vascular Diameter as Clue for the Diagnosis of Clinically and/or Dermoscopically Equivocal Pigmented and Non-Pigmented Basal Cell Carcinomas and Nodular Melanomas. *Medicina* **2022**, *58*, 1761. [CrossRef]
34. Di Matteo, E.; Pampena, R.; Pizzichetta, M.A.; Cinotti, E.; Chester, J.; Kaleci, S.; Manfredini, M.; Guida, S.; Dika, E.; Moscarella, E.; et al. Unusual dermoscopic patterns of basal cell carcinoma mimicking melanoma. *Exp. Dermatol.* **2022**, *31*, 890–898. [CrossRef]
35. Pitarch, G.; Botella-Estrada, R. Dermoscopic findings in trichoblastoma. *Actas Dermosifiliogr.* **2015**, *106*, e45–e48. [CrossRef]
36. Sławińska, M.; Płaszczyńska, A.; Lakomy, J.; Pastuszak, K.; Biernat, W.; Sikorska, M.; Nowicki, R.J.; Sobjanek, M. Significance of dermoscopy in association with clinical features in differentiation of basal cell carcinoma and benign trichoblastic tumours. *Cancers* **2022**, *14*, 3964. [CrossRef]
37. Kwock, J.T.; Casady, M.; Handfield, C.; MacLeod, A.S.; Pavlis, M.B. A trichogenic tumor with aggressive features initially diagnosed as basal cell carcinoma. *Dermatol. Online J.* **2018**, *24*, 11. [CrossRef]
38. Ghigliotti, G.; De Col, E.; Parodi, A.; Bombonato, C.; Argenziano, G. Trichoblastoma: Is a clinical or dermoscopic diagnosis possible? *J. Eur. Acad. Dermatol. Venereol.* **2016**, *30*, 1978–1980. [CrossRef]
39. Lazaridou, E.; Fotiadou, C.; Patsatsi, A.; Fotiadu, A.; Kyrmanidou, E.; Kemanetzi, C.; Ionnides, D. Solitary trichoepithelioma in an 8-year-old child: Clinical, dermoscopic, and histopathologic findings. *Dermatol. Pract. Concept.* **2014**, *4*, 55–58. [CrossRef]
40. Khelifa, E.; Masouyé, I.; Kaya, G.; Le Gal, F.A. Dermoscopy of desmoplastic trichoepithelioma reveals other criteria to distinguish it from basal cellcarcinoma. *Dermatology* **2013**, *226*, 101–104. [CrossRef]
41. Stoica, L.E.; Dascălu, R.C.; Pătraşcu, V.; Ciurea, R.N.; Brănişteanu, D.E.; Georgescu, D.M.; Ciurea, P.L. Solitary trichoepithelioma: Clinical, dermoscopic, and histopathological findings. *Rom. J. Morphol. Embryol.* **2015**, *56*, 827–832. [PubMed]
42. Kunz, M.; Kerl, K.; Braun, R.P. Basal cell carcinoma mimicking desmoplastic trichoepithelioma: A case with correlation of dermoscopy and histology. *Case Rep. Dermatol.* **2018**, *10*, 133–137. [CrossRef] [PubMed]
43. Pampena, R.; Borsari, S.; Piana, S.; Longo, C. Broadening the list of basal cell carcinoma mimickers: Dermoscopic features of trichoadenoma. *Dermatol. Pract. Concept.* **2019**, *9*, 160–161. [CrossRef]
44. Alhameedy, M.M.; Alrobaish, O.A.; Almarshoud, S.; Albahli, R. Pigmented desmoplastic trichilemmoma arising in nevus sebaceous: A potential mimicker of pigmented basal cell carcinoma. *Skin. Appendage Disord.* **2023**, *9*, 309–312. [CrossRef]
45. Muhammed, N.; Dongre, A.M.; Khopkar, U.S. Clinicopathological and dermoscopic features in a case of linear and unilateral basaloid follicular hamartoma. *Indian Dermatol. Online J.* **2019**, *10*, 710–713. [CrossRef]
46. Rekik, M.; Hammami, F.; Saguem, I.; Sellami, K.; Masmoudi, A.; Amouri, M.; Mseddi, M.; Sellami, T.; Bahloul, E.; Turki, H. Follicular basaloid hamartoma and associated cutaneous tumors: Clinical, histopathological, and dermoscopic aspects. *J. Clin. Aesthet. Dermatol.* **2023**, *16*, 43–46.
47. Llambrich, A.; Zaballos, P.; Taberner, R.; Terrasa, F.; Bañuls, J.; Pizarro, A.; Malvehy, J.; Puig, S. Dermoscopy of inverted follicular keratosis: Study of 12 cases. *Clin. Exp. Dermatol.* **2016**, *41*, 468–473. [CrossRef]
48. Ichiyama, S.; Hoashi, T.; Funasaka, Y.; Mikami, E.; Akiyama, M.; Esaki, E.; Kubo, M.; Ansai, S.I.; Tanaka, M.; Saeki, H. Pigmented poroma on the temporal region dermoscopically mimicking basal cell carcinoma: A report of two cases. *J. Dermatol.* **2018**, *45*, e94–e95. [CrossRef]
49. Bombonato, C.; Piana, S.; Moscarella, E.; Lallas, A.; Argenziano, G.; Longo, C. Pigmented eccrine poroma: Dermoscopic and confocal features. *Dermatol. Pract. Concept.* **2016**, *6*, 59–62. [CrossRef]
50. Kassuga, L.E.; Jeunon, T.; Sousa, M.A.; Campos-do-Carmo, G. Pigmented poroma with unusual location and dermatoscopic features. *Dermatol. Pract. Concept.* **2012**, *2*, 203a07. [CrossRef]
51. Avilés-Izquierdo, J.A.; Velázquez-Tarjuelo, D.; Lecona-Echevarría, M.; Lázaro-Ochaita, P. Dermoscopic features of eccrine poroma. *Actas Dermosifiliogr.* **2009**, *100*, 133–136. [CrossRef] [PubMed]
52. Kuo, H.W.; Ohara, K. Pigmented eccrine poroma: A report of two cases and study with dermatoscopy. *Dermatol. Surg.* **2003**, *29*, 10761079. [CrossRef]
53. Collgros, H.; Guitera, P. A pearly papule with arborizing vessels. *J. Am. Acad. Dermatol.* **2015**, *72*, S25–S26. [CrossRef]
54. Worley, B.; Kanigsberg, N.; Beecker, J. Differential diagnosis of a pink nodule with a blue globule. *J. Am. Acad. Dermatol.* **2014**, *71*, e191–e193. [CrossRef]

55. Ito, T.; Nomura, T.; Fujita, Y.; Abe, R.; Shimizu, H. Tubular apocrine adenoma clinically and dermoscopically mimicking basal cell carcinoma. *J. Am. Acad. Dermatol.* **2014**, *71*, e45–e46. [CrossRef]
56. Zaballos, P.; Llambrich, A.; Puig, S.; Malvehy, J. Dermoscopic findings of pilomatricomas. *Dermatology* **2008**, *217*, 225–230. [CrossRef]
57. Ning, X.; Wang, H.; Zheng, Z.; Wang, Y.; Cui, Y. Sebaceoma on the nose mimicking basal cell carcinoma: Pitfalls of dermoscopy and reflectance confocal microscopy. *Skin Res. Technol.* **2022**, *28*, 886–888. [CrossRef]
58. Cheng, C.Y.; Su, H.J.; Kuo, T.T. Dermoscopic features and differential diagnosis of sebaceous carcinoma. *J. Dermatol.* **2020**, *47*, 755–762. [CrossRef]
59. Hidalgo, L.; Abusleme, E.; Navarrete-Dechent, C.; Abarzúa-Araya, Á. Dermoscopy as an aid in the differentiation of recurrent eyelid basal cell carcinoma versus apocrine hidrocystoma. *Dermatol. Pract. Concept.* **2022**, *12*, e2022090. [CrossRef]
60. Gupta, V.; Kakkar, A.; Agarwal, S.; Sulaiman, M.; Ramam, M. Dermoscopic pitfall: Microcystic adnexal carcinoma mimicking basal cell carcinoma. *Indian J. Dermatol. Venereol. Leprol.* **2020**, *86*, 202–205. [CrossRef]
61. Ferrari, A.; Argenziano, G.; Buccini, P.; Cota, C.; Sperduti, I.; De Simone, P.; Eibenschutz, L.; Silipo, V.; Zalaudek, I.; Catricalà, C. Typical and atypical dermoscopic presentations of dermatofibroma. *J. Eur. Acad. Dermatol. Venereol.* **2013**, *27*, 1375–1380. [CrossRef] [PubMed]
62. Hanna, C.; Cook, L.; Foulke, G.; Seiverling, E.V. Scaly pink patches: Differentiating psoriasis from basal cell carcinoma. *Cutis* **2018**, *101*, 44–46. [PubMed]
63. Stefanello, B.; Rezende, P.M.; Argenziano, G.; Piana, S.; Moscarella, E.; Longo, C.; Zalaudek, I.; Lallas, A. Uncovering a hidden basal cell carcinoma. *J. Am. Acad. Dermatol.* **2014**, *70*, e99–e101. [CrossRef] [PubMed]
64. Liebman, T.N.; Wang, S.Q. Detection of early basal cell carcinoma with dermoscopy in a patient with psoriasis. *Dermatol. Online J.* **2011**, *17*, 12. [CrossRef]
65. Pan, Y.; Chamberlain, A.J.; Bailey, M.; Chong, A.H.; Haskett, M.; Kelly, J.W. Dermatoscopy aids in the diagnosis of the solitary red scaly patch or plaque—Features distinguishing superficial basal cell carcinoma, intraepidermal carcinoma, and psoriasis. *J. Am. Acad. Dermatol.* **2008**, *59*, 268–274. [CrossRef]
66. Cuellar-Barboza, A.; Cardenas-de la Garza, J.A.; Martinez-Moreno, A.; Cardenas-Gonzalez, R.; Barboza-Quintana, O.; Ocampo-Candiani, J. Giant lumbar polypoid tumor with bullae on its surface. *Acta Dermatovenerol. Croat.* **2019**, *27*, 127–128.
67. Tomasini, C.F.; Fiandrino, G.; Favale, E.M.; Antoci, F.; Barruscotti, S. Giant morpheaform basal cell carcinoma mimicking scarring alopecia: Exception prone to neglect. *Dermatopathology* **2024**, *11*, 154–160. [CrossRef]
68. Savoia, F.; Medri, M.; Stanganelli, I.; Zago, S.; Domeniconi, L.; Melandri, D.; Alaibac, M.; Tartaglia, J.; Ciolfi, C.; Sechi, A. Elongated linear vessels simulating branching vessels and diffuse structureless orange areas as prominent dermoscopic features of diffuse flat facial and extrafacial granuloma faciale: A case series. *Australas. J. Dermatol.* **2024**, *65*, 467–471. [CrossRef]
69. Lallas, A.; Sidiropoulos, T.; Lefaki, I.; Tzellos, T.; Sotiriou, E.; Apalla, Z. Photoletter to the editor: Dermoscopy of granuloma faciale. *J. Dermatol. Case Rep.* **2012**, *6*, 59–60. [CrossRef]
70. Jovic, A.; Popovic, D.; Cekic, S.; Vidovic, N.; Zivkovic, N.; Zlatanovic, Z.; Tiodorovic, D. Vulvar hidradenoma papilliferum dermoscopically mimicking basal cell carcinoma. *Dermatol. Pract. Concept.* **2021**, *11*, e2021070. [CrossRef]
71. Castro, C.G.; Vázquez-López, F.; García-García, B.; López, S.R.; Oliva, N.P. Trigeminal trophic syndrome simulating rodent ulcer basal cell carcinoma: A new clinico-dermoscopic approach. *An. Bras. Dermatol.* **2017**, *92*, 148–150. [CrossRef] [PubMed]
72. Kuraitis, D.; Pei, S. Dermoscopy of cutaneous metastasis of renal cell carcinoma. *JAAD Case Rep.* **2023**, *40*, 60–62. [CrossRef] [PubMed]
73. Horikawa, H.; Umegaki-Arao, N.; Funakoshi, T.; Amagai, M.; Tanaka, M. Dermoscopy of pigmented invasive ductal carcinoma mimicking basal cell carcinoma. *Australas. J. Dermatol.* **2017**, *58*, 326327. [CrossRef]
74. Zattar, G.A.; Cardoso, F.; Nakandakari, S.; Soares, C.T. Cutaneous histoplasmosis as a complication after anti-TNF use—Case report. *An. Bras. Dermatol.* **2015**, *90*, 104–107. [CrossRef]
75. Lozano Salazar, A.D.; Márquez García, A.; Ortega Medina, I.; Ríos-Martín, J.J. Dermal leiomyosarcoma at the end of the left eyebrow. *Actas Dermosifiliogr.* **2014**, *105*, 879–882. [CrossRef]
76. Fernández-Crehuet, P.; Fernández-Crehuet, J.L.; Ruiz-Villaverde, R.; Sanz-Trelles, A. Solitary circumscribed neuroma: A clinical and dermoscopic mimicker of basal cell carcinoma. *Int. J. Dermatol.* **2015**, *54*, e275–e277. [CrossRef]
77. Güleç, A.T. Solitary reticulohistiocytoma with arborizing vessels: A new mimicker of basal cell carcinoma. *J. Am. Acad. Dermatol.* **2016**, *74*, e5–e6. [CrossRef]
78. Enei, M.L.; Paschoal, F.M.; Valdes, R. Arborizing vessels in a targetoid hemosiderotic hemangioma: Mistaken dermoscopic diagnosis of basal cell carcinoma. *Dermatol. Pract. Concept.* **2017**, *7*, 43–47. [CrossRef]
79. Zaballos, D.P. Spot the differences between two pigmented papules. *Actas Dermosifiliogr.* **2013**, *104*, 719–720. [CrossRef]
80. Lovato, L.; Salerni, G.; Puig, S.; Carrera, C.; Palou, J.; Malvehy, J. Adult xanthogranuloma mimicking basal cell carcinoma: Dermoscopy, reflectance confocal microscopy, and pathological correlation. *Dermatology* **2010**, *220*, 66–70. [CrossRef]

81. Aydingoz, I.E.; Mansur, A.T.; Dikicioglu-Cetin, E. Arborizing vessels under dermoscopy: A case of cellular neurothekeoma instead of basal cell carcinoma. *Dermatol. Online J.* **2013**, *19*, 5. [CrossRef] [PubMed]
82. Geller, S.; Marghoob, A.A.; Scope, A.; Braun, R.P.; Myskowski, P.L. Dermoscopy and the diagnosis of primary cutaneous B-cell lymphoma. *J. Eur. Acad. Dermatol. Venereol.* **2018**, *32*, 53–56. [CrossRef] [PubMed]
83. Litaiem, N.; Karray, M.; Jones, M.; Rammeh, S.; Zeglaoui, F. Effectiveness of dermoscopy in the demarcation of surgical margins in slow Mohs surgery. *Dermatol. Ther.* **2020**, *33*, e14196. [CrossRef]
84. Dika, E.; Fanti, P.A.; Christman, H.; Ravaioli, G.M.; Patrizi, A. Videodermoscopy and curettage: The value of simple procedures during Mohs surgery. *Dermatol. Surg.* **2017**, *43*, 1411–1417. [CrossRef]
85. Yeom, S.D.; Lee, S.H.; Ko, H.S.; Chung, K.Y.; Shin, J.; Choi, G.S.; Byun, J.W. Effectiveness of dermoscopy in Mohs micrographic surgery (MMS) for nonmelanoma skin cancer (NMSC). *Int. J. Dermatol.* **2017**, *56*, e136–e139. [CrossRef]
86. Ballester Sánchez, R.; Pons Llanas, O.; Pérez Calatayud, J.; Botella Estrada, R. Dermoscopy margin delineation in radiotherapy planning for superficial or nodular basal cell carcinoma. *Br. J. Dermatol.* **2015**, *172*, 1162–1163. [CrossRef]
87. Jawed, S.I.; Goldberg, L.H.; Wang, S.Q. Dermoscopy to identify biopsy sites before Mohs surgery. *Dermatol. Surg.* **2014**, *40*, 334–337. [CrossRef]
88. Carducci, M.; Bozzetti, M.; De Marco, G.; Foscolo, A.M.; Betti, R. Usefulness of margin detection by digital dermoscopy in the traditional surgical excision of basal cell carcinomas of the head and neck including infiltrative/morpheaform type. *J. Dermatol.* **2012**, *39*, 326–330. [CrossRef]
89. Carducci, M.; Bozzetti, M.; Foscolo, A.M.; Betti, R. Margin detection using digital dermatoscopy improves the performance of traditional surgical excision of basal cell carcinomas of the head and neck. *Dermatol. Surg.* **2011**, *37*, 280–285. [CrossRef]
90. Caresana, G.; Giardini, R. Dermoscopy-guided surgery in basal cell carcinoma. *J. Eur. Acad. Dermatol. Venereol.* **2010**, *24*, 1395–1399. [CrossRef]
91. Terushkin, V.; Wang, S.Q. Mohs surgery for basal cell carcinoma assisted by dermoscopy: Report of two cases. *Dermatol. Surg.* **2009**, *35*, 2031–2035. [CrossRef] [PubMed]
92. Savant, S.S., Jr. Use of preoperative and perioperative ex vivo dermoscopy for precise mapping of margins for standard surgical excision of primary basal cell carcinoma. *Indian J. Dermatol. Venereol. Leprol.* **2023**, *89*, 793. [CrossRef] [PubMed]
93. Cerci, F.B.; Tolkachjov, S.N.; Werner, B. "DerMohscopy": Utility of Dermoscopy Combined with Mohs Micrographic Surgery for the Treatment of Basal Cell Carcinoma. *An. Bras. Dermatol.* **2022**, *97*, 250–253. [CrossRef] [PubMed]
94. Jayasekera, P.S.A.; Dodd, J.; Oliphant, T.; Langtry, J.A.A.; Lawrence, C.M. Dermoscopy Prior to Mohs Micrographic Surgery Does Not Improve Tumour Margin Assessment and Leads to Fewer Mohs Stages. *Br. J. Dermatol.* **2018**, *178*, 565–566. [CrossRef]
95. Suzuki, H.S.; Serafini, S.Z.; Sato, M.S. Utility of Dermoscopy for Demarcation of Surgical Margins in Mohs Micrographic Surgery. *An. Bras. Dermatol.* **2014**, *89*, 38–43. [CrossRef]
96. Asilian, A.; Momeni, I. Comparison Between Examination with Naked Eye, Curettage, and Dermoscopy in Determining Tumor Extension Before Mohs Micrographic Surgery. *Adv. Biomed. Res.* **2013**, *2*, 2. [CrossRef]
97. Gurgen, J.; Gatti, M. Epiluminescence Microscopy (Dermoscopy) Versus Visual Inspection During Mohs Microscopic Surgery of Infiltrative Basal Cell Carcinoma. *Dermatol. Surg.* **2012**, *38*, 1066–1069. [CrossRef]
98. Guardiano, R.A.; Grande, D.J. A Direct Comparison of Visual Inspection, Curettage, and Epiluminescence Microscopy in Determining Tumor Extent Before the Initial Margins Are Determined for Mohs Micrographic Surgery. *Dermatol. Surg.* **2010**, *36*, 1240–1244. [CrossRef]
99. Cerci, F.B.; Kubo, E.M.; Werner, B.; Tolkachjov, S.N. Surgical Margins Required for Basal Cell Carcinomas Treated with Mohs Micrographic Surgery According to Tumor Features. *J. Am. Acad. Dermatol.* **2020**, *83*, 493–500. [CrossRef]
100. Mun, J.H.; Jwa, S.W.; Song, M.; Ko, H.C.; Kim, B.S.; Kim, M.B.; Kim, H.S. Pitfalls of Using Dermoscopy in Defining Surgical Margins of Basal Cell Carcinoma. *Dermatol. Surg.* **2011**, *37*, 1704–1705. [CrossRef]
101. Cerci, F.B.; Zehnder, M.L.; Lallas, A.; Werner, B.; Tolkachjov, S.N. "Stretching Dermoscopy" to Delineate the Margins of Basal Cell Carcinoma on Photodamaged Telangiectatic Skin. *Dermatol. Pract. Concept.* **2023**, *13*, e2023148. [CrossRef]
102. Ito, T.; Inatomi, Y.; Nagae, K.; Nakano-Nakamura, M.; Nakahara, T.; Furue, M.; Uchi, H. Narrow-Margin Excision is a Safe, Reliable Treatment for Well-Defined, Primary Pigmented Basal Cell Carcinoma: An Analysis of 288 Lesions in Japan. *J. Eur. Acad. Dermatol. Venereol.* **2015**, *29*, 18281831. [CrossRef] [PubMed]
103. Imbernón-Moya, A.; Sidro, M.; Malvehy, J.; Puig, S. Negative Maple-Leaf-Like Areas: A New Clue for Basal Cell Carcinoma Margin Recognition. *Br. J. Dermatol.* **2016**, *175*, 818–820. [CrossRef] [PubMed]
104. Cerci, F.B.; Kubo, E.M.; Werner, B.; Tolkachjov, S.N. Dermoscopy Accuracy for Lateral Margin Assessment of Distinct Basal Cell Carcinoma Subtypes Treated by Mohs Micrographic Surgery in 368 Cases. *Int. J. Dermatol.* **2022**, *61*, e139–e141. [CrossRef] [PubMed]
105. Singal, A.; Daulatabad, D.; Pandhi, D.; Arora, V.K. Facial Basal Cell Carcinoma Treated with Topical 5% Imiquimod Cream with Dermoscopic Evaluation. *J. Cutan. Aesthet. Surg.* **2016**, *9*, 122–125. [CrossRef]

106. Urech, M.; Kyrgidis, A.; Argenziano, G.; Reggiani, C.; Moscarella, E.; Longo, C.; Alfano, R.; Zalaudek, I.; Lallas, A. Dermoscopic Ulceration is a Predictor of Basal Cell Carcinoma Response to Imiquimod: A Retrospective Study. *Acta Derm. Venereol.* **2017**, *97*, 117–119. [CrossRef]
107. Roldán-Marín, R.; Toussaint-Caire, S. Imiquimod 5% as Adjuvant Therapy for Incompletely Excised Infiltrative Nodular Basal Cell Carcinoma and Dermoscopy to Monitor Treatment Response. *Dermatol. Ther.* **2015**, *5*, 265–272. [CrossRef]
108. Diluvio, L.; Campione, E.; Paternò, E.J.; Orlandi, A.; Terrinoni, A.; Chimenti, S. Peculiar Clinical and Dermoscopic Remission Pattern Following Imiquimod Therapy of Basal Cell Carcinoma in Seborrhoeic Areas of the Face. *J. Dermatol. Treat.* **2009**, *20*, 124–129. [CrossRef]
109. Micantonio, T.; Fargnoli, M.C.; Piccolo, D.; Peris, K. Changes in Dermoscopic Features in Superficial Basal Cell Carcinomas Treated with Imiquimod. *Dermatol. Surg.* **2007**, *33*, 1403–1405. [CrossRef]
110. Husein-ElAhmed, H.; Fernandez-Pugnaire, M.A. Dermatoscopy-Guided Therapy of Pigmented Basal Cell Carcinoma with Imiquimod. *An. Bras. Dermatol.* **2016**, *91*, 764–769. [CrossRef]
111. Navarro-Bielsa, A.; Cerro-Muñoz, P.; Almenara-Blasco, M.; Gracia-Cazaña, T.; Gilaberte, Y. Dermoscopic Structures Predictive of Response to Photodynamic Therapy in Basal Cell Carcinoma. *Acta Derm. Venereol.* **2023**, *103*, adv00892. [CrossRef] [PubMed]
112. Apalla, Z.; Lallas, A.; Tzellos, T.; Sidiropoulos, T.; Lefaki, I.; Trakatelli, M.; Sotiriou, E.; Lazaridou, E.; Evangelou, G.; Patsatsi, A.; et al. Applicability of Dermoscopy for Evaluation of Patients' Response to Nonablative Therapies for the Treatment of Superficial Basal Cell Carcinoma. *Br. J. Dermatol.* **2014**, *170*, 809815. [CrossRef] [PubMed]
113. Diluvio, L.; Bavetta, M.; Di Prete, M.; Orlandi, A.; Bianchi, L.; Campione, E. Dermoscopic Monitoring of Efficacy of Ingenol Mebutate in the Treatment of Pigmented and Non-Pigmented Basal Cell Carcinomas. *Dermatol. Ther.* **2017**, *30*, e12438. [CrossRef] [PubMed]
114. Diluvio, L.; Lanna, C.; Lozzi, F.; Palumbo, V.; Bianchi, L.; Campione, E. Basal Cell Carcinomas Treated with 0.5% 5-Fluorouracil and 10% Salicylic Acid Topical Solution. *Dermatol. Ther.* **2019**, *32*, e12908. [CrossRef]
115. Tognetti, L.; Cinotti, E.; Fiorani, D.; Couzan, C.; Cavarretta, C.; Chazelle, M.; Labeille, B.; Pianigiani, E.; Cevenini, G.; Perrot, J.L.; et al. Long-Term Therapy of Multiple Basal Cell Carcinomas: Clinicodermoscopic Score for Monitoring of Intermittent Vismodegib Treatment. *Dermatol. Ther.* **2019**, *32*, e13097. [CrossRef]
116. Calik, J.; Sauer, N.; Woźniak, B.; Wojnar, A.; Pietkiewicz, P.; Dzięgiel, P. Pilot Study on High-Intensity Focused Ultrasound (HIFU) for Basal Cell Carcinoma: Effectiveness and Safety. *J. Clin. Med.* **2024**, *13*, 3277. [CrossRef]
117. Krzysztofiak, T.; Suchorzepka, M.; Tukiendorf, A.; Wojcieszek, P.; Kamińska-Winciorek, G. Basal Cell Carcinoma After High Dose Rate Brachytherapy: Medium-Term Dermoscopic Evaluation of Cancer's Response. *Dermatol. Ther.* **2023**, *13*, 2063–2078. [CrossRef]
118. Krzysztofiak, T.; Kamińska-Winciorek, G.; Tukiendorf, A.; Suchorzepka, M.; Wojcieszek, P. Basal Cell Carcinoma Treated with High Dose Rate (HDR) Brachytherapy—Early Evaluation of Clinical and Dermoscopic Patterns During Irradiation. *Cancers* **2021**, *13*, 5188. [CrossRef]
119. Navarrete-Dechent, C.; Cordova, M.; Liopyris, K.; Aleissa, S.; Rajadhyaksha, M.; Cohen, G.; Marghoob, A.A.; Rossi, A.M.; Barker, C.A. In Vivo Imaging Characterization of Basal Cell Carcinoma and Cutaneous Response to High-Dose Ionizing Radiation Therapy: A Prospective Study of Reflectance Confocal Microscopy, Dermoscopy, and Ultrasonography. *J. Am. Acad. Dermatol.* **2021**, *84*, 1575–1584. [CrossRef]
120. Council, M.L. Commentary on "In Vivo Imaging Characterization of Basal Cell Carcinoma Cutaneous Response to High-Dose Ionizing Radiation Therapy: A Prospective Study of Reflectance Confocal Microscopy, Dermoscopy, and Ultrasound". *J. Am. Acad. Dermatol.* **2021**, *84*, 1792–1793. [CrossRef]
121. Navarrete-Dechent, C.; Pietkiewicz, P.; Dusza, S.W.; Andreani, S.; Nehal, K.S.; Rossi, A.M.; Cordova, M.; Lee, E.H.; Chen, C.J.; Abarzua-Araya, A.; et al. Ultraviolet-Induced Fluorescent Dermoscopy for Biopsy Site Identification Prior to Dermatologic Surgery: A Retrospective Study. *J. Am. Acad. Dermatol.* **2023**, *89*, 841–843. [CrossRef] [PubMed]
122. Gil-Pallares, P.; Muelas-Rives, I.; Navarro-Bielsa, A.; Gilaberte, Y.; Suárez-Peñaranda, J.M. Identification of Skin Tumors Margins Using Wood's Light: "The Umbrella Effect". *Photodiagn. Photodyn. Ther.* **2024**, *46*, 104089. [CrossRef] [PubMed]
123. Wojtowicz, I.; Żychowska, M. Application of Ultraviolet-Enhanced Fluorescence Dermoscopy in Basal Cell Carcinoma. *Cancers* **2024**, *16*, 2685. [CrossRef] [PubMed]
124. Seidenari, S.; Bellucci, C.; Bassoli, S.; Arginelli, F.; Magnoni, C.; Ponti, G. High Magnification Digital Dermoscopy of Basal Cell Carcinoma: A Single-Centre Study on 400 Cases. *Acta Derm. Venereol.* **2014**, *94*, 677–682. [CrossRef]
125. Pogorzelska-Dyrbuś, J.; Lallas, A.; Szepietowski, J.C. Morphology of Vessels in Basal Cell Carcinoma in Optical Super-High Magnification Dermoscopy. *Acta Derm. Venereol.* **2023**, *103*, adv11966. [CrossRef]
126. Pogorzelska-Dyrbuś, J. "Oak-Leaf-Like" Loop Vessels in Super-High Magnification Dermoscopy of Basal Cell Carcinoma. *Dermatol. Pract. Concept.* **2022**, *12*, e2022147. [CrossRef]
127. Pogorzelska-Dyrbuś, J.; Cinotti, E.; Lallas, A. Differentiation of Dermal Nevus and Basal Cell Carcinoma Based on Optical-Super High Magnification Dermoscopy. *Dermatol. Pract. Concept.* **2024**, *14*, e2024094. [CrossRef]

128. Dobrosavljevic, D.; Brasanac, D.; Glumac, S.; Radojevic, S.; Matija, L.; Stanisavljevic, D. Sensitivity and Specificity of Ex Vivo Dermatoscopy: A Case Series. *Int. J. Dermatol.* **2018**, *57*, 915–921. [CrossRef]
129. Haspeslagh, M.; Vossaert, K.; Lanssens, S.; Noë, M.; Hoorens, I.; Chevolet, I.; De Wispelaere, I.; Degryse, N.; Facchetti, F.; Brochez, L. Comparison of Ex Vivo and In Vivo Dermoscopy in Dermatopathologic Evaluation of Skin Tumors. *JAMA Dermatol.* **2016**, *152*, 312–317. [CrossRef]
130. Haspeslagh, M.; Hoorens, I.; Degryse, N.; De Wispelaere, I.; Degroote, A.; Van Belle, S.; Verboven, J.; Vossaert, K.; Facchetti, F.; Van Dorpe, J.; et al. Pathologic Evaluation of Skin Tumors with ex vivo dermoscopy with derm dotting. *JAMA Dermatol.* **2017**, *153*, 154161. [CrossRef]
131. Hobelsberger, S.; Steininger, J.; Laske, J.; Berndt, K.; Meier, F.; Beissert, S.; Gellrich, F.F. Clinician's Ability to Identify Non-Melanoma Skin Cancer on 3D-Total Body Photography Sectors that Were Initially Identified During In-Person Skin Examination with Dermoscopy. *Dermatology* **2024**, *240*, 142151. [CrossRef] [PubMed]
132. Dellatorre, G.; Gadens, G.A. Wide Area Digital Dermoscopy Applied to Basal Cell Carcinoma. *An. Bras. Dermatol.* **2020**, *95*, 379–382. [CrossRef] [PubMed]
133. Lorentzen, H.F.; Eefsen, R.L.; Weismann, K. Comparison of Classical Dermatoscopy and Acrylic Globe Magnifier Dermatoscopy. *Acta Derm. Venereol.* **2008**, *88*, 139–142. [CrossRef] [PubMed]
134. Hofmann, M.A.; Keim, U.; Jagoda, A.; Forschner, A.; Fink, C.; Spänkuch, I.; Tampouri, I.; Eigentler, T.; Weide, B.; Haenssle, H.A.; et al. Dermatofluoroscopy Diagnostics in Different Pigmented Skin Lesions: Strengths and Weaknesses. *J. Dtsch. Dermatol. Ges.* **2020**, *18*, 682–690. [CrossRef]
135. Janssen, L.; Mylle, S.; Van Kelst, S.; De Smedt, J.; Diricx, B.; Kimpe, T.; Boone, M.; Verhaeghe, E.; Brochez, L.; Garmyn, M. Enhanced Visualization of Blood and Pigment in Multispectral Skin Dermoscopy. *Skin Res. Technol.* **2020**, *26*, 708–712. [CrossRef]
136. Romano, R.A.; Teixeira Rosa, R.G.; Salvio, A.G.; Jo, J.A.; Kurachi, C. Multispectral Autofluorescence Dermoscope for Skin Lesion Assessment. *Photodiagn. Photodyn. Ther.* **2020**, *30*, 101704. [CrossRef]
137. Monnier, J.; De Carvalho, N.; Harris, U.; Garfinkel, J.; Saud, A.; Navarrete-Dechent, C.; Liopyris, K.; Reiter, O.; Rubinstien, G.; Iftimia, N.; et al. Combined Reflectance Confocal Microscopy and Optical Coherence Tomography to Improve the Diagnosis of Equivocal Lesions for Basal Cell Carcinoma. *J. Am. Acad. Dermatol.* **2022**, *86*, 934–936. [CrossRef]
138. Maron, R.C.; Weichenthal, M.; Utikal, J.S.; Hekler, A.; Berking, C.; Hauschild, A.; Enk, A.H.; Haferkamp, S.; Klode, J.; Schadendorf, D.; et al. Systematic Outperformance of 112 Dermatologists in Multiclass Skin Cancer Image Classification by Convolutional Neural Networks. *Eur. J. Cancer.* **2019**, *119*, 57–65. [CrossRef]
139. Widaatalla, Y.; Wolswijk, T.; Adan, F.; Hillen, L.M.; Woodruff, H.C.; Halilaj, I.; Ibrahim, A.; Lambin, P.; Mosterd, K. The Application of Artificial Intelligence in the Detection of Basal Cell Carcinoma: A Systematic Review. *J. Eur. Acad. Dermatol. Venereol.* **2023**, *37*, 1160–1167. [CrossRef]

cancers

MDPI

Article

Application of Ultraviolet-Enhanced Fluorescence Dermoscopy in Basal Cell Carcinoma

Irena Wojtowicz and Magdalena Żychowska *

Department of Dermatology, Institute of Medical Sciences, Medical College of Rzeszow University, 35959 Rzeszow, Poland; wojtowicz.irena.maria@gmail.com
* Correspondence: magda.zychowska@gmail.com

Simple Summary: Basal cell carcinoma (BCC) is the most prevalent type of skin cancer, accounting for a significant number of cases globally each year. Most BCCs develop on the face, and, therefore, the cosmetic outcome of excision is particularly important. Early diagnosis allows for easier removal of smaller lesions, while precise excision reduces the likelihood of recurrence. This study aimed to assess the utility of a novel non-invasive imaging approach, the ultraviolet-enhanced fluorescence dermoscopy (UVFD), for imaging of BCCs. Based on the analysis of a group of 163 BCCs, we found that UVFD may provide additional valuable clues, especially in the case of tumors located on the face, small BCCs (<5 mm), non-pigmented variants and nodular subtypes.

Abstract: Introduction: Basal cell carcinoma (BCC) is the most common non-melanoma skin cancer. The aim of the current study was to analyze the ultraviolet-enhanced fluorescence dermoscopy (UVFD) characteristics of BCCs. Methods: BCCs were evaluated under polarized dermoscopy (PD) and UVFD. The findings in PD were described using predefined parameters for dermoscopic evaluation in dermato-oncology. UVFD characteristics were determined based on personal observations, and included interrupted follicle pattern, absence of pink-orange or blue-green fluorescence, well-demarcated borders, and dark silhouettes. Results: In total, 163 BCCs were analyzed. Under UVFD, the interrupted follicle pattern ($p < 0.001$), absence of pink-orange fluorescence ($p = 0.005$) and well-demarcated borders ($p = 0.031$) were more frequently noted in BCCs < 5 mm than in bigger tumors. Lesions on the face showed clearly defined borders ($p = 0.031$) and interrupted follicle pattern ($p < 0.001$) more frequently than tumors located beyond the face. Nodular BCCs displayed interrupted follicle pattern ($p = 0.001$) and absence of pink-orange fluorescence ($p < 0.001$) more commonly than superficial subtypes. Non-pigmented BCCs more frequently showed lack of blue-green fluorescence ($p = 0.007$) and interrupted follicle pattern ($p = 0.018$) compared to pigmented variants. Conclusions: UVFD may be a valuable, complementary to PD, tool in the diagnosis of BCC, particularly in small tumors, lesions located on the face and nodular or non-pigmented subtypes.

Keywords: basal cell carcinoma; dermoscopy; dermatoscopy; ultraviolet; UVFD

Citation: Wojtowicz, I.; Żychowska, M. Application of Ultraviolet-Enhanced Fluorescence Dermoscopy in Basal Cell Carcinoma. *Cancers* **2024**, *16*, 2685. https://doi.org/10.3390/cancers16152685

Academic Editors: Paola Savoia and Elisa Zavattaro

Received: 25 June 2024
Revised: 23 July 2024
Accepted: 25 July 2024
Published: 28 July 2024

1. Introduction

Basal cell carcinoma (BCC) is the most frequent form of non-melanoma skin cancer, predominantly affecting fair-skinned individuals. The lifetime risk is estimated to be 33% to 39% in white men and 23% to 28% in white women [1]. Diagnosis is based on clinico-dermoscopic features, although histopathological examination remains the gold standard [2]. According to the systematic review of studies on BCC diagnosis, naked eye examination had a sensitivity of 66.9% and specificity of 97.2%, which increased to 85.0% and 98.2%, respectively, with the addition of dermatoscopy [3].

Additionally, a novel diagnostic approach, the integration of ultraviolet light into dermatoscopes (ultraviolet-enhanced fluorescence dermoscopy—UVFD), has shown promise in facilitating more precise evaluations of many skin lesions. This technique may be useful

for assessing neoplastic conditions, such as melanoma, BCC, glomus tumor and apocrine hidrocystoma [4–8]. It also proves effective for evaluating non-neoplastic dermatoses, including alopecia, vitiligo, melasma, porokeratosis, psoriasis and various fungal, bacterial, viral and parasitic infections [4,9–21].

Ultraviolet (UV) light functions through a process known as the Stokes shift. The UVA spectrum ranges from 320 to 400 nm, with the DL5 dermatoscope specifically emitting at 365 nm. Chromophores in the skin, such as melanin and hemoglobin, absorb the UV light, exciting their electrons to higher energy levels. As the electrons return to their ground state, they emit photons at longer wavelengths within the visible spectrum, producing fluorescence. This fluorescence increases the visibility of skin structures by highlighting differences in absorption and reflection among various chromophores, leading to improved diagnostic imaging in dermatology [4].

So far, UVFD has been reported to be helpful in identifying biopsy sites for BCC prior to Mohs micrographic surgery. The surgical site tended to be more apparent (darker than the surrounding skin) under UVFD compared to the images obtained with traditional polarized dermoscopy (PD) [4,22]. Moreover, UVFD was suggested to help in detecting fresh erosions (one of the dermoscopic phenomena in BCC) in skin lesions due to the presence of bilirubin in dried-out crust [4,23]. However, to the best of our knowledge, the UVFD features of BCCs have not been analyzed, yet.

The aim of the current study was to comprehensively analyze the UVFD characteristics of BCCs in patients with Fitzpatrick skin phototype I–III, with particular emphasis on lesion location, diameter and clinical subtype.

2. Methods

The research was carried out at the Department of Dermatology in Rzeszow, located in southeastern Poland. Patients with a clinical and dermoscopic suspicion of BCC, who presented to the department between May and December 2023 were recruited for the study. The preliminary diagnosis was histopathologically confirmed in each patient.

Clinical data collected in each case included patient's sex, Fitzpatrick skin phototype, location of the tumor, diameter and clinical subtype. Dermoscopic examinations, both PD and UVFD, were performed with a Dermlite DL5 dermatoscope. For each lesion at least one image was captured under PD, and one using UV light (365 nm). The images were obtained using an iPhone 7 Plus and were stored until analysis. Cases were excluded if the diagnosis was unverified or the quality of dermoscopic photos was poor. The images were analyzed by two dermatologists with experience in dermoscopy (IW and MŻ). All discrepancies were discussed until consensus was reached.

Predefined dermoscopic criteria in dermato-oncology were applied to characterize the findings seen in PD [24]. The phenomena included vascular patterns (arborizing vessels, short fine telangiectasia, hairpin vessels), pigmented structures (maple leaf-like areas, gray ovoid nests, spoke wheel areas, blue-gray globules, blue-white veil, blue-gray peppering, concentric structures, peripheral striations) and other (hemorrhage, multiple erosions, red-white homogenous area, white structureless areas, milia-like cysts, comedo-like openings, scale, follicular plugging, a peri-follicular white ring, keratin masses, shiny white lines and well-demarcated borders).

UVFD features have not been defined in the literature, yet. Based on personal observations of the authors, the following findings were distinguished: dark silhouettes, interrupted follicle pattern, erosions/ulcerations, white-blue scales, arborizing vessels, lack of blue-green fluorescence, pink-orange fluorescence, lack of pink-orange fluorescence, blue-fluorescent fibers, black globules, white depigmentation, white clods, well-demarcated borders.

A BCC was defined to have a "dark silhouette" if the tumor area was darker than the surrounding skin. "Interrupted follicle pattern" meant that regular dark round or oval structures corresponding to follicular ostia were present in the surrounding skin, but not in the tumor area. Similarly, "lack of blue-green fluorescence" and "lack of pink-orange

fluorescence" were defined as presence of follicular fluorescence, either blue-green or pink-orange, in the surrounding skin, but not in the tumor area. "White depigmentation" referred to whitish structureless area that was brighter than the rest of the tumor area and the surrounding skin. In turn, "well-demarcated borders" referred to sharply defined borders separating the tumor from the surrounding skin.

This study was conducted according to the guidelines of the Declaration of Helsinki. Informed written consent was obtained from all subjects for participation in the study and the publication of images.

Statistical Analysis

Statistical analysis was conducted using SPSS. Categorical data were represented as absolute numbers and percentages, while continuous data were shown as mean ± standard deviation (SD) and median (range). Fisher's exact test was used to assess differences in the frequencies of dermoscopic features. A *p*-value of less than 0.05 was deemed statistically significant.

3. Results

3.1. Clinical Characteristics

A total of 52 patients (29 women and 23 men), with a total number of 163 BCCs, were included in the study. All patients had Fitzpatrick skin phototypes I–III. The most frequent tumor locations were the face (*n* = 83; 50.9%) and back (*n* = 45; 27.6%), with a smaller number of BCCs located on the upper limbs (*n* = 7; 4.3%). None of the patients had BCCs located on the lower limbs. The BCCs were divided into two clinical subtypes: nodular (*n* = 72; 44.2%) and superficial (*n* = 91; 55.8%). Among these, 73 (44.8%) tumors were identified as pigmented BCCs. The mean diameter of the BCCs was 8.1 ± 5 mm. Table 1 displays the demographic and clinical data of the study participants.

Table 1. Clinical characteristics (BCC—basal cell carcinoma; *n*—number of cases; SD—standard deviation).

Clinical Characteristics	
Patients	*n* = 52
Gender, *n* (%)	
Male	23 (44.2)
female	29 (55.8)
Fitzpatrick skin phototype, *n* (%)	
I	29 (55.8)
II	22 (42.3)
III	1 (1.9)
Total number of BCC	*n* = 163
Location of BCC, *n* BCC (% BCC)	
face	83 (50.9)
scalp	9 (5.5)
nape	1 (0.6)
upper limbs	7 (4.3)
back	45 (27.6)
chest	6 (3.7)
abdomen	12 (7.4)

Table 1. *Cont.*

Clinical Characteristics	
Clinical subtype, *n* BCC (% BCC)	
nodular	72 (44.2)
superficial	91 (55.8)
pigmented	73 (44.8)
non-pigmented	90 (55.2)
Diameter of BCC (mm), *n* BCC (% BCC)	
Mean ± SD	8.1 ± 5
Diameter 0–4 mm	63 (38.6)
Diameter 5–10 mm	64 (39.3)
Diameter > 10 mm	36 (22.1)

3.2. UVFD Findings and Association with PD Features

Dermoscopic examination, including both PD and UVFD, identified the most frequent features. Table 2 lists these features along with their occurrence frequencies.

Table 2. Findings in BCC observed with polarized dermoscopy and ultraviolet-induced fluorescent dermoscopy (*n*—number of BCCs).

	Total *n* = 163	**%**
Polarized Dermoscopy (PD)		
ulcerations/micro-ulcerations	56	34.4
maple leaf-like areas	31	19.0
gray ovoid nests	10	6.1
spoke wheel areas	21	12.9
blue-gray globules	35	21.5
arborizing vessels	50	30.7
multiple erosions	27	16.6
short fine teleangiectasias	79	48.5
concentric structures	8	4.9
red-white homogenous areas	84	51.5
blue-white veil	1	0.6
blue-gray peppering	31	19.0
milia-like cysts	10	6.1
comedo-like openings	2	1.2
scales	47	28.8
peripheral striations	10	6.1
follicular pluggings	2	1.2
peri-follicular white rings	4	2.5
keratin masses	5	3.1
hairpin vessels	1	0.6
hemorrhages	22	13.5

Table 2. *Cont.*

	Total n = 163	%
Polarized Dermoscopy (PD)		
white structureless areas	51	31.3
shiny white lines	9	5.5
well-demarcated borders	27	16.6
Ultraviolet-Induced Fluorescent Dermoscopy (UVFD)		
dark silhouettes	134	82.2
interrupted follicle pattern	52	31.9
erosions/ulcerations	12	7.4
white-blue scales	47	28.8
arborizing vessels	28	17.2
lack of blue-green fluorescence	54	33.1
pink-orange fluorescence	3	1.8
lack of pink-orange fluorescence	43	26.4
blue-fluorescent fibers	4	2.5
black globules	48	29.4
white depigmentation	15	9.2
white clods	8	4.9
well-demarcated borders	39	23.9

3.2.1. PD

Under PD, the common findings included homogeneous red-white areas (51.5%), ulcerations/micro-ulcerations (34.4%), structureless white areas (31.3%), scales (28.8%) and vascular morphologies such as short fine telangiectasias (48.5%) and arborizing vessels (30.7%).

3.2.2. UVFD

UVFD revealed dark silhouettes (82.2%) with interrupted follicle pattern (31.9%), absence of blue-green fluorescence (33.1%) within the tumor compared to the surrounding healthy skin, black globules (29.4%), white-blue scales (28.8%), lack of pink-orange fluorescence (26.4%), well-demarcated borders (23.9%) and arborizing vessels (17.2%). Less frequently observed findings included white depigmentation (9.2%), erosion/ulceration (7.4%), white clods (4.9%), presence of blue-fluorescent fibers (2.5%) and pink-orange fluorescence (1.8%). Sample UVFD images showing all described features are presented in Figure 1.

Moreover, statistical analysis was performed to evaluate the association between UVFD findings and PD features.

Dark Silhouette

Dark silhouettes were more commonly observed under UVFD, if BCC showed short fine telangiectasias (92.1% vs. 73.6%, $p = 0.002$) or red-white homogeneous areas (90.5% vs. 73.4%; $p = 0.007$) in PD. However, they were significantly less frequent in BCCs displaying white structureless areas (59.6% vs. 92.8%; $p < 0.001$) in PD.

Interrupted Follicle Pattern

The interrupted follicle pattern was less common under UVFD in BCCs with peripheral striations (0% vs. 34.2% without peripheral striations, $p = 0.031$), maple leaf-like areas (9.7% vs. 37.1%, $p = 0.003$), ulcerations/micro-ulcerations (17.9% vs. 39.3%, $p = 0.008$), red-white

homogenous areas (23.8% vs. 40.5%; $p = 0.029$) and scales (18.8% vs. 37.4%; $p = 0.026$) in PD. On the other hand, the interrupted follicle pattern was more frequent in tumors with arborizing vessels (51.0% vs. 23.2%; $p < 0.001$). It was also significantly more commonly noted in BCCs showing well-demarcated borders under PD (55.6% vs. 27.2%; $p = 0.006$).

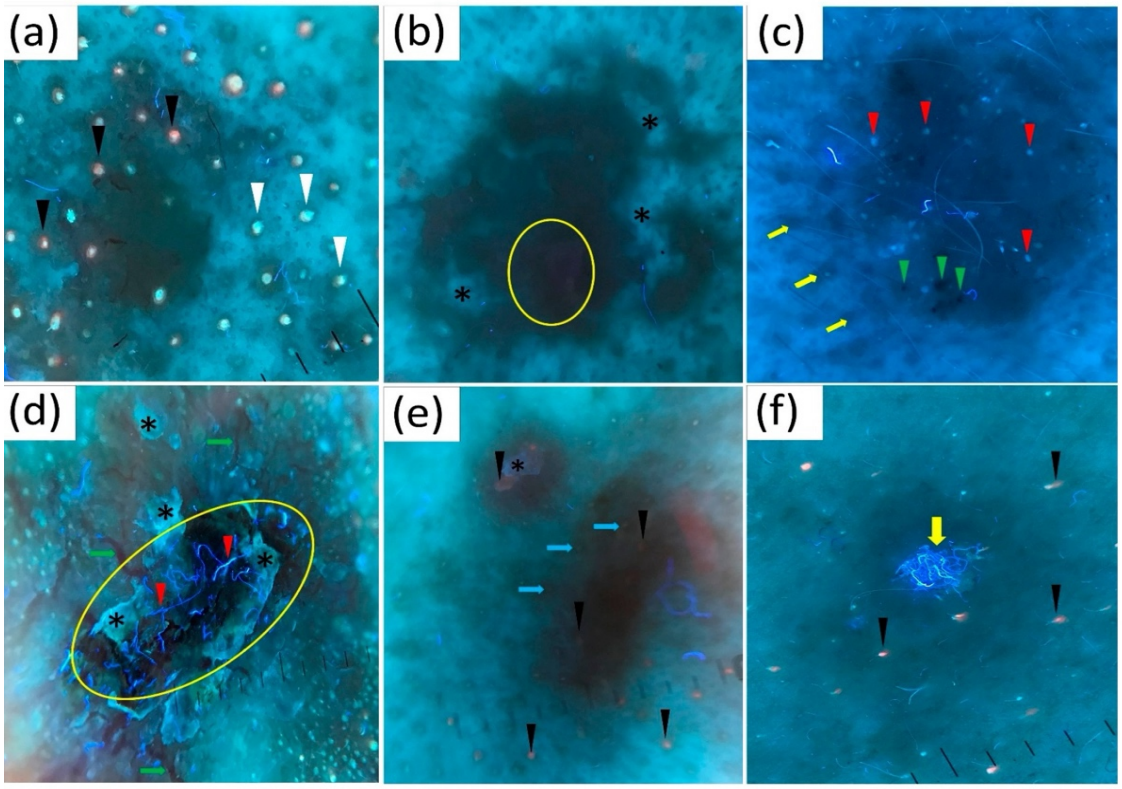

Figure 1. Structures present in basal cell carcinoma (BCC) in ultraviolet-enhanced fluorescence dermoscopy (UVFD). (**a**) Dark silhouette of the lesion, pink-orange follicular fluorescence (black arrowheads) and blue-green follicular fluorescence (white arrowheads) present in the surrounding normal skin but absent in the tumor area. (**b**) Dark silhouette of the lesion, white depigmentation (black asterisks), pink-orange fluorescence (yellow circle). (**c**) Dark silhouette of the BCC, white clods (red arrowheads), black globules (green arrowheads), normal follicle pattern (yellow arrows) in the surrounding skin and interruption of the follicle pattern within the lesion. (**d**) White-blue scale (black asterisks), blue-fluorescent fibers (red arrowheads), arborizing vessels (green arrows). (**e**) Dark silhouette of the lesion, pink-orange follicular fluorescence (black arrowheads) in the surrounding skin and absent in the tumor area, white-blue scale (black asterisk), regular follicle pattern in the surrounding skin and interrupted follicle pattern within the lesion (blue arrows). (**f**) Blue-fluorescent fibers (yellow arrow), pink-orange follicular fluorescence (black arrowheads).

Erosions/Ulcerations

Erosions or ulcerations were visualized with UVFD in only 12 out of 56 (21.4%) BCCs showing this feature in PD ($p < 0.001$). In addition, they were significantly more frequently observed in tumors with hemorrhages under PD (30.4% vs. 3.6%; $p < 0.001$).

White-Blue Scales

White-blue scales was present under UVFD significantly more frequently in BCCs showing ulcerations/microulcerations (67.9% vs. 9.3%; $p < 0.001$), multiple erosions (76.9% vs. 20.4%; $p < 0.001$), short fine teleangiectasia (40.8% vs. 19.5%; $p = 0.003$), red-white homogenous areas (45.2% vs. 12.7%; $p < 0.001$) or hemorrhages (69.6% vs. 22.9%; $p < 0.001$) under PD. Interestingly, this UVFD finding was significantly less common in tumors with white structureless areas in PD (13.5% vs. 36.9%; $p = 0.003$).

White-blue fluorescent scales were observed in the majority of BCCs (77.1%) showing presence of scales under classical PD. However, this feature was also noted under UVFD in 11 out of 115 (9.6%) cases lacking scales in PD—$p < 0.001$.

Arborizing Vessels

Under UVFD, arborizing vessels were noted only in 25 out of 51 (49.0%) tumors showing this feature in PD ($p < 0.001$).

Absence of Blue-Green Fluorescence

The absence of blue-green fluorescence in UVFD was observed less frequently in BCCs with peripheral striations (0% vs. 35.5%; $p = 0.032$), spoke wheel areas (9.5% vs. 36.6%; $p = 0.013$) or maple leaf-like areas (12.9% vs. 37.9%; $p = 0.01$) in PD. Conversely, this UVFD finding was significantly more frequent in BCCs showing presence of arborizing vessels (60.8% vs. 20.5%; $p < 0.001$) or well-demarcated borders (51.9% vs. 29.4%; $p = 0.042$) in PD.

Absence of Pink-Orange Fluorescence

The absence of pink-orange fluorescence was significantly less common in BCCs with maple leaf-like areas (9.7% vs. 30.3%, $p = 0.022$) or spoke wheel areas (4.8% vs. 29.6% $p = 0.016$) in PD. However, it was significantly more frequently observed in tumors showing arborizing vessels (49.0% vs. 16.1%; $p < 0.001$) and well-demarcated borders (44.4% vs. 22.8%; $p = 0.03$) in PD.

Blue-Fluorescent Fibers

All BCCs with blue-fluorescent fibers in UVFD also exhibited ulcerations/micro-ulcerations in PD. This strongly indicates that the presence of blue-fluorescent fibers under UV light should prompt a search for ulcerations in the lesion.

Black Globules

Under UVFD, black globules are observed significantly more frequently in BCCs with spoke wheel areas (81% vs. 21.8%; $p < 0.001$), blue-gray globules (70.6% vs. 18.6%; $p < 0.001$), peripheral striations (70.0% vs. 27.0%; $p = 0.008$), maple leaf-like areas (64.5% vs. 21.2%; $p < 0.001$) and blue-gray peppering (63.3% vs. 21.8%; $p < 0.001$) in PD.

White Depigmentation

White depigmentation under UVFD was more commonly observed in tumors showing white structureless areas (21.2% vs. 4.5%; $p = 0.002$) in PD.

White Clods

White clods (globules) were more frequently observed in BCCs showing milia-like cysts in PD (50% vs. 2.0%; $p < 0.001$).

Well-Demarcated Borders

Well-demarcated borders were present under UVFD less frequently in BCCs with white structureless areas (7.7% vs. 31.5%; $p < 0.001$) in PD. On the other hand, they were significantly more frequent in tumors, which were also well-defined under PD (62.7% vs. 16.2%; $p < 0.001$). However, it should be emphasized, that over half of BCCs (22 out of 39; 56.4%) with well-demarcated borders under UVFD did not show this feature under PD.

3.3. UVFD Findings by Tumor Location

Taking into consideration anatomical differences, two groups were distinguished—BCCs located on the face ($n = 83$; 50.9%) and BCCs located beyond the face ($n = 80$; 49.1%). The demarcation of BCC borders was more distinct in UVFD than in PD (23.9% vs. 16.6%), particularly on the face (38.6% vs. 26.5%). The areas where UVFD markedly enhanced margin visibility compared with PD were the nose (60% vs. 35%) and the forehead (41.7%

vs. 16.7%). Overall, UVFD showed clearly defined borders in 38.6% of BCCs on the face and in only 8.8% of BCCs located beyond the face ($p = 0.031$).

The interrupted follicle pattern was more prominently observed in UVFD on the face compared to other body regions (53% vs. 10%, $p \leq 0.001$), with the highest frequency on the nose (75%). Similarly, lack of pink-orange fluorescence was more common in BCCs located on the face (43.4% vs. 8.8%, $p = 0.005$). Erosions/ulcerations were also more frequently noted on the face (12% vs. 2.5%, p-value = 0.008). On the other hand, UVFD more frequently revealed white scales in BCCs located on areas beyond the face than on the face (35% vs. 22.9%, $p \leq 0.001$).

Table 3 and Figure 2 summarize the UVFD findings according to the location of the lesion.

Table 3. UVFD findings according to the location of the BCCs (n—number of BCCs).

Location of BCC, n (%)	Face n = 83	%	Beyond Face n = 80	%	p-Value
dark silhouettes	69	83.1	65	81.3	0.819
interrupted follicle pattern	44	53.0	8	10.0	<0.001
erosions/ulcerations	10	12.0	2	2.5	0.008
white-blue scales	19	22.9	28	35.0	<0.001
arborizing vessels	25	30.1	3	3.8	0.166
lack of blue-green fluorescence	43	51.8	11	13.8	0.073
pink-orange fluorescence	3	3.6	0	0,0	0.635
lack of pink-orange fluorescence	36	43.4	7	8.8	0.005
blue-fluorescent fibers	1	1.2	3	3.8	0.311
black globules	17	20.5	31	38.8	0.084
white depigmentation	3	3.6	12	15.0	0.105
white clods	4	4.8	4	5.0	0.115
well-demarcated borders	32	38.6	7	8.8	0.031

3.4. UVFD Findings by Tumor Diameter

BCCs were categorized based on their diameter into small (<5 mm; n = 63; 38.6%), medium (5–10 mm; n = 64; 39.3%) and large (>10 mm; n = 36; 22.1%).

In smaller BCCs, UVFD showed an interrupted follicle pattern (41.3% vs. 29.7% vs. 19.4%, $p < 0.01$), lack of pink-orange fluorescence (38.1% vs. 21.9% vs. 13.9%, $p = 0.005$) and well-demarcated borders (33.3% vs. 20.3% vs. 13.9%, $p = 0.031$) significantly more frequently. Conversely, UVFD displayed white-blue scales (58.3% vs. 31.3% vs. 9.5%, $p < 0.001$) and erosions/ulcerations (19.4% vs. 6.3% vs. 1.6%, $p = 0.008$) more frequently in BCCs with larger diameters.

Table 4 and Figure 3 present the UVFD characteristics categorized by the size of the BCCs.

3.5. UVFD Findings by Clinical Subtype

Based on clinical features, all BCCs were divided into nodular (n = 72; 44.2%) or superficial types (n = 91; 55.8%) and pigmented (n = 73; 44.8%) or non-pigmented (n = 90; 55.2%) variants.

Notably, UVFD demonstrated a significantly more frequent absence of follicular fluorescence, either blue-green or pink-orange in nodular BCCs than in superficial ones, with respective frequencies of 55.1% vs. 17.6% for blue-green ($p \leq 0.001$) and 44.9% vs. 13.2% for pink-orange ($p \leq 0.001$). Moreover, the majority of BCCs showing erosions/ulcerations (83.3%), arborizing vessels (65.5%), interrupted follicle pattern (63.5%) and well-demarcated borders (61.5%) in UVFD were nodular. White depigmentation was predominantly observed in superficial BCCs (87.5%). Pigmented BCCs displayed black globules under UV light with significantly higher frequency than non-pigmented BCCs (52.1% vs. 11.1%,

$p \leq 0.001$). In contrast, non-pigmented lesions exhibited a higher incidence of several specific features in UVFD compared to pigmented ones: lack of blue-green fluorescence (42.2% vs. 21.9%, $p = 0.007$), an interrupted follicle pattern (40% vs. 21.9%, $p = 0.018$), lack of pink-orange fluorescence (35.5% vs. 15.1%, $p = 0.004$) and presence of arborizing vessels (24.4% vs. 9.6%, $p = 0.014$).

Tables 5 and 6 and Figures 4 and 5 present UVFD characteristics according to the clinical type of BCCs.

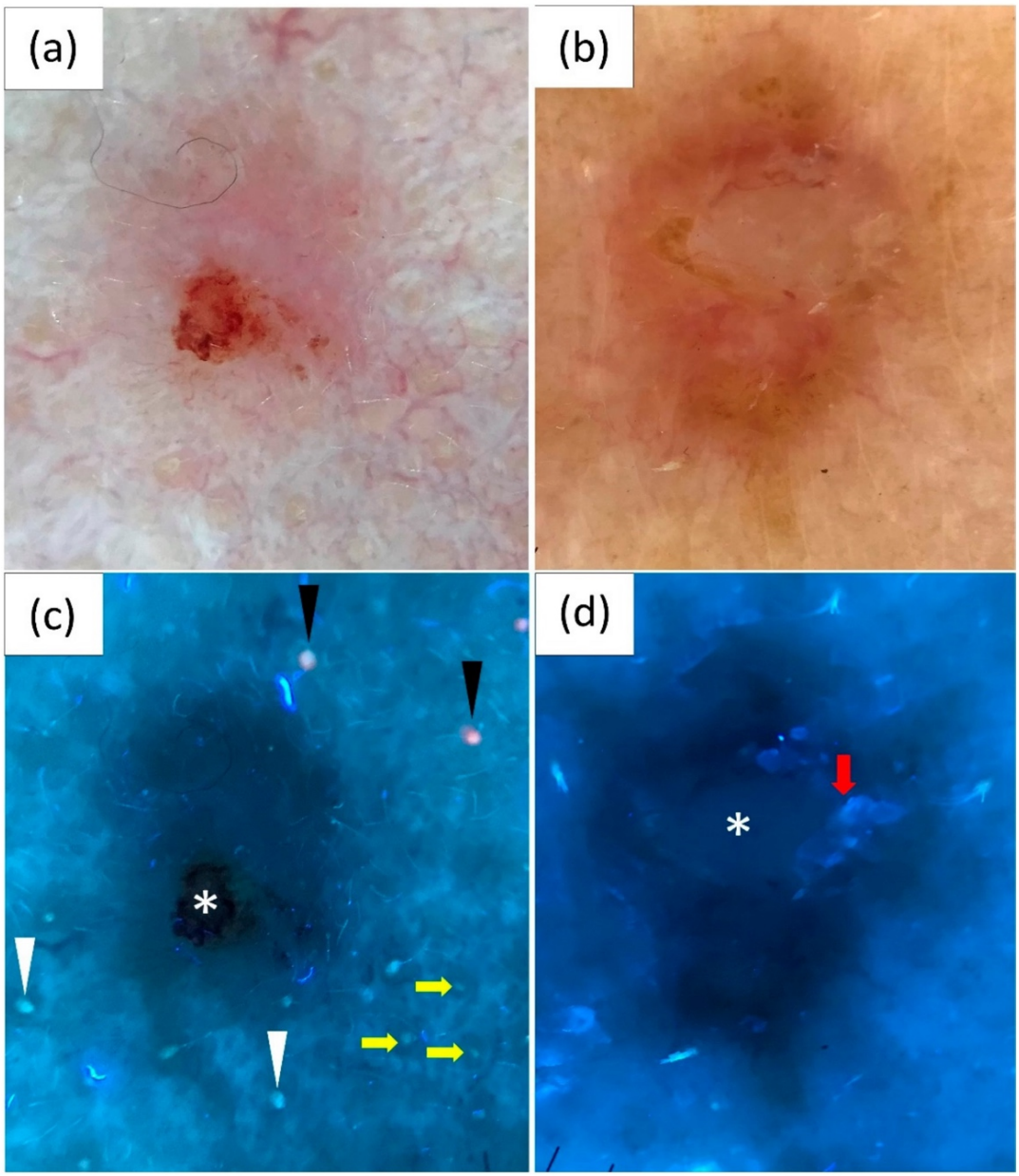

Figure 2. Polarized light dermoscopy (PD) presentation of basal cell carcinoma (BCC) on the (**a**) face and (**b**) beyond the face (back). (**c**,**d**) Corresponding images in ultraviolet-enhanced fluorescence dermoscopy (UVFD). (**c**) Dark silhouette, erosion (white asterisk), pink-orange follicular fluorescence at the periphery of the tumor (black arrowheads), blue-green follicular fluorescence at the periphery of the BCC (white arrowheads), absence of both types of fluorescence within the BCC, follicle pattern in the surrounding skin (yellow arrows), interrupted follicle pattern within the lesion. (**d**) Dark silhouette, white-blue scale (red arrow), white depigmentation (white asterisk).

Table 4. Ultraviolet-enhanced fluorescence dermoscopy (UVFD) characteristics categorized by the size of the basal cell carcinomas (BCCs); (*n*—number of BCCs).

Diameter of BCC, *n* (%)	<5 mm *n* = 63	%	5–10 mm *n* = 64	%	>10 mm *n* = 36	%	*p*-Value
dark silhouettes	51	81.0	53	82.8	30	83.3	0.819
interrupted follicle pattern	26	41.3	19	29.7	7	19.4	<0.001
erosions/ulcerations	1	1.6	4	6.3	7	19.4	0.008
white-blue scales	6	9.5	20	31.3	21	58.3	<0.001
arborizing vessels	13	20.6	8	12.5	8	22.2	0.166
lack of blue-green fluorescence	24	38.1	23	35.9	7	19.4	0.073
pink-orange fluorescence	2	3.2	1	1.6	0	0.0	0.635
lack of pink-orange fluorescence	24	38.1	14	21.9	5	13.9	0.005
blue-fluorescent fibers	1	1.6	1	1.6	2	5.6	0.311
black globules	20	31.7	20	31.3	8	22.2	0.084
white depigmentation	4	6.3	4	6.3	7	19.4	0.105
white clods	4	6.3	4	6.3	0	0.0	0.115
well-demarcated borders	21	33.3	13	20.3	5	13.9	0.031

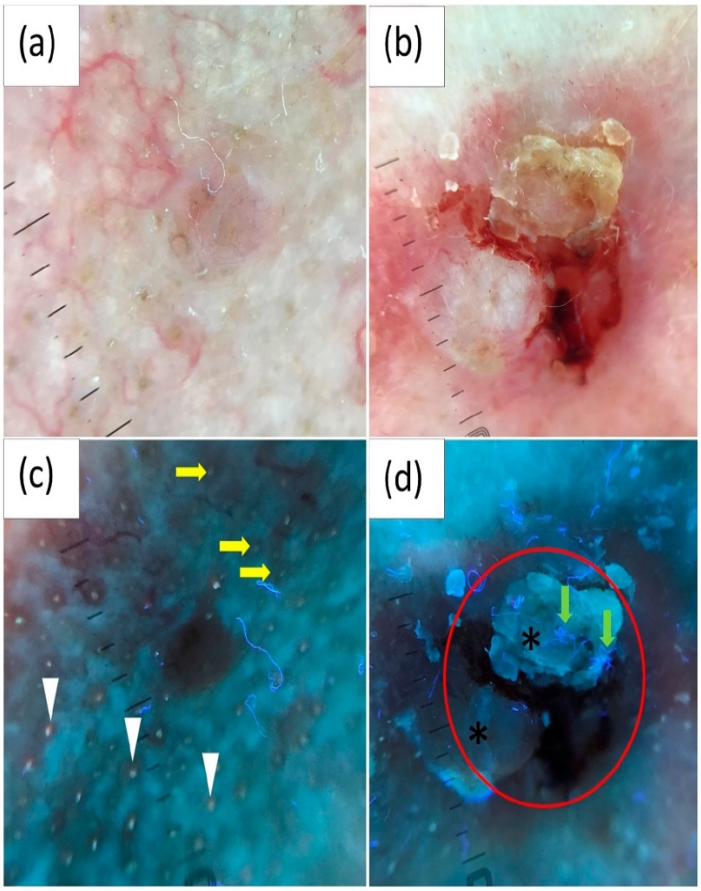

Figure 3. Polarized light dermoscopy (PD) presentation of (**a**) small (diameter < 5 mm) and (**b**) medium (diameter 5–10 mm) basal cell carcinoma (BCC). (**c**,**d**) Corresponding images in ultraviolet-enhanced fluorescence dermoscopy (UVFD). (**c**) Dark silhouette, pink-orange follicular fluorescence in the surrounding skin (white arrowheads), lack of this fluorescence within the BCC, regular follicle pattern at the periphery of the tumor (yellow arrows), interrupted follicle pattern within the lesion. (**d**) Ulceration (red circle), blue-fluorescent fibers (green arrows), scale (black asterisks).

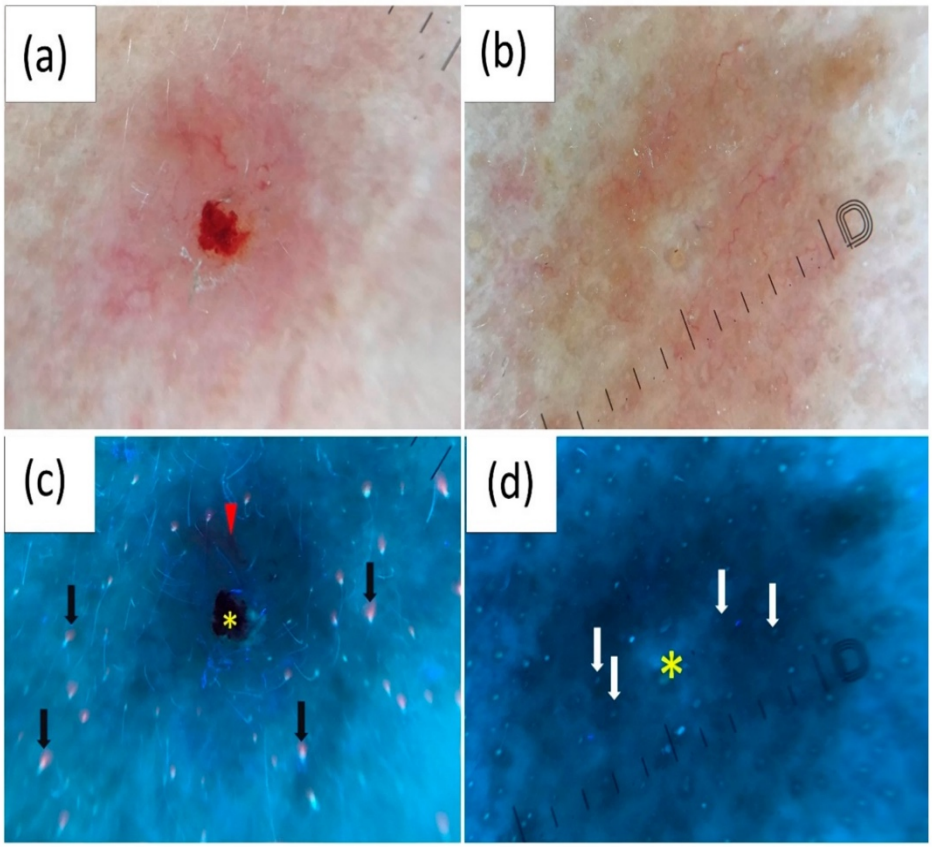

Figure 4. Polarized light dermoscopy (PD) presentation of (**a**) nodular and (**b**) superficial basal cell carcinoma (BCC). (**c**,**d**) Corresponding images in ultraviolet-enhanced fluorescence dermoscopy (UVFD). (**c**) Erosion (yellow asterisk), arborizing vessel (red arrowhead), pink-orange fluorescence in the surrounding skin (black arrows), lack of this fluorescence within the BCC. (**d**) White depigmentation (yellow asterisk) and follicle pattern (white arrows) are also present within the lesion.

Table 5. Ultraviolet-enhanced fluorescence dermoscopy (UVFD) characteristics of nodular and superficial basal cell carcinomas (BCCs); (*n*—number of BCCs).

Clinical Type of BCC, *n* (%)	Nodular *n* = 72	%	Superficial *n* = 91	%	*p*-Value
dark silhouettes	62	89.9	72	79.1	0.304
interrupted follicle pattern	33	47.8	19	20.9	0.001
erosions/ulcerations	10	14.5	2	2.2	0.006
white-blue scales	18	26.1	29	31.9	0.302
arborizing vessels	19	27.5	10	11.0	0.013
lack of blue-green fluorescence	38	55.1	16	17.6	<0.001
pink-orange fluorescence	1	1.4	2	2.2	1.000
lack of pink-orange fluorescence	31	44.9	12	13.2	<0.001
blue-fluorescent fibers	2	2.9	2	2.2	1.000
black globules	19	27.5	29	31.9	0.492
white depigmentation	2	2.9	13	14.3	0.007
white clods	5	7.2	3	3.3	0.304
well-demarcated borders	24	34.8	15	16.5	0.016

Table 6. Ultraviolet-enhanced fluorescence dermoscopy (UVFD) characteristics of pigmented and non-pigmented basal cell carcinomas (BCCs); (*n*—number of BCCs).

Clinical Type of BCC, *n* (%)	Pigmented *n* = 73	%	Non-Pigmented *n* = 90	%	*p*-Value
dark silhouettes	64	87.7	70	77.8	0.149
interrupted follicle pattern	16	21.9	36	40.0	0.018
erosions/ulcerations	2	2.7	10	11.1	0.067
white-blue scales	19	26.0	29	32.2	0.490
arborizing vessels	7	9.6	22	24.4	0.014
lack of blue-green fluorescence	16	21.9	38	42.2	0.007
pink-orange fluorescence	0	0.0	3	3.3	0.254
lack of pink-orange fluorescence	11	15.1	32	35.6	0.004
blue-fluorescent fibers	2	2.7	2	2.2	1.000
black globules	38	52.1	10	11.1	<0.001
white depigmentation	8	11.0	8	8.9	0.793
white clods	5	6.8	3	3.3	0.469
well-demarcated borders	17	23.3	22	24.4	1.000

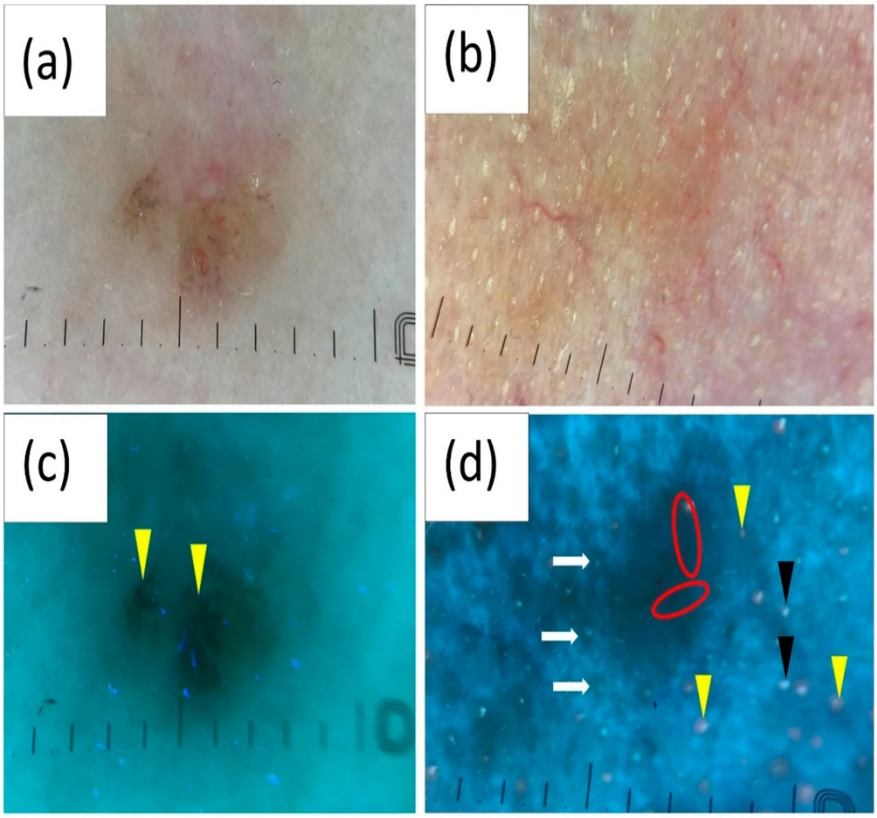

Figure 5. Polarized light dermoscopy (PD) presentation of (**a**) pigmented and (**b**) non-pigmented basal cell carcinoma (BCC). (**c**,**d**) Corresponding images in ultraviolet-enhanced fluorescence dermoscopy (UVFD). (**c**) Black globules (yellow arrowheads). (**d**) Arborizing vessels (red circles), follicle pattern (white arrows), interrupted follicle pattern within the lesion, pink-orange follicular fluorescence in the surrounding skin (yellow arrowheads), blue-green fluorescence in the surrounding skin (black arrowheads), lack of both types of fluorescence within the BCC.

4. Discussion

PD has become a key method for preliminary identification of BCCs. Its utility continues to expand. It has proven to be helpful in detecting small (<5 mm) lesions, which exhibit characteristic dermoscopic features from their onset [25]. PD aids in recognizing various histologic subtypes of BCC [26–29]. However, UVFD appears to be a new valuable supplementary method for detecting BCCs. So far, UVFD has been reported to help to identify biopsy site prior to Mohs micrographic surgery [22]. In a recent study by Navarrete-Dechent et al. [22], the authors showed that the area affected by the BCC appears darker than the surrounding skin under UVFD, which makes it easier to precisely determine the surgical area. However, to the best of our knowledge, there are no other studies that characterize in depth the UVFD features in BCCs. In our analysis, a dark silhouette was the most common finding, observed in the vast majority of lesions. However, BCCs showing white structureless areas in PD were also more likely to display white depigmentation rather than a dark silhouette under UVFD.

Combining UVFD with PD could enhance both the sensitivity and specificity of dermoscopy in identifying BCCs. Furthermore, clinical experience shows that defining the borders of a lesion prior to excision is often more challenging than the diagnosis itself. PD helps to identify the borders of BCCs [30,31], but UVFD offers extra details, often highlighting the edges more clearly than PD. The interrupted follicle pattern and lack of follicular fluorescence that is observed in the surrounding skin further increases tumor visibility.

UVFD has, undoubtedly, several limitations. Its sensitivity in visualization of erosions or ulcerations was much lower compared to classical PD, 78.6% of erosions present in PD were not observed under UVFD. It was similar in the case of vascular structures. Although UVFD enabled visualization of thicker arborizing vessels as black branching lines, most of the vascular structures present in PD were not visible under UVFD.

The usefulness of UVFD also seems to depend on the location of the tumor, its size and clinical subtype. This method primarily provides additional diagnostic clues in the case of lesions located on the face, where interrupted follicle pattern, lack of pink-orange follicle fluorescence and well-demarcated borders were more frequently noted. This may, of course, result from a certain anatomical difference of the face, a larger number of dilated follicle openings and increased activity of the sebaceous glands. The pink-orange fluorescence of the follicle openings within healthy skin is most probably linked to colonization with *Cutibacterium acnes*, which is more commonly observed on the face and in seborrheic locations. Therefore, it should not be surprising that disruption of the normal skin architecture by the growing tumor mass leads to interruption of the follicle pattern and, subsequently, lack of follicle fluorescence.

In the presented population, the usefulness of UVFD was greater for BCCs with a diameter of less than 10 mm, or even less than 5 mm. In smaller tumors, UVFD findings such as interrupted follicle pattern, lack of pink-orange fluorescence and well-demarcated borders were more frequently noted and provided additional clues to the classical PD. In bigger BCCs, UVFD showed presence of scales or ulcerations more frequently, but these features were also clearly visible in PD, so it seems that in this respect the benefit of using UVFD is limited.

When it comes to clinical subtype, UVFD seems to have an advantage in nodular BCCs, in which the method frequently shows well-defined borders, interrupted follicle pattern and lack of follicle fluorescence. This may also indirectly result from the location of the tumors—superficial subtypes were more commonly found on the trunk and upper extremities, where the fluorescence within the hair follicles is less frequently observed under normal conditions.

Similarly, UVFD showed advantages in non-pigmented BCCs, in which interrupted follicle pattern and lack of follicle fluorescence were more frequently noted.

5. Conclusions

UVFD is a novel non-invasive diagnostic method providing additional features of BCCs—dark silhouettes, interrupted follicle pattern, absence of blue-green fluorescence within the tumor compared to the surrounding healthy skin, presence of black globules, white-blue scales, lack of pink-orange fluorescence, presence of well-demarcated borders, arborizing vessels, white depigmentation, erosions/ulcerations, white clods, presence of blue-fluorescent fibers and pink-orange fluorescence. Despite its limitations, UVFD may be a valuable complementary method to classical PD in the preliminary diagnosis of BCC. This method seems to be more beneficial for the evaluation of lesions located on the face, small tumors and nodular or non-pigmented subtypes.

Author Contributions: Concept and design: I.W. and M.Ż.; methodology: I.W. and M.Ż.; data acquisition: M.Ż.; statistical analysis: M.Ż.; manuscript—draft preparation: I.W.; manuscript—final version editing: M.Ż. All authors have read and agreed to the published version of the manuscript.

Funding: The study was not supported by any funding or sponsorship. Dermlite DL5 dermatoscope was purchased from the grant funds no. INM/33/2023 of the University of Rzeszów awarded to Magdalena Żychowska.

Institutional Review Board Statement: This study was conducted according to the guidelines of the Declaration of Helsinki. Since this study is an analysis of data obtained in clinical routine care in an academic university setting, consent of the Ethics Committee was not required. According to the Polish statute, this is a non-interventional study (Article 37a (1) of the Pharmaceutical Law) and therefore, within the meaning of the Act on the professions of doctors and dentists of 5 December 1996, it does not require the Opinion of the Bioethical Committee and does not constitute a clinical trial.

Informed Consent Statement: Informed written consent was obtained from all subjects for the participation in the study and publication of images.

Data Availability Statement: The datasets generated during and/or analyzed during the current study are available from the corresponding author on reasonable request.

Conflicts of Interest: The authors declare that they have no conflicts of interest.

References

1. Iwańczuk, P. Basal cell carcinoma—The most common form of skin cancer. Methods of treatment. *J. Educ. Health Sport* **2024**, *58*, 144–153. [CrossRef]
2. Peris, K.; Fargnoli, M.C.; Kaufmann, R.; Arenberger, P.; Bastholt, L.; Seguin, N.B.; Bataille, V.; Brochez, L.; Del Marmol, V.; Dummer, R.; et al. European consensus-based interdisciplinary guideline for diagnosis and treatment of basal cell carcinoma-update 2023. *Eur. J. Cancer* **2023**, *192*, 113254. [CrossRef]
3. Reiter, O.; Mimouni, I.; Gdalevich, M.; Marghoob, A.A.; Levi, A.; Hodak, E.; Leshem, Y.A. The diagnostic accuracy of dermoscopy for basal cell carcinoma: A systematic review and meta-analysis. *J. Am. Acad. Dermatol.* **2019**, *80*, 1380–1388. [CrossRef]
4. Pietkiewicz, P.; Navarrete-Dechent, C.; Togawa, Y.; Szlązak, P.; Salwowska, N.; Marghoob, A.A.; Leszczyńska-Pietkiewicz, A.; Errichetti, E. Applications of Ultraviolet and Sub-ultraviolet Dermatoscopy in Neoplastic and Non-neoplastic Dermatoses: A Systematic Review. *Dermatol. Ther.* **2024**, *14*, 361–390. [CrossRef] [PubMed]
5. Thatte, S.S.; Chikhalkar, S.B.; Khopkar, U.S. "Pink glow": A new sign for the diagnosis of glomus tumor on ultraviolet light dermoscopy. *Indian Dermatol. Online J.* **2015**, *6* (Suppl. S1), 21–23. [CrossRef] [PubMed]
6. Minagawa, A.; Meling, M.T.; Koga, H.; Okuyama, R. Near-ultraviolet light dermoscopy for identification of pigmented skin tumours. *Acta Derm. Venereol.* **2023**, *103*, 00876. [CrossRef]
7. Sano, T.; Minagawa, A.; Suzuki, R.; Koga, H.; Okuyama, R. Dermoscopy with near-ultraviolet light highlights the demarcation of melanin distribution in cutaneous melanoma. *J. Am. Acad. Dermatol.* **2021**, *84*, 23–24. [CrossRef]
8. Shu, J.; Yamamoto, Y.; Aoyama, K.; Togawa, Y.; Kishimoto, T.; Matsue, H. Assessment of malignant melanoma lesions using violet-light dermoscopy: A case report. *J. Dermatol.* **2022**, *49*, 710–713. [CrossRef] [PubMed]
9. Pietkiewicz, P.; Navarrete-Dechent, C.; Goldust, M.; Korecka, K.; Todorovska, V.; Errichetti, E. Differentiating Fordyce Spots from Their Common Simulators Using Ultraviolet-Induced Fluorescence Dermatoscopy-Retrospective Study. *Diagnostics* **2023**, *13*, 985. [CrossRef]
10. Errichetti, E.; Pietkiewicz, P.; Bhat, Y.J.; Salwowska, N.; Szlązak, P.; Stinco, G. Diagnostic accuracy of ultraviolet-induced fluorescence dermoscopy in non-neoplastic dermatoses (general dermatology): A multicentric retrospective comparative study. *J. Eur. Acad. Dermatol. Venereol.* **2024**. [CrossRef]

11. Yuan, M.; Xie, Y.; Zheng, Y.; Zhang, Z.; Yang, C.; Li, J. Novel ultraviolet-dermoscopy: Early diagnosis and activity evaluation of vitiligo. *Skin Res. Technol.* **2023**, *29*, 13249. [CrossRef] [PubMed]
12. Pietkiewicz, P.; Navarrete-Dechent, C.; Mayisoğlu, H.; Jolly, G.; Kutlu, Ö.; Errichetti, E. Pink-red fluorescence observed in ultraviolet-induced fluorescence dermoscopy of psoriatic plaques. *Dermatol. Pract. Concept.* **2023**, *13*, 2023243. [CrossRef]
13. Singh, N.; Yang, H.; Pradhan, S.; Ran, X.; Ran, Y. Image gallery: Wandering demodex mite in vivo under ultraviolet dermoscopy of rosacea. *Br. J. Dermatol.* **2020**, *182*, 2. [CrossRef] [PubMed]
14. Yürekli, A. A new sign with UV dermoscope in the diagnosis of scabies: Ball sign. *Skin Res. Technol.* **2023**, *29*, 13336. [CrossRef] [PubMed]
15. Pietkiewicz, P.; Navarrete-Dechent, C. Scabies mite is bright green under UV dermatoscopy. *Dermatol. Pract. Concept.* **2023**, *13*, 2023135. [CrossRef]
16. Fujimoto, M.; Sakai, H.; Watanabe, R.; Fujimoto, M. Glittering trail: Feces of scabies indicated by high-power–field dermatoscopy using UV-A light. *J. Am. Acad. Dermatol.* **2023**, *90*, E17–E18. [CrossRef] [PubMed]
17. Tang, J.; Ran, Y. Polarized and ultraviolet dermoscopy for the diagnosis of dermatophytosis of vellus hair. *Indian J. Dermatol. Venereol. Leprol.* **2020**, *86*, 607. [PubMed]
18. Rudnicka, L.; Olszewska, M.; Rakowska, A.; Slowinska, M. Trichoscopy update 2011. *J. Dermatol. Case Rep.* **2011**, *5*, 82–88. [CrossRef] [PubMed]
19. Pietkiewicz, P.; Korecka, K.; Salwowska, N.; Kohut, I.; Adhikari, A.; Bowszyc-Dmochowska, M.; Pogorzelska-Antkowiak, A.; Navarrete-Dechent, C. Porokeratoses—A comprehensive review on the genetics and metabolomics, imaging methods and management of common clinical variants. *Metabolites* **2023**, *13*, 1176. [CrossRef]
20. Rodrigues-Barata, A.R.; Moreno-Arrones, O.M.; Corralo, D.S.; Galvan, S.V. The 'starry night sky sign' using ultraviolet-light-enhanced trichoscopy: A new sign that may predict efficacy of treatment in frontal fibrosing alopecia. *Int. J. Trichol.* **2018**, *10*, 241–243. [CrossRef]
21. Li, X.; Zhou, C. Ultraviolet-induced fluorescence dermoscopy aids in distinguishing scarring and nonscarring alopecia: Enhancing Identification of Hair Follicle Openings: The Potential of Ultraviolet-induced Fluorescence Dermoscopy in Hair Loss Diagnosis. *J. Am. Acad. Dermatol.* **2024**, *91*, E1–E2. [CrossRef] [PubMed]
22. Navarrete-Dechent, C.; Pietkiewicz, P.; Dusza, S.W.; Andreani, S.; Nehal, K.S.; Rossi, A.M.; Cordova, M.; Lee, E.H.; Chen, C.J.; Abarzua-Araya, A.; et al. Ultraviolet-induced fluorescent dermoscopy for biopsy site identification prior to dermatologic surgery: A retrospective study. *J. Am. Acad. Dermatol.* **2023**, *89*, 841–843. [CrossRef] [PubMed]
23. Kearse, K.P. Ultraviolet fluorescent detection of elevated bilirubin in dried blood serum. *J. Foren. Sci. Res.* **2022**, *6*, 49–52.
24. Marghoob, A.; Braun, R.; Jaimes, N. *Atlas of Dermoscopy*, 3rd ed.; CRC Press: Boca Raton, FL, USA, 2023; pp. 97–101. [CrossRef]
25. Longo, C.; Specchio, F.; Ribero, S.; Coco, V.; Kyrgidis, A.; Moscarella, E.; Ragazzi, M.; Peris, K.; Argenziano, G. Dermoscopy of small-size basal cell carcinoma: A case-control study. *J. Eur. Acad. Dermatol. Venereol.* **2017**, *31*, 273–274. [CrossRef]
26. Álvarez-Salafranca, M.; Ara, M.; Zaballos, P. Dermoscopy in Basal Cell Carcinoma: An Updated Review. *Actas Dermosifiliogr.* **2021**, *112*, 330–338. [CrossRef] [PubMed]
27. Popadić, M.; Brasanac, D. The use of dermoscopy in distinguishing the histopathological subtypes of basal cell carcinoma: A retrospective, morphological study. *Indian J. Dermatol. Venereol. Leprol.* **2022**, *88*, 598–607. [CrossRef]
28. Camela, E.; Ilut Anca, P.; Lallas, K.; Papageorgiou, C.; Manoli, S.M.; Gkentsidi, T.; Eftychidou, P.; Liopyris, K.; Sgouros, D.; Apalla, Z.; et al. Dermoscopic Clues of Histopathologically Aggressive Basal Cell Carcinoma Subtypes. *Medicina* **2023**, *59*, 349. [CrossRef]
29. Pampena, R.; Parisi, G.; Benati, M.; Borsari, S.; Lai, M.; Paolino, G.; Cesinaro, A.M.; Ciardo, S.; Farnetani, F.; Bassoli, S.; et al. Clinical and Dermoscopic Factors for the Identification of Aggressive Histologic Subtypes of Basal Cell Carcinoma. *Front. Oncol.* **2021**, *10*, 630458. [CrossRef]
30. Chen, W.; Liu, Z.R.; Zhou, Y.; Liu, M.X.; Wang, X.Q.; Wang, D.G. The effect of dermoscopy in assisting on defining surgical margins of basal cell carcinoma. *Dermatol. Ther.* **2022**, *35*, 15711. [CrossRef]
31. Litaiem, N.; Hayder, F.; Benlagha, I.; Karray, M.; Dziri, C.; Zeglaoui, F. The Use of Dermoscopy in the Delineation of Basal Cell Carcinoma for Mohs Micrographic Surgery: A Systematic Review with Meta-Analysis. *Dermatol. Pract. Concept.* **2022**, *12*, 2022176. [CrossRef]

Dermatol Ther (Heidelb)
https://doi.org/10.1007/s13555-025-01432-z

ORIGINAL RESEARCH

Polarized Dermoscopy and Ultraviolet-Induced Fluorescence Dermoscopy of Basal Cell Carcinomas in the H- and Non-H-Zones of the Head and Neck

Irena M. Wojtowicz · Adam A. Reich · Magdalena Żychowska

Received: March 23, 2025 / Accepted: April 17, 2025

ABSTRACT

Introduction: Basal cell carcinoma (BCC) is the most common skin cancer, primarily affecting the head and neck region. This study aimed to evaluate the characteristics of BCCs in different facial areas using polarized dermoscopy (PD) and ultraviolet-induced fluorescence dermoscopy (UVFD).

Methods: BCCs were examined using a Dermlite DL5 dermatoscope in polarized and UVFD modes. The tumors were categorized based on their location within the high-risk H-zone (ear and periauricular region, temple, eyes and periorbital area, nose and paranasal region, oral region, chin) and non-H-zone (forehead, cheek, rest of the face, scalp, neck). PD features were characterized according to standard dermoscopic criteria for skin cancer assessment. UVFD characteristics included dark silhouettes, interrupted follicle patterns, ulcerations/erosions, white-blue scales, arborizing vessels, absence of pink-orange or blue-green fluorescence, blue-fluorescent fibers, pink-orange fluorescence, black globules, white depigmentation, white clods, and well-defined margins.

Results: A total of 151 BCCs were analyzed, with 61.6% located in the H-zone, where the nose and paranasal region were the most affected area (37.6%). Nodular (65.6%) and non-pigmented (86%) subtypes predominated in the H-zone. PD most commonly revealed arborizing vessels (52.7%), short fine telangiectasias (46.2%), red-white homogeneous areas (40.9%), and ulcerations/micro-ulcerations (40.9%). Under UVFD, BCCs in the H-zone frequently exhibited dark silhouettes (77.4%), interrupted follicle patterns (51.6%), absence of blue-green (51.6%) or pink-orange fluorescence (44%), and well-defined lesion borders (43%). Compared to non-H-zone tumors, BCCs in the H-zone were significantly more likely to display ulcerations/micro-ulcerations under PD ($p=0.021$), and erosions/ulcerations ($p=0.019$), blue-fluorescent fibers ($p=0.009$), and absence of blue-green fluorescence ($p=0.019$) under UVFD.

Conclusion: BCCs in the head and neck exhibit distinct characteristics under UVFD, with certain findings more commonly observed in H-zone tumors. The addition of UVFD to PD serves as a valuable, noninvasive diagnostic tool that enhances early detection of BCCs in this anatomically and cosmetically significant region.

I. M. Wojtowicz · A. A. Reich · M. Żychowska (✉)
Department of Dermatology, Faculty of Medicine, Collegium Medicum, University of Rzeszów, Ul. Szopena 2, 35-055 Rzeszów, Poland
e-mail: magda.zychowska@gmail.com

Keywords: Dermoscopy; Dermatoscopy; Basal cell carcinoma; UV-dermoscopy; Ultraviolet-induced fluorescence dermoscopy; Head; Skin cancer

Published online: 28 April 2025

Key Summary Points
Accurate diagnosis of basal cell carcinoma (BCC) is essential for effective treatment, especially in the high-risk facial region—H-zone.
This study examined the findings in ultraviolet-induced fluorescence dermoscopy (UVFD) alongside polarized dermoscopy (PD) in BCCs in different areas of the head and neck.
UVFD revealed erosions or ulcerations, the presence of blue fluorescent fibers, and the absence of blue-green fluorescence significantly more frequently in tumors located in the H-zone than in the non-H-zone.
UVFD provides additional clues, such as the presence of interrupted follicle patterns or absence of follicular fluorescence within the tumor, especially for lesions located within the nose and paranasal area, oral region, or on the neck.
This study underscores the complementary role of UVFD alongside PD in the evaluation of BCCs of the head and neck area.

INTRODUCTION

Basal cell carcinoma (BCC) is the most common type of skin cancer and the most frequently diagnosed cancer overall [1, 2]. According to global statistics, one in five individuals will develop BCC in their lifetime, with incidence increasing with age [3]. Although its prognosis is generally favorable owing to its rare metastatic potential (the reason why the classical TNM cancer classification is not typically applied), BCC remains locally aggressive [4]. As it grows, it progressively invades and destroys surrounding tissues, with a high recurrence rate, particularly in non-pigmented subtypes [5].

BCC predominantly develops in sun-exposed areas, particularly on the head and neck, where cosmetic outcomes are of significant concern [6]. Therefore, early detection methods that improve treatment outcomes and aesthetics are highly desirable. The advancement of dermoscopy has been a major breakthrough in this field. Its role in the diagnosis, treatment planning, and monitoring of BCC has been extensively studied and well established [5, 7, 8]. However, despite its proven utility, there is still a need for improved diagnostic accuracy, as certain benign and malignant tumors may remain difficult to differentiate using conventional dermoscopy alone [8].

In recent years, ultraviolet-induced fluorescence dermoscopy (UVFD) has emerged as a novel approach, integrating UV light (365 nm) into dermoscopic imaging. The present study aimed to analyze the PD and UVFD characteristics of BCCs located in the head and neck region, with a particular focus on the H-zone—a high-risk area known for its aggressive tumor behavior and increased recurrence rates [9, 10]. Understanding UVFD patterns in these locations could enhance early detection strategies and improve treatment outcomes.

METHODS

The study was conducted at the Department of Dermatology in Rzeszów, southeastern Poland. Patients who visited the department with clinical and dermoscopic features suggestive BCC were enrolled.

For each patient, clinical data were collected, including sex, Fitzpatrick skin phototype, tumor location, lesion diameter, and clinical subtype. The tumor locations were categorized using the surface anatomy terminology described by Beltrami et al. in 2024 [11]. Subsequently, these regions were further classified into H-zone and non-H-zone categories following the scheme presented by Blechman et al. [12]. The H-zone consisted of the ear and periauricular region, temple, eyes and periorbital region, nose and paranasal region, as well as the oral region and chin. The non-H-zone included the forehead, cheeks, remaining facial areas (including malar eminence, mandibular region, angle of jaw), scalp and neck.

Dermoscopic imaging was performed using a Dermlite DL5 dermatoscope, employing both PD

and UVFD. Each lesion was photographed under PD and UV light (365 nm) using an iPhone 7 Plus, and the images were stored for subsequent analysis.

Histopathological examination was performed in all cases to confirm the preliminary diagnosis of BCC. Cases with other histopathological diagnoses or with poor-quality dermoscopic images were excluded. Two experienced dermatologists (IW and MŻ) analyzed the images independently and resolved any disagreements through discussion.

The dermoscopic evaluation was based on established criteria in dermato-oncology for categorizing the features seen in PD [13]. The analysis included vascular patterns, pigmented structures, and other notable findings. Vascular patterns included arborizing vessels, short fine telangiectasia, and hairpin vessels. Pigmented structures encompassed gray ovoid nests, maple leaf-like areas, spoke wheel areas, concentric structures, blue-gray globules, blue-gray peppering, blue-white veil, and peripheral striations. Additionally, various other findings were assessed, such as the presence of multiple erosions, hemorrhage, red-white homogeneous areas, shiny white lines, white structureless zones, milia-like cysts, comedo-like openings, scaling, follicular plugging, perifollicular white rings, keratin masses, and well-defined lesion borders.

The UVFD features of BCC were previously described by the authors in the scientific literature [14]. That study, based on clinical observations, identified a spectrum of diagnostic features including arborizing vessels, white clods, blue-fluorescent fibers, white-blue scales, and black globules. Alterations in fluorescence patterns were also noted, such as the presence or absence of pink-orange follicular fluorescence and the loss of the typical blue-green background signal. Additional hallmarks included dark silhouettes, interrupted follicular patterns, erosions or ulcerations, white depigmented areas, and well-demarcated lesion borders. All of these previously described features were systematically re-evaluated and analyzed in the present study.

A "dark silhouette" was identified when the tumor area exhibited a noticeably darker shade than the surrounding skin. The "interrupted follicle pattern" was described as the presence of evenly spaced, round or oval dark structures—corresponding to follicular ostia—in the unaffected skin, while being absent within the tumor itself. The "lack of blue-green fluorescence" and "lack of pink-orange fluorescence" referred to the presence of these fluorescence patterns in the surrounding skin but their complete absence within the tumor. Additionally, "white depigmentation" was characterized by a bright, structureless whitish zone that stood out against both the tumor and the adjacent skin. The term "well-demarcated borders" was used to describe tumors with sharply outlined edges that distinctly separated them from surrounding tissue.

This research was carried out in compliance with the ethical principles outlined in the Declaration of Helsinki. Prior to participation, all individuals provided written informed consent, which also covered the use of clinical images for publication purposes.

Statistical Analysis

Data analysis was performed using SPSS. Categorical variables were expressed as absolute counts and percentages, while continuous variables were reported as means ± standard deviations (SD) and medians with ranges. Fisher's exact test was applied to compare the distribution of dermoscopic features, with statistical significance set at $p < 0.05$.

RESULTS

Clinical Characteristics

In total, 80 patients (52 women and 28 men) with histopathologically confirmed 151 BCCs, all located on the head and neck region, were included in the study. Twelve patients with 18 lesions, clinically suspected to be BCC, were

excluded because of different histopathological diagnoses (mainly adnexal tumors or squamous cell carcinoma). One patient was excluded because of poor quality of dermoscopic images.

All participants had Fitzpatrick skin phototypes I–III. The BCCs were categorized into two clinical subtypes: nodular ($n=90$; 59.6%) and superficial ($n=61$; 40.4%). The majority of the tumors were nonpigmented ($n=119$; 78.8%). The average tumor size measured 8.3 ± 6 mm. Detailed demographic and clinical characteristics of the patients are summarized in Table 1.

PD Findings

Head and neck BCCs under PD most frequently showed vascular structures, including arborizing vessels (52.3%) and short fine telangiectasias (45.7%), occurring on red-white homogeneous areas (40.4%) with ulcerations or micro-ulcerations (33.8%). The occurrence frequencies of these and other dermoscopic features are presented in detail in Table 2.

Table 1 Clinical characteristics

Clinical characteristics	
Patients, *n*	80
Gender, *n* (%)	
Male	28 (35.0)
Female	52 (65.0)
Fitzpatrick skin phototype, *n* (%)	
I	68 (45.0)
II	79 (52.3)
III	4 (2.6)
Total number of BCC, *n*	151
Location of BCC, *n* (%)	
Face	141 (93.4)
Scalp	6 (4.0)
Neck	4 (2.6)

BCC basal cell carcinoma, *n* number of cases, *SD* standard deviation

UVFD Findings

Under UVFD, BCCs appeared as dark silhouettes (78.8%) with an interrupted follicle pattern (53.0%), lacking follicular fluorescence observed in the area surrounding the tumor—either blue-green (44.4%) or pink-orange (39.7%). A considerable number of lesions showed well-demarcated borders (43%). Table 2 presents the occurrence frequencies of these findings.

H-Zone and Non-H-Zone

A total of 61.6% (93/151) of the analyzed BCCs on the head and neck were located within the H-zone. Among these, 65.6% (61/93) were classified as nodular, while 34.4% (32/93) were superficial. The majority of tumors in this region (86%, 80/93) were non-pigmented, whereas 14% (13/93) exhibited pigmentation. Regarding tumor size, 24.7% (23/93) measured between 0–4 mm in diameter, 53.8% (50/93) were within the 5–10 mm range, and 21.5% (20/93) exceeded 10 mm. One large BCC extended across both the H-zone and non-H-zone.

No statistically significant difference was found in the size or clinical subtype between tumors located in the H-zone and non-H-zone. However, the non-pigmented subtype was significantly more frequent in the H-zone ($p=0.008$).

Under PD, ulcerations/micro-ulcerations (40.9% vs. 23.7%, $p=0.021$) and hemorrhages (24.7% vs. 11.9%, $p=0.033$) were observed more frequently in the H-zone compared to the non-H-zone. Similarly, under UVFD, a higher prevalence of erosions/ulcerations (30.1% vs. 15.3%, $p=0.019$) and blue-fluorescent fibers (14% vs. 3.4%, $p=0.009$) was noted in the H-zone. Moreover, lack of blue-green fluorescence (51.6% vs. 32.2%, $p=0.019$) within the tumor was observed more frequently in the H-zone.

Table 2 and Figs. 1 and 2 present the clinical and dermoscopic characteristics of BCCs by location in the H-zone or non-H-zone.

Specific Locations

The frequency of pigmented BCCs varied significantly ($p<0.001$) according to anatomical

Table 2 Comparison of the clinical characteristics, polarized dermoscopy findings, and ultraviolet-induced fluorescence dermoscopy features of BCCs located in the H-zone and non-H-zone

	Total $n = 151$	%	H-zone ($n = 93$)	%	Non-H-zone ($n = 59$)	%	p value
Clinical subtype							
Nodular	90	59.6	61	65.6	30	50.8	0.227
Superficial	61	40.4	32	34.4	29	49.2	
Pigmented	32	21.2	13	14.0	19	32.2	< 0.001
Non-pigmented	119	78.8	80	86.0	40	67.8	
Size							
Mean ± SD	8.3 ± 6		8.2 ± 6		8.3 ± 6		0.550
Diameter 0–4 mm	38	25.2	23	24.7	15	25.4	0.331
Diameter 5–10 mm	86	56.9	50	53.8	36	61.0	
Diameter > 10 mm	27	17.9	20	21.5	8	13.6	
PD findings							
Vascular structures							
Arborizing vessels	79	52.3	49	52.7	31	52.5	1.000
Short fine telangiectasias	69	45.7	43	46.2	26	44.1	0.868
Hairpin vessels	2	1.3	1	1.1	1	1.7	1.000
Linear irregular vessels	51	33.8	34	36.6	17	28.8	0.387
Pigmented structures							
Maple leaf-like areas	13	8.6	7	7.5	6	10.2	0.570
Gray ovoid nests	11	7.3	5	5.4	6	10.2	0.341
Spoke wheel areas	6	4.0	2	2.2	4	6.8	0.210
Blue-gray globules	17	11.3	7	7.5	10	16.9	0.069
Concentric structures	7	4.6	6	6.5	1	1.7	0.483
Blue-gray peppering	23	15.2	13	14.0	10	16.9	0.649
Peripheral striations	2	1.3	1	1.1	1	1.7	0.561
Blue-white veils	2	1.3	2	2.2	0	0.0	0.521
Other findings							
Ulcerations/micro-ulcerations	51	33.8	38	40.9	14	23.7	0.021
Multiple erosions	19	12.6	14	15.1	5	8.5	0.463
Hemorrhages	29	19.2	23	24.7	7	11.9	0.033
Red-white homogenous areas	61	40.4	38	40.9	25	42.4	1.000

Table 2 continued

	Total $n = 151$	%	H-zone ($n = 93$)	%	Non-H-zone ($n = 59$)	%	p value
Milia-like cysts	11	7.3	5	5.4	6	10.2	0.341
Comedo-like openings	1	0.7	1	1.1	0	0.0	1.000
Follicular pluggings	7	4.6	6	6.5	1	1.7	0.405
Perifollicular white rings	5	3.3	4	4.3	1	1.7	0.649
Keratin masses	6	4.0	5	5.4	1	1.7	0.405
Scales	44	29.1	29	31.2	15	25.4	0.467
White structureless areas	37	24.5	24	25.8	14	23.7	0.699
Shiny white lines	8	5.3	6	6.5	2	3.4	0.483
Well-demarcated borders	54	35.8	34	36.6	21	35.6	0.731
UVFD findings							
Dark silhouettes	119	78.8	72	77.4	48	81.4	0.685
Interrupted follicle pattern	80	53.0	48	51.6	32	54.2	0.741
Erosions/ulcerations	36	23.8	28	30.1	9	15.3	0.019
White-blue scales	50	33.1	35	37.6	15	25.4	0.115
Arborizing vessels	49	32.5	29	31.2	21	35.6	0.859
Lack of blue-green fluorescence	67	44.4	48	51.6	19	32.2	0.019
Pink-orange fluorescence	7	4.6	4	4.3	3	5.1	1.000
Lack of pink-orange fluorescence	60	39.7	41	44.1	19	32.2	0.173
Blue-fluorescent fibers	14	9.3	13	14.0	2	3.4	0.009
Black globules	36	23.8	20	21.5	16	27.1	0.339
White depigmentation	9	6.0	5	5.4	4	6.8	0.712
White clods	17	11.3	8	8.6	9	15.3	0.291
Well-demarcated borders	65	43.0	40	43.0	26	44.1	1.000

PD polarized dermoscopy, *UVFD* ultraviolet-induced fluorescence dermoscopy, *n* number of BCCs

site. All of the scalp BCCs were pigmented followed by tumors located in the forehead region (42.1%), eyes and periorbital region (22.2%), rest of the face (18.2%), cheeks (15.8%), oral region (12.5%), nose and paranasal region (11.4%). Lower frequencies were noted in the temple or ears and periauricular region (each 9%) while no pigmented BCCs were detected on the neck.

PD and UVFD revealed several significant differences in the dermoscopic presentations of BCCs across specific anatomical sites. Under PD, red-white homogeneous areas ($p = 0.045$) were most frequently observed on the temple (90.9%), followed by the neck (50.0%), nose and paranasal region (45.7%), rest of the face (45.5%), cheek (42.1%), and oral region

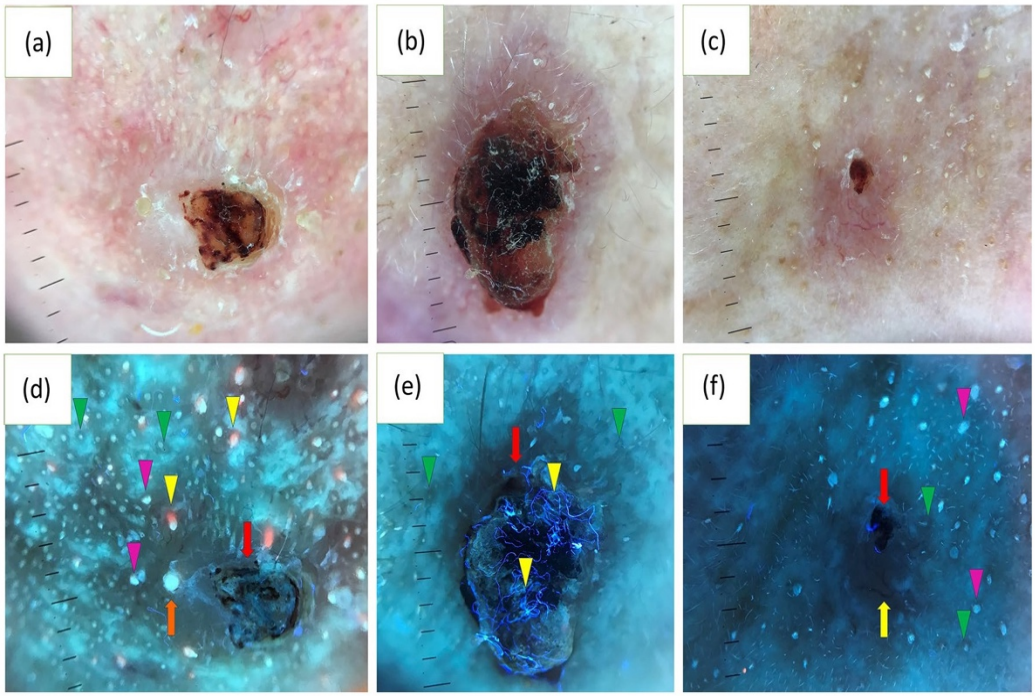

Fig. 1 Polarized light dermoscopy (PD) presentation of basal cell carcinoma (BCC) in the H-zone of the face including BCC (**a**, **c**) on the nose and (**b**) in the oral region. **d**–**f** Corresponding images in ultraviolet-induced fluorescence dermoscopy (UVFD). **d** Dark silhouette, ulceration (red arrow), pink-orange follicular fluorescence at the periphery of the tumor (yellow arrowheads), blue-green follicular fluorescence at the periphery of the tumor (pink arrowheads), absence of both types of fluorescence within the BCC, follicle pattern in the surrounding skin (green arrowheads), interrupted follicle pattern within the lesion, follicular plugging (orange arrow). **e** Dark silhouette, ulceration (red arrow), blue fluorescent fibers (yellow arrowheads), follicle pattern in the surrounding skin (green arrowheads), interrupted follicle pattern within the lesion. **f** Dark silhouette, erosion (red arrow), arborizing vessels (yellow arrow), follicle pattern in the surrounding skin (green arrowheads), interrupted follicle pattern within the lesion, blue-green follicular fluorescence at the periphery of the tumor (pink arrowheads), absence of this type of fluorescence within the BCC

(31.3%). Blue-gray globules showed the highest occurrence ($p=0.004$) on the scalp (66.7%), with lower frequencies on the forehead (21.0%), ears and periauricular region (18.2%), and temple (18.2%). Moreover, the blue-white veil ($p=0.004$)—a feature often associated with melanoma—was exclusively seen in the ears and periauricular region with an 18.2% occurrence at these sites.

Under UVFD, an interrupted follicle pattern ($p=0.012$) was most frequently observed in the oral region (75.0%), followed by the nose and paranasal region (71.4%), forehead (57.9%), and cheeks (52.6%). Erosions or ulcerations ($p=0.04$) were most common on the neck (50.0%), followed by the ears and periauricular region (45.5%), nose and paranasal region (40.0%), scalp (33.3%), and oral region (31.3%). A lack of blue-green fluorescence ($p<0.001$) showed the highest occurrence in the neck (75%), nose and paranasal region (74.3%), and oral region (62.5%). Similarly, the absence of pink-orange fluorescence ($p=0.001$) was most frequent in the nose and paranasal region (65.7%) and oral region (56.3%).

Tables 3 presents the frequencies of PD features across various anatomical locations, while Table 4 summarizes the distribution of UVFD findings. Examples of BCCs in the nose and paranasal region are presented in Fig. 3, while those in the oral region are shown in Fig. 4.

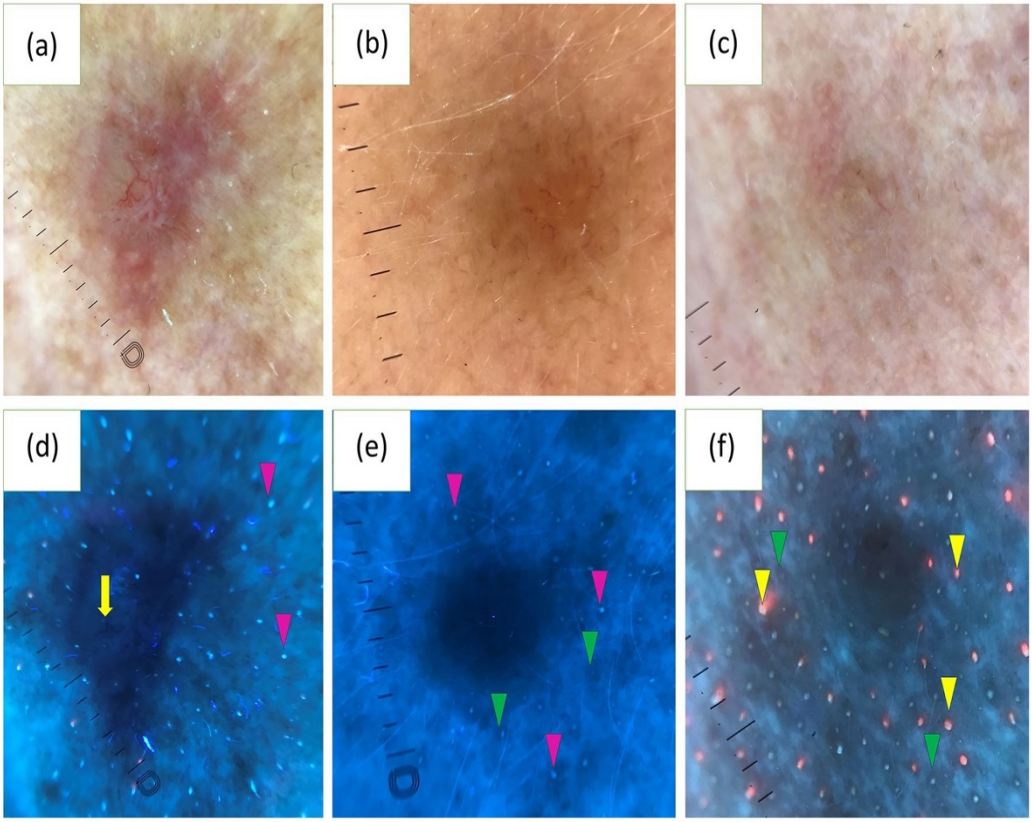

Fig. 2 PD presentation of BCC in the **a–c** non-H-zone of the face including BCC (**a**) on the neck and (**b**, **c**) on the cheek. **d–f** Corresponding images in UVFD. **d** Dark silhouette, arborizing vessel (yellow arrow), blue-green follicular fluorescence at the periphery of the tumor (pink arrowheads), absence of this type of fluorescence within the BCC. **e** Dark silhouette, follicle pattern in the surrounding skin (green arrowheads), interrupted follicle pattern within the lesion, blue-green follicular fluorescence at the periphery of the tumor (pink arrowheads), absence of this type of fluorescence within the BCC. **f** Dark silhouette, pink-orange follicular fluorescence at the periphery of the tumor (yellow arrowheads), absence of this type of fluorescence within the BCC, follicle pattern in the surrounding skin (green arrowheads), interrupted follicle pattern within the lesion

DISCUSSION

The available data on the application of UVFD in BCCs has been limited [14–16]. In a recent study by Navarrete-Dechent et al. [16], the authors underscored the role of UVFD in detecting the white-bluish fluorescence of the multiple aggregated yellow-white (MAY) globules. In the aforementioned study, UVFD contributed to the better visualization of MAY globules (95% under UVFD vs. 81% under PD). In another study, UVFD was demonstrated to facilitate biopsy site identification prior to BCC surgery [15]. However, the biggest comprehensive study to date on the UVFD findings in BCCs was conducted by the authors in 2024 [14]. UVFD has been recognized as a valuable complementary tool to PD, particularly for detecting small lesions (<5 mm), facial tumors, and nodular or non-pigmented BCC subtypes [14].

To better understand the features of BCC, it is necessary to know what normal skin looks like under UVFD. In most cases, regularly distributed gray round/oval structures corresponding to the follicular openings are present. Within the openings of hair follicles, more or less regular fluorescence may be visible—either pink-orange or green-blue. In sebum-rich areas, the follicles often display pink-orange fluorescence associated with porphyrins produced by *Cutibacterium*

Table 3 Prevalence of PD features in various anatomical locations

Location of BCC, *n* (%)	Nose and paranasal region (*n* = 35)	Forehead (*n* = 19)	Cheeks (*n* = 19)	Eyes and periorbital region (*n* = 18)	Oral region (*n* = 16)	Temple (*n* = 11)	Ears and periauricular region (*n* = 11)	Chin (*n* = 1)	Rest of face (*n* = 11)	Scalp (*n* = 6)	Neck (*n* = 4)	*p* value
Vascular structures												
Arborizing vessels	19 (54.3)	12 (63.2)	9 (47.4)	11 (61.1)	10 (62.5)	4 (36.4)	4 (36.4)	0 (0.0)	6 (54.5)	2 (33.3)	2 (50.0)	0.763
Short fine teleangiectasias	17 (48.6)	10 (52.6)	4 (21.1)	7 (38.9)	8 (50.0)	6 (54.5)	5 (45.5)	0 (0.0)	7 (63.6)	1 (16.7)	4 (100.0)	0.132
Hairpin vessels	1 (2.9)	0 (0.0)	0 (0.0)	0 (0.0)	0 (0.0)	0 (0.0)	0 (0.0)	0 (0.0)	1 (9.1)	0 (0.0)	0 (0.0)	0.715
Linear irregular vessels	12 (34.3)	5 (26.3)	4 (21.1)	7 (38.9)	5 (31.3)	4 (36.4)	6 (54.5)	0 (0.0)	4 (36.4)	3 (50.0)	1 (25.0)	0.844
Pigmented structures												
Maple leaf-like areas	1 (2.9)	4 (21.1)	1 (5.3)	3 (16.7)	2 (12.5)	0 (0.0)	1 (9.1)	0 (0.0)	0 (0.0)	1 (16.7)	0 (0.0)	0.413
Gray ovoid nests	0 (0.0)	2 (10.5)	0 (0.0)	1 (5.6)	1 (6.3)	1 (9.1)	2 (18.2)	0 (0.0)	2 (18.2)	2 (33.3)	0 (0.0)	0.133
Spoke wheel areas	1 (2.9)	3 (15.8)	1 (5.3)	0 (0.0)	1 (6.3)	0 (0.0)	0 (0.0)	0 (0.0)	0 (0.0)	0 (0.0)	0 (0.0)	0.446
Blue-gray globules	1 (2.9)	4 (21.1)	1 (5.3)	1 (5.6)	1 (6.3)	2 (18.2)	2 (18.2)	0 (0.0)	1 (9.1)	4 (66.7)	0 (0.0)	0.004

Table 3 continued

Location of BCC, *n* (%)	Nose and paranasal region (*n* = 35)	Forehead (*n* = 19)	Cheeks (*n* = 19)	Eyes and periorbital region (*n* = 18)	Oral region (*n* = 16)	Temple (*n* = 11)	Ears and periauricular region (*n* = 11)	Chin (*n* = 1)	Rest of face (*n* = 11)	Scalp (*n* = 6)	Neck (*n* = 4)	*p* value
Concentric structures	2 (5.7)	1 (5.3)	0 (0.0)	0 (0.0)	2 (12.5)	1 (9.1)	1 (9.1)	0 (0.0)	0 (0.0)	0 (0.0)	0 (0.0)	0.798
Blue-gray peppering	6 (17.1)	3 (15.8)	2 (10.5)	3 (16.7)	1 (6.3)	1 (9.1)	1 (9.1)	1 (100.0)	1 (9.1)	3 (50.0)	1 (25.0)	0.178
Peripheral striations	0 (0.0)	0 (0.0)	1 (5.3)	1 (5.6)	0 (0.0)	0 (0.0)	0 (0.0)	0 (0.0)	0 (0.0)	0 (0.0)	0 (0.0)	0.794
Blue-white veils	0 (0.0)	0 (0.0)	0 (0.0)	0 (0.0)	0 (0.0)	0 (0.0)	2 (18.2)	0 (0.0)	0 (0.0)	0 (0.0)	0 (0.0)	0.004
Other findings												
Ulcerations/microulcerations	17 (48.6)	2 (10.5)	4 (21.1)	7 (38.9)	6 (37.5)	2 (18.2)	5 (45.5)	0 (0.0)	3 (27.3)	3 (50.0)	2 (50.0)	0.199
Multiple erosions	5 (14.3)	1 (5.3)	1 (5.3)	2 (11.1)	2 (12.5)	1 (9.1)	4 (36.4)	0 (0.0)	1 (9.1)	2 (33.3)	0 (0.0)	0.369
Hemorrhages	11 (31.4)	0 (0.0)	2 (10.5)	5 (27.8)	2 (12.5)	2 (18.2)	2 (18.2)	0 (0.0)	1 (9.1)	3 (50.0)	1 (25.0)	0.137

Table 3 continued

Location of BCC, *n* (%)	Nose and paranasal region (*n* = 35)	Forehead (*n* = 19)	Cheeks (*n* = 19)	Eyes and periorbital region (*n* = 18)	Oral region (*n* = 16)	Temple (*n* = 11)	Ears and periauricular region (*n* = 11)	Chin (*n* = 1)	Rest of face (*n* = 11)	Scalp (*n* = 6)	Neck (*n* = 4)	*p* value
Red-white homogenous areas	16 (45.7)	6 (31.6)	8 (42.1)	3 (16.7)	5 (31.3)	10 (90.9)	4 (36.4)	0 (0.0)	5 (45.5)	2 (33.3)	2 (50.0)	0.045
Milia-like cysts	2 (5.7)	3 (15.8)	0 (0.0)	3 (16.7)	0 (0.0)	0 (0.0)	0 (0.0)	0 (0.0)	2 (18.2)	1 (16.7)	0 (0.0)	0.279
Comedo-like openings	0 (0.0)	0 (0.0)	0 (0.0)	0 (0.0)	1 (6.3)	0 (0.0)	0 (0.0)	0 (0.0)	0 (0.0)	0 (0.0)	0 (0.0)	0.581
Follicular pluggings	4 (11.4)	1 (5.3)	0 (0.0)	0 (0.0)	2 (12.5)	0 (0.0)	0 (0.0)	0 (0.0)	0 (0.0)	0 (0.0)	0 (0.0)	0.454
Perifollicular white rings	1 (2.9)	1 (5.3)	0 (0.0)	0 (0.0)	2 (12.5)	0 (0.0)	1 (9.1)	0 (0.0)	0 (0.0)	0 (0.0)	0 (0.0)	0.628
Keratin masses	2 (5.7)	0 (0.0)	0 (0.0)	0 (0.0)	1 (6.3)	1 (9.1)	1 (9.1)	0 (0.0)	0 (0.0)	1 (16.7)	0 (0.0)	0.676
Scales	13 (37.1)	1 (5.3)	6 (31.6)	5 (27.8)	4 (25.0)	2 (18.2)	5 (45.5)	0 (0.0)	4 (36.4)	2 (33.3)	2 (50.0)	0.425
White structureless areas	7 (20.0)	2 (10.5)	5 (26.3)	6 (33.3)	5 (31.3)	1 (9.1)	3 (27.3)	1 (100.0)	2 (18.2)	2 (33.3)	3 (75.0)	0.168

Table 3 continued

Location of BCC, *n* (%)	Nose and paranasal region (*n* = 35)	Forehead (*n* = 19)	Cheeks (*n* = 19)	Eyes and periorbital region (*n* = 18)	Oral region (*n* = 16)	Temple (*n* = 11)	Ears and periauricular region (*n* = 11)	Chin (*n* = 1)	Rest of face (*n* = 11)	Scalp (*n* = 6)	Neck (*n* = 4)	*p* value
Shiny white lines	2 (5.7)	1 (5.3)	0 (0.0)	0 (0.0)	1 (6.3)	2 (18.2)	1 (9.1)	0 (0.0)	0 (0.0)	0 (0.0)	1 (25.0)	0.426
Well-demarcated borders	13 (37.1)	5 (26.3)	9 (47.4)	8 (44.4)	6 (37.5)	4 (36.4)	2 (18.2)	0 (0.0)	5 (45.5)	0 (0.0)	2 (50.0)	0.563

n number of BCCs

acnes. This phenomenon is most prominent in younger individuals with higher sebaceous activity [17–19]. On the other hand, green-blue follicular fluorescence has been identified as a probable marker of *Malassezia* colonization, particularly in seborrheic areas [20–22].

In the current study, the most frequently observed UVFD feature of BCCs was the presence of dark silhouettes (78.8%), consistent with the authors' previous research and the findings of Navarrete-Dechent et al. [14, 15]. These studies demonstrated that BCC-affected areas appear darker than the surrounding skin under UVFD, aiding in precise surgical margin delineation. This characteristic is particularly useful for distinguishing BCCs from healthy tissue, especially in non-pigmented facial lesions, where conventional PD may be less effective. UVFD enhance the visualization of lesion margins, which were determined to be well demarcated in 43.0% of tumors examined under UVFD, compared to 35.8% of cases visualized under PD. This may offer practical advantages in preoperative planning, particularly in the high-risk H-zone of the face, where complete tumor removal is critical to reducing recurrence rates. In addition to its oncologic significance, precise excision is also essential for aesthetic outcomes, particularly important in cosmetically sensitive areas, which is undoubtedly the face region.

Additionally, UVFD showed interrupted follicle pattern and the absence of blue-green or pink-orange follicular fluorescence within the tumor compared to the surrounding unaffected skin. These features were significantly more frequently noted in the nose, paranasal, and oral regions. This likely corresponds to the increased number of dilated follicular openings and higher sebaceous gland activity in these areas.

The absence of fluorescence patterns in BCC-affected areas may suggest that tumor growth disrupts follicular structures and alters the local microenvironment. We postulate that this feature, observed only under UV light, may constitute another premise for the preliminary diagnosis of BCC. However, as highlighted before, one of the main assumptions of this clue is that the fluorescence is present in the surrounding healthy skin. In our analysis, the phenomenon was particularly common (> 50% of cases) in

Table 4 Summary of the distribution of UVFD findings

Location of BCC, *n* (%)	Nose and paranasal region (*n* = 35)	Forehead (*n* = 19)	Cheeks (*n* = 19)	Eyes and periorbital region (*n* = 18)	Oral region (*n* = 16)	Temple (*n* = 11)	Ears and periauricular region (*n* = 11)	Chin (*n* = 1)	Rest of face (*n* = 11)	Scalp (*n* = 6)	Neck (*n* = 4)	*p* value
Dark silhouettes	28 (80.0)	15 (78.9)	15 (78.9)	13 (72.2)	9 (56.3)	10 (90.9)	10 (90.9)	1 (100.0)	8 (72.7)	6 (100.0)	4 (100.0)	0.398
Interrupted follicle pattern	25 (71.4)	11 (57.9)	10 (52.6)	3 (16.7)	12 (75.0)	4 (36.4)	3 (27.3)	1 (100.0)	6 (54.5)	3 (50.0)	2 (50.0)	0.012
Erosions/ulcerations	14 (40.0)	1 (5.3)	2 (10.5)	2 (11.1)	5 (31.3)	1 (9.1)	5 (45.5)	0 (0.0)	2 (18.2)	2 (33.3)	2 (50.0)	0.040
White-blue scales	17 (48.6)	2 (10.5)	6 (31.6)	5 (27.8)	4 (25.0)	2 (18.2)	7 (63.6)	0 (0.0)	4 (36.4)	1 (16.7)	2 (50.0)	0.088
Arborizing vessels	14 (40.0)	8 (42.1)	6 (31.6)	5 (27.8)	4 (25.0)	2 (18.2)	3 (27.3)	0 (0.0)	5 (45.5)	0 (0.0)	2 (50.0)	0.606
Lack of blue-green fluorescence	26 (74.3)	7 (36.8)	4 (21.1)	4 (22.2)	10 (62.5)	4 (36.4)	3 (27.3)	1 (100.0)	5 (45.5)	0 (0.0)	3 (75.0)	< 0.001
Pink-orange fluorescence	2 (5.7)	2 (10.5)	1 (5.3)	0 (0.0)	0 (0.0)	0 (0.0)	2 (18.2)	0 (0.0)	0 (0.0)	0 (0.0)	0 (0.0)	0.492
Lack of pink-orange fluorescence	23 (65.7)	4 (21.1)	9 (47.4)	2 (11.1)	9 (56.3)	2 (18.2)	4 (36.4)	1 (100.0)	4 (36.4)	0 (0.0)	2 (50.0)	0.001

Table 4 continued

Location of BCC, *n* (%)	Nose and paranasal region (*n* = 35)	Forehead (*n* = 19)	Cheeks (*n* = 19)	Eyes and periorbital region (*n* = 18)	Oral region (*n* = 16)	Temple (*n* = 11)	Ears and periauricular region (*n* = 11)	Chin (*n* = 1)	Rest of face (*n* = 11)	Scalp (*n* = 6)	Neck (*n* = 4)	*p* value
Blue-fluorescent fibers	5 (14.3)	0 (0.0)	1 (5.3)	1 (5.6)	2 (12.5)	1 (9.1)	3 (27.3)	0 (0.0)	0 (0.0)	0 (0.0)	1 (25.0)	0.350
Black globules	6 (17.1)	8 (42.1)	4 (21.1)	7 (38.9)	3 (18.8)	3 (27.3)	0 (0.0)	1 (100.0)	1 (9.1)	2 (33.3)	1 (25.0)	0.124
White depigmentation	0 (0.0)	1 (5.3)	2 (10.5)	0 (0.0)	3 (18.8)	2 (18.2)	0 (0.0)	0 (0.0)	1 (9.1)	0 (0.0)	0 (0.0)	0.209
White clods	4 (11.4)	3 (15.8)	2 (10.5)	2 (11.1)	0 (0.0)	2 (18.2)	0 (0.0)	0 (0.0)	2 (18.2)	2 (33.3)	0 (0.0)	0.586
Well-demarcated borders	19 (54.3)	9 (47.4)	9 (47.4)	8 (44.4)	4 (25.0)	5 (45.5)	2 (18.2)	1 (100.0)	6 (54.5)	0 (0.0)	2 (50.0)	0.194

n number of BCCs

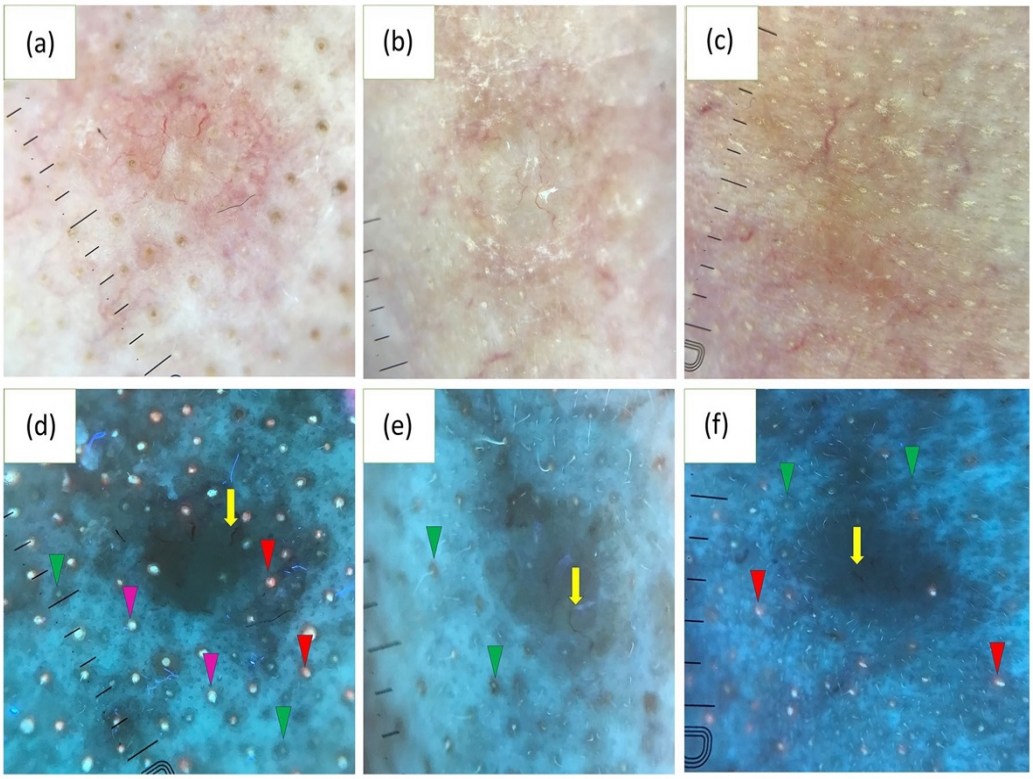

Fig. 3 PD presentation of BCC in the **a**, **b** nose and **c** paranasal region. **d–f** Corresponding images in UVFD. **d** Dark silhouette, arborizing vessel (yellow arrow), pink-orange follicular fluorescence at the periphery of the tumor (red arrowheads), blue-green follicular fluorescence at the periphery of the tumor (pink arrowheads), absence of both types of fluorescence within the BCC, follicle pattern in the surrounding skin (green arrowheads), interrupted follicle pattern within the lesion. **e** Dark silhouette, arborizing vessel (yellow arrow), follicle pattern in the surrounding skin (green arrowheads), interrupted follicle pattern within the lesion. **f** Dark silhouette, arborizing vessel (yellow arrow), pink-orange follicular fluorescence at the periphery of the tumor (red arrowheads), absence of this type of fluorescence within the BCC, follicle pattern in the surrounding skin (green arrowheads), interrupted follicle pattern within the lesion

specific areas of the head and neck, namely the nose and paranasal area, the oral region, and the neck. Presumably, it is in the assessment of tumors in these locations that the UVFD may be particularly useful.

Despite its advantages, UVFD has certain drawbacks. The technique enables detection of erosions or ulcerations at a lower rate than PD (23.8% vs. 33.8%). Similarly, in the current study vascular structures were less frequently noted under UVFD than under classical PD examination (32.5% vs. 52.3%). It should be underscored at this point that both erosions/ulcerations and arborizing vessels constitute important dermoscopic clues for BCC. These observations are in line with those reported in our previous study [2], highlighting the need to consider UVFD as a complementary rather than a standalone diagnostic tool. This strengthens the importance of an integrative approach in BCC assessment.

There are some limitations to this study that should be acknowledged. The relatively small number of BCCs in certain anatomical regions, such as the chin, scalp, and neck, may have affected statistical power and the generalizability of our findings. Future studies should focus on expanding sample sizes. Additionally, investigating the potential of UVFD in distinguishing BCC from other non-melanoma skin cancers could further refine its clinical utility.

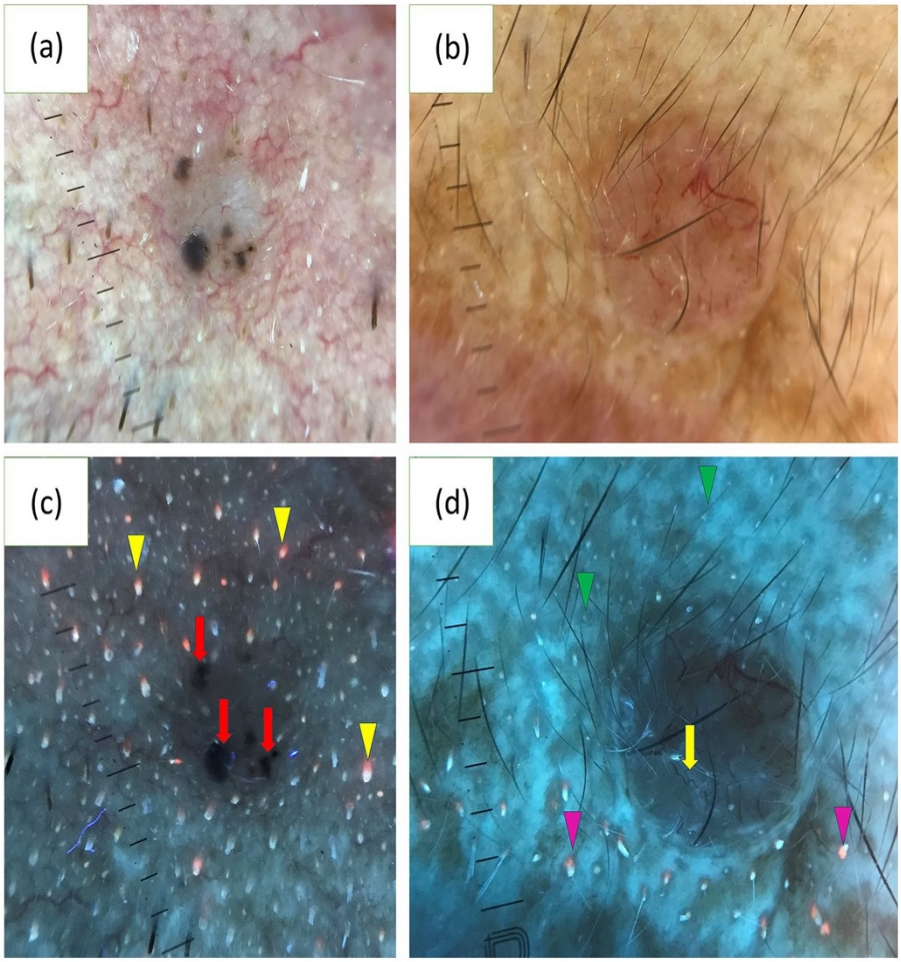

Fig. 4 **a**, **b** PD presentation of BCC in the oral region. **c**, **d** Corresponding images in UVFD. **c** Dark silhouette, black globules (red arrows), pink-orange follicular fluorescence at the periphery of the tumor (yellow arrowheads), absence of this type of fluorescence within the BCC. **e** Dark silhouette, arborizing vessel (yellow arrow), pink-orange follicular fluorescence at the periphery of the tumor (pink arrowheads), absence of this type of fluorescence within the BCC, follicle pattern in the surrounding skin (green arrowheads), interrupted follicle pattern within the lesion

CONCLUSIONS

This study underscores the complementary role of UVFD alongside PD in the evaluation of BCCs of the head and neck area. UVFD revealed erosions or ulcerations, the presence of blue fluorescent fibers, and the absence of blue-green fluorescence significantly more frequently in tumors located in the H-zone than in the non-H-zone. UVFD provides additional clues, such as presence of interrupted follicle patterns or absence of follicular fluorescence within the tumor, especially for lesions located in the nose and paranasal area, oral region, or on the neck.

ACKNOWLEDGEMENTS

We thank the participants of the study.

Author Contribution. Irena Wojtowicz: Data curation, Methodology, Writing—Original draft preparation; Adam Reich: Supervision; Magdalena Żychowska: Conceptualization, Methodology, Supervision. All named authors

meet the International Committee of Medical Journal Editors (ICMJE) criteria for authorship for this article, take responsibility for the integrity of the work as a whole, and have given their approval for this version to be published.

Funding. No funding or sponsorship was received for this study or publication of this article.

Data Availability. The datasets generated during and/or analyzed during the current study are available from the corresponding author on reasonable request.

Declarations

Conflict of Interest. Adam Reich is an Editorial Board member of *Dermatology and Therapy*. Adam Reich was not involved in the selection of peer reviewers for the manuscript nor any of the subsequent editorial decisions. Irena Wojtowicz and Magdalena Zychowska have nothing to disclose.

Ethical Approval. The study was conducted in accordance with the Declaration of Helsinki and approved by the Ethics Committee at the Regional Medical Chamber in Rzeszow (protocol code 50/2024/B, date of approval 21st October 2024). The patients in this manuscript have given written informed consent to the publication of their case details.

REFERENCES

1. Longo C, Guida S, Mirra M, et al. Dermatoscopy and reflectance confocal microscopy for basal cell carcinoma diagnosis and diagnosis prediction score: a prospective and multicenter study on 1005 lesions. J Am Acad Dermatol. 2024;90(5):994–1001. https://doi.org/10.1016/j.jaad.2024.01.035.

2. Coppola R, Barone M, Zanframundo S, et al. Basal cell carcinoma thickness evaluated by high-frequency ultrasounds and correlation with dermoscopic features. Ital J Dermatol Venerol. 2021;156(5):610–5. https://doi.org/10.23736/S2784-8671.20.06576-1.

3. Wang WE, Chen YT, Wang CH, et al. Dermoscopic features of pigmented basal cell carcinoma according to size. Int J Dermatol. 2024;63(7):916–21. https://doi.org/10.1111/ijd.17042.

4. Yuki A, Takatsuka S, Abe R, et al. Diagnostic accuracy of dermoscopy for 934 basal cell carcinomas: a single-center retrospective study. J Dermatol. 2023;50(1):64–71. https://doi.org/10.1111/1346-8138.16607.

5. Wojtowicz I, Żychowska M. Dermoscopy of basal cell carcinoma part 1: dermoscopic findings and diagnostic accuracy—a systematic literature review. Cancers (Basel). 2025;17(3):493. https://doi.org/10.3390/cancers17030493.

6. Peris K, Fargnoli MC, Kaufmann R, et al. European consensus-based interdisciplinary guideline for diagnosis and treatment of basal cell carcinoma—update 2023. Eur J Cancer. 2023;192:113254. https://doi.org/10.1016/j.ejca.2023.113254.

7. Wojtowicz I, Żychowska M. Dermoscopy of basal cell carcinoma part 2: dermoscopic findings by lesion subtype, location, age of onset, size and patient phototype. Cancers (Basel). 2025;17(2):176. https://doi.org/10.3390/cancers17020176.

8. Wojtowicz I, Żychowska M. Dermoscopy of basal cell carcinoma part 3: differential diagnosis, treatment monitoring and novel technologies. Cancers (Basel). 2025;17(6):1025. https://doi.org/10.3390/cancers17061025.

9. Pogorzelska-Dyrbuś J, Salwowska N, Bergler-Czop B. Vascular pattern in dermoscopy of basal cell carcinoma in the H- and non-H-zone. Postepy Dermatol Alergol. 2023;40(2):273–6. https://doi.org/10.5114/ada.2023.127643.

10. Murray C, Sivajohanathan D, Hanna TP, et al. Patient indications for Mohs micrographic surgery: a systematic review. J Cutan Med Surg. 2019;23(1):75–90. https://doi.org/10.1177/1203475418786208.

11. Beltrami EJ, Johnson T, Ngo T, et al. Surface anatomy in dermatology: part I—clinical importance, diagnostic utility, and impact on medical management. J Am Acad Dermatol. 2024;91(2):207–20. https://doi.org/10.1016/j.jaad.2023.07.001.

12. Blechman AB, Patterson JW, Russell MA. Application of Mohs micrographic surgery appropriateuse criteria to skin cancers at a university health system. J Am Acad Dermatol. 2014;71(1):31–6.

13. Marghoob A, Braun R, Jaimes N. Atlas of dermoscopy. 3rd ed. Boca Raton: CRC; 2023. p. 97–101.

14. Wojtowicz I, Żychowska M. Application of ultraviolet-enhanced fluorescence dermoscopy in basal cell carcinoma. Cancers (Basel). 2024;16(15):2685. https://doi.org/10.3390/cancers16152685.

15. Navarrete-Dechent C, Pietkiewicz P, Dusza SW, et al. Ultraviolet-induced fluorescent dermoscopy for biopsy site identification prior to dermatologic surgery: a retrospective study. J Am Acad Dermatol. 2023;89(4):841–3. https://doi.org/10.1016/j.jaad.2023.05.089.

16. Navarrete-Dechent C, Pietkiewicz P, Astronave G, et al. The role of ultraviolet-induced fluorescence dermatoscopy for the detection of multiple aggregated yellow-white globules in basal cell carcinoma. J Am Acad Dermatol. 2024;91(6):1250–2.

17. Barnard E, Johnson T, Ngo T, et al. Porphyrin production and regulation in cutaneous *Propionibacteria*. mSphere. 2020;5(1):e00793-e819. https://doi.org/10.1128/mSphere.00793-19.

18. Songsantiphap C, Asawanonda P. The correlations between follicular fluorescence and casual sebum levels in subjects with normal skin. J Clin Aesthet Dermatol. 2019;12(8):24–7.

19. Wu Y, Li X, Ma Y, et al. Characterizing the skin porphyrins in healthy individuals using ultraviolet-induced fluorescence photography. Skin Res Technol. 2021;27(6):956–64. https://doi.org/10.1111/srt.13005.

20. Pietkiewicz P, Navarrete-Dechent C, Togawa Y, et al. Applications of ultraviolet and sub-ultraviolet dermatoscopy in neoplastic and non-neoplastic dermatoses: a systematic review. Dermatol Ther (Heidelb). 2024;14(2):361–90. https://doi.org/10.1007/s13555-024-01104-4.

21. Silva AMG, Michalany AO, de Sá Menezes Carvalho G. UV dermoscopy for the diagnosis of *Pityrosporum* folliculitis. Dermatol Pract Concept. 2024;14(1):e2024092. https://doi.org/10.5826/dpc.1401a92.

22. Errichetti E, Scaggiante A, Stinco G. Ultraviolet-induced fluorescence dermoscopy for non-neoplastic dermatoses: a prospective study on its diagnostic accuracy. J Eur Acad Dermatol Venereol. 2024;38(1):e38–41. https://doi.org/10.1111/jdv.19459.

Rozdział 10.

Wnioski

1. Klasyczna dermoskopia jest cennym narzędziem we wczesnym wykrywaniu BCC, wyznaczaniu granic przed zabiegiem chirurgicznym i w monitorowaniu skuteczności leczenia. Jednak połączenie z innymi nieinwazyjnymi metodami obrazowania może zwiększyć czułość i swoistość diagnostyczną.

2. W UVFD, BCC wykazują szereg charakterystycznych cech, a na szczególną uwagę zasługują te, które nie są widoczne w klasycznej dermoskopii – ciemna sylwetka nowotworu, zaburzenie wzorca ujść mieszków włosowych, brak niebiesko-zielonej lub różowo-pomarańczowej fluorescencji mieszkowej lub obecność błękitnych włókien fluorescencyjnych.

3. Liczne korelacje pomiędzy strukturami obserwowanymi w UVFD oraz PD wskazują na komplementarność obu technik. Przykładowo obecność niebieskich fluorescencyjnych włókien w UVFD wskazuje na obecność nadżerki/ owrzodzenia. Dlatego też UVFD może stanowić cenne uzupełnienie klasycznego badania dermoskopowego.

4. Obecność poszczególnych struktur w UVFD jest zależna od lokalizacji BCC, wielkości guza i podtypu klinicznego. Stąd też metoda ta może być szczególnie przydatna w przypadku małych, bezbarwnikowych guzów, zlokalizowanych na twarzy.

5. BCC zlokalizowane w tzw. strefie H cechują się pewnymi odmiennościami dermoskopowymi nie tylko w PD, ale również w UVFD.

Rozdział 11.

Piśmiennictwo

1. Palmisano G., Orte Cano C., Fontaine M. i wsp. Dermoscopic criteria explained by LC-OCT: Negative maple leaf-like areas. J Eur Acad Dermatol Venereol 2024;38(3):e271–e273.
2. Wang W.E., Chen Y.T., Wang C.H. i wsp. Dermoscopic features of pigmented basal cell carcinoma according to size. Int J Dermatol 2024;63(7):916–921.
3. Manca R., Dattolo A., Valenzano F. i wsp. Proposal of a new dermoscopic criterion for pigmented basal cell carcinoma: a multicentre retrospective study. Dermatol Reports 2023;16(1):9691.
4. Carroll D.M., Billingsley E.M., Helm K.F. Diagnosing basal cell carcinoma by dermatoscopy. J Cutan Med Surg 1998;3(2):62–67.
5. Nelson S.A., Scope A., Rishpon A. i wsp. Accuracy and confidence in the clinical diagnosis of basal cell cancer using dermoscopy and reflex confocal microscopy. Int J Dermatol 2016;55:1351–1356.
6. Rosendahl C., Tschandl P., Cameron A. i wsp. Diagnostic accuracy of dermatoscopy for melanocytic and nonmelanocytic pigmented lesions. J Am Acad Dermatol 2011;64:1068–1073.
7. Ahnlide I., Bjellerup M. Accuracy of clinical skin tumour diagnosis in a dermatological setting. Acta Derm Venereol 2013;93:305–308.
8. Mansur A.T., Yildiz S. A Diagnostic Challenge: Inflamed and Pigmented Seborrheic Keratosis. Clinical, Dermoscopic, and Histopathological Correlation. Dermatol Online J 2019;25:14.
9. Álvarez-Salafranca M., Gómez-Martín I., Bañuls J. i wsp. Dermoscopy of Inflamed Seborrheic Keratosis: A Great Mimic of Malignancy. Australas J Dermatol 2022;63:53–61.
10. Ferrari A., Argenziano G., Buccini P. i wsp. Typical and atypical dermoscopic presentations of dermatofibroma. J Eur Acad Dermatol Venereol 2013;27:1375–1380.
11. Papageorgiou C., Apalla Z., Variaah G. i wsp. Accuracy of Dermoscopic Criteria for the Differentiation Between Superficial Basal Cell Carcinoma and Bowen's Disease. J Eur Acad Dermatol Venereol 2018;32:1914–1919.

12. Aydingoz I.E., Mansur A.T., Dikicioglu-Cetin E. Arborizing vessels under dermoscopy: A case of cellular neurothekeoma instead of basal cell carcinoma. Dermatol Online J 2013;19:5.
13. Lozano Salazar A.D., Márquez García A., Ortega Medina I. i wsp. Dermal leiomyosarcoma at the end of the left eyebrow. Actas Dermosifiliogr. 2014;105:879–882.
14. Zaballos P., Gómez-Martín I., Martin J.M. i wsp. Dermoscopy of Adnexal Tumors. Dermatol Clin 2018;36(4):397–412.
15. Kuraitis D., Pei S. Dermoscopy of cutaneous metastasis of renal cell carcinoma. JAAD Case Rep 2023;40:60–62.
16. Zattar G.A., Cardoso F., Nakandakari S. i wsp. Cutaneous histoplasmosis as a complication after anti-TNF use—Case report. An Bras Dermatol 2015;90:104–107.
17. Geller S., Marghoob A.A., Scope A. i wsp. Dermoscopy and the diagnosis of primary cutaneous B-cell lymphoma. J Eur Acad Dermatol Venereol 2018;32:53–56.
18. Pietkiewicz P., Navarrete-Dechent C., Togawa Y. i wsp. Applications of ultraviolet and sub-ultraviolet dermatoscopy in neoplastic and non-neoplastic dermatoses: a systematic review. *Dermatol Ther* 2024;14:361–390.
19. Page M.J., McKenzie J.E., Bossuyt P.M. i wsp. The PRISMA 2020 statement: an updated guideline for reporting systematic reviews. BMJ 2021;372:n71.
20. Guitera P., Menzies S.W., Argenziano G., Longo C., Losi A., Drummond M., Scolyer R.A., Pellacani G. Dermoscopy and in vivo confocal microscopy are complementary techniques for diagnosis of difficult amelanotic and light-coloured skin lesions. Br. J. Dermatol. 2016;175(6):1311–1319.
21. Ahnlide I., Zalaudek I., Nilsson F., Bjellerup M., Nielsen K. Preoperative prediction of histopathological outcome in basal cell carcinoma: Flat surface and multiple small erosions predict superficial basal cell carcinoma in lighter skin types. Br. J. Dermatol. 2016;175(4):751–761.

Rozdział 12.

Streszczenie w języku polskim

Rak podstawnokomórkowy (ang. *basal cell carcinoma*, BCC) to najczęstszy nowotwór złośliwy skóry, a w jego wczesnej diagnostyce pomocna jest dermoskopia. Mimo wysokiej czułości tej metody, wciąż istnieją przypadki o nietypowym obrazie dermoskopowym, w których rozpoznanie może sprawiać trudności. Jednym z kierunków doskonalenia nieinwazyjnej diagnostyki nowotworów skóry jest zastosowanie nowatorskiej metody - dermoskopii wzmocnionej ultrafioletem (ang. *ultraviolet-enhanced fluorescence dermoscopy*, UVFD).

Celem niniejszej pracy była analiza dotychczasowej wiedzy na temat wykorzystania dermoskopii w diagnostyce BCC oraz ocena zastosowania w tym wskazaniu UVFD, w tym identyfikacja struktur widocznych w tej technice.

Badania przeprowadzono w Klinice Dermatologii w Rzeszowie. Rozpoznanie BCC każdorazowo potwierdzano histopatologicznie. Do obrazowania zmian użyto dermatoskop Dermlite DL5, umożliwiający wizualizację w trybie dermoskopii spolaryzowanej (ang. *polarized dermoscopy*, PD) oraz UVFD.

Na podstawie własnych obserwacji wyróżniono następujące cechy BCC w UVFD: ciemną sylwetkę nowotworu, zaburzony wzorzec ujść mieszków włosowych, utratę niebiesko-zielonej i różowo-pomarańczowej fluorescencji, obecność różowo-pomarańczowej fluorescencji, błękitne włókna fluorescencyjne, nadżerki i owrzodzenia, naczynia rozgałęziające się drzewkowato, ogniska białej depigmentacji, białe grudki/globule, czarne globule, biało-niebieską łuskę oraz dobrze widoczne granice guza.

Najczęściej występującymi cechami były: ciemna sylwetka, zaburzony wzorzec ujść mieszków włosowych i utrata niebiesko-zielonej fluorescencji mieszkowej.

BCC zlokalizowane na twarzy częściej prezentowały w UVFD cechy takie jak wyraźne granice, zaburzenie wzorca ujść mieszków włosowych, utratę różowo-pomarańczowej fluorescencji oraz obecność nadżerek i owrzodzeń. Guzy zlokalizowane w strefie H na twarzy częściej wykazywały owrzodzenia, obecność błękitnych włókien fluorescencyjnych i brak niebiesko-zielonej fluorescencji. BCC o średnicy poniżej 5 mm

częściej cechowały się wyraźnymi granicami, utratą różowo-pomarańczowej fluorescencji i zaburzonym wzorcem ujść mieszków włosowych, natomiast większe guzy częściej wykazywały obecność nadżerek i owrzodzeń oraz biało-niebieskiej łuski. BCC guzkowe charakteryzowały się zaburzoną architekturą ujść mieszków włosowych, brakiem fluorescencji mieszkowej, obecnością naczyń rozgałęziających się drzewkowato oraz nadżerek i owrzodzeń, natomiast powierzchowne – ogniskami białej depigmentacji. Barwnikowe guzy wykazywały obecność czarnych globul, a bezbarwnikowe – zaburzoną architekturę ujść mieszków włosowych, obecność naczyń rozgałęziających się drzewkowato oraz utratę fluorescencji mieszkowej.

Zastosowanie UVFD umożliwia potencjalnie lepsze uwidocznienie granic BCC, zwłaszcza w zmianach zlokalizowanych na głowie i szyi, co może mieć istotne znaczenie w planowaniu leczenia chirurgicznego. Jednocześnie, UVFD okazało się mniej czułe w wykrywaniu niektórych struktur, takich jak naczynia czy nadżerki, w porównaniu do PD.

Wnioski te potwierdzają, że UVFD stanowi cenne narzędzie uzupełniające w diagnostyce BCC, wzbogacające możliwości klasycznej dermoskopii.

Rozdział 13.

Abstract (streszczenie w języku angielskim)

Basal cell carcinoma (BCC) is the most common malignant skin tumor and dermoscopy is a helpful tool in its early diagnosis. Despite the high sensitivity of this method, there are still cases with atypical dermoscopic features, in which establishing the diagnosis may be challenging. One of the directions in improving non-invasive skin cancer diagnostics is the implementation of an innovative technique—ultraviolet-enhanced fluorescence dermoscopy (UVFD).

The aim of this study was to review the current knowledge on the use of dermoscopy in the diagnosis of BCC and to assess the utility of UVFD in this indication, including the identification of structures observable with this technique.

The study was conducted at the Department of Dermatology in Rzeszów. The diagnosis of BCC was confirmed histopathologically in all cases. A Dermlite DL5 dermatoscope was used for imaging, enabling visualization in polarized dermoscopy (PD) and UVFD modes.

Based on the authors' observations, the following UVFD features of BCC were identified: dark silhouette, interrupted follicular pattern, lack of blue-green and pink-orange fluorescence, presence of pink-orange fluorescence, blue fluorescent fibers, erosions and ulcerations, arborizing vessels, white depigmentation, white clods, black globules, white-blue scales and well-demarcated borders.

The most frequent features were: dark silhouette, interrupted follicular pattern and lack of blue-green fluorescence.

BCCs located on the face more often exhibited features such as well-defined borders, interrupted follicular pattern, lack of pink-orange fluorescence and presence of erosions and ulcerations. Tumors situated within the H-zone of the face more frequently showed ulcerations, blue fluorescent fibers and lack of blue-green fluorescence. Tumors smaller than 5 mm in diameter more commonly demonstrated well-demarcated borders, lack of pink-orange fluorescence and interrupted follicular pattern, while larger tumors more often showed erosions, ulcerations and white-blue scales. Nodular BCCs were

characterized by interrupted follicular pattern, lack of follicular fluorescence, arborizing vessels and the presence of erosions and ulcerations, whereas superficial BCCs showed white depigmentation. Pigmented tumors exhibited black globules, while non-pigmented tumors were marked by interrupted follicular pattern, arborizing vessels and lack of follicular fluorescence.

The use of UVFD potentially allows for improved visualization of BCC margins, particularly in lesions located on the head and neck, which may be of clinical importance when planning surgical treatment. At the same time, UVFD was found to be less sensitive than PD in detecting certain structures, such as vessels and erosions.

These findings confirm that UVFD is a valuable complementary tool in BCC diagnostics, enhancing the capabilities of conventional dermoscopy.

Rozdział 14.

Oświadczenia współautorów

Magdalena Żychowska
(Imię i nazwisko autora)

Rzeszów, 01.06.2025
(miejscowość i data)

OŚWIADCZENIE
o merytorycznym wkładzie współautora

Oświadczam, że w pracy:

Wojtowicz I, Żychowska M. *Dermoscopy of Basal Cell Carcinoma Part 1: Dermoscopic Findings and Diagnostic Accuracy-A Systematic Literature Review*. Cancers (Basel). 2025 Feb 1;17(3):493. doi: 10.3390/cancers17030493,
mój udział polegał na:

- współtworzeniu koncepcji badania,
- opracowaniu metodologii,
- udziale w redakcji końcowej wersji manuskryptu przed jego przesłaniem do czasopisma.

dr hab. n. med. Magdalena Żychowska
prof. UR
specjalista dermatologii i wenerologii
2867525

Magdalena Żychowska
(podpis osoby składającej oświadczenie)

Magdalena Żychowska
(Imię i nazwisko autora)

Rzeszów, 01.06.2025
(miejscowość i data)

OŚWIADCZENIE
o merytorycznym wkładzie współautora

Oświadczam, że w pracy:

Wojtowicz I, Żychowska M. *Dermoscopy of Basal Cell Carcinoma Part 2: Dermoscopic Findings by Lesion Subtype, Location, Age of Onset, Size and Patient Phototype*. Cancers (Basel). 2025 Jan 8;17(2):176. doi: 10.3390/cancers17020176,
mój udział polegał na:

- współtworzeniu koncepcji badania,
- opracowaniu metodologii,
- udziale w redakcji końcowej wersji manuskryptu przed jego przesłaniem do czasopisma.

dr hab. n. med. Magdalena Żychowska
prof. UR
specjalista dermatologii i wenerologii
2867525

Magdalena Żychowska
(podpis osoby składającej oświadczenie)

Magdalena Żychowska
(Imię i nazwisko autora)

Rzeszów, 01.06.2025
(miejscowość i data)

OŚWIADCZENIE
o merytorycznym wkładzie współautora

Oświadczam, że w pracy:

Wojtowicz I, Żychowska M. *Dermoscopy of Basal Cell Carcinoma Part 3: Differential Diagnosis, Treatment Monitoring and Novel Technologies*. Cancers (Basel). 2025 Mar 19;17(6):1025. doi: 10.3390/cancers17061025,
mój udział polegał na:

- współtworzeniu koncepcji badania,
- opracowaniu metodologii,
- udziale w redakcji końcowej wersji manuskryptu przed jego przesłaniem do czasopisma.

dr hab. n. med. Magdalena Żychowska
prof. UR
specjalista dermatologii i wenerologii
2867525

(podpis osoby składającej oświadczenie)

Magdalena Żychowska
(Imię i nazwisko autora)

Rzeszów, 01.06.2025
(miejscowość i data)

OŚWIADCZENIE
o merytorycznym wkładzie współautora

Oświadczam, że w pracy:

Wojtowicz I, Żychowska M. *Application of Ultraviolet-Enhanced Fluorescence Dermoscopy in Basal Cell Carcinoma.* Cancers (Basel). 2024 Jul 28;16(15):2685. doi: 10.3390/cancers16152685,
mój udział polegał na:

- współtworzeniu koncepcji badania,
- opracowaniu metodologii,
- pozyskaniu danych do analizy,
- przeprowadzeniu analizy statystycznej,
- redakcji końcowej wersji manuskryptu przed jego przesłaniem do czasopisma.

dr hab. n. med. Magdalena Żychowska
prof. UR
specjalista dermatologii i wenerologii
2867525

Magdalena Żychowska
(podpis osoby składającej oświadczenie)

Magdalena Żychowska
(Imię i nazwisko autora)

Rzeszów, 01.06.2025
(miejscowość i data)

OŚWIADCZENIE
o merytorycznym wkładzie współautora

Oświadczam, że w pracy:

Wojtowicz IM, Reich AA, Żychowska M. *Polarized Dermoscopy and Ultraviolet-Induced Fluorescence Dermoscopy of Basal Cell Carcinomas in the H- and Non-H-Zones of the Head and Neck*. Dermatol Ther (Heidelb). 2025 Jun;15(6):1507-1522. doi: 10.1007/s13555-025-01432-z,

mój udział polegał na:

- współtworzeniu koncepcji badania,
- opracowaniu metodologii,
- nadzorze nad przebiegiem projektu,
- udziale w analizie i interpretacji danych,
- krytycznej ocenie i korekcie treści manuskryptu przed jego przesłaniem do czasopisma.

dr hab. n. med. Magdalena Żychowska
prof. UR
specjalista dermatologii i wenerologii
2867525

(podpis osoby składającej oświadczenie)

Prof. dr hab. n. med. Adam Reich
KIEROWNIK KLINIKI DERMATOLOGII
Uniwersytecki Szpital Kliniczny
im. Fryderyka Chopina w Rzeszowie

.....
(Imię i nazwisko autora)

Rzeszów, 03.06.2025
.....
(miejscowość i data)

OŚWIADCZENIE
o merytorycznym wkładzie współautora

Oświadczam, że w pracy:

Wojtowicz IM, Reich AA, Żychowska M. *Polarized Dermoscopy and Ultraviolet-Induced Fluorescence Dermoscopy of Basal Cell Carcinomas in the H- and Non-H-Zones of the Head and Neck*. Dermatol Ther (Heidelb). 2025 Jun;15(6):1507-1522. doi: 10.1007/s13555-025-01432-z,

mój udział polegał na nadzorze nad przebiegiem projektu oraz krytycznej ocenie i korekcie treści manuskryptu przed jego przesłaniem do czasopisma.

Prof. dr hab. n. med. Adam Reich
KIEROWNIK KLINIKI DERMATOLOGII
Uniwersytecki Szpital Kliniczny
im. Fryderyka Chopina w Rzeszowie

.....
(podpis osoby składającej oświadczenie)

Rozdział 15..

Załączniki

Zgoda Komisji Bioetycznej

Komisja Bioetyczna
przy Okręgowej Izbie Lekarskiej
35-030 Rzeszów, ul. Dekerta 2
tel. 17 717 77 17

UCHWAŁA Nr 50/2024/B
Komisji Bioetycznej Okręgowej Izby Lekarskiej
z dnia 21 października 2024 r.

Komisja Bioetyczna Okręgowej Izby Lekarskiej w Rzeszowie działając na podstawie art. 29 ust. 3 pkt. 2 ustawy z dnia 5.12.1996 r. o zawodzie lekarza (Dz. U. z dnia 26.03.1997 r. Nr 28, poz. 152), działając zgodnie z Rozporządzeniem Ministra Zdrowia i Opieki Społecznej z dnia 11 maja 1999 r. (Dz. U. Nr 47 poz. 480 z 1999 r.) w sprawie szczegółowych zasad powoływania i finansowania , oraz trybu działania Komisji Bioetycznych, Kodeksu Etyki Lekarskiej, z uwzględnieniem zasad Deklaracji Helsińskiej (Declaration of Helsinki) oraz zasad prawidłowego prowadzenia badań klinicznych (Good Clinical Practice) i Międzynarodowej Konferencji na rzecz harmonizacji wymogów technicznych dla rejestracji środków farmaceutycznych (International Conference on Harmonisation of Technical Requirements for Registration of Pharmaceutical for Human Use (ICH), po zapoznaniu się z dokumentami przedłożonymi wraz ze „Zgłoszeniem badań" oraz po wysłuchaniu dodatkowych informacji złożonych przez wnioskodawcę :

postanawia

w wyniku przeprowadzonej dyskusji i głosowania, Komisja pozytywnie zaopiniowała projekt badania pt. :

„ Zastosowanie dermatoskopii i dermatoskopii wzmocnionej ultrafioletem w ocenie raka podstawnokomórkowego".

Badacz : lek. Irena Wojtowicz

Ośrodek :

Klinika Dermatologii Uniwersyteckiego Szpitala Klinicznego
35-005 Rzeszów, ul. Szopena 2

Przewodniczący
Komisji Bioetycznej
Okręgowej Izby Lekarskiej w Rzeszowie
dr hab. n. med. Andrzej Pluta

Irena Wojtowicz
Imię i nazwisko

Rzeszów, 04.06.2025r.

OŚWIADCZENIE

Ja, niżej podpisana Irena Wojtowicz oświadczam, że przygotowana dysertacja pt. „Zastosowanie dermatoskopii i dermatoskopii wzmocnionej ultrafioletem w ocenie raka podstawnokomórkowego", którą przedkładam w przewodzie doktorskim procedowanym na Uniwersytecie Rzeszowskim została przygotowana i w pełni odpowiada założeniom projektu badawczego o tym samym tytule, który uzyskał pozytywną opinię Komisji Bioetycznej Okręgowej Izby Lekarskiej w Rzeszowie (uchwała nr 50/2024/B wydana w dniu 21 października 2024r.).

Magdalena Gacuta
(promotor)

Irena Wojtowicz
(składający oświadczenie)